Universidade de Aveiro
2023

Sónia Isabel Neto Pedro

Formulações à base de solventes eutécticos profundos para o desenvolvimento de sistemas de administração de fármacos

Deep eutectic solvent formulations for the development of drug delivery systems

Universidade de Aveiro
2023

Sónia Isabel Neto Pedro

Formulações à base de solventes eutécticos profundos para o desenvolvimento de sistemas de administração de fármacos

Deep eutectic solvent formulations for the development of drug delivery systems

Tese apresentada à Universidade de Aveiro para cumprimento dos requisitos necessários à obtenção do grau de Doutor em Bioquímica, realizada sob a orientação científica da Doutora Carmen Sofia da Rocha Freire Barros, Investigadora Principal com Agregação do Departamento de Química da Universidade de Aveiro, do Professor Armando Jorge Domingues Silvestre, Professor Catedrático do Departamento de Química da Universidade de Aveiro e da Doutora Mara Guadalupe Freire Martins, Investigadora Coordenadora do Departamento de Química da Universidade de Aveiro.

o júri

Presidente
Doutora Anabela Botelho Veloso
Professora Catedrática da Universidade de Aveiro

Vogais
Doutora Maria Adelaide de Pinho Almeida
Professora Catedrática da Universidade de Aveiro

Doutor Hélder Almeida Santos
Professor Catedrático do Centro Médico Universitário de Groningen

Doutora Carmen Sofia da Rocha Freire Barros
Investigadora Principal com Agregação da Universidade de Aveiro

Doutor Simão Pedro de Almeida Pinho
Professor Coordenador do Instituto Politécnico de Bragança

Doutor Alexandre Babo de Almeida Paiva
Investigador Auxiliar da Universidade Nova de Lisboa

Agradecimentos

Em todos os momentos da vida é absolutamente necessário estar no sítio certo, mas acima de tudo, com as pessoas certas. Este percurso tem sido um longo caminho de descobertas felizes, não só a nível da ciência, mas especialmente pessoais. Esta Universidade deu-me, desde o primeiro dia, mais do que alguma vez sonhei e eu nunca esquecerei isso. São mais de 10 anos de aprendizagem, descobertas e boas amizades. Estes anos de doutoramento não são exceção.

Acho necessário agradecer primeiro aos avaliadores da FCT que aprovaram a minha bolsa. Agradeço terem visto neste trabalho o mesmo potencial que eu vi. Sem nunca me terem conhecido fizeram de mim uma pessoa incrivelmente mais realizada a nível profissional.

Aos meus orientadores, pelo constante reforço positivo que me fizeram nestes anos. Sempre questionada sobre ter três orientadores, hoje posso dizer que, foi o melhor que me aconteceu. Aprendi a ver sempre tudo com três diferentes perspetivas e isso acabou por melhorar a minha visão na investigação, levo isso comigo. O vosso incentivo e a vossa confiança em mim fez-me querer ser melhor. A liberdade que me deram para fazer o que gosto tornou-me melhor no meu trabalho. Estou-vos eternamente grata por isso, e também pelo carinho e pela disponibilidade.

Ao professor Paulo Claro, pela oportunidade que me deu de trabalhar com ele durante este doutoramento numa área diferente e por ser um dos motivos que me mantiveram neste curso.

Agradeço à professora Adelaide ter-me acolhido no seu laboratório, pela disponibilidade e pela motivação nos nossos trabalhos que permitiram que esta tese ficasse mais completa. À Drª Ana Gomes, o meu especial agradecimento, por tudo o que me ensinou na área da Biologia e que hoje me permite poder ser independente no trabalho. A ela agradeço também as palavras de amizade e a possibilidade de ter conhecido a Drª Rosa Fernandes, a quem agradeço também pela contribuição e ajuda.

Não posso deixar de agradecer à professora Helena Amaral, por me ter recebido no seu laboratório, por todo o conhecimento que me transmitiu, a sua relação com os alunos e pela simpatia.

Deixo também o meu agradecimento a todos os restantes envolvidos na realização do meu doutoramento. À Drª Isabel Almeida, ao professor Paulo Costa e à Drª Carla Vitorino pela oportunidade de ter feito os ensaios de permeação.

Ao prof. Bruno Neves e à Drª Helena Oliveira a sua disponibilidade na realização dos ensaios de citotoxicidade. Um especial agradecimento à Drª Carla Vilela por toda a ajuda e contribuição nos trabalhos realizados.

Nenhum sucesso é resultado do trabalho de um só, somos também o que nos rodeia, por isso gostaria de deixar o meu mais profundo agradecimento aos excelentes colegas e amigos que ganhei durante este percurso. Aos colegas da Biologia por me mostrarem o verdadeiro espírito de entreajuda, por terem sempre um tempinho para mim e por todas as horas passadas em conjunto à frente das câmaras. Aos meus colegas e amigos dos grupos Biopol4Fun e Path, pelo apoio, pela troca de conhecimento, por todas as boas memórias que partilhámos ao longo destes anos. Gostaria de deixar um agradecimento especial ao Bruno Pinheiro, Bruno Valente (um especial ao Brubru), Fábio, João, Maria do Céu, Nicole, Nuno Hélder, Rodrigo, Samuel e ao Tiago, pela amizade que ficou, pela partilha dos dias de laboratório, a boa disposição e todas as pausas para lanche.

Aos meus amigos, demasiados para listar, aos que Aveiro me deu, aos de infância, e aos amigos dos meus pais que são também meus amigos, por estarem sempre a torcer por mim, obrigado por todo o apoio nesta etapa e por me deixarem um sorriso no rosto. Gostaria, porém, de fazer um agradecimento muito especial aos amigos (que são como família) que estão comigo desde o primeiro dia da Universidade e aos que decidiram juntar-se depois neste percurso até ao doutoramento, o Carlos, a Eduarda, a Inês, o João, o Luís, a Sara, o Vasco e o Vítor. Obrigada por tudo o que aprendi convosco, sem saberem, vocês fazem de mim uma pessoa melhor, o vosso carinho, apoio e compreensão faz de mim uma pessoa mais feliz e torna os dias mais leves. Obrigada por todos os risos, e por estarem em todas as memórias mais queridas que tenho. Um especial à Dinha, pela dupla fantástica que criámos, pelos anos de casa e pelas boas histórias partilhadas.

À minha família, que apesar de pequena é feita de grandes pessoas com as quais posso sempre contar. Aos meus avós, José e Manuel por me terem ensinado que só somos verdadeiramente felizes quando fazemos o que gostamos. Às minhas avós, Conceição e Palmira, por serem um modelo de como é possível ser forte e doce ao mesmo tempo. À minha madrinha, que é um exemplo de dedicação e de força, agradeço todo o carinho, preocupação e apoio.

Por fim, às melhores pessoas que conheço e aos meus melhores amigos, os meus pais. Tudo o que aprendi fora desta tese, foi convosco, mas também acabou por ser essencial para fazê-la. Vocês são o motivo do meu sorriso todos os dias. Talvez nunca chegue a merecer a sorte que é ter-vos. Obrigado pelo vosso apoio que, durante esta tese não teve limites. Pelo vosso entusiasmo com tudo o que faço e pela vossa motivação, compreensão, boa disposição e carinho, que me dão sempre força. Tudo o que alcancei até hoje é nosso, e ainda bem que seremos sempre os três. Mal posso esperar pelo que o futuro nos reserva.

(Todas as pessoas listadas na mesma frase estão por ordem alfabética, porque no meu coração todos ocupam um mesmo lugar.)

Palavras-chave   Princípios ativos, reformulação de fármacos, solventes eutécticos profundos, biopolímeros, sistemas de administração de fármacos, eficácia terapêutica

Resumo   A indústria farmacêutica é caraterizada por mudanças e exigências constantes, originadas pela necessidade de desenvolver novos fármacos, ou formulações de fármacos existentes, que sejam mais eficazes e seguras. Neste contexto, são frequentemente utilizadas estratégias como a reformulação farmacêutica para ultrapassar muitas das desvantagens associadas aos fármacos existentes, dado o menor custo desta abordagem.

As estratégias usadas para aumentar a solubilidade, estabilidade e permeação de fármacos são cruciais para melhorar a sua eficácia terapêutica. Assim, compreender os problemas associados aos princípios ativos já existentes, desenvolver estratégias mais eficazes para a sua solubilização e administração, assim como a seleção de solventes ou excipientes apropriados, são aspetos cruciais para melhorar a eficácia terapêutica. Adicionalmente, a possibilidade de incorporar estes componentes, nomeadamente os solventes, em sistemas de administração de fármacos é apelativa para modelar as suas propriedades.

Recentemente, solventes alternativos como os solventes eutécticos profundos (DES) têm sido explorados na área farmacêutica, mostrando uma elevada capacidade de solvatação e de permeação de fármacos através de membranas biológicas, bem como da sua estabilização. Adicionalmente, a versatilidade destes solventes possibilita a sua incorporação em diferentes sistemas de administração de fármacos, sendo inclusive possível o uso de biopolímeros hidrofílicos. Esta combinação resulta em efeitos positivos nas propriedades dos materiais biopoliméricos, permitindo em particular o ajuste das suas propriedades mecânicas e dos perfis de libertação dos respetivos fármacos.

Neste contexto, o principal objetivo da presente tese centrou-se no desenvolvimento de formulações de DES e na sua utilização em novos sistemas de administração de fármacos já existentes, visando a melhoria da sua eficácia. Os trabalhos desenvolvidos envolveram o design racional dessas formulações e a avaliação do seu impacto no desempenho do sistema. Dada as crescentes preocupações associadas aos agentes antimicrobianos, incluindo antibióticos, esta classe de fármacos foi uma das mais estudadas.

O primeiro trabalho focou-se no desenvolvimento de soluções aquosas de DES, tais como cloreto de colina:ureia:ácido malónico, prolina:ureia:ácido malónico e ácido cítrico:xilitol, para melhorar a solubilidade, a estabilidade e a eficácia terapêutica do antibiótico ciprofloxacina.

As formulações desenvolvidas permitiram aumentar a solubilidade do fármaco 430 vezes comparativamente à sua solubilidade em água, e a suscetibilidade de bactérias Gram-negativas e Gram-positivas à ciprofloxacina 2 a 4 vezes, respetivamente, sendo não tóxicas para células humanas nas concentrações estudadas. Foi ainda demonstrada a capacidade de melhorar a eficácia terapêutica do antibiótico sem promover o desenvolvimento de tolerância antimicrobiana ao mesmo.

O trabalho seguinte teve como objetivo a utilização de soluções aquosas de DES à base de betaína, nomeadamente betaína:glicerol e betaína:xilitol, no desenvolvimento de sistemas de administração de fármacos para administração ocular, especificamente microemulsões com carácter termo-responsivo, cuja viscosidade aumenta quando em contato com o ambiente ocular. Estes sistemas permitiram obter uma libertação contínua e uma maior permeação do antibiótico cloranfenicol através da córnea. Por fim, foi demonstrada uma maior atividade antimicrobiana e uma ação mais rápida em caso de infeção por bactérias multirresistentes, usando estas microemulsões, comparativamente com uma formulação comercial.

A versatilidade das formulações aquosas de DES foi também explorada no desenvolvimento de sistemas tópicos de administração de fármacos à base de biopolímeros. Neste sentido, foram desenvolvidos filmes adesivos baseados em pululano para aplicação em terapia fotodinâmica antimicrobiana (TFDa). Com este propósito, foram utilizados DES à base de betaína (betaína:ácido levulínico)) para melhorar a solubilidade e fotoestabilidade da curcumina, um fotossensibilizador natural. A incorporação das formulações de DES nos filmes de pululano permitiu ajustar as suas propriedades, tendo-se obtido sistemas com maior extensibilidade do que os correspondentes originais. Estes filmes possuem ainda capacidade de absorver a humidade da pele e passar para a forma de hidrogel com maior adesividade do que os hidrogéis comerciais. O uso destes sistemas em combinação com uma abordagem de TFDa permitiu erradicar estirpes resistentes a antibióticos comuns, abaixo do limite de deteção do método, em amostras de pele *ex vivo*, sendo estes sistemas não tóxicos para as células da pele.

A combinação de DES e biopolímeros foi também investigada para a administração transdérmica de fármacos anti-inflamatórios. Foram utilizadas soluções aquosas de DES à base de arginina:glicerol para aumentar a solubilidade do ibuprofeno (até 7917 vezes em comparação com a solubilidade em água). Estas formulações não apresentaram citotoxicidade para macrófagos e preservaram a ação anti-inflamatória do fármaco. A sua incorporação em hidrogéis de alginato resultou em materiais com maior flexibilidade, e que apresentam uma libertação sustentada do fármaco. Adicionalmente, estes hidrogéis promoveram um aumento da permeação do fármaco na pele humana em comparação com o sistema homólogo contento apenas ibuprofeno.

Em suma, a presente tese demonstra a versatilidade e as vantagens das formulações aquosas de DES na melhoria da administração e na eficácia terapêutica de diferentes fármacos existentes.

keywords
Active pharmaceutical ingredients, drug reformulation, deep eutectic solvents, biopolymers, drug delivery systems, therapeutic efficacy

abstract
The pharmaceutical industry is characterized by constant changes and demands, driven by the need to develop new drugs, or drug formulations of existing drugs, that are more efficient and safer. In this context, strategies such as drug reformulation are frequently applied to overcome many of the drawbacks associated with the existing pharmaceuticals, given the lower cost of this approach.

Approaches to enhance drug solubility, stability, and permeation are crucial to improve their therapeutic efficacy. Therefore, understanding the problems associated with the existing active pharmaceutical ingredients, developing more effective strategies for their solubilization and administration, as well as to select proper solvents or excipients, are main aspects to improve therapeutic efficacy. Additionally, the possibility to incorporate these components, namely the solvents, in the drug delivery system, to tune their properties is appealing.

Recently, alternative solvents, such as deep eutectic solvents (DES), have been explored in the pharmaceutical field, showing high solvation ability and high drug permeation across biological membranes, as well as drug stabilization. Furthermore, the versatility displayed by these solvents enables their incorporation into different drug delivery systems, being even possible the use of hydrophilic biopolymers. This partnership results in positive effects in the properties of biopolymer-based materials, allowing to particularly tune the mechanical properties and the respective drug release profiles.

In this context, the main goal of this thesis is focused on the development of DES formulations of existing drugs and their incorporation in delivery systems, envisioning the improvement of their efficacy. The works developed involved the rational design of these formulations and the evaluation of their impact on system's performance. Given the rising concerns associated with antimicrobial agents, including antibiotics, this was the class mainly studied.

The first study focused on the development of DES aqueous solutions of cholinium chloride:urea:malonic acid, proline:urea:malonic acid and citric acid:xylitol, to remarkably improve the solubility, stability, and therapeutic efficacy of the antibiotic ciprofloxacin. The developed formulations enhanced the drug solubility up to 430-fold, in comparison to water, and the susceptibility of Gram-negative and Gram-positive bacteria to ciprofloxacin by 2- to 4-fold, respectively, while being non-toxic to human cells at the studied concentrations.

The ability to improve the therapeutic efficacy of the antibiotic while avoiding the development of antimicrobial tolerance was demonstrated.

The following study aimed to use betaine-based DES aqueous solutions, such as betaine:glycerol and betaine:xylitol, in the development of ocular drug delivery systems, namely thermo-responsive microemulsions that increase their viscosity upon contact with the ocular environment. These systems allowed a sustained-release and a higher permeation of the antibiotic chloramphenicol through the cornea. Finally, a higher antimicrobial activity and faster action in case of infection caused by multi-resistant bacteria was demonstrated using these microemulsions in comparison to a commercialized formulation.

The versatility of DES formulations was also explored in the development of biopolymer-based drug delivery systems. In this sense, pullulan-based adhesive films were developed for application in antimicrobial photodynamic therapy (aPDT). For this purpose, betaine-based DES (betaine:levulinic acid) were applied to improve the solubility and photostability of the natural photosensitizer, curcumin. The incorporation of the DES formulations in the films, permitted to tune pullulan's properties, obtaining systems with higher extensibility than the pristine materials. These films also present capability to absorb skin moisture and transit into a hydrogel with and higher adhesiveness than commercial hydrogels. The use of these systems in combination with an aPDT approach, allowed to eradicate common drug-resistant strains below the detection limit in *ex vivo* skin samples while being non-toxic to skin cells.

The partnership between DES and biopolymers was also investigated for the transdermal delivery of anti-inflammatory drugs. DES aqueous solutions, based on arginine:glycerol, were used to increase the solubility of ibuprofen (up to 7917-fold, in comparison to water). These formulations were non-cytotoxic to macrophages and shown to preserve the anti-inflammatory action of the drug. Their incorporation into alginate-based hydrogels resulted in materials with higher flexibility, that presented a sustained release of the drug. Additionally, these hydrogels promoted an enhancement in the drug permeation across human skin in comparison to their counterpart containing only ibuprofen.

In conclusion, the present thesis demonstrates the versatility and advantages of DES formulations in the improvement of drug delivery and therapeutic efficacy of known drugs.

Table of Contents

Publications and Communications

Patents:

Pedro, S. N.; Gomes, A. T. P. C.; Oliveira, H.; Almeida, A.; Freire, M. G.; Silvestre, A. J. D.; Freire, C. S. R. Processo de separação de preparação de formulações à base de solventes eutécticos profundos e de princípios ativos e utilização destas formulações para melhoria da ação terapêutica de fármacos, PT/116953, 16 Dez, 2020 (provisional order).

Scientific papers developed within the thesis scope:

Pedro, S. N.; Freire, M. G.; Freire, C. S. R.; Silvestre, A. J. D. Deep eutectic solvents comprising active pharmaceutical ingredients in the development of drug delivery systems (2019) Expert Opinion on Drug Delivery, 16 (5), 497-506. DOI: 10.1080/17425247.2019.1604680 (IF= 5.847 in 2020, Q1).

Pedro, S. N.; Freire, C.S.R.; Silvestre, A. J. D.; Freire, M. G. The Role of Ionic Liquids in the Pharmaceutical Field: An Overview of Relevant Applications (2020) International Journal of Molecular Sciences, 21, 8298. DOI: 10.3390/ijms21218298. (IF=6.208 in 2021, Q1).

Pedro, S. N.; Freire, C. S. R.; Silvestre, A. J. D.; Freire, M. G. Ionic Liquids in Drug Delivery (2021) Encyclopedia, 1(2), 324–339. DOI: https://doi.org/10.3390/encyclopedia1020027.

Pedro, S. N.; Freire, C. S. R.; Silvestre, A. J. D.; Freire, M. G. Deep Eutectic Solvents and Pharmaceuticals (2021) Encyclopedia, 1(3), 942-963. DOI: https://doi.org/10.3390/encyclopedia1030072.

Pedro, S. N.; Gomes, A. T. P. C.; Oskoei, P.; Oliveira, H.; Almeida, A.; Freire, M.G.; Silvestre, A. J. D.; Freire, C. S. R. Boosting Antibiotics Performance by New Formulations with Deep Eutectic Solvents (2022) International Journal of Pharmaceutics, 616, 121566. DOI: https://doi.org/10.1016/j.ijpharm.2022.121566. (IF=6.51 in 2022-2023, Q1).

Pedro, S. N.; Mendes, M. S. M.; Neves, B. M.; Almeida I. F.; Costa, P.; Correia-Sá, I.; Vilela, C.; Freire, M. G.; Silvestre, A. J. D.; Freire, C. S. R. Deep Eutectic Solvent Formulations and Alginate-Based Hydrogels as a New Partnership for the Transdermal Administration of Anti-Inflammatory Drugs (2022) Pharmaceutics, 14(4), 827. DOI: https://doi.org/10.3390/pharmaceutics14040827. (IF=6.525 in 2022-2023, Q1).

Pedro, S. N.; Gomes, A. T. P. C.; Vilela, C.; Vitorino, C.; Fernandes, R.; Almeida A.; Amaral, M. H.; M. G. Freire; Silvestre, A. J. D.; Freire, C. S. R. Thermo-responsive microemulsions containing deep eutectic-based antibiotic formulations for improved treatment of resistant bacterial ocular infections (2023) Advanced Therapeutics, 2200235. DOI: 10.1002/adtp.202200235. (IF=5.20 in 2021, Q1).

Pedro, S. N.; Valente, B. F.; Vilela, C.; Oliveira, H.; Almeida, A.; Freire, M.G.; Silvestre, A. J. D.; Freire, C. S. R. Photodynamical Switchable Adhesive Pullulan Films Loaded with a Deep Eutectic Solvent Formulation Containing Curcumin to Treat Multi-Resistant Skin Infections (2023) Materials Today Bio, 22, 100733. DOI: https://doi.org/10.1016/j.mtbio.2023.100733. (IF=10.761 in 2023, Q1).

Book chapters developed within the thesis scope:

Pedro, S. N.; Freire, C. S. R.; Silvestre, A. J. D.; Freire, M. G. Chapter 7- Advances brought by ionic liquids in the development of polymer-based drug delivery systems, In: Application of Ionic Liquids in Drug Delivery (2021) Springer, 113-135. DOI:10.1007/978-981-16-4365-1_7.

Oral communications:

By invitation: <u>Pedro, S. N.</u>; Freire, M. G.; Silvestre, A. J. D.; Freire, C. S. R.; Eutectic solvents comprising active pharmaceutical ingredients, an improvement in therapeutics (2019) In Path Spring workshop 2019, held in University of Aveiro, Aveiro, Portugal.

By invitation: <u>Pedro, S. N.</u>; Freire, M. G.; Silvestre, A. J. D.; Freire, C. S. R. The Successful Partnership Between Deep Eutectic Solvent Formulations and Biopolymers in the Transdermal Delivery of NSAIDs (2022) In

PATh/IL2BioPro/mVACCIL workshop 2022, held in University of Aveiro, Aveiro, Portugal.

Other:

Pedro, S. N.; Freire, M. G.; Silvestre, A. J. D.; Freire, C. S. R. Deep eutectic solvents comprising active pharmaceutical ingredients- antibiotic-based liquid formulations for drug delivery (2019) In ISGC 2019, held in La Rochelle, France.

Pedro, S. N.; Freire, M. G.; Silvestre, A. J. D.; Freire, C. S. R. Eutectic Solvents Comprising Antibiotics - A Breakthrough In Topical Treatment (2019) In 1st International Meeting on Deep Eutectic Solvents, held in Universidade Nova de Lisboa, Lisboa, Portugal.

Pedro, S. N.; Freire, M. G.; Silvestre, A. J. D.; Freire, C. S. R. Deep eutectic solvents comprising active pharmaceutical ingredients for incorporation in biopolymer-based drug delivery systems (2019). Research Summit, University of Aveiro, Aveiro, Portugal.

Pedro, S. N.; Freire, M. G.; Silvestre, A. J. D.; Freire, C. S. R. Deep eutectic solvents comprising active pharmaceutical ingredients, searching new therapeutic approaches International (online) Workshop on Deep Eutectic Solvents for Environmental Remediation and Energy Storage Department of Chemical Engineering, IIT Guwahati (2020), India.

Pedro, S. N.; Freire, M. G.; Silvestre, A. J. D.; Freire, C. S. R. Deep eutectic solvents comprising active pharmaceutical ingredients for incorporation in biopolymer-based drug delivery systems (2020). Research Summit (online), Aveiro, Portugal.

Pedro, S. N.; Mendes, M. S M.; Neves, B. M.; Freire, M. G.; Silvestre, A. J. D.; Freire, C. S. R. Delivery of Deep Eutectic Solvents Comprising Nonsteroidal Anti-inflammatory Drugs using Biopolymer-Based Systems (2021) In 2nd International Meeting on Deep Eutectic Solvents, held by Universidade Nova de Lisboa, Lisboa, Portugal.

Pedro, S. N.; Freire, M. G.; Silvestre, A. J. D.; Freire, C. S. R., Deep eutectic solvents comprising active pharmaceutical ingredients for incorporation in

biopolymer-based drug delivery systems (2021). Research Summit (online), Aveiro, Portugal.

Pedro, S. N.; Freire, M. G.; Silvestre, A. J. D.; Freire, C. S. R. Deep eutectic solvents comprising active pharmaceutical ingredients for incorporation in biopolymer-based drug delivery systems (2022). Research Summit, University of Aveiro, Aveiro, Portugal.

Poster communications:

Pedro, S. N.; Freire, M. G.; Silvestre, A. J. D.; Freire, C. S. R. "Deep eutectic solvents as active pharmaceutical ingredients- novel liquid formulations for cell therapy". Presented in 12th Symposium of the European Society of Biochemical Engineering Sciences, 2018.

Pedro, S. N.; Freire, M. G.; Silvestre, A. J. D.; Freire, C. S. R. "Therapeutic formulations based on deep eutectic solvents as new strategies to tackle Pseudomonas aeruginosa infections". Presented in Jornadas CICECO 2019, 2019.

Pedro, S. N.; Freire, M. G.; Silvestre, A. J. D.; Freire, C. S. R. "Boosting the therapeutic efficiency of antibiotics with novel formulations based on deep eutectic solvents". Presented in Jornadas CICECO 2020, 2020.

Pedro, S. N.; Freire, M. G.; Silvestre, A. J. D.; Freire, C. S. R. "Deep eutectic solvents as new tools to fight bacterial resistance to antibiotics". Paper presented in Jornadas CICECO 2021, 2021.

Pedro, S. N.; Valente, B. F. A.; Vilela, C.; Oliveira, H.; Almeida, A.; Freire, M. G.; Silvestre, A. J. D.; Freire, C. S. R. "Adhesive pullulan-based films comprising deep eutectic-curcumin formulations to overcome antimicrobial multi-resistance". Paper presented in Jornadas CICECO 2022, 2022.

Awards:

Best Poster awards:

Pedro, S. N.; Freire, M. G.; Silvestre, A. J. D.; Freire, C. S. R. "Therapeutic formulations based on deep eutectic solvents as new strategies to tackle Pseudomonas aeruginosa infections". Presented in Jornadas CICECO 2019, 2019.

X

Pedro, S. N.; Valente, B. F. A.; Vilela, C.; Oliveira, H.; Almeida, A.; Freire, M. G.; Silvestre, A. J. D.; Freire, C. S. R. "Adhesive pullulan-based films comprising deep eutectic-curcumin formulations to overcome antimicrobial multi-resistance". Jornadas CICECO 2022, 2022.

Best communication awards:

Pedro, S. N.; Freire, M. G.; Silvestre, A. J. D.; Freire, C. S. R. Deep eutectic solvents comprising active pharmaceutical ingredients for incorporation in biopolymer-based drug delivery systems (2019). Research Summit, University of Aveiro, Aveiro, Portugal.

Pedro, S. N.; Freire, M. G.; Silvestre, A. J. D.; Freire, C. S. R. Deep eutectic solvents comprising active pharmaceutical ingredients for incorporation in biopolymer-based drug delivery systems (2022). Research Summit, University of Aveiro, Aveiro, Portugal.

Pedro, S. N.; Freire, M. G.; Silvestre, A. J. D.; Freire, C. S. R. The Successful Partnership Between Deep Eutectic Solvent Formulations and Biopolymers in the Transdermal Delivery of NSAIDs (2022) PATh/IL2BioPro/mVACCIL workshop University of Aveiro, Aveiro, Portugal.

Projects:

ISIS Neutron and Muon Source, Rutherford Appleton Laboratory (Oxford, UK) Experiment number 1920244 (November 13 18 2019 TEAM MEMBER) "API DES improving drug solubility with deep eutectic solvents by inelastic neutron scattering".

Other Distinctions:

Highly Cited Papers of IJMS in 2020 - "The Role of Ionic Liquids in the Pharmaceutical Field: An Overview of Relevant Applications".

Best photo in materials@AVEIRO Award University of Aveiro CICECO, "Treasure in a bottle".

2nd Place- Best PhD video, University of de Aveiro CICECO, "Shaping the future of pharmaceuticals.

Trainings and workshops:

2018 - Workshop on MultiBiorefinery, III Path Spring Meeting 2018, University of Aveiro, Portugal.

2020 – Workshop PATh IonCytDevice, University of Aveiro, Portugal.

2021- Interdisciplinary Training Program on Principles Applications and Nanotechnology Innovation in Pharmaceutical Sciences Biological Engineering and Medicine, University of Texas at Austin, USA & Associação para a Inovação e Desenvolvimento da FCT, Portugal.

Promotion and Dissemination of Science

Speaker

2019, 2020, 2021- Research Summit, Aveiro, Portugal

2019- Biochemistry Day, University of Aveiro, Portugal.

Presence in Events

TECHDAYS 2018 – Representing the Project DEEPBIOREFINERY (PTDC/AGR-TEC/1191/2014) and MULTIBIOREFINERY (POCI-01-0145-FEDER-016403).

Other scientific papers resulting from collaborative work outside the scope of the thesis:

Nolasco, M. M.; Pedro, S.N.; Vilela, C.; Vaz, P. D.; Ribeiro-Claro, P.; Rudić, S.; Parker, S. F.; Freire, C. S. R.; Freire, M. G.; Silvestre, A. J. D. Water in Deep Eutectic Solvents: New Insights From Inelastic Neutron Scattering Spectroscopy (2022) Frontiers in Physics, 10, 834571. DOI: https://doi.org/10.3389/fphy.2022.834571. (IF=3.718 in 2022-2023, Q2).

Pereira, M. M.; Pedro, S. N.; Quental, M. V.; Mohamadou, A.; Coutinho, J. A. P.; Freire M. G. Integrated Approach to Extract and Purify Proteins from Honey by Ionic Liquid-Based Three-Phase Partitioning (2022) ACS Sustainable Chemistry & Engineering, 10, 29, 9275–9281. DOI: https://doi.org/10.1021/acssuschemeng.2c01782. (IF=9.224 in 2022, Q1).

Carvalho, T.; Bártolo, R.; Pedro, S. N.; Valente, B. F. A.; Pinto, R. J. B.; Vilela, C.; Shahbazi, M.-A; Santos, H. A.; Freire, C. S. R. "Injectable nanocomposite

hydrogels of gelatin-hyaluronic acid reinforced with hybrid lysozyme nanofibrils gold nanoparticles for regeneration of damaged myocardium" ACS Applied Materials and Interfaces (submitted)

Batista, V.F.; Pedro, S.N.; Freire, M.G.; Pinto, D.C.G.A; Silvestre, A.J.D.; Silva, A.M.S. "Deep eutectic solvent as a recyclable solvent for the diazo amination reaction catalyzed by iron porphyrins" (to be submitted).

Nolasco, M. M.; Pedro, S.N.; Vilela, C.; Vaz, P. D.; Ribeiro-Claro, P.; Rudić, S.; Parker, S.F.; Freire, C.S.R.; Freire, M.G.; Silvestre, A.J.D. Understanding the water impact in Deep Eutectic Solvents comprising active pharmaceutical ingredients using Inelastic Neutron Scattering Spectroscopy (under preparation).

Vieira, C.; Pedro, S.N.; Bartolomeu, M.; Dias, C. J.; Gamelas, S. R. D.; Lourenço, L. M. O.; Gomes, A. T. P. C.; Freire, C. S. R.; Neves, M. G. P.M.S.; Faustino, M. A. F.; Almeida A. "Deep Eutectic Solvents (DES) as alternative solvents for Photodynamic Inactivation of microrganismos" (under preparation).

Oral communications resulting from collaborative work outside the scope of the thesis:

Vieira, C.; Pedro, S. N.; Mesquita, M. Q.; Bartolomeu, M.; Gomes, A. T. P. C.; Freire, C. S. R.; Ramos, P.; Neves, M. Graça P. M. S.; Faustino, M. A. F.; Almeida, A. "Antimicrobial Photodynamic Therapy as an innovative approach for the inactivation of pathogenic bacteria on fish fillet" (2021) VI PhD Students Meeting in Environment and Agriculture. University of Évora. Évora, Portugal.

Poster communications resulting from collaborative work outside the scope of the thesis:

Pedro, S. N.; Quental, M. V.; Pereira, M. M.; Ferreira, A. M.; Shahriari, S.; Mohamadou, A.; Coutinho, J. A. P.; Freire, M. G. (2018) "Sustainable Separation Plataforms based on Aqueous Biphasic Systems formed by Ionic Liquid and Carbohydrates" 6PYCheM – 6 th Portuguese Young Chemists Meeting, Setúbal, Portugal.

Pedro, S. N.; Quental, M. V.; Pereira, M. M.; Ferreira, A. M.; Shahriari, S.; Mohamadou, A.; Coutinho, J. A. P.; Freire, M. G. (2018) "Ionic liquids and carbohydrates in aqueous media: Novel sustainable separation platforms" 13th International Chemical and Biological Engineering Conference, Aveiro, Portugal.

Vieira, C.; Pedro, S. N.; Mesquita, M. Q.; Gomes, A. T. P. C.; Freire, C. S. R.; Ramos, P.; Neves, M. Graça P. M. S.; Faustino, M. A. F.; Almeida, A. (2021) "Antimicrobial Photodynamic Therapy as an innovative approach to inactivate Escherichia coli on Sea Bass Fillets" 3rd Online International Conference on Aquaculture and Fisheries, Coalesce Research Group.

Other distinctions:

Selected cover of the issue 29 of the journal ACS Sustainable Chemistry & Engineering 2022- Pereira, M. M.; Pedro, S. N.; Quental, M. V.; Mohamadou, A.; Coutinho, J. A. P.; Freire M. G. Integrated Approach to Extract and Purify Proteins from Honey by Ionic Liquid-Based Three-Phase Partitioning (2022) ACS Sustainable Chemistry & Engineering, 10, 29, 9275–9281.

Other activities:

2018-2022 – Biochemistry Day@UA, (member of poster section evaluation panel).

2019-2020 – Co-founding member of PhD Students Council (CAD) of CICECO, Aveiro Institute of Materials, at University of Aveiro.

2020 – 1st AIM Further PhD students meeting event PCI Creative Science Park, Aveiro, Portugal (Member of the Organizing Committee).

2020/2021 – WrtitingLeague@UA- Co-founder of the first group of scientific and creative writing in University of Aveiro.

2020 – Stylish Academic Writing (with participation of the internationally recognized Profª Helen Sword (Member of the Organizing Committee).

List of Tables

List of Figures

Abbreviations

A375	Human malignant melanoma cell line
Alg	Alginate hydrogel
Alg-DES	Alginate hydrogel with the Arg:Gly aqueous solution
Alg-(DES + Ibu)	Alginate hydrogel with the with ibuprofen solubilized in the Arg:Gly aqueous solution
Alg-Ibu	Alginate hydrogel with ibuprofen.
API	Active pharmaceutical ingredients
API-DES	Deep eutectic solvents comprising active pharmaceutical ingredients
aPDT	Antimicrobial photodynamic therapy
Arg:Gly	Arginine:Glycerol
ARPE-19	Human adult retinal pigment epithelial cells
B16F10	Mouse skin cancer cell line
BCS	Biophramaceutical classification system
Bet:gly	Betaine:glycerol
Bet:xyl	Betaine:xylitol
CA:Xyl	Citric acid:xylitol
[Ch]Cl	Cholinium chloride
[Ch]Cl:U:MA	Cholinium chloride:urea:malonic acid
CaOV3	Human ovarian cancer cell line
COX-1	Cyclooxygenase 1
COX-2	Cyclooxygenase 2
CFU	Colony forming units
CLSI	Clinical and Laboratory Standards Institute
DES	Deep eutectic solvents
DMEM	Dulbecco's modified Eagle's medium
DMSO	Dimethyl sulfoxide
EHEC	Ethyl(hydroxyethyl)cellulose
EMLA	Eutectic Mixture of Local Anesthetic

EUCAST	European Committee on Antimicrobial Susceptibility Testing
FBS	Fetal bovine serum
FTIR-ATR	Fourier Transform Infrared with Attenuated Total Reflectance
HaCat	Immortalized human epidermal keratinocytes
HBA	Hydrogen bond acceptors
HBD	Hydrogen bond donors
HelaS3	Human cervical cancer cell line
HPLC-DAD	High-performance liquid chromatography with photodiode-array detection
ILs	Ionic liquids
IFN-α2	Human interferon-α2
LPS	Lipopolysaccharide
MCF-7	Human breast cancer cell line
MIC	Minimum Inhibitory Concentration
MTT	3- (4,5-dimethylthiazol-2-yl)-2,5-diphenyltetrazolium bromide
NMR	Nuclear magnetic resonance
NSAIDs	Nonsteroidal anti-inflammatory drugs
O.D.	Optical density
o/w	Oil/water
PBS	Phosphate buffered saline
PC3	Human prostate cancer cell line
PEG	Poly(ethylene glycol)
PF-127	Pluronic® F-127
PL	Pullulan film
PL-C	Pullulan film with curcumin solubilized in aqueous solution with acetone
PL-DES	Pullulan film with the Bet:Lev aqueous solution

PL-(DES+C)	Pullulan film and with curcumin solution in aqueous Bet:Lev
PPG	Poly(propylene glycol)
Pro:U:MA	Proline:urea:malonic acid
ROS	Reactive oxygen species
$scCO_2$	Supercritical CO_2 sintering
SEM	Scanning electron microscopy
SPCL	Poly-ε-caprolactone
TEM	Transmission electron microscopy
TGA	Thermogravimetric analysis
THPP	5,10,15,20-tetrakis(4-hydroxyphenyl)-porphyrin
TMSP	Trimethylsilyl propanoic acid
TSA	Trypic Soy Agar
TSB	Trypic Soy Broth
w/o	Water/oil
w/o/w	Water-in-oil-in-water

Contextualization and thesis outline

The modern era of pharmaceuticals impacted life quality in ways that were not possible nor even predictable before.[1] Despite the rising number of people affected by different diseases worldwide, the improvement in global health has allowed to extend life expectancy and save an uncountable number of lives. Although the pharmaceutical industry is known for its innovation and research driven character, as well as for its high degree of social and economic responsibility, the overall investments in this area not always reflect more treatment choices for patients or additional effective therapeutics.[2] Thought the pharmaceutical sector holds a 19% share of all business spending on R&D worldwide, the number of new approved pharmaceuticals per billion US dollars spent on R&D has halved every 9 years since 1950.[3] The R&D process has become more knowledge-based, and the costs associated have increased several folds over the same time, being now governed by generic products that control many traditional therapeutic areas.[4]

On average, new pharmaceuticals take about 15 years to reach the market, and in between, most of the time is dedicated to expensive clinical trials.[5] The global COVID-19 pandemic scenario demonstrated that, in some cases, this period can be potentially shortened without significantly impacting the product safety, but more importantly, it shifted the global medical needs.[6] Overall, this atypic situation showed that reimagining R&D in pharmaceuticals demands a change in the drug development and formulation and in the strategies to address the patients' needs. One alternative to reduce the time and costs associated with the development of new drugs is to start from known drugs and improve their formulations.[7] The development of new and more effective formulations of existing drugs should preclude the necessity for extensive preclinical formulation and toxicology studies and, thereby, significantly reduce the development time.[8] It is interesting to note that even though this PhD project began before the pandemic, it already followed this view.

New drug formulations are mainly designed to improve therapeutic efficacy, patient compliance and clinical outcomes.[9] Finding new ways to design or modify a formulation to achieve those goals, might allow existing drugs to stay longer in the market, avoiding patents expiring and enables the release products that can compete with generic options. This might be beneficial to tackle the pharmaceutical

productivity shortfalls in many therapeutic sectors, as well as promising to increase the patients' treatment options and efficacy.

One of the most affected therapeutic sectors has been the antibiotic pipeline.[10] Since the 1960s, the rise in antimicrobial resistance has led to an increasing number of deaths each year motivated by infections, and is estimated to surpass by 2050 the number of deaths caused by cancer if no action is taken.[11,12] Despite this evolving risk and the clear need for more effective antimicrobial agents, discovering and bringing new antibiotics to the market is often too long and hardly profitable for pharmaceutical companies.[13] Therefore, this class of pharmaceutical agents may highly benefit from the development and research of more effective formulations.

Main objectives

Motivated by the high number of pharmaceuticals in the market that present efficacy drawbacks, this PhD thesis focused on the development of new formulations that can simultaneously improve water-solubility, permeation and/or stability of existing drugs, and their incorporation in different drug delivery systems, considering the intended therapeutic target. For this purpose, the solubilization of existing active pharmaceutical ingredients (APIs) in alternative solvents, namely aqueous solutions of deep eutectic solvents (DES), was investigated. The stability of the several APIs in the new solvents was conducted under different time periods, temperature and light conditions and compared to the conventional formulations. Furthermore, the works developed focused on understanding the DES influence in the properties of the final drug delivery systems. For this purpose, different types of drug delivery systems (liquid, semi-solid and solid dosage forms) were prepared, the combination of DES and biopolymers was studied, and distinct administration routes were considered (ocular, topical and transdermal ones). The impact of the DES incorporation in pharmaceutical formulations in the final therapeutic efficacy was evaluated, aiming to expose the benefits of their use. Overall, the results obtained are highly promising, further encouraging the expansion of knowledge in this field towards the development of more efficient therapeutics.

4

Thesis outline

The current PhD thesis is organized in 6 chapters. For a better understanding of the thesis organization, a graphical layout is portrayed in Figure 0.
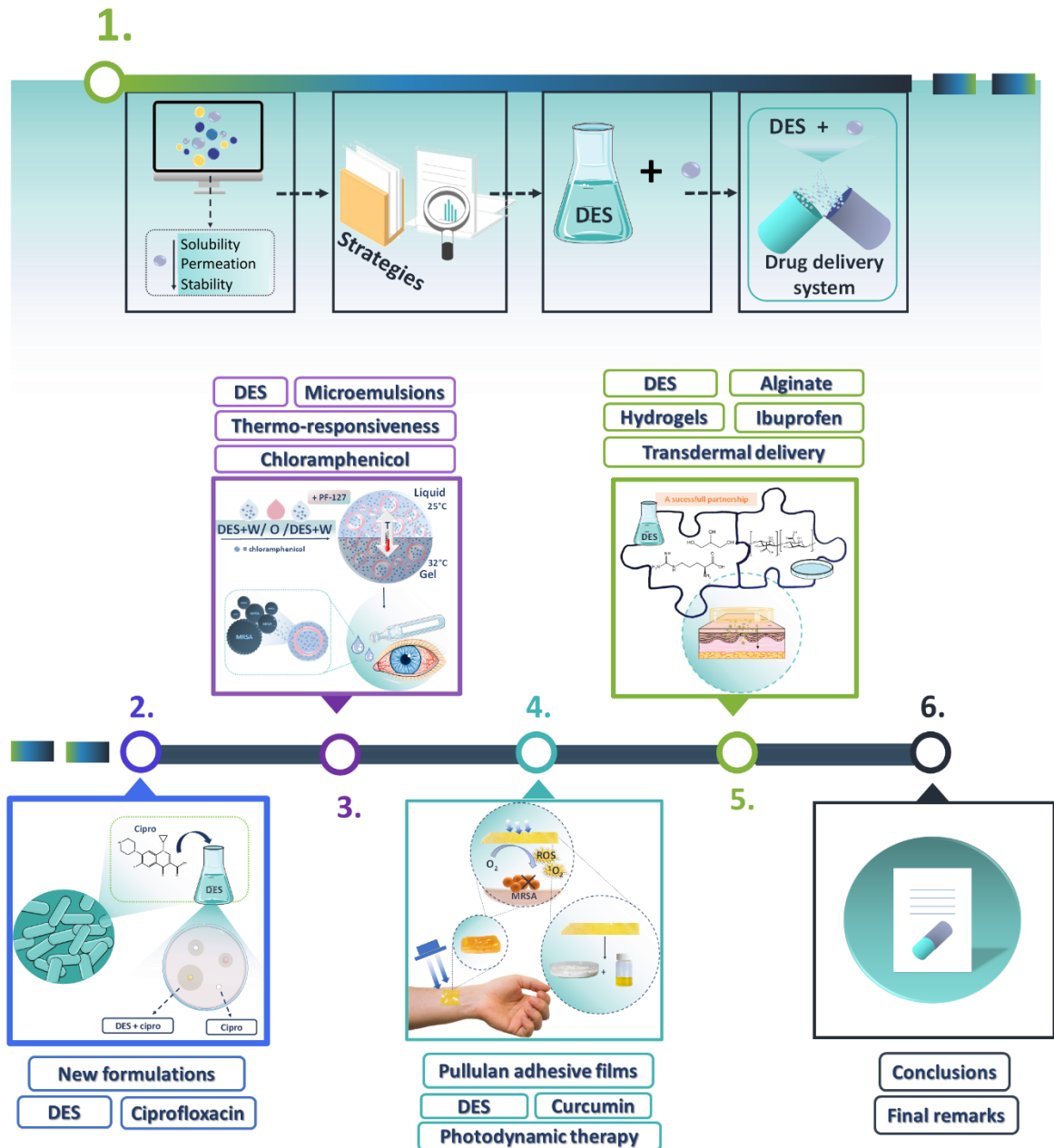
Figure 0. Visual overview of the PhD thesis structure: from the literature survey provided in chapter 1. Introduction to the application of DES in drug formulation, development and delivery systems and future perspectives (chapters 2-6).

Chapter 1 provides a contextualization of the main concepts and topics addressed during the thesis, creating a guideline of the rational thinking behind all developed studies (Figure 0). A literature overview of the path to the development of innovative and more effective drug formulations is first introduced, highlighting how drug's characteristics impact their formulation, performance and therapeutic efficacy. Following these challenges, a summary of the methodologies commonly applied to tackle these limitations is presented. Then, the emerging use of DES and their applications in the pharmaceutical field is emphasized as a new strategy to be considered. Finally, the main features of biopolymers and the applications of DES in the development of polymeric drug delivery systems are appraised.

This chapter was adapted from the published manuscripts/Book chapters: Pedro, S. N.; Freire, M. G.; Freire, C. S. R.; Silvestre, A. J. D. Deep eutectic solvents comprising active pharmaceutical ingredients in the development of drug delivery systems (2019) Expert Opinion on drug delivery, 16 (5), 497-506.

Pedro, S. N.; Freire, C. S. R.; Silvestre, A. J. D.; Freire, M. G. Deep Eutectic Solvents and Pharmaceuticals (2021) Encyclopedia, 1(3), 942-963.

Pedro, S. N.; Freire, C. S. R.; Silvestre, A. J. D.; Freire, M. G. Chapter 7- Advances brought by ionic liquids in the development of polymer-based drug delivery systems, In: Application of Ionic Liquids in Drug Delivery (2021) Springer, 113-135.

Chapters 2 to 5 present the main experiment results of this thesis. They provide a detailed perspective on the path to design and develop delivery systems with DES formulations, from simple aqueous solutions to biopolymer-based materials.

Chapter 2 focuses on the design of aqueous DES formulations containing the antibiotic ciprofloxacin, showing improved drug solubility, stability and therapeutic efficacy. The rational selection of the DES components was explored as well as their concentration in the final formulation, allowing successful enhancements of the solubility, stability and antimicrobial action of the antibiotic, without cytotoxicity associated.

This chapter has been adapted from the published manuscript: Pedro, S. N.; Gomes, A. T. P. C.; Oskoei, P.; Oliveira, H.; Almeida, A.; Freire, M.G.; Silvestre, A.

J. D.; Freire, C. S. R. Boosting Antibiotics Performance by New Formulations with Deep Eutectic Solvents (2022) International Journal of Pharmaceutics, 616, 121566.

Chapter 3 is dedicated to the incorporation of aqueous DES formulations comprising the antibiotic chloramphenicol in liquid drug delivery systems. Aqueous solutions of DES were used in the preparation of water-in-oil-in-water thermo-responsive microemulsions. This work emphases the beneficial and multifunctional role of DES and how they allow the improvement of the solubility, stability, permeation and therapeutic action of the drug, avoiding the use of multiple excipients in the final delivery system.

This chapter has been adapted from the published manuscript: Pedro, S. N.; Gomes, A. T. P. C.; Vilela, C.; Vitorino, C.; Fernandes, R.; Almeida A.; Amaral, M. H.; M. G. Freire; Silvestre, A. J. D.; Freire, C. S. R. Thermo-responsive microemulsions containing deep eutectic-based antibiotic formulations for improved treatment of resistant bacterial ocular infections (2023) Advanced Therapeutics, 2200235.

In **Chapter 4**, the incorporation of aqueous DES formulations containing curcumin (a natural photosensitizer) in biopolymer-based systems, namely pullulan-based adhesive films for application in antimicrobial photodynamic therapy, is presented. The DES formulations enhanced the photostability and antimicrobial action of curcumin, and their incorporation in the pullulan films improved their properties, namely the adhesiveness and mechanical performance. The *ex vivo* eradication of multi-resistant bacteria from skin samples was successfully demonstrated. Moreover, the beneficial use of DES in the development of drug delivery systems is shown and compared with the usage of common organic solvents.

This chapter has been adapted from the following submitted manuscript: Pedro, S. N.; Valente, B. F.; Vilela, C.; Oliveira, H.; Almeida, A.; Freire, M.G.; Silvestre, A. J. D.; Freire, C. S. R. Photodynamical Switchable Adhesive Pullulan Films Loaded with a Deep Eutectic Solvent Formulation Containing Curcumin to Treat Multi-Resistant Skin Infections (2023) Materials Today Bio, 22, 100733.

Finally, in **Chapter 5**, aqueous DES formulations are considered to overcome the solubility and the permeation drawbacks of other types of drugs, such as non-steroidal anti-inflammatory ones, namely ibuprofen. These formulations were combined with alginate to produce new hydrogel-based systems, with improved mechanical properties, capable of preserving the therapeutic efficacy of the drug while improving its transdermal administration. This study also aimed to demonstrate that the use of DES might allow the administration of pharmaceuticals by alternative routes of administration.

This chapter has been adapted from the published manuscript: Pedro, S. N.; Mendes, M. S. M.; Neves, B. M.; Almeida I. F.; Costa, P.; Correia-Sá, I.; Vilela, C.; Freire, M. G.; Silvestre, A. J. D.; Freire, C. S. R. Deep Eutectic Solvent Formulations and Alginate-Based Hydrogels as a New Partnership for the Transdermal Administration of Anti-Inflammatory Drugs (2022) Pharmaceutics, 14 (4), 827.

In **Chapter 6**, the final remarks of this thesis are provided, along with an overview of the future trends to be considered in this field. Finally, proposals of future work that emerged from the presented studies are mentioned, aiming to open the door for future research in this area and to the pharmaceutical approval of these systems in the future.

Chapter 1. Introduction

Research in the pharmaceutical industry remains circled with difficulties, for most of which no obvious solutions seem to emerge. Several strategies have become available attempting to surpass the different drawbacks, where drug reformulation is seen as an advantageous alternative since many initial screening tests may be avoided.[9]

Most pharmaceutical drug candidates pass through a long process, as illustrated in Figure 1 where they are initially screened by high-throughput techniques capable to run >100 000 compounds per day.[14] This drug discovery process is designed to identify only substances that exhibit specific biological activities, and usually a refinement step is needed to reduce the results to one or two candidates for further investigation. The pre-clinical stage comprehends the drug manufacture, the pre-formulation and formulation study, and design and evaluation of the drug through analytical and bioanalytical methods, pharmacokinetics and toxicological studies.[15] These intend to provide full documentation of the drug product to be used in clinical trials. These trials present several phases and require tests in many subjects to guarantee the product's safety and efficacy, until it reaches final approval.

The pharmaceutical industry might spend billions of dollars in this time-consuming process, which might face an extremely high overall rate of failure, which even in a final stage can be higher than 90%.[5] Despite all the careful planning of the process, problems such as drug poor solubility, undesirable side effects, poor biodistribution by the proposed clinical route of administration and poor efficacy in clinical trials are problems usually encountered.[15] Therefore, pharmaceutical companies need cost-effective and reduced-risk alternatives to develop drug products.[16] In this context, developing a new and more effective formulation of a marketed drug can be considered an appealing strategy for pharmaceutical companies. Drug reformulation can comprehend changes in active ingredient concentrations, in pharmaceutical excipients,[17] changes in the means of drug delivery or a combination of them.[18] This way, it is possible to cut the initial screening mentioned above, excluding several years of development. Also, when dealing with already approved drugs, the data used for the original approval can often be used

to support the new formulation.[19] In this sense, reformulation can also signify a shortcut to pass some regulatory obstacles.
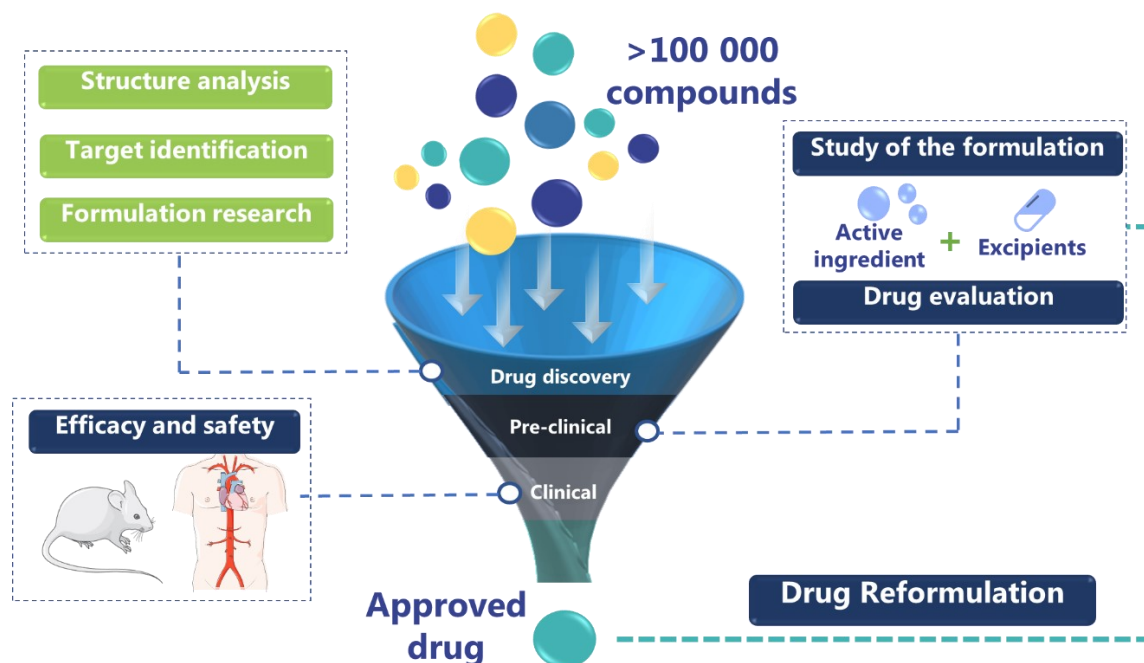
Figure 1. Schematic illustration of the several stages of drug research, development and reformulation. Images of the Efficacy and safety section made with Servier Medical Art and adapted by the authors according with Servier under the CC-BY 3.0 License (at https://smart.servier.com/, accessed on 10 September 2022).

Even though reformulation presents less waste production, for the reason that some experiments are avoided, it can still contribute to the high environmental impact of the pharmaceutical industry.[20] This industry, known for its global health and environmental impact, is still one of the largest users of organic solvents per amount of the final product (E factor ranging from 25 to greater than 100), and relies mainly on synthetic non-biodegradable and petroleum-based compounds.[21] Pharmaceutical companies need to apply more sustainable practices in their research and pipeline. This change might also be beneficial from an economic point of view.[20,22] The adoption of sustainable practices, can consider, for example, the use of alternative solvents with low cytotoxicity to solubilize a given drug and integrate the final formulation, excluding steps of recovery and reuse.[23–25] Furthermore, the thriving exploration of excipients from natural and renewable sources, such as natural polymers, might help to meet these goals.[26] Therefore, the search for options that can fit into a more "green chemistry" approach needs to

captivate the pharmaceutical industry to shift into novel and more sustainable strategies, offering clear advantages that, among other solutions, can address the problems associated with the pharmaceuticals performance.

Notwithstanding, new strategies to be applied in drug reformulation must aim, above all, at the improvement of the drug therapeutic efficacy.[27] Particularly, characteristics such as stability (both in aqueous media and in solid state), water solubility (or other relevant solvents) and permeation ability must be scrutinized.[28] Based on the exposed, the following subchapters will address each one of these issues and their impact in formulation development and excipient selection, and their influence in the drug efficacy.

1.1 Challenges faced by active pharmaceutical ingredients

It might seem surprising, but there is not a straightforward answer to the question: what is a pharmaceutical? Active pharmaceutical ingredients (APIs) cannot be treated as a class of substances since they do not all share the same chemical, physical, structural or biological similarities.[16] The main relation between all these compounds is their application. Therefore, any chemical substance capable of modifying biological functions in the organism, resulting in functional or somatic changes that can be applied with beneficial effects to treat a specific health condition, can integrate this group of compounds. [29]

Every dosage form is a combination of an API and the non-active components, the so termed excipients/additives.[30] These can be used to give to the dosage form a particular shape, to improve solubility, stability and/or permeation, to mask a bitter taste, to allow for a proper dosage delivery or control the drug release profile and, ultimately, to enhance the drug's bioavailability while improving safety.[31] For drug molecules to reach quickly their therapeutic goal and minimize the side-effects along their path, they must be freely soluble in biological fluids.[32] Thus, the pharmaceuticals' stability, solubility and permeation are fundamental factors to achieve successful treatments and dictate the strategy to be selected for the formulation process.

1.1.1 The stability of active pharmaceutical ingredients

Instability issues in a drug formulation result in a reduction of efficacy or, more seriously, in the formation of toxic degradation products.[33] Testing drug stability usually follows specific guidelines[34] that focus on the duration and frequency of testing, number of samples and replicates per time interval, storage conditions (duration of storage, type of storage, temperatures and packaging) and analysis methods (from which high-performance liquid chromatography is predominantly used). Such variables are intended to cover the detection of degradation products resulting from physical or chemical degradation of the formulations. Degradation studies also usually cover stress factors (pH, temperature and light) that impact the drug during manufacturing, handling and storage.[35]

The most studied drug degradation process is the hydrolytic degradation, since water is commonly used in isolation or formulation strategies.[36,37] Usually water acts as nucleophile attacking organic bonds in the drug (e.g.: lactam, ester, amide, etc.) via neutral, acid- or base-catalyzed conditions.[36,37] Therefore, in drug formulation one must prove that a given drug is stable under the different pH conditions found under storage and at the local of administration. Several options can be considered to avoid drug hydrolysis in a formulation, depending on the type of drug and formulation.[38] For example, if the dosage form is a liquid, then pH adjustment can improve the shelf life. When considering the hydrolysis of hydrophobic drugs, the selection of surfactant-based systems (such as micelles) can be an alternative to protect the drug from the aqueous environment and reduce degradation.[38]

The rate and extension of the chemical degradation of drugs is impacted by several factors, in addition to the pH, temperature is highly relevant.[39] Therefore, storage temperature conditions of the final formulation are normally adjusted to ensure the product stability and safety.[40] To understand the mechanisms of thermal decomposition, initially stability tests in accelerated conditions are performed, in which high temperatures (40–80 °C) are applied for short periods of time.[41] The drug degradation tests both in solid-state and in solution form intend to identify degradation products that might allow to predict the real behavior under long-term storage conditions.[35]

14

Likewise photo-instability might also be responsible for efficacy loss, uncertain efficacy, and adverse side effects.[42] Many photosensitive drugs find their concentration to be abruptly decreased when stored or handled under light exposure.[43] Usually, packing the drug formulations with appropriate protective packaging solves the photodegradation problematics;[44] however, some drugs present such a fast photodegradation rate and instability, even in solid forms that numerous methods of photo-stabilization must be applied in early formulation (e.g.: light absorbers,[45] inclusion in cyclodextrins[46] or encapsulation[47]). Overall, the strategies defined to improve drug stability might also result on the enhancement of other drug characteristics, such as solubility, fundamental for successful drug performance, which will be discussed in the following subchapter.

1.1.2 Solubility of active pharmaceutical ingredients

Solubility is one of the main characteristics to be evaluated in the development of a drug formulation.[48] It is particularly relevant since it might impact on reaching the desired systemic concentration and obtaining an optimal therapeutic response. However, marketed drugs and under development present low water-solubility, which might implicate the therapeutic efficacy and therefore fail in later stages of development.[49] This means a burden shifted to the patient who has more side-effects due to the higher doses administrated than the ones needed.[50,51] In general, determining the solubility of a compound in biorelevant media, its dissolution rate and its permeability across biological membranes is essential to determine the rate and extent of drug absorption.[32,52] Dissolution rates for weakly acidic and basic drugs can be improved by administering a salt form, normally with higher solubility compared to the non-salt one.[53] However, due to the complexity of the human physiology (as for instance changes in the pH environment and temperature) the *in vivo* solubility of a drug can be different than that tested in different media. Physiologically adapted media and buffers have been increasingly applied with the purpose to better predict the *in vivo* solubility of drugs.

Based on the drug solubility and permeability, formulation developers might also consider the Biopharmaceutical Classification System (BCS) as a tool.[54] This system can be helpful to predict the potential effect of formulations and physiological

variables on the drug bioavailability. Drugs can be classified into four BCS categories, from class I (very well absorbed) to class IV (very poor bioavailability), as depicted in Figure 2. For the BSC application, a drug can be classified as "highly soluble" when the highest clinical dose strength is soluble in 250 mL (or less) of aqueous media over a pH between 1 to 7.5 at 37 °C.[55] More than the intrinsic solubility of the molecule, the solubility criterion in this system considers the physiological conditions and the corresponding targeted therapeutic dose. Many drugs are classified as BCS Class II, which denote good permeability but low aqueous solubility, which is, the most common drawback encountered.[56] Drugs from each class demand different approaches for solubility enhancement, and, usually, advancing in the system classification (from I to IV) generally means less chances of developing an oral dosage form.[57]
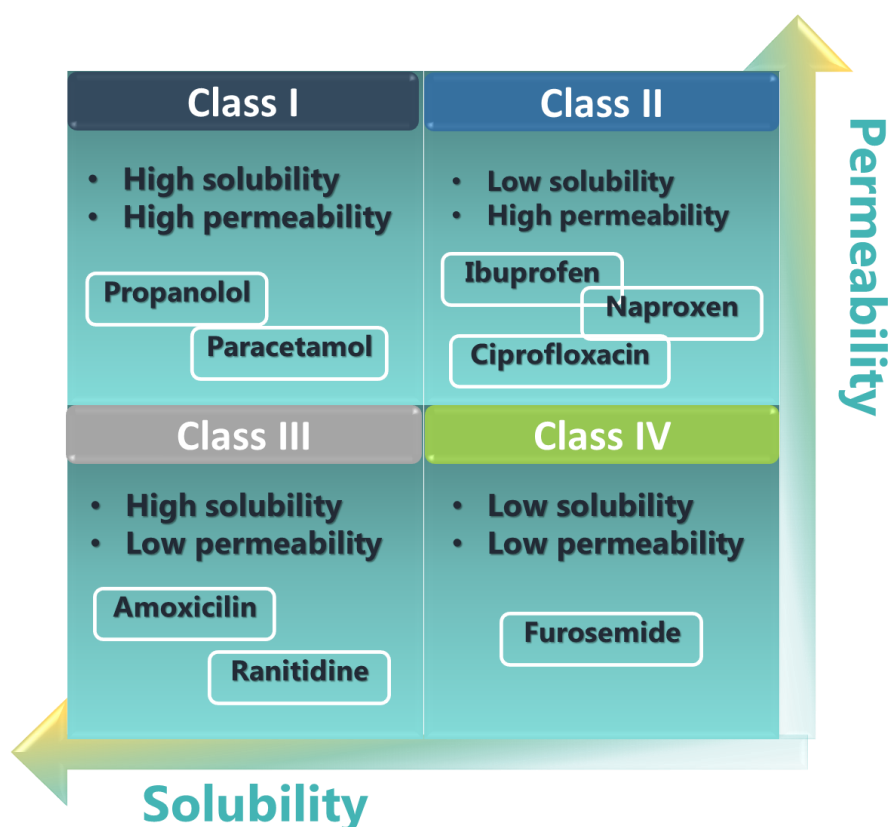
Figure 2. Biopharmaceutical Classification System (BCS) and examples of drugs from each class (adapted from [54]).

1.1.3 The permeation of active pharmaceutical ingredients across biological membranes

In early stages of drug development and pre-formulation, lipophilicity is another property that must be considered, since it may help to predict the transport of drug molecules across biological membranes.[58] Whereas lipophilic molecules are mostly transported through partition, hydrophilic ones need a specific transport mechanism.[59] Thus, most drugs have to cross the alternating lipids and aqueous domains by partitioning into the lipid bilayer and diffusing to the inner side. In this sense, lipophilicity intends to designate the affinity of a compound to be in a lipid-like environment, which increases the potency and the duration of the drug action.[60] Thus, a balance between lipophilicity and hydrophilicity is desired to avoid not only problems of solubility and permeation, but also due to its impact in pharmacokinetic, pharmacodynamic and toxicological profile.[61]

Based on this notion, lipophilicity can be satisfactorily associated with drug permeability. This relationship might be predictive and imply, for example, that lower drug lipophilicity can mean lower permeability across biological membranes.[62] According to the BSC, drug substances are classified as "highly permeable" when an administered dose presents an absorption extension in humans of more than 90%, determined based on a mass balance or in comparison to an intravenous reference dose.[54] In addition to the drug permeation in the gastrointestinal media, transdermal[63] and ocular[64] routes might be appealing alternatives of administration that present clear advantages (avoiding systemic side-effects), high patient compliance, and which depend mostly on the permeation ability.

In the case of transdermal delivery, so far, only less than 20 drugs have been fully approved.[67] The restricted number of available drugs that fit the requirements for transdermal administration reflects the struggle of the dual compromise between a potent pharmacological activity and the right physicochemical properties. If a drug molecule has low molecular weight (<500 Da), is lipophilic (LogP <5) and presents a significant solubility in both aqueous and lipidic media, formulations for skin application can be considered.[65] After the administration of these formulations, the drug can permeate the skin tissue through the *stratum corneum* or adnexal orifices (i.e., hair follicles, sweat and sebaceous glands).[65] For a better understanding of the

skin outer layers that form this protective barrier, a schematic illustration is provided in Figure 3.
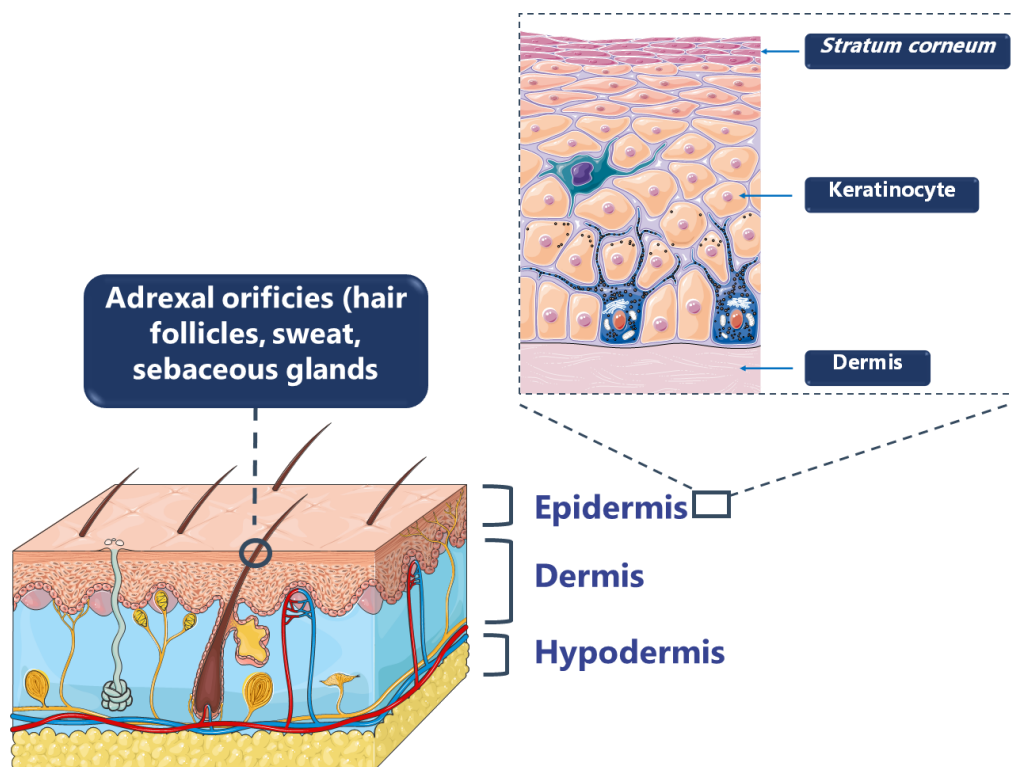
Figure 3. Schematic illustration of the skin layers and epidermal differentiation that contributes to the skin permeability barrier. Skin image made with Servier Medical Art and adapted by the authors according with Servier under the CC-BY 3.0 License (at https://smart.servier.com/, accessed on 10 September 2022).

When considering permeation through ocular barriers, drugs formulated in eye drops account for 90% of the marketed formulations, due to their easiness in administration and patient compliance.[66] However, these formulations present a low ocular associated bioavailability. The tear turnover, nasolacrimal drainage, reflex blinking, and ocular barriers (illustrated in Figure 4) represent a challenge to a more efficient drug permeation. Drug administration by this route usually comprehends ~35–56 µL of the formulation applied into the eye, which in healthy conditions presents a turnover rate of 0.5–2.2 µL·min^{-1}.[67] Since the tear volume is only of ~7–9 µL, the excess volume is drained by the nasolacrimal duct or reflex blinking. All these difficulties result in a drug loss of ~95% after administration. The remaining amount will permeate trough the corneal epithelial barrier, which might involve the effect of the thigh junctions, the nature of the epithelium and drug efflux pumps.[68]

18

For this reason, only a small amount of the topically applied dose reaches deeper ocular tissues. These obstacles prevent reaching the therapeutic drug concentration into posterior segment ocular tissues.

To overcome the ocular barriers and enhance the ocular permeation and, thereby, bioavailability, several strategies, such as the use of ointments,[69] nanoparticles,[70] contact lenses[71] among others, have been explored. However, there is still not an ideal system for this purpose.
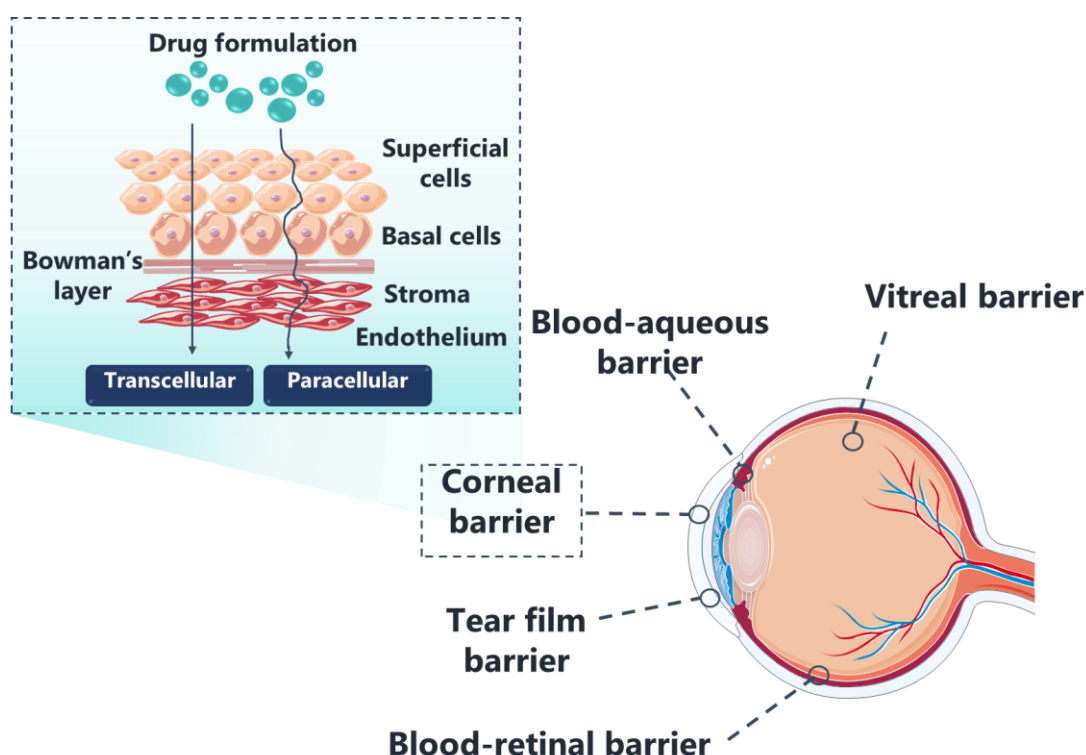
Figure 4. Physiological barriers on ophthalmic drug administration. Image made with Servier Medical Art and adapted by the authors according with Servier under the CC-BY 3.0 License (at https://smart.servier.com/, accessed on 10 September 2022).

The knowledge and understanding of all these downsides about drug design and development must instigate the selection of the proper strategies, capable to tackle these drawbacks, and allow to improve drugs characteristics by new means, while ensuring effectiveness and safety of the final drug formulation.

1.2 Approaches to enhance the solubility and permeation of active pharmaceutical ingredients

Numerous techniques have been developed over the past years to improve drugs' solubility and permeation.[49,72] Selecting the optimal method must take into consideration the properties of the drugs, the route of administration, the absorption site, the dose to be administered and the stability of the drug.

Among the existing methods for drug solubilization, the use of co-solvents, hydrotropes and eutectic mixtures should be particularly highlighted due to the relevant solubility enhancements in water achieved for hydrophobic drugs.[73,74] Despite these strategies are all used to improve the drugs' water solubility, they display different features and mechanisms of solubilization. Therefore, they deserve more intensive research for their comprehension and application. On the other hand, methodologies used to improve the permeation of drugs might comprehend the use of permeation enhancers and different drug delivery strategies (microemulsions, liposomes, etc.).[75]

Although several reviews highlight the application of many strategies to improve drugs' performance and discuss the multiple advances made in this field, some methods demand special attention to be drawn as the ones herein explored.[49,75,76]

1.2.1 Strategies to enhance the aqueous solubility of active pharmaceutical ingredients

Co-solvents can be defined as water-miscible solvents that can be used in liquid drug formulations to enhance the solubility of poorly water-soluble drugs and, in some cases, also their chemical stability.[77] Although a comprehensive image is still missing, co-solvents have been hypothesized to act in active pharmaceutical ingredients solubilization in water due to the reduction of the interfacial tension between the aqueous solvent and the hydrophobic solute.[78] In aqueous formulations, co-solvents such as ethanol,[79] glycerol,[80] propylene glycol[80] and polyethylene glycols[81] have been mostly used in the pharmaceutical context.

Hydrotropes, on the other hand, work mainly by an aggregation behavior.[82] Abranches *et al.*[83] have shown that the driving force for this mechanism is mainly

dictated by the apolarity of the hydrotrope and the solute. Both seem to display strong interactions in the presence of water, established between their hydrophobic moieties. If the hydrophobicity of the hydrotrope and solute are similar, the hydrotrope aggregation around the solute is maximum (Figure 5). This happens because the hydrophobic moieties of both molecules interact weakly with water, being more driven out to associate between them and agglomerate. The classification of hydrotropes solely based on their molecular structure is difficult, since a wide variety of compounds have been shown to present a hydrotropic behavior. The most common examples are ethanol, catechol, salicylates, alkaloids, like caffeine and nicotine, and latterly ionic liquids (ILs).
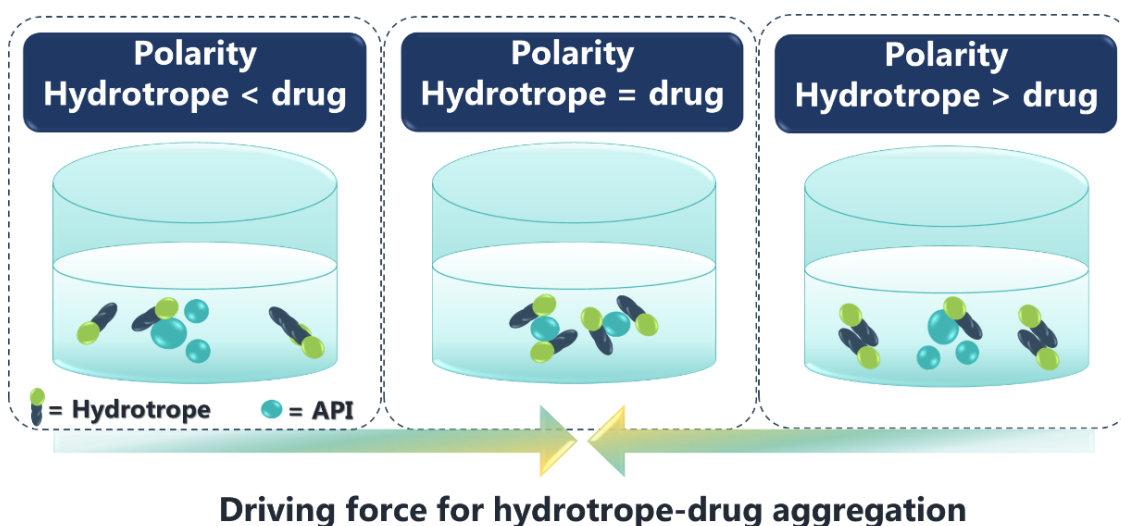
Figure 5. Mechanism of hydrotropy (adapted from Abrances *et.al* [83]).

Another strategy to improve the solubility of a given drug is the use of eutectic mixtures.[49] These mixtures result from the combination of two or more components that do not interact through covalent bonding, resulting in a mixture with a lower melting temperature than the pristine components.[49] Eutectic mixtures comprising APIs date back to the 60s, when Sekiguchi[84] studied the absorption differences between sulfathiazole and its eutectic mixture with urea. This was the first study showing the higher absorption and excretion of a drug when orally administrated in the form of a eutectic mixture. After this pioneering work, the exploitation of this strategy has been increasingly observed in the pharmaceutical context.[85,86]

1.2.2 Permeation enhancers

Permeation enhancers can exert their effect by direct action on the membrane barrier (ex.: skin or ocular membranes) or by indirect effects on the formulation, such as by improving the drug solubility in the final system.[87] In this sense, in the case of skin permeation, some permeation enhancers might act directly on the lipids, disrupting their highly ordered structure on the *stratum corneum*, as for the use of fatty acids and terpenes.[88] On the other hand, permeation enhancers, such as ethanol, might also act by extracting lipids from the *stratum corneum*.[89] Additionally, these compounds can improve the solubility and the partitioning of the drug from the formulation into the *stratum corneum*, as it happens with the incorporation of surfactants in formulations.[90] This class of enhancers can comprehend a wide variety of compounds with different functional groups, including low molecular weight solvents, amphiphiles and even peptides. Figure 6 provides a summary of the impact of permeation enhancers on the lipidic barrier, aiming a better understanding of their effect on drug's efficacy.
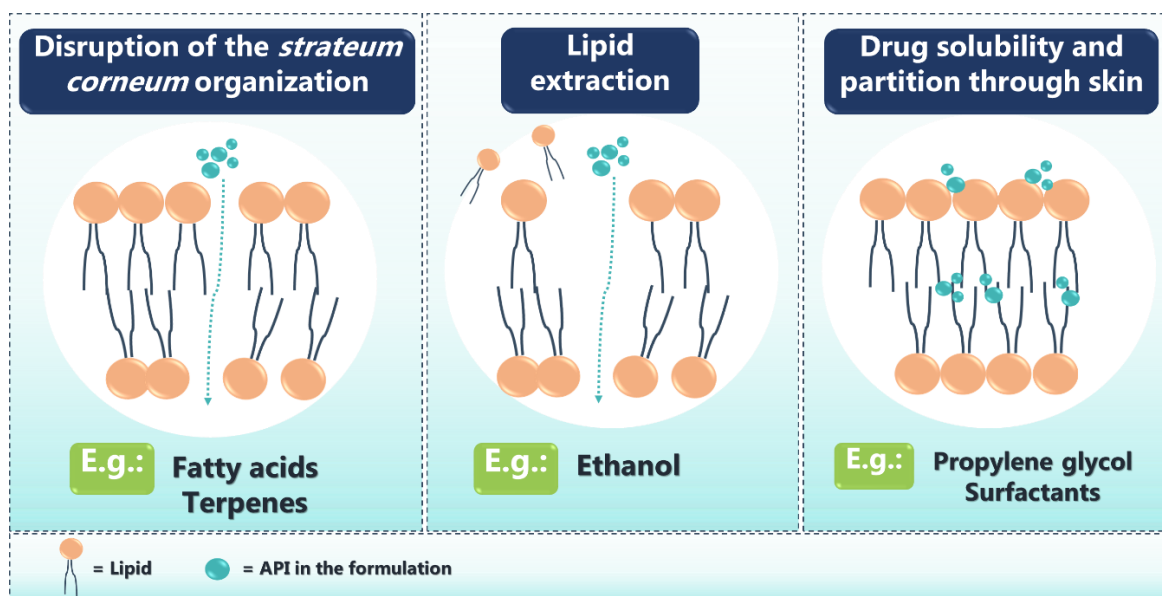
Figure 6. Effect of permeation enhancers on the lipidic bilayer of biological membranes.

When considering the action of permeation enhancers on other membranes, such as the ocular one, they must target the modification of the tear film and mucous layer;[91] the modification of the membrane components (lipid bilayers of epithelial cells);[92] and the loosening of the epithelial tight junctions.[91] Compounds such as

cyclodextrins,[93] chelating agents,[94] cell-penetrating peptides[95] and amphiphilic compounds[96] have been also applied in this context. Among these, cyclodextrins are commonly found excipients in marketed ophthalmic formulations.[93] In addition to the permeability enhancement, these compounds can act also as solubility enhancers in the final formulation. Due to the multiple roles of many permeation enhancers, and their versatility of application, they enable the development of suspensions, creams, gels or patches,[97] contributing to their wide acceptance since the drug administration is simple and non-invasive.

Eutectic mixtures can also be applied to improve drug permeation, while presenting an easy preparation and higher stability than the crystalline form of the drug, which makes them more appealing in this area in comparison to amorphous materials. Patents and commercialized drugs with eutectic mixtures are mostly dedicated to the delivery of drugs by dermal administration.[98] One of the oldest patented and marketed eutectic mixture is the anesthetic cream EMLA® (Eutectic Mixture of Local Anaesthetic), with a melting temperature of 16 °C used in transdermal applications.[99] This system composed of prilocaine (melting temperature of 38 °C) and lidocaine (melting temperature of 68 °C) represents a landmark in drugs' solubilization and permeation enhancement strategies, being widely used worldwide. However, EMLA®'s adverse side effects, mainly associated to prilocaine, led to the creation of other dual function eutectic mixtures, namely lidocaine:procaine and lidocaine:tetracaine.[100] The lidocaine:tetracaine mixture is also liquid at room temperature, presenting a melting temperature (ca. 18 °C) similar to that of EMLA® . The facilitation of the transdermal drug delivery brought by EMLA® and the possibility to include this eutectic mixture in different drug delivery systems, motivated a broad spectrum of studies in this field, expanding their application.[101,102] Given the progress in the development and application of eutectic mixtures throughout recent years, and more recently, deep eutectic solvents (DES) have emerged as an advantageous alternative when considering the drug incorporation, which will be discussed in the following section.

1.3 Deep eutectic solvents (DES) in the pharmaceutical field

Within eutectic mixtures, DES stand out for their strong deviations from the ideal solid–liquid phase behavior (Figure 7).[103] DES were first presented by Abbott *et al.*[104], in 2003, to describe mixtures of amides with quaternary ammonium salts, with melting temperatures far below those of their pure components. The negative deviations from the ideal solid-liquid phase behavior can be of such extent that they melt far below room or the human body's temperatures.[104,105] Moreover, these solvents can be considered designer solvents since they can be prepared from a wide variety of combinations of hydrogen bond donors (HBDs) with hydrogen bond acceptors (HBAs).[23,106]
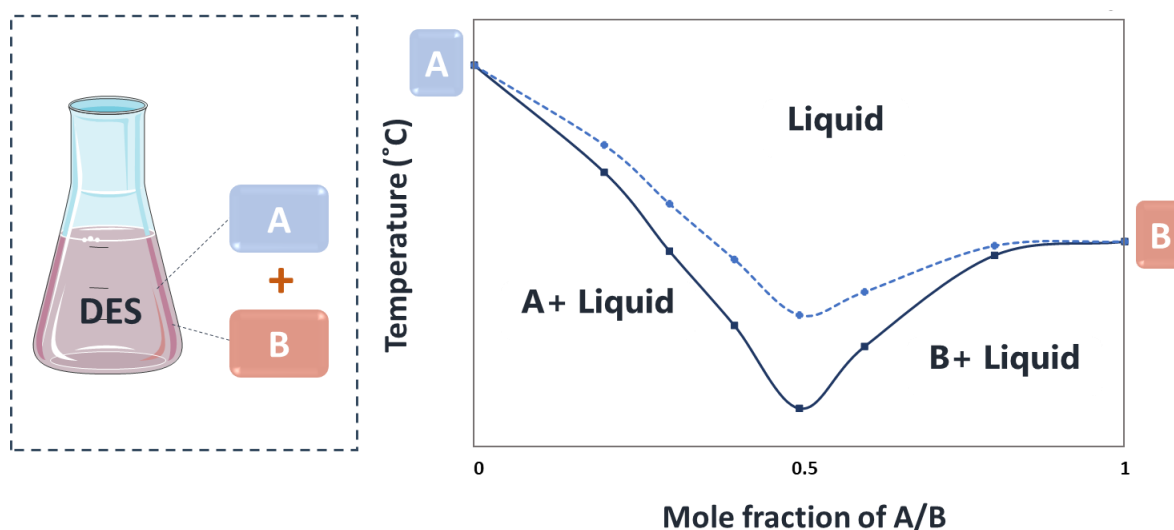
Figure 7. Solid-liquid phase diagram of a hypothetical DES (continuous line) and its comparison with the ideal solid-liquid phase behavior (dashed line): The formation of hydrogen bonds between the two components (A and B) is represented.

The DES characteristics and toxicity can be tuned according to the compounds' selection. Therefore, among the existing possibilities, there is a panoply of biobased compounds available, for which the combination of quaternary ammonium derivatives, such as cholinium chloride ([Ch]Cl), betaine, proline, alanine, among others, with other metabolites or permeation enhancers can be highlighted, as portrayed in Figure 8.[107] The resultant mixtures can be either hydrophilic or hydrophobic, enabling the "phobic" behavior to be tunable for specific applications.[108,109] Ultimately, DES can be designed with a specific biological activity envisioning the production of formulations that can be applied to solubilize drugs

and integrate drug delivery systems with a specific role.[110] In this case, the component selection must focus on the application and consider the intended route of administration.
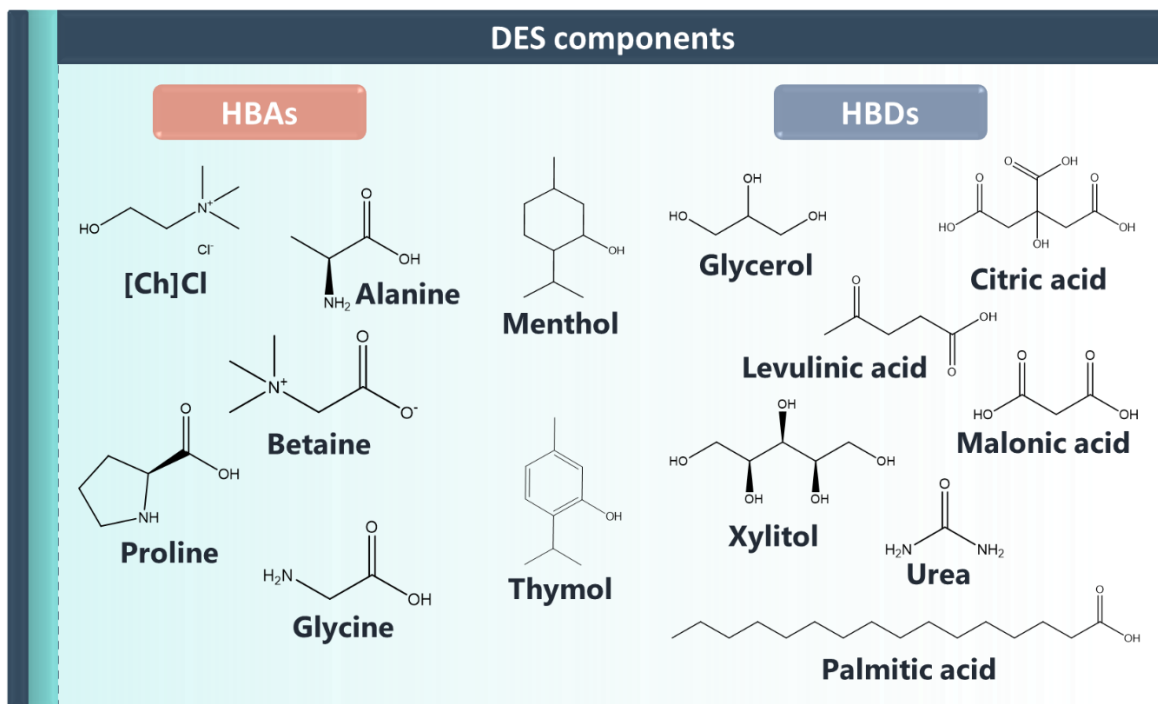
Figure 8. Examples of chemical structures of HBAs and HBDs commonly used in the preparation of DES.

DES can also be designed to enhance APIs' solubility while avoiding drug polymorphism.[111] This can be achieved by the conversion of the API into its liquid form, i.e., through the formation of deep eutectic solvents comprising the target active pharmaceutical ingredient (API-DES), also addressed in literature as therapeutic deep eutectic solvents (THEDES).[108,111] These drug liquid forms can be obtained by the combination of APIs with a wide variety of compounds, namely metabolites or permeation enhancers, but also by the selection of two different APIs, resulting in dual function liquid forms (Figure 9).[111–113] Some DES can also present a polymerizable character when comprising APIs combined with compounds with polymerizable moieties, further allowing the tuning of their delivery profile.[114] Despite all the possible combinations, and the fact that APIs can act as both HBAs and HBDs, most of the API-DES reported up to date are prepared using the API as the HBD species.[115–117]
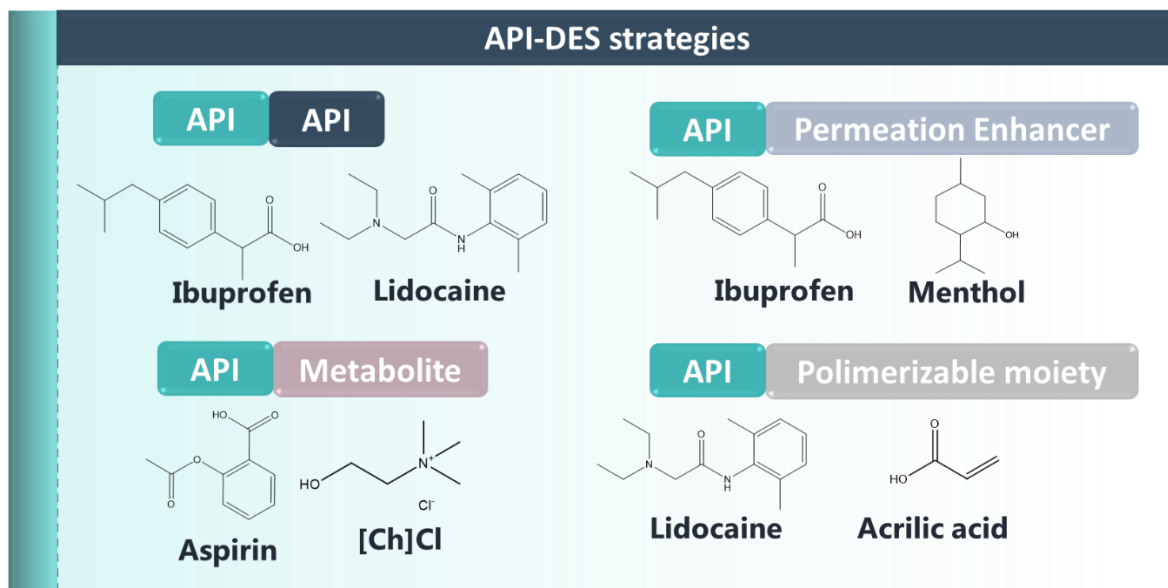
Figure 9. Possible API–DES strategies according with the individual starting components selection.

Among the existing DES preparation methods, freeze-drying, vacuum evaporation, grinding, microwave, ultrasound irradiation and, the most employed, the heating and stirring of the mixture of the HBA and the HBD, are some examples.[118] The latter method usually comprehends the combination of both DES components, in a specific molar ratio, under constant heat and stirring, until a uniform colorless liquid is obtained.[23] Since no chemical reaction is involved it presents 100% of the atom economy, fitting within one of the "green chemistry" principles.[105] Thus, if no degradation occurs, the purity of the DES is only dependent on the purity of the individual starting components.

The properties of DES can be defined by their composition and molar ratio.[114] Thus, DES might present different physicochemical properties, such as density, viscosity, ionic conductivity or polarity, and interesting characteristics, including non-flammability, non-volatility, thermal stability and biodegradability. One example the influence of the composition and molar ratio on the resultant properties of DES is their impact in viscosity, which is most often higher than the water viscosity (>1 mPa.s).[119][120] While [Ch]Cl:urea displays a viscosity of 750 mPa.s, other DES, such as sugar-based ones like [Ch]Cl:glucose, can achieve as much as 34400 mPa.s at room temperature. To fit into a specific application and reduce the mixture viscosity, this can be tuned by the addition of water or polyols such as glycerol.[121]

26

The preparation of aqueous solutions of DES allows not only the manipulation of the viscosity of the mixture but also an increase in the solvation ability in comparison to the neat DES. [82] Although water is the most desirable solvent for pharmaceuticals, since the vast majority presents low-water solubility, organic solvents are generally employed, such as alcohols, acetone or dimethyl sulfoxide (DMSO).[122] On the other hand, DES can be designed to present non-toxic character and to be used in aqueous solutions to fit the drug delivery system's needs. The solubilization of pharmaceuticals and even biopolymers[108,123,124] in DES aqueous solutions might result in systems with different properties to those obtained with the direct dissolution of the DES' components separately in water.[125] Both the DES solution and the components in water have a distinct impact in the resultant properties of the biopolymer-based system, being a clear advantage in this case the solubilization of the DES in water, since better mechanical properties can be achieved. Due to the advantages of the use of neat DES and their aqueous solutions in the pharmaceutical context, they have been applied in several steps of drug formulation and drug delivery development.

1.3.1 DES to improve the solubility of active pharmaceutical ingredients

DES can be ideally designed to solubilize selected APIs and integrate the drug delivery system without affecting the cytotoxicity of the pharmaceutical formulation.[126] These mixtures have been widely studied in the solubilization of anti-inflammatory,[110] antipyretic,[127] analgesic and antimicrobial drugs[128–130] as well as for the solubilization of nutraceuticals.[131,132] Promising results on the solubilization of these drugs have been reported using different DES, as summarized in Table 1. It has been shown that the solubility enhancements achieved by DES can greatly surpass those obtained with conventional co-solvents, hydrotropes and organic solvents already applied for pharmaceuticals' solubilization. For example, this has been verified for anti-inflammatory drugs like ibuprofen.[110,133] Ibuprofen's solubility in aqueous solutions with common co-solvents, such as propylene glycol and polyethylene glycol (PEG 300), presents solubility enhancements of 193-fold and 700-fold, respectively, whereas, ibuprofen's solubility can be increased more than

5,400-fold in specific DES, namely tetrapropylammonium bromide:1,2-propanediol or camphor:menthol, when compared with its solubility in water.[110]

Examples with of other drugs have also been investigated, Li and co-workers[134] demonstrated solubility enhancements for itraconazole, piroxicam, lidocaine, and posaconazole of 6700-, 430-, 28-, and 6,400-fold, respectively, compared to their solubility in water, using a DES based on [Ch]Cl and glycolic acid (molar ratio 1:2). A solubility enhancement for itraconazole of 53,600-fold by adding a third component, namely oxalic acid, into this DES, at a molar ratio of 1:1.6:0.4 ([Ch]Cl:glycolic acid:oxalic acid), has also been reported.[134] Contrarily, by solubilizing ibuprofen in the mixture menthol:camphor (1:1) only a 4-fold increase in the water solubility is achieved.[135] Other drugs, such as antifungals like danazol, also benefit from the use of DES. The solubilization of this drug in [Ch]Cl:malonic acid (1:1) allows a 320-fold solubility increase, compared to its aqueous solution.[128]

Although drugs can be solubilized in the neat DES, they can also be solubilized in aqueous solutions containing DES, as previously mentioned. Since most of these drugs are intended for human treatment, solubility in aqueous solutions of DES should be preferred. The solubility of different drugs, such as itraconazone,[128] griseofulvin[128] and dapsone,[129] has been studied in aqueous solutions of DES; however, few studies report the full solubility curves that allow to choose the best DES:water ratio.

The results reported up to date show how the solubility of APIs in a DES can be controlled by its proper design, since the interaction of the DES components with the relevant sites of the drug structure might translate into the high solvation abilities observed. Ultimately, the solubility of the drugs can be improved while enhancing other characteristics such as the permeation ability.

Table 1. Summary of APIs solubility improvements in DES (and DES aqueous solutions) at room temperature.

API	Solubility in water (mg.mL^{-1})	DES (molar ratio, HBA:HBD) (%of DES in water)	Solubility in DES (mg.mL^{-1})	Ref
Aspirin	7.03	[Ch]Cl:1,2-propanediol (1:2)	202.00	[110]
Acetaminophen	19.95	[Ch]Cl:1,2-propanediol (1:2)	324.00	[110]
Berberine	2.1	Proline:urea (2:1)	12.3	[132]
Carvedilol	0.09	Thymol:camphor (1:1) Menthol:camphor (2:1) Thymol:menthol (1:1)	12.66 24.52 28.10	[130]
Curcumin	Insoluble	[Ch]Cl:glycerol (1:1) [Ch]Cl:maleic acid (3:1) Glucose:sucrose (1:1)	7.25 0.07 0.05	[136]
Danazol	<0.0005	[Ch]Cl:urea (1:2) [Ch]Cl:malonic acid (1:2)	0.05 0.16	[128]
Dapsone	0.38	[Ch]Cl:ascorbic acid (2:1) (80% of DES in water) [Ch]Cl:propylene glycol (1:3)	200.00 500.00	[129]
Furosemide	0.02	Thymol:camphor (1:1) Menthol:camphor (2:1) Thymol:menthol (1:1)	6.99 0.85	[130]
Griseofulvin	0.007	[Ch]Cl:urea (1:2) [Ch]Cl:urea (1:2) (75% of DES in water) [Ch]Cl:malonic acid (1:2) [Ch]Cl:malonic acid (1:2) (75% of DES in water)	0.03 0.02 1.00 0.10	[128]
Ibuprofen	0.07	Camphor:menthol (1:1) Tetrapropylammonium bromide:1,2-propanediol	282.11 383.40	[135] [110]
Itraconazole	<0.001	[Ch]Cl:glycolic acid:oxalic acid (1:1.6:0.4) [Ch]Cl:malonic acid (1:2) [Ch]Cl:malonic acid (1:2) (75% of DES in water)	53.60 22 6.60	[134] [128]
Lidocaine	3.63	[Ch]Cl:glycolic acid:oxalic acid (1:1.7:0.3)	295.40	[134]
Ketoprofen	0.34	[Ch]Cl:levulinic acid (1:2)	329.10	[110]
Naproxen	0.06	[Ch]Cl:1,2-propanediol (1:2)	45.26	[110]
Nitrofurantoin	0.08	Thymol:camphor (1:1) Menthol:camphor (2:1) Thymol:menthol (1:1)	0.50 0.10 0.52	[130]
Piroxicam	0.02	[Ch]Cl:glycolic acid (1:2)	9.90	[134]
Posaconazole	0.01	[Ch]Cl:glycolic acid:oxalic acid (1:1.7:0.3)	88.40	[134]
Rutin	0.12	[Ch]Cl:proline (3:1)	2.79	[131]
Tetracycline	0.23	Thymol:camphor (1:1) Menthol:camphor (2:1) Thymol:menthol (1:1)	24.55 23.17 37.88	[130]

1.3.2 DES as permeation enhancers of active pharmaceutical ingredients

Until recently, the majority of DES were designed for transdermal purposes and included drugs and permeation enhancers in their preparation, like anti-inflammatory drugs and terpenes or fatty acids, respectively. This trend dates back to 1998, when Stott and co-workers[137] reported a series of API-DES based on ibuprofen and different permeation enhancers, namely L-menthol, L-menthone, thymol, D-limonene, 1,8-cineole and *p*-cymene. These mixtures presented melting temperatures below body's temperature, and since the recrystallization of the API at lower temperatures was avoided, the API stability under storage could be potentially improved. Due to its relevance, the DES menthol:ibuprofen has been characterized (T_m=13 °C), studied regarding its efficacy in transdermal delivery and applied in drug delivery systems to enhance the release of ibuprofen.[108,137]

In a different approach, the APIs' permeation was improved not by using the API in the DES preparation but by the dissolution of the drug in a given DES. This type of DES has been designed with permeation enhancers in their composition to facilitate the transportation of the drug across the biological membrane. Such an approach was recently reported by Silva *et al.*[138] that studied the preparation of DES with menthol and fatty acids (such as stearic, myristic, and lauric acids) for wound healing applications. Among these, the mixture menthol:stearic acid showed to be particularly relevant since it possesses two permeation enhancers in its composition, but also interesting biological activities, namely enhanced wound healing and antibacterial properties. The advantageous use of these formulations is their application versatility. DES with permeation enhancing ability can be incorporated into different dosage forms, including topical creams, in a safe way.[100,139] For example, *in vivo* studies on albino rabbits have confirmed that topical application of DESs, composed of capric acid:menthol, do not cause skin irritation.[140] Ultimately, these systems have been applied for the solubilization of fluconazole and mometasone, antifungal and anti-allergic drugs, respectively, and their formulation and application as a topical cream was studied. Interestingly, it has been shown that the drug, the DES and cream components do not cause skin edema or inflammation, being safe for topical application.[140]

Given the versatility in the design of DES, they can exert multiple roles, offering the possibility to have new drug delivery options, which represent a step forward in the development of novel drug delivery systems.

1.3.3 DES as stability enhancers

DES have also been reported to enhance the stability of pharmaceuticals, since many of them are known to decompose through a variety of pathways in aqueous solution (as summarized in Table 2).

Table 2. Impact of DES in drug stability under different storage conditions.

API	Reference Solvent	DES	Storage Conditions	Stability Improvement in DES Media	Ref
Hydrolysis					
Aspirin	Water	[Ch]Cl:1,2-propanediol	14 h at 80 °C	Cleavage into salicylic and acetic acids is 8.2 times slower	110
Imipenem	Water	Betaine:urea	7-day storage at 25 °C	7-fold less degradation	141
Clavulanic acid	Water			2.5-fold less degradation	
Photochemical					
5,10,15,20-tetrakis(4-hydroxyphenyl)-porphyrin (THPP)	Methanol	Citric acid:glucose	3 to 5 h exposure to 765 W·m^{-2} (310–800 nm) irradiation to an endpoint of 8 h corresponding to 1.2 × 10^6 lux·h (400–800 nm)	Lower rate of photodegradation	142
Curcumin	Methanol	[Ch]Cl:glycerol	2 h exposure to sunlight	Decreases photodegradation under sunlight exposure	136
Thermal					
Chondroitinase ABCI	Phosphate buffer	[Ch]Cl:glycerol Betaine–glycerol	15 days storage at −20 °C	Enzyme activity retention of 95% and 80%, respectively, vs loss of activity after 5 days in its absence	143
Human interferon-α2	Phosphate buffer	[Ch]Cl:fructose	Short-term (2 h) and long-term (3 months) storage at 37 °C	Preservation of structural integrity and activity	144

For instance, many ester-containing APIs, like aspirin, undergo hydrolysis upon a long period storage in water.[35] The hydrolysis of aspirin into salicylic and acetic acids is 8.2 times slower in a 50% (w/w) aqueous solution of [Ch]Cl:1,2-propanediol (1:2) than in water, at high temperatures (80 °C). In the same line, some

β-lactam antibiotics can be unstable, due to β-lactam hydrolysis, resulting in antimicrobial activity loss.[141] To overcome this drawback, the DES betaine:urea (1:2) with 2% (w/w) of water was studied to improve the stability of the β-lactams imipenem and clavulanic acid. These formulations enhanced the antibiotics stability by 7- and 2.5-fold, respectively, compared to aqueous formulations in a 7-day storage period at room temperature. DES also allow the prevention of thermal and photochemical degradations of APIs. As an example, porphyrins display photophysical properties attractive for their application in photodynamic therapy.[145] The rate of porphyrins degradation is significantly higher in methanol than in neat [Ch]Cl and glucose-based DES; however, upon dilution of the DES porphyrin solution in water (1:50), the degradation profile is inverted. In this case, the use of the DES as media instead its aqueous solution can be advantageous, especially when considering high water concentrations.[142]

In addition to porphyrins, curcumin can also be applied as a photosensitizer.[146] Its poor water solubility and high photo and thermal sensitivity, might, however, limit its application. By storing curcumin in DES media, namely [Ch]Cl:glycerol (1:2), it is possible to prevent the degradation of the photosensitizer over 2 h even when exposed to sunlight, while, when stored in methanol in the same conditions, curcumin concentration decreases to less than 5% of its initial amount.[136]

DES can also decrease or prevent the thermal degradation of therapeutic proteins.[147] The stability of chondroitinase ABCl, an important clinical enzyme in the treatment of spinal lesions and of human interferon-α2 (IFN-α2), a therapeutic protein used in the treatment of hepatitis B and C and leukemia, have been enhanced using [Ch]Cl:glycerol (1:2) and betaine:glycerol[143] and [Ch]Cl:fructose,[144] respectively. The use of these solvents increases the thermal stability of the proteins in comparison with their aqueous formulations under different storing temperature conditions, and also from short to long-term storing periods.

Despite the promising results achieved with the use of DES to improve drug stability, more extensive data are still needed so that their careful design can be accomplished.

1.3.4 Cytotoxicity and biological activity of deep eutectic solvents

Considering the increased potential application of these solvents in the pharmaceutical area, the cytotoxicity of DES and their impact in the final formulation must be addressed for a more efficient selection and acceptance for drug formulation purposes.[148,149] Initial studies have focused on the cytotoxicity of cholinium-based DES tested in prokaryotic microorganisms, like bacteria.[138,150,151] Lately, the effect of DES in more complex systems, such as eukaryotic organisms like yeasts,[152] human[153] and animal cell lines,[154] and even animal models has been studied.[155] The use of different animal models with progressive degrees of complexity might help to clarify the impact of DES in the organism after administration and its mechanisms of action. These studies have highlighted that DES present a different toxicity pattern to that observed for the individual components. Furthermore, when in aqueous media, DES present low cytotoxicity (below 3000 µM) and low impact on aquatic organisms turning them appellative for incorporation in pharmaceutical formulations.[156] However, when considering oral administration, the selection of DES components must be carefully considered. Many studies comprise [Ch]Cl:urea as a model system to explore DES applications. Yet, the toxicity of this DES has been increasingly reported and, more recently, studies on mice have confirmed this drawback.[153] After the administration of the DES, the metabolic profiling of the liver, kidney, and serum samples were evaluated, revealing that ammonia was putatively responsible for the DES toxic effect.[157] Other types of DES and the assessment of proper DES concentrations to be regulated should be studied in the future.

Therefore, to avoid significant toxicity, the DES preparation method should be considered, and the DES components carefully selected, since this can impact the final cytotoxicity.[151,158] If properly designed, the DES can be fine-tuned to a specific formulation purpose, however this possibility it is still shortly investigated. When appropriately considered, the DES formulation can complement or amplify the therapeutic action of a drug solubilized in this media. This possibility makes DES not only appealing solvents but also valuable excipients to incorporate into

pharmaceutical formulations, a possibility further explored through the present thesis.

Table 3 summarizes the DES reported so far with anti-tumoral and antimicrobial activities against the respective microorganisms/cell lines. The antimicrobial activity of a variety of [Ch]Cl-based DES has been evaluated against fungal species, such as *Candida albicans*,[138] *Phanerochaete chrysosporium, Aspergillus niger, Lentinus tigrinus* and *Candida cylindracea*;[152] and against Gram-positive (*Staphylococcus aureus* and *Listeria monocytogenes*) and Gram-negative (*Escherichia coli* and *Salmonella enteritidis*) bacteria.[138,150,151,159] Alcohol- and sugar-based DES do not inhibit bacterial growth since these components can be used as nutrient sources.[150,151] On the other hand, it has been shown that the selection of DES with organic acids can have an enhanced effect of bacterial inactivation. DES with high acidity or basicity can denature proteins located on the cell wall, resulting in cell collapse and death.[150] Furthermore, the use of DES based on fatty acids can promote biofilm detachment/removal in gram-positive (*S. aureus*), gram-negative (*E. coli*) bacteria and fungus such as *Candida albicans*.[138]

The *in vitro* anti-tumoral potential of DES has also been explored in several tumoral cell lines.[151,153] For example, [Ch]Cl combined with different HBDs, namely glycerol, ethylene glycol, triethylene glycol and urea were investigated regarding their effect on human prostate cancer (PC3), human malignant melanoma (A375), human colon adenocarcinoma (HT29) and human breast cancer (MCF-7) cell lines.[153] The investigated DES inhibited cancer cell growth at certain dosages (11–70 µg·mL^{-1}), presenting selectivity to a specific cell line according to the DES composition. All the studied DES present, in a dose dependent manner, the ability to provoke cell death and increase reactive oxygen species (ROS) production in cancer cell lines. In general, DES did not cause DNA damage but enhanced ROS production and induced apoptosis in treated cancer cells. However, *in vivo* administration in mice revealed that the dose concentration for administration should be carefully manipulated to avoid the toxicity to healthy tissue/organs.[153]

Table 3. DES with impact on the respective microorganisms and cell lines studied.

DES	Molar Ratio	Microorganism	Bacterial inhibition (cm)	Ref
Antibacterial activity				
[Ch]Cl:*p*-toluenesulfonic acid	1:1		1.71±0.09	
[Ch]Cl:oxalic acid	1:1		2.48±0.03	
[Ch]Cl:levulinic acid	1:2		1.65±0.05	
[Ch]Cl:malonic acid		*E. coli*	1.53±0.03	
[Ch]Cl:malic acid	1:1		1.92±0.08	
[Ch]Cl:citric acid			1.93±0.13	
[Ch]Cl:tartaric acid	2:1		1.76±0.14	
[Ch]Cl:*p*-toluenesulfonic acid	1:1		1.20±0.01	
[Ch]Cl:oxalic acid	1:1		1.93±0.07	
[Ch]Cl:levulinic acid	1:2	*S. enteritidis*	1.60±0.10	
[Ch]Cl:malonic acid			1.17±0.03	150
[Ch]Cl:malic acid	1:1		1.22±0.03	
[Ch]Cl:citric acid			1.77±0.03	
[Ch]Cl:tartaric acid	2:1		1.50±0.01	
[Ch]Cl:*p*-toluenesulfonic acid	1:1		1.12±0.02	
[Ch]Cl:oxalic acid	1:1		1.97±0.07	
[Ch]Cl:levulinic acid	1:2		1.00±0.01	
[Ch]Cl:malonic acid			1.32±0.03	
[Ch]Cl:malic acid	1:1	*S. aureus*	1.50±0.05	
[Ch]Cl:citric acid			1.58±0.08	
[Ch]Cl:tartaric acid	2:1		1.50±0.19	
Caprylic acid:myristic acid	3:1		1.40±1.00	
Caprylic acid:stearic acid	4:1		1.47±0.58	138
Caprylic acid:lauric acid	2:1		1.57±0.58	
[Ch]Cl:*p*-toluenesulfonic acid	1:1		0.70±0.01	
[Ch]Cl:oxalic acid	1:1		1.50±0.01	
[Ch]Cl:levulinic acid	1:2		0.97±0.08	
[Ch]Cl:malonic acid		*L. moncytogenes*	0.93±0.07	150
[Ch]Cl:malic acid	1:1		1.10±0.10	
[Ch]Cl:citric acid			1.30±0.05	
[Ch]Cl:tartaric acid	2:1		1.10±0.05	
Caprylic acid:myristic acid	3:1		1.43±0.47	
Caprylic acid:stearic acid	4:1	*MRSA*	1.57±0.47	
Caprylic acid:lauric acid	2:1		1.65±0.41	138
Caprylic acid:myristic acid	3:1		1.57±0.47	
Caprylic acid:stearic acid	4:1	*MRSE*	2.00±0.82	
Caprylic acid:lauric acid	2:1		1.50±0.82	
Antifungal activity				
Caprylic acid:myristic acid	3:1		1.27±0.47	
Caprylic acid:stearic acid	4:1	C. albicans	1.50±0.50	138
Caprylic acid:lauric acid	2:1		1.35±0.41	
[Ch]Cl:*p*-toluenesulfonic acid	1:3		0.50±0.10	
[Ch]Cl:ZnCl$_2$	1:2	*P. chrysosporium*	1.60±0.20	
[Ch]Cl:malonic acid	1:1		0.70±0.03	
[Ch]Cl:*p*-toluenesulfonic acid	1:3		0.40±0.20	138
[Ch]Cl:ZnCl$_2$	1:2	*A. niger*	1.70±0.40	
[Ch]Cl:malonic acid	1:1		0.60±0.02	
[Ch]Cl:*p*-toluenesulfonic acid	1:3		0.30±0.20	
[Ch]Cl:ZnCl$_2$	1:2	*L. tigrinus*	1.50±0.10	
[Ch]Cl:malonic acid	1:1		0.50±0.20	

Table 3. (cont.)

DES	Molar Ratio	Cell line	IC$_{50}$	Ref
[Ch]Cl:*p*-toluenesulfonic acid	1:3		0.70±0.40	
[Ch]Cl:ZnCl$_2$	1:2	*C. cylindracea*	1.70±0.40	
[Ch]Cl:malonic acid	1:1		0.90±0.20	
Anti-tumoral activity				
[Ch]Cl:glycerol			30.65 ± 2.82 [a]	
[Ch]Cl:ethylene glycol		PC3	32.88 ± 5.82 [a]	
[Ch]Cl:urea			27.78 ± 3.92 [a]	
[Ch]Cl:triethylene glycol			20.32 ± 2.34 [a]	
[Ch]Cl:glycerol			21.86 ± 2.54 [a]	
[Ch]Cl:ethylene glycol		MCF-7	27.02 ± 1.31 [a]	
[Ch]Cl:urea	1:3		29.37 ± 4.83 [a]	153
[Ch]Cl:triethylene glycol			16.09 ± 1.23 [a]	
[Ch]Cl:glycerol			18.07 ± 1.62 [a]	
[Ch]Cl:ethylene glycol		A375	35.23 ± 4.40 [a]	
[Ch]Cl:urea			59.61 ± 8.28 [a]	
[Ch]Cl:triethylene glycol			12.29 ± 3.07 [a]	
[Ch]Cl:glycerol			28.44 ± 3.28 [a]	
[Ch]Cl:ethylene glycol		HT29	30.54 ± 3.68 [a]	
[Ch]Cl:urea			36.21 ± 4.98 [a]	
[Ch]Cl:triethylene glycol			17.42 ± 2.55 [a]	
[Ch]Cl:fructose	5:2		177±7.30 [b]	
[Ch]Cl:glucose		Human cervical cancer (HelaS3)	182±7.60 [b]	
[Ch]Cl:sucrose	4:1		166±5.80 [b]	
[Ch]Cl:glycerol	1:2		427±11.0 [b]	
[Ch]Cl:malonic acid	1:1		20±8.40 [b]	
[Ch]Cl:fructose	5:2		206±7.50 [b]	
[Ch]Cl:glucose		Human ovarian cancer (CaOV3)	193±7.50 [b]	
[Ch]Cl:sucrose	4:1		154±5.60 [b]	154
[Ch]Cl:glycerol	1:2		483±11.0 [b]	
[Ch]Cl:malonic acid	1:1		15±8.20 [b]	
[Ch]Cl:fructose	5:2		195±7.70 [b]	
[Ch]Cl:glucose		Mouse skin cancer (B16F10)	211±8.0 [b]	
[Ch]Cl:sucrose	4:1		136±5.70 [b]	
[Ch]Cl:glycerol	1:2		340±10.3 [b]	
[Ch]Cl:malonic acid	1:1		35±8.8 [b]	

[a]: $\mu g \cdot mL^{-1}$
[b]: mM

1.4 DES in the development of drug delivery systems

Drug delivery has evolved as a strategy of processes or devices designed to enhance the efficacy of therapeutic agents taking into consideration the carrier, the route and the target.[160] In 1952, Smith Klein Beecham[161] introduced, for the first time, the possibility to formulate a sustained release system for the delivery of dextroamphetamine (Dexedrine), a stimulant used to treat attention deficit hyperactivity disorder. This new system was able to control the drug release kinetics

over 12 h. After this pioneering evidence, delivery strategies and technologies have quickly emerged to tackle drug delivery needs and enabled to develop different systems with improved release profiles, extending therapeutic effect from 12 h to long-acting systems (up to 3 years), depending on characteristics of the drug and delivery system.[162,163] Research focused essentially on drug delivery systems aimed at effectively reducing the dosage frequency, while maintaining the drug concentration in targeted organs/tissues for longer periods of time.[164] After years of advances in drug delivery technologies, the different release profiles, targets and efficacy had a strong contribution from the advances in polymer science (Figure 10).

Due to the diversity and versatility of synthetic and natural polymeric materials, their applications are nowadays widespread and essential across all sectors of human activity, spanning from extremely low added-value (yet essential) packaging materials to high-technology and high added-value materials, in which biomedical and pharmaceutical applications are often included.[165,166] The first drug delivery polymer-based systems developed, so called First-generation delivery systems (Figure 10), were highly successful. These systems were mainly for oral and transdermal purposes, and the *in vivo* pharmacokinetic profiles could be controlled by adjusting the drug release kinetics.[167] Thus, their success was mainly based on engineering manipulations.

Among the existing drug administration routes, the oral route has been the most used for both conventional and novel drug delivery systems.[160] The reasons for this preference are the easiness of administration and widespread acceptance by the patients. However, orally administrated drugs often present variable absorption rates and variable serum concentrations, which may be unpredictable.[168] Furthermore, many drugs present undesired side-effects, that often patients intend to avoid. Alternative to oral route, topical (skin or ocular) and transdermal drug delivery approaches have been widely studied to deliver drugs through biological membranes.[169] Following this, the development of novel drug release systems, which include not only oral controlled release systems, but also fast dispersing dosage forms, modulated release profiles and nano-drug delivery systems, emerged as second-generation strategies,[166] as depicted in Figure 10.
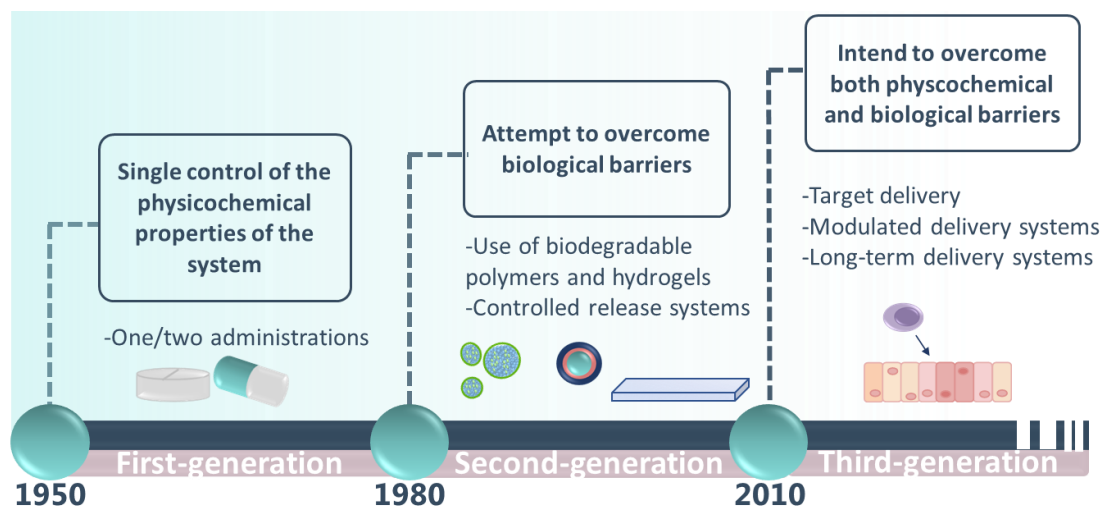
Figure 10. Evolution of drug delivery strategies.

These strategies, however, have experienced difficulties due to the lack of regulatory regimes and reproducibility issues.[170,171] Although second-generation systems are formulated to surpass biological barriers, their efficacy is expected to be different from conventional systems and their biological response needs to be studied in more detail. The pharmacokinetics of these formulations is mainly driven by the body's response rather than by the delivery system itself.[172] Third-generation drug delivery technologies pursue to tackle these limitations, being designed to overcome both physicochemical and biological barriers, such as site-specific intracellular delivery.[170] Thus, the future of these drug delivery systems relies in the development of new approaches to correct initial burst release, creating more controlled systems (as for example in injectable depot formulations) and for the formulation of poorly soluble drugs for which the use of DES can be advantageous. The progress brought by DES in drug formulation and delivery has been briefly reviewed,[173–175] highlighting the versatility of these solvents in different types of drug delivery systems which will be discussed in more detail in the next subchapters.

1.4.1 DES in the development of new aqueous drug delivery systems

Liquid formulations are designed to provide the maximum therapeutic response and to produce rapid therapeutic effects.[176] These dosage forms can be divided according to the number of phases into monophasic (solutions) and biphasic

(suspensions, emulsions, etc.) systems.[177] Due to the variety of possible of biphasic delivery systems, they can envisage different administration means such as oral, other non-parenteral (ophthalmic, nasal, transdermal) and parenteral routes.[178] Among the numerous strategies in this area, nano and microemulsions represent a versatile option for the delivery of drugs through lipophilic barriers and an alternative approach to overcome drug low solubility and instability in aqueous media.[179] The nature of the continuous and discontinuous phases also impacts the nature of each colloidal system, making it possible to prepare water/oil (w/o) or oil/water (o/w) dispersions.[180,181]

Due to the coexistence of both phases, it is possible to solubilize both lipophilic and hydrophilic active ingredients in these formulations.[182] Therefore, water-insoluble compounds will prefer to be dispersed in the oil phase and/or hydrophobic tail region of the surfactant, whereas water-soluble drugs will favorably be dispersed in the aqueous phase.[183,184] Additionally, the viscosity of the microemulsion can be adjusted for a given application, either by formulation changes, or by the addition of specific gelling agents (such as *in situ* gelling synthetic polymers or biopolymers).[185] Among the gelling agents it is possible to highlight synthetic polymers like Lutrol, Carbopol and Pluronics, or biopolymers such as xanthan gum, alginate and hydroxypropyl methylcellulose.[185–187] Owing to the range of possibilities allowed by the development of nano and microemulsions, several drugs have been incorporated into this type of formulations and many pharmaceutical products are available in the market that employ this type of formulations.[188–191] Despite most of these systems are designed for transdermal delivery, the application of microemulsions for ocular drug delivery has gained special attention due to their advantages in comparison to typical eye-drops.[192] Due to the phase transition behavior, microemulsions can create *in situ* precorneal deposits, improving the drug retention and, thus, making the release of incorporated drug prolonged.[179] Furthermore, the correct selection of the lipidic phase (mostly medium-chain triglycerides), the surfactant phase, and the cosurfactant might enable the delivery of the drug in a precise and controlled manner.[179]

DES have only recently started to be applied in the development of microemulsions. So far, DES have integrated these systems as oil phases since

hydrophobic DES, based in fatty acids like *n*-decanoic and octanoic acids, were mainly selected.[193,194] Furthermore, these can be applied for the delivery of compounds with low water-solubility, such as curcumin.[194] Systems with octanoic acid:menthol-in-water proved to be suitable carriers for curcumin, resulting in microemulsions with 90% of curcumin in the system after a 30 days storage at 4 °C. Interestingly, these systems have shown enhanced anti-inflammatory action, by suppressing NO release and reduced cytokines production in lipopolysaccharide (LPS)-activated murine and differentiated human macrophages, when compared to common formulations of curcumin solubilized in organic solvents, such as DMSO.[194] Despite being in its infancy, the application of DES in water-based formulations can foresee interesting results and allow the development of novel drug delivery systems with improved efficacy.

1.4.2 DES incorporation in semi-solid and solid biopolymer-based drug delivery systems

Solid dosage forms emerged as unit doses such as capsules, pills, tablets, chewable and effervescent tablets, granules and represent a simple approach to oral drug delivery systems.[177] Semisolid dosage forms, on the contrary, have been developed mostly for external use, attempting to reduce the drug's side effects and allowing a local application at the target site.[195] These systems have evolved from simple dosage forms, such as ointments or creams, to advanced controlled release systems like transdermal patches or hydrogel adhesives, from which biopolymers have been widely studied.

Biopolymers can be divided into three major classes according to their chemical structure: polysaccharides, proteins, and polyesters.[196] Polysaccharides, in particular, consist of monosaccharides linked by *O*-glycosidic linkages. Differences in the monosaccharide composition, linkage types and patterns, and molecular weight dictate their physical properties, such as solubility, viscosity, gelling potential, and/or surface and interfacial properties.[197–199] Since they are derived from renewable feedstocks, such as plants, algae, or microorganisms, they can ultimately answer to the demand for more environmentally friendly options for the pharmaceutical industry.[200] From the vast range of known polysaccharides,

40

alginate,[201] cellulose,[202,203] starch,[204] chitosan[205] and pullulan[206] are the most frequently used in the development of drug delivery systems.

The use of biopolymers is advantageous, since they can reduce the stimulation of chronic inflammation or immunological reactions and toxicity, in comparison to the side-effects associated with the use of synthetic polymers.[207] Materials such as films,[208–210] membranes,[211,212] hydrogels,[213,214] and micro- and nanoparticle-based systems,[215] have been developed. These materials can be prepared through a variety of methods, from solvent casting[216] to electrospinning.[217] In addition to the reasons mentioned above, the interest in the study of biopolymers for drug delivery systems also relies in the possibility of developing novel approaches that are less invasive and can offer a more personalized and effective treatment. These systems can protect the active ingredients and provide their controlled release to the targeted area, while offering the possibility to improve the pharmacokinetics and pharmacodynamics of small drugs.[218]

Biopolymers and their derivatives have been applied in the development of drug delivery systems comprising eutectic mixtures and later DES. One of the oldest applications of eutectic mixtures in drug delivery is the application of the previously mentioned EMLA® mixture, commercialized as a cream or in a patch form.[219] In the latter case, a single-dose unit of EMLA® is incorporated into a cellulose absorbent disc. Although EMLA® patches have been developed and highlighted for their easy application, they seem to exert the same effect as the cream form in cutaneous pain relief.[139] After this, the lidocaine and prilocaine mixture used in EMLA® has been studied for the development of a local delivery system to the periodontal pocket.[220] Cellulose derivatives, such as ethyl(hydroxyethyl)cellulose (EHEC) and a hydrophobically modified EHEC, have been tested as potential carrier systems for the anesthesia mixture's delivery, demonstrating a sustained drug release over a minimum of 1 h.[220] The cellulose derivative EHEC was combined with surfactants to advantageously increase the viscosity of the system upon increasing the temperature. This behavior allows to administrate an API in a low viscous polymer system that thickens in contact with the body. The obtained data indicated the possibility of formulating a temperature-sensitive system where small amounts of

the eutectic mixture can be incorporated, without severely affecting the gelation behavior of the polymer.[220]

The combination of DES formulations with biopolymers has allowed to expand the possibilities of delivering APIs in a more effective way.[221–223] DES have been applied as novel solvents for drug and biopolymer solubilization,[124,224] as API formulations (API-DES)[111] or as agents with specific role (permeation enhancers, plasticizers or porosity enhancers) that can fit the needs for the design of drug delivery systems for distinct routes of administration.[108,113,225] These mixtures have been conjugated with different biopolymers (such as gelatin, alginate and chitosan) producing varied drug delivery systems, such as hydrogels,[223,226] particles[227] and nanofibers,[228] among others. Figure 11 highlights the role of DESs in biopolymeric drug delivery systems and their function in the development of systems with improved therapeutic action. Based on the exposed, along the description of the works developed so far in this area, a particular emphasis will be given to pullulan and alginate due to their specific properties and their use in the present PhD thesis.
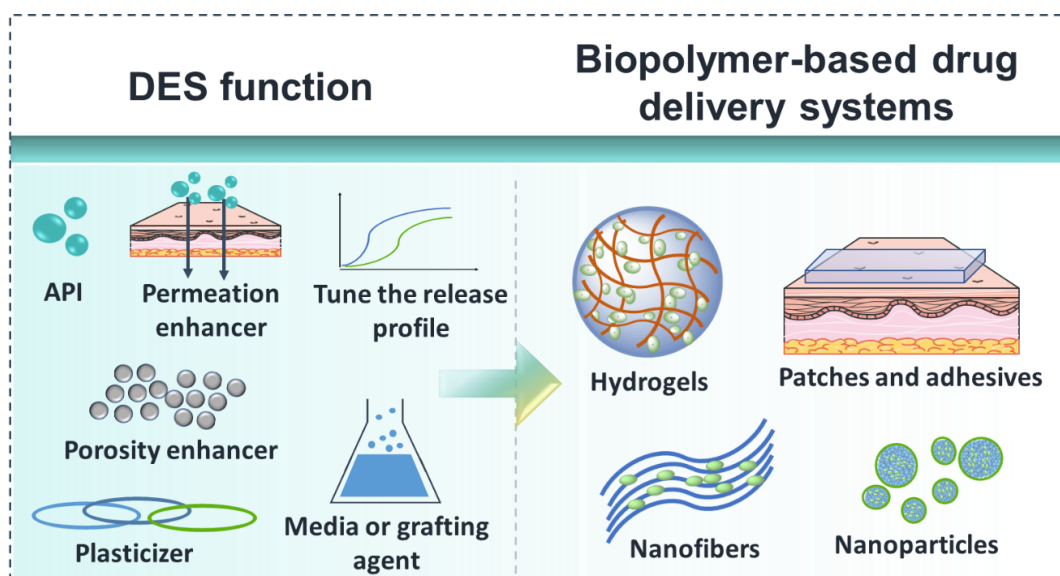
Figure 11. Schematic representation of the role of DES in the development of different biopolymer-based drug delivery systems. Skin image made with Servier Medical Art and adapted by the authors according with Servier under the CC-BY 3.0 License (at https://smart.servier.com/, accessed on 10 Septemper 2022).

Pullulan is a linear polysaccharide composed of maltotriose units (three glucose units connected by α–1,4 glycosidic bonds) that are linked between each other by α–1,6 glycosidic bonds,[187] as shown in Figure 12. Pullulan is obtained by

extracellular production of the fungus *Aureobasidium pullulans* under a fermentation process.[229] This biopolymer presents interesting features that make it appealing for the biomedical and pharmaceutical field, namely it is inert, antimicrobial, hemocompatible, nonimmunogenic, noncarcinogenic .[229,230] In contrast with many biopolymers, it is readily water soluble, originating low viscous solutions, that enable the preparation of microparticles,[231] nanoparticles,[232] micelles[233] and hydrogels.[234] In addition due to its filmogenic ability, pullulan is applied to produce films aimed at topical applications.[235]

Owning to pullulan's chain flexibility and hydroxyl groups, chemical modifications can be made to produce derivatives, such as pullulan acetate[236] or carboxymethyl pullulan.[237] These modifications intend to optimize the hydrophilic–hydrophobic balance, to adjust the release profile and to allow the conjugation of this biopolymer with hydrophobic drugs.[238,239] This is particularly relevant to achieve properties that, otherwise, the biopolymer itself might not comprise (e.g.: self-assembling). Although its use in drug delivery systems has only recently been reported, systems with this biopolymer hold great promise in the development of targeted delivery for the treatment of numerous diseases, such as topical ones.[235,240–242]
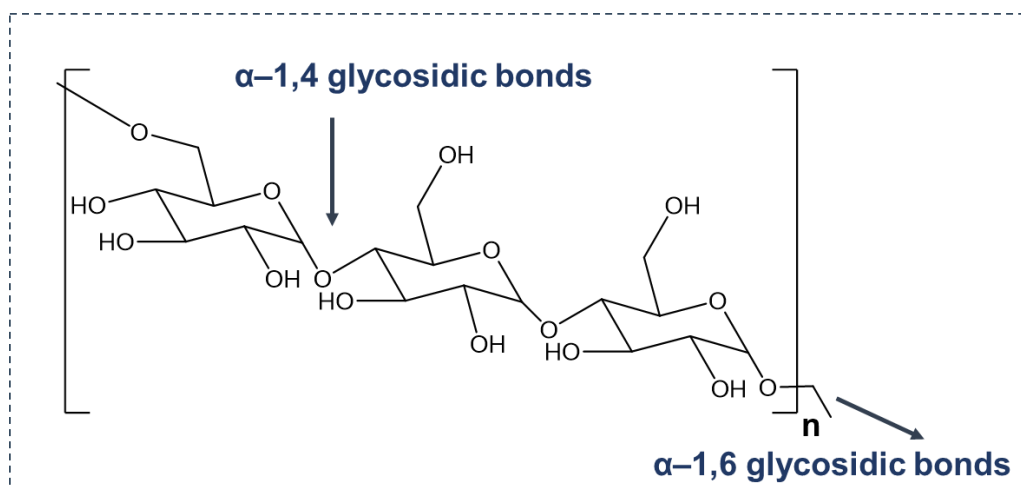
Figure 12. Structure of pullulan, highlighting the glycosidic bonds between glucose units (α−1,4) and between maltotriose units (α−1,6).

More recently, pullulan has been reported for its ability to improve wounds re-epithelialization, dermal regeneration, blood vessels formation and collagen synthesis,[243] proving that pullulan gels could be potential wound healing agents.

Materials containing pullulan might affect the cellular response to the delivery system, promoting faster healing time that can overcome the already commercialized hydrogels.[244] Regardless of all these promising properties, the use of DES in the production of pullulan-based materials for drug delivery is almost not investigated. Only one study by Silva *et al.*[216] was reported concerning the use of [Ch]Cl:carboxylic acid-based DES as efficient and timesaving fibrillation agents to produce protein nanofibers, which were applied as reinforcing additives of pullulan-based films. However, in this case the DES were not directly used in combination with pullulan.

Alginate is a highly viscous anionic polysaccharide with gelling properties, being mainly produced by brown seaweeds.[245] This biopolymer is constituted by polymeric chains made of D-mannuronate and L-guluronate units, as illustrated in Figure 13a, which can arrange in different proportions and present distinct molecular weights (10—600 kDa).[246] The anti-inflammatory activity of alginate combined to its nonimmunogenic, haemostatic and biocompatible features make it an important biopolymer in the pharmaceutical industry with a wide range of applications.[214,247,248] In fact, drug delivery systems, such as hydrogels, can be prepared with this biopolymer by ionotropic gelation with divalent cations (such as Ca^{2+}).[249] The coupling of continuous α-L-guluronate blocks of adjacent polymer chains with entrapment of Ca^{2+} within the resultant cavities, the so-called egg-box model of cross-linking, is the key for the formation of these alginate hydrogels.[245] Consequently, the L-guluronate unit content is particularly relevant to the resultant hydrogel properties, affecting the viscosity, elasticity, and pore size of the system.[245] Furthermore, the existence of carboxylic groups in the alginate's structure, negatively charged at pH values above 4, turns this biopolymer more soluble in neutral and alkaline conditions.[245,250] This ability has been advantageously used by the pharmaceutical industry for the design of drug delivery systems of drugs with preferential absorption in the intestinal tract or drugs that require a higher protection and modulation of the release profile.[251–253]

Hydrogels present a high amount of water in their 3D network owing to the multiple hydrophilic groups in the polymer chains.[254] Due to this ability to retain water, hydrogels acquire high adaptability to living tissues and an elastic behavior,

widening their application to different administration routes.[255] However, the resultant materials can present limitations, such as low tensile strength, nonuniformity in drug loading of hydrophobic drugs and fast drug release. These factors have urged the search for alternative strategies to be combined with these systems. One of these possibilities is the incorporation of nanoparticles into hydrogels to improve their performance (Figure 13b).[256]
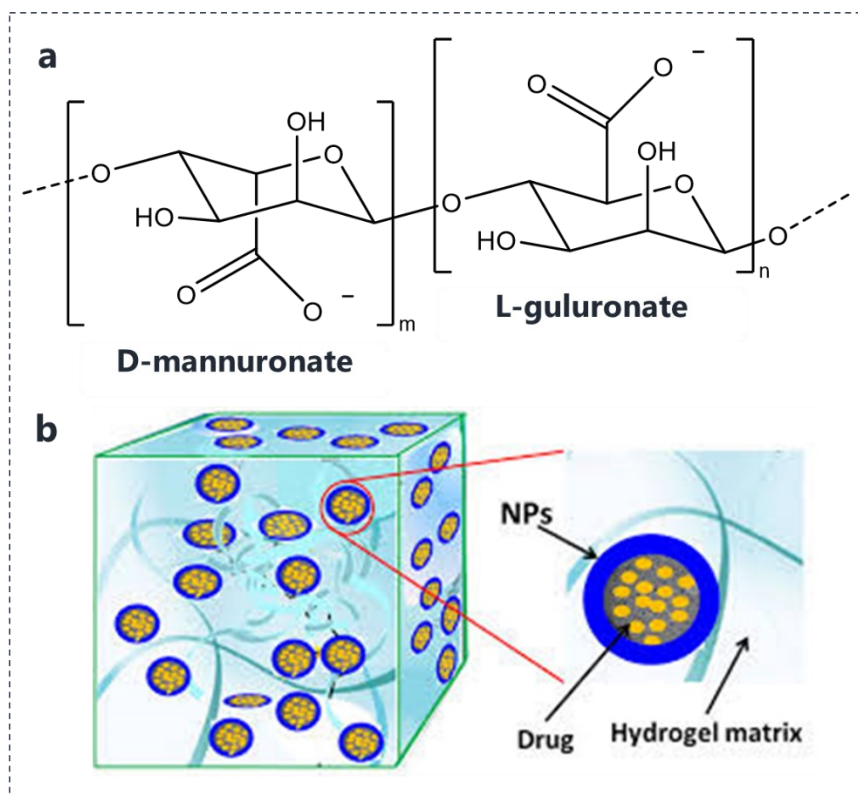
Figure 13. (a) Alginate structure units containing blocks of (1,4)-linked D-mannuronate and L-guluronate residues. (b) Alginate hydrogel loaded with nanoparticles (NPs) (adapted from [257]).

Alginate hydrogels have shown to be particularly relevant for the development of beads,[252] films,[208] wound dressings[201,258] and, more recently, for transdermal delivery systems with liquid formulations incorporated.[257] Although still less explored, the use of alginate hydrogels for transdermal delivery has shown the possibility to produce self-adhesive systems with good mechanical properties (stretchability and elasticity) and fast release profiles.[259]

Among the liquid formulations that can be incorporated into biopolymer-based hydrogels, the entrapment of DES formulations comprising APIs has shown promising results, not only in drug solubilization but also in the resulting properties

of the delivery system. DES have been combined with alginate and chitosan to produce hydrogel beads with pH-responsive behavior.[226] The DES [Ch]Cl:glycerol (1:1) was used as dissolution media for the low water-soluble agent, curcumin. The DES could enhance the drug solubility by several orders of magnitude, while it also improved the loading capacity of these hydrogels. The formulation was added to the alginate aqueous solution (ideally 6% (w/v)) and coagulated with calcium chloride, and then coated with 0.2% (w/v) of chitosan. The concentration of DES used in the beads' preparation was also screened. It was possible to verify that amounts lower than 25 wt% of DES are more indicated to retain the beads' shape (Figure 14a). Since these hydrogel systems present a pH-responsiveness behavior, due to the nature of the biopolymers selected, the drug release was lower in the simulated gastric fluid (pH=1.2) than in the simulated intestinal fluid (pH=6.8). A burst release associated with the beads' disintegration was also observed after 2 h and at 1 h in both fluids, respectively. Within the period of the assay the release percentage of curcumin in the gastric media ranged between 3.59% and 6.49%, whereas 31.97% to 57.73% was released in the intestinal media. Furthermore, it is possible to achieve 89.49% and 97.49% of curcumin release when simulating colonic conditions, at pH=7.4 (Figure 14b). [226]
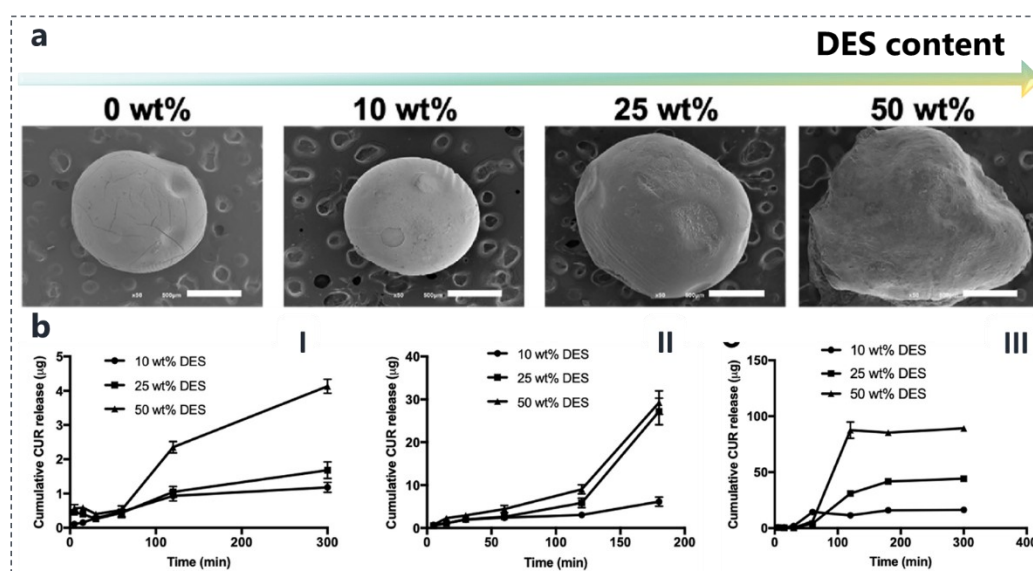
Figure 14. (a) Scanning electron microscopy (SEM) images of the vacuum-dried hydrogel beads with different DES content. The scale bar is 500 µm. (b) Cumulative release of curcumin from hydrogel beads with different DES-Curcumin content tested in gastric (I), intestinal (II) and colonic (III) simulated fluids (adapted from [226]).

Not only the use of DES is advantageous to improve the loading of higher amounts of drug, since they increase the API solubility, it also enables the possibility to tune the release profile to fit the intended application, ranging from controlled and pH-responsive release profiles as previously stated to fast-release systems. The work of Mano *et al.*[228] focused on the development of fast-dissolving delivery systems that dissolve or disintegrate in the mouth rapidly. These systems usually enable a rapid onset of action with a significant increase in the drug's bioavailability when compared to common oral administration systems. With this purpose in mind, ChCl:mandelic acid mixture was used as an API-DES model to evaluate the capacity of these mixtures and active ingredients to be encapsulated in gelatin fibers produced by electrospinning. Cytotoxicity studies showed that the gelatin fibers with DES do not display negative influence on cell proliferation, being suitable for drug delivery purposes.[228]

DES have been also applied in the development of nanocarriers for application in oral administration of chemotherapy agents.[260] For this purpose, serine:lactic acid (1:3) was used to improve the solubility of chitosan and the thermal stability of the system by being grafted to chitosan, via a simple condensation reaction between the acidic group of DES and the hydroxyl groups of the biopolymer (Figure 15a).[260] In the building process, the DES-*g*-chitosan was conjugated with the targeted ligand of the biotin molecule, obtaining the nanocarrier DES-*g*-chitosan-biotin. This nanocarrier was loaded with doxorubicin, used in cancer treatment, and the resultant system was characterized and evaluated regarding its activity and cytotoxicity. The drug delivery system showed high cytotoxicity towards cancer cells, namely the HeLa cell line, while presenting low cytotoxicity against healthy cell lines (L929) (Figure 15b).

Although the rise in the number of oral[113] and even nasal[221] drug delivery has broadened the use and application of DES in drug delivery, topical and transdermal systems are still the mostly reported.[175,223,261] The design of these transdermal patches is based on the drug loading into a polymeric or viscous adhesive.[262] Therefore, the development of these systems usually employs a multi-layered structure with several components. Among these, an impermeable backing film, a preparation comprising the APIs and the respective excipient(s), an adhesive and a

protective release liner to peel off before the application.[263] Since these are intended for a precise local administration of the drug, poor adhesion can result in improper dosing and an increasing cost to the patients, once the systems have to be more often replaced.[263]
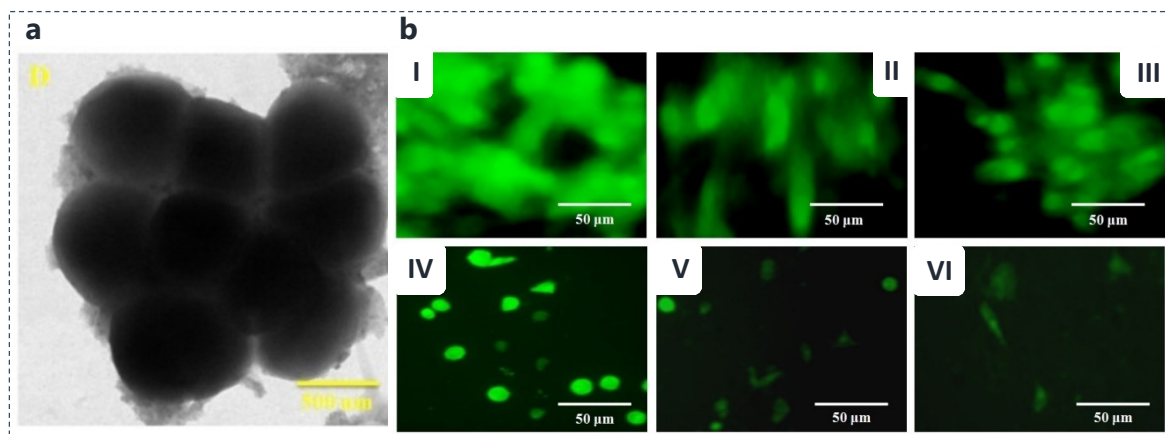
Figure 15. (a) Transmission electron microscopy (TEM) image of drug loaded DES-g-chitosan-biotin nanocarrier. (b) Apoptosis of HeLa cancer cell treated with doxorrubicin loaded DES-g-chitosan-biotin nanocarrier from 2 h to 24 h (adapted from [260]).

To evaluate the ability of new delivery systems to provide an adequate adhesion to skin, peel adhesion tests are usually conducted, where the force required to peel away an adhesive once it has been attached to a surface is quantified.[264–266] Equally, the shear adhesion test can be important to be tested for the measurement of the cohesive strength of the adhesive polymer to the skin.[266] The advances made so far in this area comprise the research of novel transdermal adhesive patches combined with strategies such as iontophoresis,[267] microneedles[242,268,269] and "smart" systems triggered by remote monitor signals.[270] The delivery devices will allow to improve the individualized and controlled treatment that is responsive to bio-feedback, benefiting the patients.

Aiming to apply DES in the development of transdermal systems, recently Abbot and coworkers[223] combined [Ch]Cl with catechol (1:1), aspirin (1:1) and imipramine to produce API-DES. These mixtures were then applied to plasticize gelatin films, showing no difference in the properties of the resulting biopolymeric systems according to the API formulation incorporated. In general, the API-DES enabled a fast drug dispersion in aqueous media achieving higher drug concentrations. *In vitro* tests on hydrated bovine hide and a porcine loin cut exhibited

48

that the transdermal delivery of the API-DES was superior to the pristine drugs from the gelatin matrix. One major example is the transdermal delivery of imipramine which was found to reach 65% of drug content in 15 min when in the API-DES form in the gelatin film, while systems with only imipramine can released only 20% within the same period.[223]

In addition to all the promising diversity of systems to be developed with DES highlighted above, these solvents can strongly influence the biopolymer-based materials' properties, particularly mechanical ones, mostly associated with their plasticizer effect.[271] DES such as [Ch]Cl:urea, [Ch]Cl:lactic acid, [Ch]Cl:malonic acid and [Ch]Cl:glycerol have been the most applied mixtures as biopolymer plasticizers.[272] They have shown to reduce cohesion forces between the biopolymer chains to improve the final system stretchability, flexibility and processability, as it happens with biopolymer-based films and as summarized in Table 4.[225,273–275]

Table 4. Effect of DES on the mechanical properties of polysaccharide-based films.

Biopolymer-based film	DES (molar ratio)	Amount of DES (%)	Young's modulus (MPa) ± SD	Tensile strength (MPa) ± SD	Elongation at break (%) ± SD	Ref
Agar	-	0	656 ± 153	34.3 ± 7.7	25.3 ± 9.9	273
	[Ch]Cl:urea (1:2)	-	55.2 ± 12.6	7.3 ± 0.7	59.2 ± 9.4	
Cellulose		0	414.20 ± 76.61	60.83 ± 7.02	2.22 ± 0.42	274
	[Ch]Cl:urea (1:2)	62	14.80 ± 1.57	4.14 ± 0.37	34.88 ± 0.11	
Chitosan	-	0	570 ± 70	31 ± 03	16 ± 05	
	[Ch]Cl:Lactic acid (1:1)	0	42.8 ± 1.9	33.8 ± 3.8	2.1 ± 0.3	225
		10	30.1 ± 3.6	20.5 ± 2.0	3.6 ± 0.3	
		20	21.6 ± 2.4	16.9 ± 2.6	6.5 ± 0.5	
		30	15.7 ± 1.3	13.2 ± 1.5	19.0 ± 2.1	
	[Ch]Cl:Malonic acid (1:1)	82	16 ± 02	2.8 ± 0.4	35 ± 09	275

The inclusion of DES in the delivery system can be also beneficial to change the resultant porosity, which also impacts the release profile of the API. An example has been demonstrated with the DES menthol:ibuprofen (3:1 molar ratio).[108] By impregnation of a polymeric blend (composed of starch and poly-ε-caprolactone (SPCL)) with the DES, after supercritical CO_2 ($scCO_2$) sintering, a drug delivery system was obtained. This foaming process with the DES allows to obtain a porous matrix impregnated with the intended API. The liquid DES contributes to a significant modification in the aggregation of the polymer particles, leading to a higher porosity

and interconnectivity. *In vitro* dissolution studies demonstrated similar dissolution profiles between pure ibuprofen and its liquid form with menthol; however, ibuprofen presented a faster release rate from the polymeric carrier impregnated with API-DES than in its pristine form. More recently, using the same polymeric blend and the same approach based on scCO$_2$ sintering, it was possible to develop a controlled drug delivery system with a DES based on [Ch]Cl and ascorbic acid.[113] This DES was used to increase the solubility of dexamethasone in several orders of magnitude and applied in the development of a drug delivery system also with blends of starch and SPCL. The drug release was studied *in vitro* in physiological-like conditions (37 °C, pH 7.4 in PBS solution), showing that the release plateau of this system is achieved after 3 days.[113] Such a fact highlights the advantage of using DES and biopolymer-based systems to tune the APIs release profile by modification of the system's properties.

Due to the ability of DES to increase the solubility, stability and permeation of drugs and biopolymers in aqueous media, they allow different types of systems to be prepared. In addition, and owing to their versatility, they are not only compatible with different strategies for materials' preparation, but also different types of administration can be envisaged. Regardless of the potential of DES in this field, there is still an insufficient number of works to fully understand the interaction of DES with biopolymers that could contribute to the conscious development of more effective drug delivery systems, and which needs to be expanded. The works herein revised support a new direction for the use of DES in the pharmaceutical area, with promising potential for implementation in the market.

Chapter 2. Boosting Active Pharmaceutical Ingredients Performance by New Formulations with DES
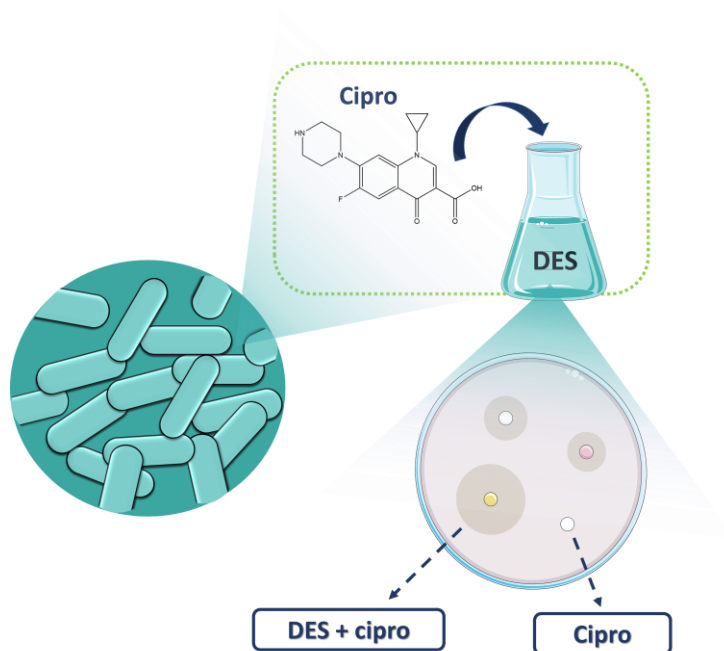
2.1 Abstract

The critical scenario of antimicrobial resistance to antibiotics highlights the need for improved therapeutics and/or formulations. Herein, is demonstrate that DES formulations are very promising to remarkably improve the solubility, stability and therapeutic efficacy of antibiotics, such as ciprofloxacin. DES aqueous solutions enhance the solubility of ciprofloxacin up to 430-fold while extending the antibiotic stability. The developed formulations can improve, by 2 to 4-fold, the susceptibility of Gram-negative (*Escherichia coli* and *Pseudomonas aeruginosa*) and Gram-positive (*Staphylococcus aureus*) bacteria to the antibiotic. They also improve the therapeutic efficacy at concentrations where bacteria present resistance, without promoting tolerance development to ciprofloxacin. Furthermore, the incorporation of DES decreases the toxicity of ciprofloxacin towards immortalized human epidermal keratinocytes (HaCat cells). The results herein reveal the pioneering use of DES in fluoroquinolone-based formulations and their impact on the antibiotic's characteristics and on its therapeutic action.

2.2 Introduction

In an era of increased resistance to antibiotics and consequent decreased antimicrobials' susceptibility, the risk of failure of standard therapies has become one of the major health challenges of society.[276] The ongoing emergence of new resistant bacteria has challenged the pharmaceutical industry's research and production; yet the development of new effective antibiotics has not been sufficiently successful to tackle this challenge. Given this critical scenario, other therapeutic strategies, such as bacteriophages with anti-CRISPR genes, monoclonal antibodies, host modulation and microbiome approaches have started to be investigated.[277]

Antibiotics regularly face economic drawbacks as older ones remain first in line for use in clinical practice, whereas new options in clinical pipeline are scarcely adopted or safeguarded as the last resort.[278,279] To pursue more profitable and effective alternatives, the improvement of the already existing formulations can help boost antibiotic performance for bacteria eradication.[280] Examples of this strategy include the research on nanoparticle-based systems with extended antibiotic release[281] and the use of antibiotic adjuvants, which have insufficient antibacterial activity, but when combined can augment or transform the activity of antibiotics.[282]

An example of progressive decrease in the susceptibility of several pathogens to antibiotics and increasing resistance mechanisms corresponds to the clinical use of antibiotics belonging to the quinolone family.[283] Among these, fluoroquinolones have been increasingly prescribed due to their broad-spectrum of action.[284] Ciprofloxacin, in particular, is ranked as one of the most important antimicrobials for human medicine applications.[279] Although Gram-negative bacteria like *enterobacteriaceae* are highly susceptible to this antibiotic, as well as *Pseudomonas aeruginosa*, some Gram-positive bacteria, like the *Staphylococcus* species, also present some susceptibility to this fluoroquinolone.[285] Unfortunately, due to its wide application, in the last decade an increased resistance rate to ciprofloxacin has been verified for these strains.[286] Therefore, the design of novel ciprofloxacin-based formulations must ensure higher efficacy, drug concentration above subinhibitory levels and prevent the development of resistance that will limit therapeutic efficacy.[287] However, ciprofloxacin, as many other antibiotics, is poorly water-

soluble, being its application in different dosage forms limited.[288] Therefore, the possibility to design formulations that can not only improve the solubility of the antibiotic in water but also improve its antimicrobial action is a mandatory demand.

In the present work, it is proposed an innovative formulation for antibiotics based, namely ciprofloxacin, on aqueous solutions of DES, that significantly boosts the drug's performance by overcoming its solubility, stability, susceptibility and resistance drawbacks. The therapeutic efficacy of drugs solubilized in DES is still shortly addressed and the potential brought by the numerous possibilities of design is not fully explored. So far, no reports on the application of DES to improve the antimicrobial activity of antibiotics have been found nor their potential to avoid bacterial resistance. Furthermore, DES are mainly investigated as neat compounds, being, as previously mentioned, aqueous solutions of DES less studied in the field of pharmaceuticals and APIs.[128,129]

Herein, is demonstrated the possibility to achieve remarkable solubility enhancements for ciprofloxacin in aqueous solutions of DES, while providing detailed insights towards the understanding of the simultaneous influence of the adequate DES design and the formulation of antibiotics in DES aqueous solutions in tackling therapeutic efficacy problems and antibiotic resistance. To this purpose it is shown the improved therapeutic effect achieved with these novel formulations on Gram-negative (*E. coli* and *P. aeruginosa*) and Gram-positive (*S. aureus*) bacteria.

2.3 Experimental section

2.3.1 Materials

The DES studied in this work were prepared using different HBD and HBA species. [Ch]Cl (≥ 99% purity) and urea (≥ 99% purity) were supplied by Sigma-Aldrich. Malonic acid (≥ 98% purity) was purchased by Fluka and L-proline (≥ 99% purity) by TCI chemicals. The citric acid (≥ 99% purity) was supplied by Panreac, and xylitol (≥ 99% purity) by Acros Organics. The antibiotic, ciprofloxacin, was acquired from Sigma-Aldrich (≥ 98% purity).

2.3.2 DES preparation and characterization

The DES investigated were prepared by mixing the respective precursors (HBAs and HBDs) in sealed glass vials with constant heating and stirring, until a homogeneous transparent liquid was formed (maximum temperature of 90 °C). The mixtures were then kept for one hour at this maximum temperature before returning to room temperature. DES were prepared at the following molar ratios: [Ch]Cl:urea:malonic acid ([Ch]Cl:U:MA), 1:2:0.05; proline:urea:malonic acid (Pro:U:MA), 1:1:0.05; and citric acid:xylitol (CA:Xyl), 2:1. The respective DES components' integrities were confirmed by ^{13}C and ^{1}H nuclear magnetic resonance (NMR). The ^{1}H NMR and ^{13}C NMR spectra were recorded using a Bruker Avance 300 at 300.13 MHz and 75.47 MHz, respectively, by previously dissolving the mixtures in deuterated water and using trimethylsilyl propanoic acid (TMSP) as an internal reference.

Cholinium Chloride:Urea: ^{1}H NMR (300.13 MHz, D_2O): δ 3.08 (9H, d, N(CH$_3$)$_3$); 3.39 (2H, m, H-2); 3.93 (2H, m, H-1) ppm. ^{13}C NMR (75.47 MHz, D_2O): δ 53.86 (N(CH$_3$)$_3$); 55.6 C-2); 67.38 (C-1); 162.40 (C-1').

Proline:Urea: ^{1}H NMR (300.13 MHz, D_2O): δ 1.84 (2H, m, H-4); 2.18 (2H, m, H-3); 3.20 (2H, m, H-5); 3.97 [1H, dd, H-2) ppm. ^{13}C NMR (75.47 MHz, D_2O): δ 23.69 (C-4); 28.87 (C-3); 45.97 (C-5); 60.90 (C-2); 162.90 (C-1); 174.34 (C-1') ppm.

Citric acic:xylitol: ^{1}H NMR (300.13 MHz, D_2O): δ 2.64 (4 H, dd, H-2,5); 3.26 - 3.58 (1H, m, H-3', 2H, m, H-2',4', 4H, m, H-1',5') ppm. ^{13}C NMR (75.47 MHz, D_2O):

δ 43.00 (C-2,5); 62.38 (C-1',5'); 70.51 (C-2',4'); 71.68 (C-3'); 73.01 (C-3); 173.12 (C-1,6); 176.39 (C-4) ppm.

2.3.3 Ciprofloxacin's solubility assays

Ciprofloxacin was added in excess to 2.0 g of each DES aqueous solution (0-60% (w/w) of DES) and pure water and placed in sealed glass vials with a stirring bar. These mixtures were allowed to equilibrate in a specific aluminum disk placed on a stirring plate with heat control, at constant temperature (25 and 37 °C) and stirring (900 rpm) over 72 h. Due to the high viscosity of the obtained solutions, it was only possible to study ciprofloxacin's solubility up to 60% (w/w) of DES in an aqueous solution. After saturation of the DES aqueous solutions, the samples were centrifuged, and a supernatant aliquot was taken and diluted in water. After this, the sample was carefully filtered with a 0.45 μm syringe filter to remove any solid from the liquid phase and subsequently quantified by high-performance liquid chromatography with diode-array detection (HPLC-DAD, Shimadzu, model PROMINENCE). HPLC analyses were performed with an analytical C18 reversed-phase column (250 × 4.60 mm), Kinetex 5 μm C18 100 Å, from Phenomenex. The mobile phase consisted of 25% (v/v) of acetonitrile and 75% (v/v) of ultra-pure water with 0.3% (v/v) of orto-phosporic acid. The separation was conducted in isocratic mode, at a flow rate of 0.8 mL·min^{-1} and using an injection volume of 10 μL. The column oven and the autosampler operated at 35 °C. The wavelength was set at 280 nm and each sample was analyzed at least in duplicate form. Calibration curves were obtained using the pure ciprofloxacin dissolved in the mobile phase. Under these conditions, ciprofloxacin displays a retention time of 3.3 min.

2.3.4 Stability of DES formulations

To evaluate the stability of the drug in the DES aqueous solutions and in pure water, the drug was dissolved 10 times below its solubility limit (at 3.00×10^{-5} mol·mL^{-3}) in water, to guarantee its full solubility. The same amount of drug was solubilized in each DES aqueous solution. An aliquot of each solution was collected and analyzed by HPLC-DAD to obtain the initial profile for each formulation. Then, the formulations were kept in the dark at 25 °C and 75−80% relative humidity for 30

days. After this period new samples were collected and analyzed. The drug concentration in water and in the DES' formulations was quantified by HPLC-DAD using the method described above. The stability of the DES aqueous solution in the absence of the antibiotic was conducted by Fourier Transform Infrared with Attenuated Total Reflectance (FTIR-ATR) to evaluate changes in the functional groups of the DES components. The spectrum of each sample was acquired in a FTIR system Spectrum BX, PerkinElmer, equipped with a diamond crystal and a single horizontal Golden Gate ATR cell. The analyses of the solutions at 40% (w/w) of DES were performed at room temperature (25 ± 2) °C with controlled relative humidity (75—80%). Samples were collected on the day of preparation of the DES solutions and after 30 days at the storage conditions. All data were recorded in the range of 4000—400 cm^{-1} with a resolution of 4 cm^{-1} and by accumulating 32 scans with an interval of 1 cm^{-1}. For all the spectra acquired, the background air spectrum was subtracted, and the results were recorded as transmittance values.

2.3.5 Bacterial strains and culture conditions

The strains of *Echerichia coli* ATCC 25922, *Pseudomonas aeruginosa* ATCC 27853 and *Staphylococcus aureus* ATCC 6538 were grown on solid medium Trypic Soy Agar (TSA) (Liofilchem) at 37 °C during 24 h and posteriorly kept at 4 °C. Each bacterium strain was inoculated whenever necessary in liquid medium Trypic Soy Broth (TSB) and grown aerobically at 37 °C for 24 h under stirring (100 rpm). For each assay, an aliquot of this culture (300 µL) was transferred twice into a new fresh TSB medium (subcultured in 30 mL) and grew overnight at 37 °C under stirring.

2.3.6 Minimum Inhibitory Concentration (MIC) of ciprofloxacin formulated in DES aqueous solutions

Minimum Inhibitory Concentration (MIC) determination for *E. coli*, *P. aeruginosa* and *S. aureus* was achieved by broth dilution method.[289] Dilutions of standardized microbial suspension adjusted to 0.5 McFarland scale in TSB were prepared and dispensed in a 96-well microtitration plate. Ciprofloxacin solutions in water and formulated in DES were freshly prepared for a starting concentration of 10 µg·mL^{-1} of ciprofloxacin, and each were two-fold diluted along the 96-well

microtitration plate (12 concentrations for each ciprofloxacin formulated in DES were evaluated in the range 10—0.00244 µg·mL^{-1}). DES alone were also tested in the same concentration to infer their influence in the antimicrobial effect. After well-mixing, the optical density (O.D.) at 600 nm was read, and 96-well microtitration plate was incubated under suitable conditions at 37 °C for 24 h. After this time, O.D. at 600 nm was read and the MIC was achieved by the lowest concentration of antimicrobial agent that inhibits growth of each microorganism.

2.3.7 Antimicrobial susceptibility to ciprofloxacin in DES aqueous solutions

Antimicrobial activity of ciprofloxacin and DES formulations with the antibiotic was assessed by dissolving the pure antibiotic in water and in the DES [Ch]Cl:U:MA, Pro:U:MA and CA:Xyl aqueous solutions against *E. coli* ATCC 25922, *P. aeruginosa* ATCC 27853 and *S. aureus* ATCC 6538 strains. The susceptibility test was performed using the modified Kirby-Bauer disk diffusion method. Each bacterial suspension in physiological saline solution (PBS), with a turbidity of 0.5 on the McFarland scale, was prepared by peaking up 1–2 colonies from pure cultures. The suspension was spread plated using a swab on Mueller-Hinton Agar. Antimicrobial-impregnated disks were (BD BBL, Sensi-Disc) placed onto the cultures' medium surface. Disks containing 0.5 and 5 µg·mL^{-1} of the drug were used for *E. coli*, *P. aeruginosa* and *S. aureus* evaluation. The disks with the antibiotic in water and in aqueous solutions of DES with the antibiotic were placed and incubated at 37 °C for 18–24 h. Each DES was evaluated without the drug to determine its impact on the antimicrobial susceptibility. The antimicrobial efficacy of each formulation was determined by measuring the diameter of the zones of inhibition and compared with the zone diameter breakpoint established by EUCAST, European Committee on Antimicrobial Susceptibility Testing, and accordingly to the Clinical and Laboratory Standards Institute [CLSI].[290,291]

2.3.8 Bacterial inactivation efficacy by ciprofloxacin in DES solutions

The bacterial cultures (*E. coli*, *P. aeruginosa* and *S. aureus*) were grown overnight and were diluted and adjusted to 0.5 Macfarland scale in PBS, pH 7.4. The bacterial suspensions were equally distributed in 2 mL tubes. Afterwards, appropriate volumes of ciprofloxacin, CA:Xyl and Pro:U:MA alone and both deep eutectic solvent formulations with ciprofloxacin were added to achieve a final concentration of 0.5 µg·mL^{-1} of the antibiotic. A bacterium positive control (Ct) containing only the bacterial inoculum in PBS was also carried out. The inactivation efficiency of ciprofloxacin, each DES and DES formulations with ciprofloxacin were evaluated by quantifying the number of Colony Forming Units per mililiter (CFU·mL^{-1}). Aliquots of samples and control were taken at different incubation times (0, 1, 2, 3, 4, 6, 12 and 24 h). Each solution was serially diluted in PBS and each sample dilution was pour-plated TSA. The plates were incubated at 37 °C for 24 h and the CFU·mL^{-1} was counted. Experiments were carried out in duplicate and repeated three times.

2.3.9 Bacterial tolerance to ciprofloxacin in DES formulations

In order to verify the development of tolerance to the treatment with ciprofloxacin and the antibiotic formulated in the DES solutions, 7 cycles of inactivation under the conditions previously described were performed. The concentration of ciprofloxacin was equal to the previous ones used in the inactivation profile (0.5 µg·mL^{-1}). The time of exposure used was chosen based on the reduction of ca. ~50% in the CFU levels, 4 h for *E. coli* and 6 h for *P. aeruginosa*. After each cycle of treatment with pure ciprofloxacin and ciprofloxacin formulated in DES solutions, the *E. coli* or *P. aeruginosa* colonies that survived to the previous cycle of inactivation were aseptically removed from the TSA plates and re-suspended in PBS, and then undertook the same inactivation protocol. The optical density of both bacteria suspension, before each assay, was measured to prevent differences in the treatment efficiency. Three independent assays in duplicate were performed for each strain.

2.3.10 Keratinocytes cell culture and cytotoxicity assay

Immortalized human epidermal keratinocytes (HaCaT cells) obtained from Cell Lines Services (Eppelheim, Germany) were cultured in Dulbecco's modified Eagle's medium (DMEM) supplemented with 10% of fetal bovine serum (FBS) and 1% of L-glutamine, penicillin– streptomycin and fungizone (Life Technologies, Grand Island, NY, USA) and incubated in a humidified atmosphere at 37 °C and 5% CO_2. Cytotoxic effect of ciprofloxacin aqueous solution, of ciprofloxacin formulated in DES aqueous solutions and of the DES formulations without the drug was assessed on HaCat cells by the colorimetric MTT (3- (4,5-dimethylthiazol-2-yl)-2,5-diphenyltetrazolium bromide) assay. For this purpose, HaCaT cells were seeded in 96-well plates at a concentration of 15 000 cells·mL^{-1} and allowed to adhere for 24h. After adhesion, cells were exposed to a range of five concentrations (0.05–0.75 µg·mL^{-1}), of the tested compounds diluted in DMEM medium (these previously sterilized with a 0.22 µm syringe filter) and incubated for 72 h at 37 °C in 5% of CO_2. After this period, the wells were washed with PBS, and 100 µL of fresh medium was placed in each well, as well as 50 µL of MTT solution (1 mg·mL^{-1} in PBS, pH 7.2) was added to each well. After 4 h of incubation, the medium was replaced with 150 µL of DMSO to dissolve the formazan crystals. Posteriorly, the plate was shaken for approximately 2 h, protected from light. Cell viability was measured through the optical density of reduced MTT at 570 nm using a microplate reader (Synergy HT from BioTeK Instruments Inc., Winooski, VT, USA). The percentage of viable cells was calculated as the ratio between the absorbance of treated versus control cells.

2.4 Results and discussion

2.4.1 Selection and preparation of DES for ciprofloxacin solubilization

The DES components used in this work were carefully selected given the intended purpose, i.e., of improving the antibiotic's therapeutic action and to allow different administration routes for drug delivery. After an initial screening of potential biocompatible DES components, three DES with different hydrogen-bond acceptors and donors, namely [Ch]Cl:urea ([Ch]Cl:U (1:2)), proline:urea (Pro:U (1:1)) and citric

acid:xylitol (CA:Xyl (2:1)) were selected. [Ch]Cl was chosen since it is a strong hydrogen-bond acceptor and one of the most extensively explored compounds to create DES.[127] Urea was selected since it has been one of the most investigated hydrogen-bond donor species coupled to [Ch]Cl to create DES,[104] whereas citric acid was selected due to its effective results reported for the control of skin and soft tissue infections,[292] The additional hydrogen-bond acceptor, proline, was chosen based on the reported capability of proline-based DES to improve the *in vivo* pharmacokinetic parameters of nutraceuticals,[131] with the DES Pro:U allowing a direct comparison with [Ch]Cl:U. Finally, xylitol was considered due to its antibacterial and antioxidant properties.[293] All these DES were prepared by the heat method, being in a jellified form at body's temperature, with the exception of [Ch]Cl:U that is liquid at this temperature.

It is known that the pH of wounds can influence the effectiveness and performance of antibiotics and antiseptics or potentially alter the metabolic state of bacteria.[294] Alkaline media allow bacterial growth and acquired resistance; in this sense, an acidic environment is more promising for the effective treatment of infections. When considering a topical application purpose, for instance, the alkaline pH associated with the urea-based DES used in this work could compromise the therapeutic action of the formulation. Thus, the pH of the investigated DES was adjusted to a more suitable value to fulfil the requirements for a wide range of applications. For this purpose, malonic acid was used at a fixed molar ratio in the DES [Ch]Cl:urea:malonic acid ([Ch]Cl:U:MA (1:2:0.05)) and proline:urea:malonic acid (Pro:U:MA (1:1:0.5)) to adjust the pH of the mixtures to a final pH near 4.5.

The hydrogen-bond donors/acceptors integrity was maintained over the DES' preparation; the respective chemical stability of the components was confirmed for the remaining DES formulations based on ^{1}H and ^{13}C NMR. The results reveal the components' integrity due to the similarity of the characteristic resonances of the individual components to those obtained for each DES. The ^{1}H NMR spectrum of [Ch]Cl:U (Figure 16a) presented the typical resonances of [Ch]Cl, presenting the proton resonances of $N(CH_3)_3$ at 3.08 ppm, of the CH_2 protons (H-2,1), as multiplets at 3.39 ppm and 3.93 ppm, respectively. Similarly, the ^{13}C NMR spectrum of this DES (Figure 16b) presented the carbon resonance from $N(CH_3)_3$ of [Ch]Cl at 53.86

ppm and the ones from C-2 and C-1 at 67.38 ppm and 55.6 ppm, respectively. The carbon resonance of C-1' from urea can be observed at 162.40 ppm, matching those found in literature.[295]
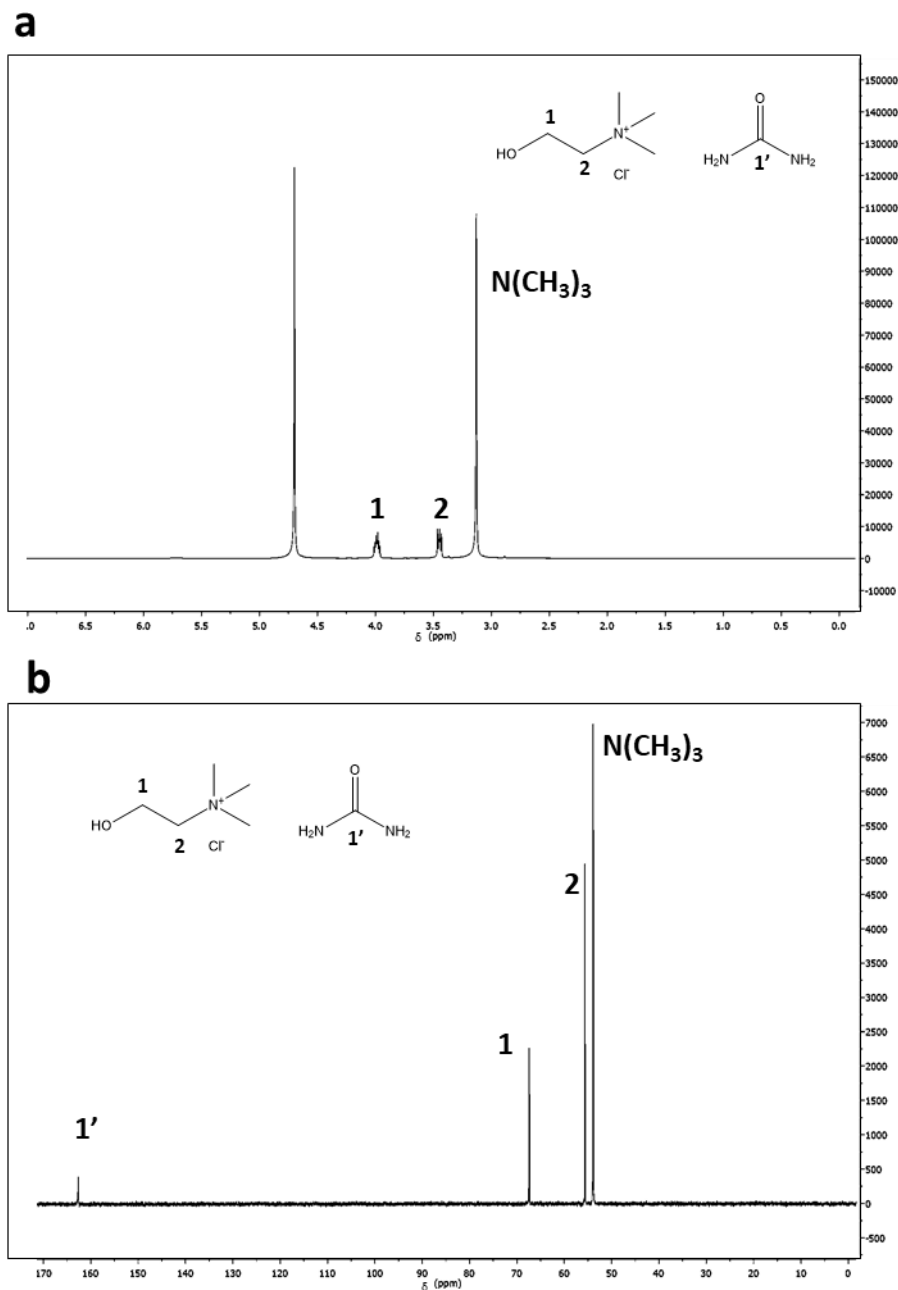
Figure 16. ^{1}H NMR (a) and ^{13}C NMR spectra (**b**) spectra of [Ch]Cl:U DES in D$_2$O.

In Figure 17a is presented the ^{1}H NMR spectrum of Pro:U, were likewise the observed resonances are coincident with those expected for the single components, being possible to observe the proton resonances from H-4,3,5 of proline's ring at 1.84 ppm, 2.18 ppm and 3.20 ppm, as well as the resonance of H-2 at 3.97 ppm.

The ^{13}C NMR spectrum (Figure 17b) shows carbon resonances of from the CH_2 groups of proline's ring at 23.69 ppm, 28.87 ppm and 45.97 ppm, and of the C-1 group at 60.90 ppm. The resonances of the carboxyl and carbonyl group of proline (C-1) and urea's (C-1') appear at 162.90 ppm and 174.34 ppm, respectively.
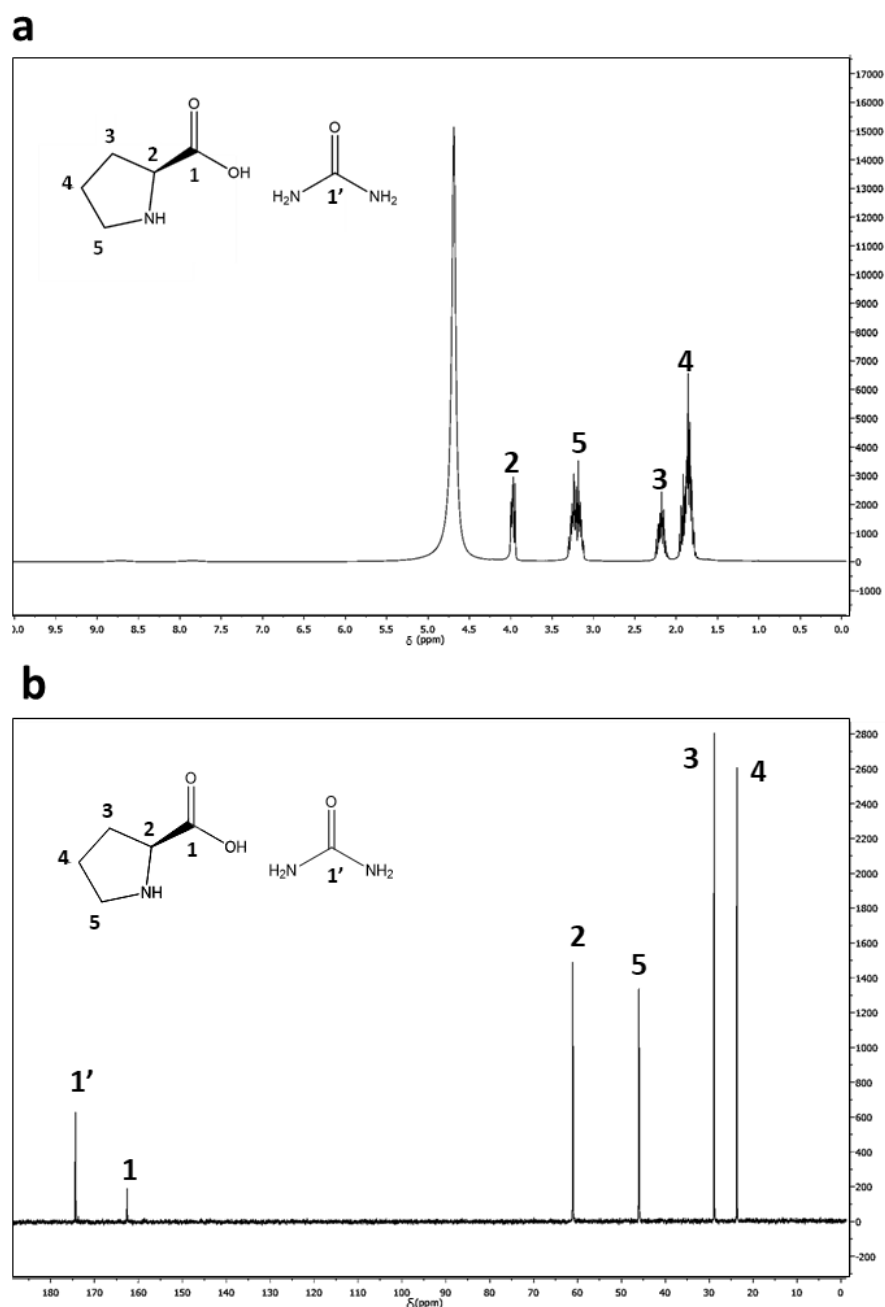
Figure 17. ^1H NMR (**a**) and ^{13}C NMR spectra (**b**) spectra Pro:U DES in D_2O.

The ^1H NMR spectrum of CA:Xyl, depicted in Figure 18a, also confirms the components integrity. The proton resonances from the CH_2 protons (H-2,5) of citric

acid, appear as expected as a double duplet at 2.64 ppm, while the proton resonances from the H-3', H-2',4' and H-1',5' of xylitol can be observed as multiplets in the range of 3.26 -3.58 ppm. In the same way, the resonances in the ^{13}C NMR spectrum of this DES (Figure 18b) shows the carbon resonance of C-2,5 of citric acid (43.00 ppm) and xylitol's (C-1',5' at 63.38 ppm and C-2',4' at 70.51 ppm). Also, the C-3' of xylitol and C-3 of citric acid were found at 71.68 ppm and 73.01 ppm, respectively. The carboxyl groups of citric acid (C-2,6 and C-4) appear, at higher chemical shifts, being observed at 173.12 ppm and 176.39 ppm.
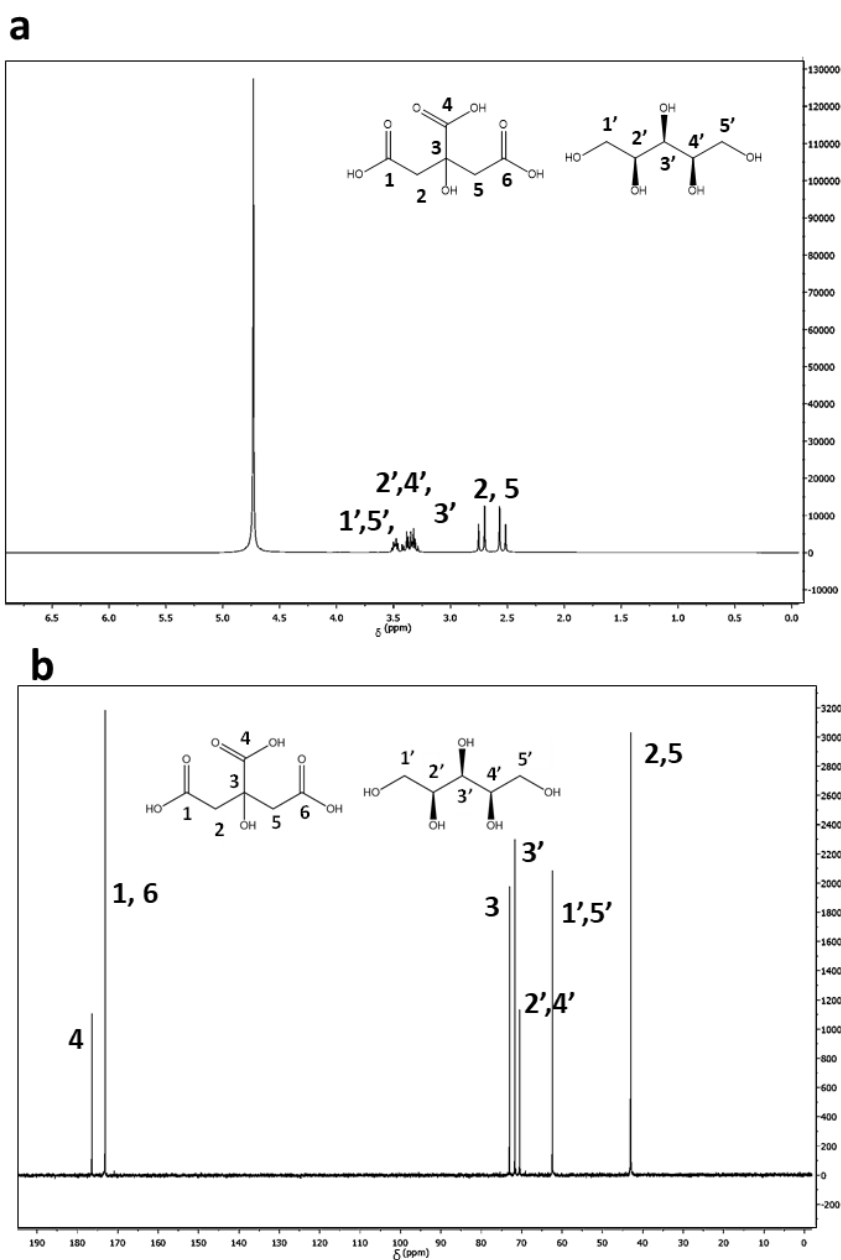
Figure 18. ^{1}H NMR (a) and ^{13}C NMR spectra (b) spectra of CA:Xyl DES in D$_2$O.

2.4.2 Ciprofloxacin solubility in aqueous solutions of DES

The three selected DES ([Ch]Cl:U (1:2), Pro:U (1:1) and CA:Xyl (2:1)) were tested allowing to appraise the effect of their HBDs (urea, xylitol) and HBAs ([Ch]Cl, proline, citric acid) on the solubilization of ciprofloxacin. Solubility was tested up to 60% (w/w) of DES due to the high viscosity of the solvent above these concentrations. To better understand which concentrations should be applied in the formulations, the ciprofloxacin's solubility enhancement in each DES aqueous solution was assessed at both room (25 °C) and human body (37 °C) temperatures. Figure 19 depicts the solubility curves and the results in solubility enhancement determined for each DES aqueous solution (S/S_0, where S corresponds to the solubility of ciprofloxacin in the DES aqueous solution and S_0 to the solubility of ciprofloxacin in water at the same temperature and at the same pH of 4.5).
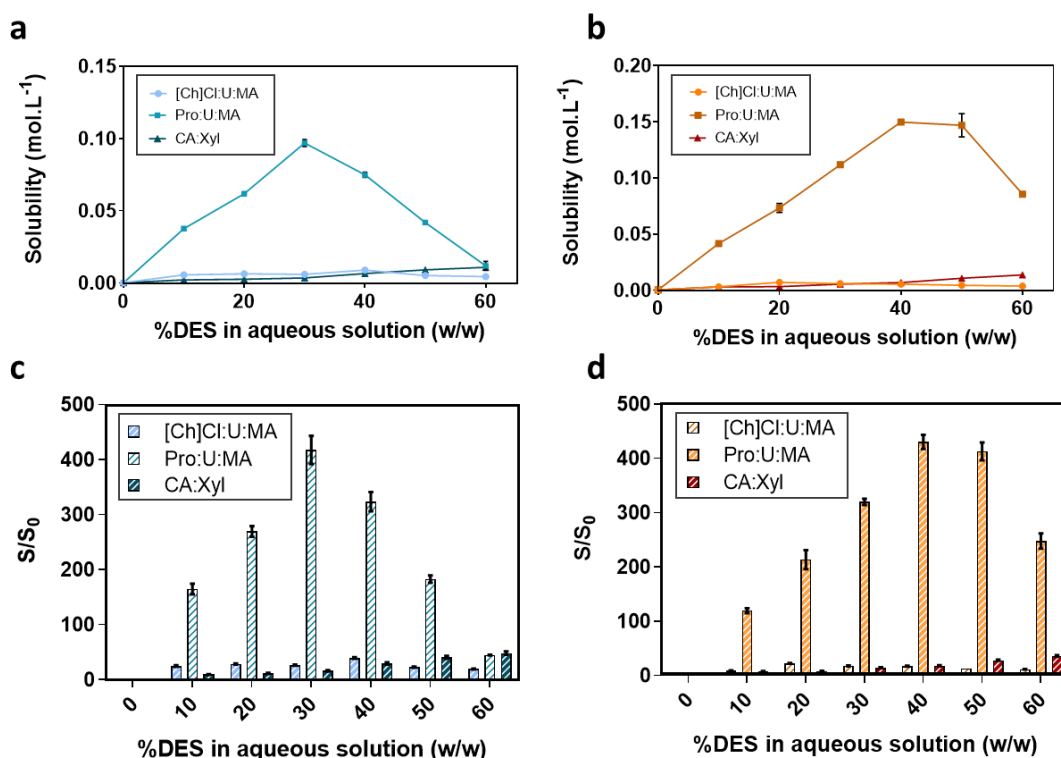
Figure 19. Solubility behavior of ciprofloxacin in [Ch]Cl:U:MA, Pro:U:MA and CA:Xyl aqueous solutions. (a) Solubility studies at room and (b) human body's temperature. The solubility values (mol·L^{-1}) were determined after 72 h of equilibrium. All solutions were studied at the same pH and temperature conditions. Solubility enhancement of ciprofloxacin in DES aqueous solutions (c) at room temperature and (d) human body's temperature. The results are expressed as the mean ± SD of three independent measurements.

66

Ciprofloxacin shows low solubility in common organic solvents such as ethanol, 2-propanol or acetone[296] and notably in water ($<3.00 \times 10^{-4}$ mol·mL^{-1} at pH=4.5), limiting its formulation. In fact, ethanol seems to exhibit lower capability than water and acetone to solubilize this antibiotic, and even lower for its hydrochloride form.[296] Due to the pH-dependent solubility of ciprofloxacin in aqueous media, its solubility is higher at pH values below 5.5.[297] Generally, improvements in solubilization are achieved by addition of diluted hydrochloric acid (as used in this work), and in case of intravenous formulations, using lactic acid achieving pH values up to 4.6.[298] Although DES are known for their high solvation ability for some APIs, such as anti-inflammatory, analgesic or antifungal drugs,[110,134] the study of the influence of DES aqueous solutions solubilization of APIs has only been recently been described. [128,129] The pH adjustment of these mixtures for a specific application has not been fully explored for pharmaceutical purposes.

As determined in the present study, the ciprofloxacin solubility in water was found to be $(2.28 \pm 0.01) \times 10^{-4}$ mol·mL^{-1} and $(3.61 \pm 0.20) \times 10^{-4}$ mol·mL^{-1} at room and human body temperatures, respectively (which is in the range of the values mentioned above). Remarkably, the studied aqueous solutions of DES allowed to enhance the solubility of ciprofloxacin in aqueous media to $(9.70 \pm 0.20) \times 10^{-2}$ mol·mL^{-1} at room temperature (Figure 19a) and $(1.50 \pm 0.04) \times 10^{-1}$ mol·mL^{-1} at body's temperature (Figure 19b), respectively, using Pro:U:MA. This DES allowed solubility enhancements up to 430-fold using only at 30% of Pro:U:MA in solution (w/w) at room temperature (25 °C, Figure 19c) and at 40% (w/w) at body's temperature (37 °C, Figure 19d).

The Pro:U:MA DES is not only among the best DES aqueous solutions studied, but also allows a similar to higher solubilization ability for ciprofloxacin than its hydrochloride form (by 2 orders of magnitude).[296] This DES, allows a non-monotonic solubility enhancement in aqueous media at both temperatures, with a solubility behavior indicative of an hydrotrope- mediated mechanism.[299] At room temperature, is possible to enhance ciprofloxacin's solubility from 160-fold (using 10% (w/w) of DES) to 430-fold at 30% (w/w) of DES. The solubility enhancement then decreases when higher DES concentrations are used, achieving a 44-fold increase at 60% (w/w) of DES (Figure 19c). Considering the results at body's temperature, a similar

behavior is observed, solubility improvements from 117-fold, at 10% (w/w) of DES, to 430-fold at 40% (w/w) of DES are observed, reaching also a minimum at 60% (w/w) of DES, where a 238-fold increase in ciprofloxacin's solubility could be obtained (Figure 19d).

Aqueous solutions of the DES CA:Xyl present a monotonic increase of solubility within the studied DES concentration range, with a minimum at 10% (w/w) of DES (10-fold, at body's temperature (Figure 19c) and 8-fold, at body's temperature (Figure 19d)). The maximum in the solubility enhancement occurred at 60% (w/w) of DES for both room (50-fold, Figure 19c) and body's temperature (35-fold, Figure 19d). The observed behavior is in accordance with a co-solvency mechanism.[300] Aqueous solutions of [Ch]Cl:U:MA exhibited the lower ciprofloxacin solubility enhancement among the studied DES, presenting a maximum of approximately 40-fold increase at 40% (w/w) at 25 °C (Figure 19c) and up to 20-fold at 37 °C at 20% (w/w) of DES (Figure 19d). The [Ch]Cl:U:MA presents the same mechanism of solubilization of Pro:U:MA, hydrotrope-mediated. It is possible to increase the solubility of the antibiotic from 24-fold (using 10 % (w/w) of DES) to its maximum at 40% (w/w) of DES, and similarly to the Pro:U:MA behavior find a minimum at 60% (w/w) of DES (19-fold, Figure 19c) at room temperature. At body's temperature, the solubility enhancements at 10% (w/w) of DES are similar to those obtained using a 60% (w/w) DES solution (10-fold, Figure 19d). This DES presents the lowest ability of all DES aqueous solutions to solubilize the antibiotic. Although [Ch]Cl and proline seem to play a significant role in this mechanism, the [Ch]Cl had a lower impact on the solubilization ability.

Recent studies have been dedicated to understanding the influence of amino acid-based DES on antibiotics' solvation, namely β-lactam ones.[301] These findings highlight the strong solute−solvent intermolecular interactions along with a slight volume expansion. In the case of ciprofloxacin solubilization, the key for the observed efficacy of the studied DES relies also in the interactions with the DES components taking advantage of the different types of HBA/HBD sites in the antibiotic structure, that lead to highly effective interactions in the case of Pro:U:MA. Given the high solubility enhancements achieved at 40% (w/w) of all DES in

68

aqueous solution at room temperature, this DES concentration was selected for further studies.

2.4.3 Ciprofloxacin stability in aqueous solutions of DES

Prior to the solubilization of the components in aqueous media, the physical appearance of the three DES with solubilized ciprofloxacin was monitored over one week. These formulations were monitored for changes in color, homogeneity and drug precipitation. No physical changes were verified for the formulations at room temperature conditions (25 °C) as depicted in Figure 20a. To determine the shelf-life of ciprofloxacin in the novel aqueous formulations, the stability of the solvents (DES aqueous solutions at 40% (w/w)) and of the API formulated in the DES aqueous solutions was accessed. Stability experiments were carried out at storage conditions of 25 °C and 75—80% relative humidity, in the dark. The drug concentration in the DES formulations was determined during a one-month period (T_{30}) at the same storage conditions. DES formulations containing the API were prepared by dissolving ciprofloxacin below its solubility limit, namely 3.00×10^{-5} mol·mL^{-1}, in aqueous solutions of DES and by direct dissolution in water at the same pH=4.5 for direct comparison purposes. Table 5 presents the ciprofloxacin content in each DES formulation and when solubilized in water (T_{30}), relative to initial drug concentration (at T_0).

Table 5. Effect of the solvent on ciprofloxacin's stability in aqueous media when stored at room temperature for 30 days.

Ciprofloxacin content (% ± SD)		
Solvent	T_0	T_{30}
Water	100 ± 0	52.3 ± 3.1
Water + 40% [Ch]Cl:U:MA	100 ± 0	80.7 ± 0.7
Water + 40% Pro:U:MA	100 ± 0	98.4 ± 0.5
Water + 40% CA:Xyl	100 ± 0	94.7 ± 0.6

It is known that ciprofloxacin aqueous solutions have limited stability at room temperature, thus being stored at low temperatures (-18 to 4 °C) to decrease degradation.[302] Alternatively, in aqueous solution, the antibiotic can be stable for 14 days at room temperature with addition of either 5% dextrose or 0.9% sodium

chloride;[298,303] the stability of the mentioned solutions can be further improved up to one month, through their storage in polyvinylchloride minibags.[303] DES have also been explored to improve the chemical, thermal, and photostability of drugs, being proved to be effective pharmaceutical excipients to enhance the stability of formulations during the storage.[141,143]
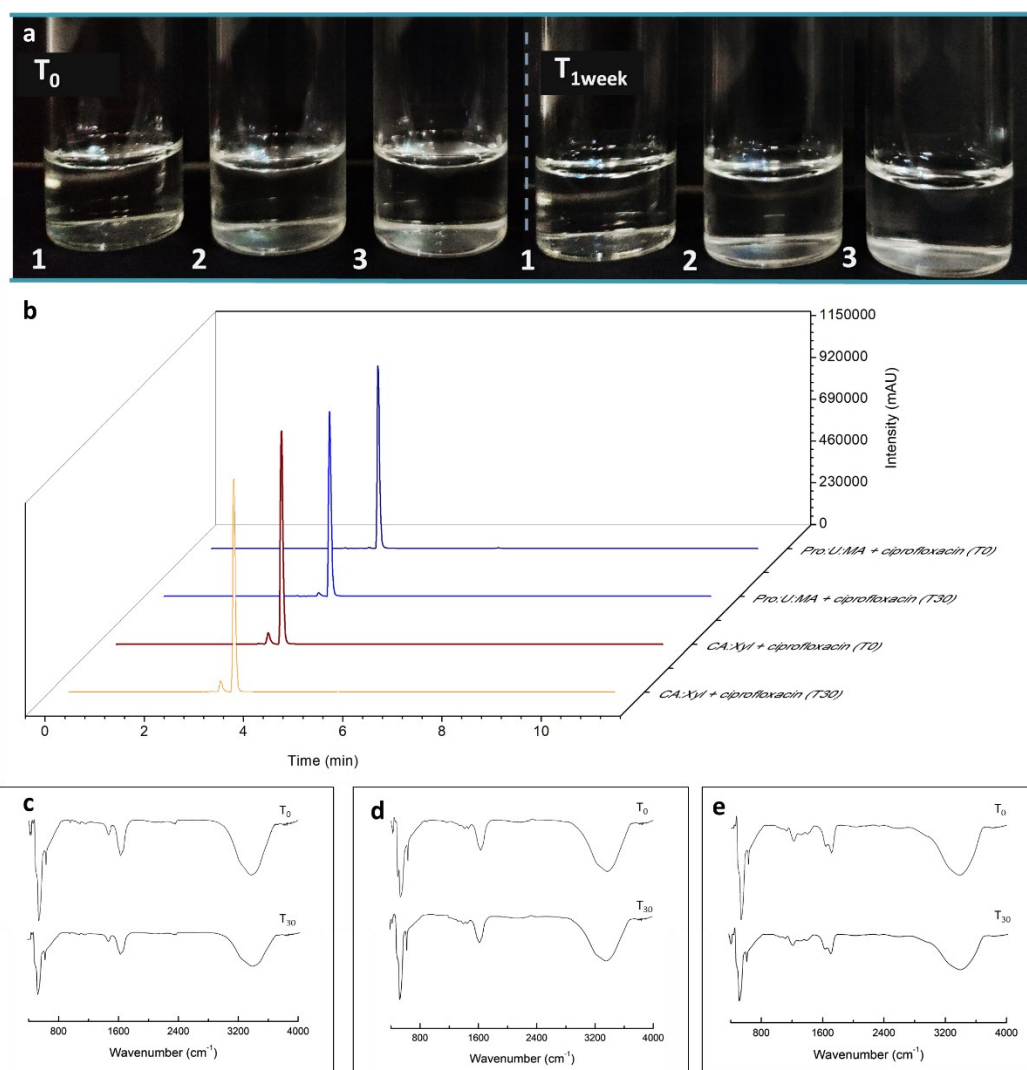
Figure 20. (a) Physical appearance of DES formulations comprising ciprofloxacin (1 mg·mL-1) after preparation and after one week at 25 °C and 75-80% relative humidity: (1) [Ch]Cl:U :MA, (2) Pro:U :MA, (3) CA:Xyl. (b) Stability of ciprofloxacin in DES formulations (Pro:U:MA and CA:Xyl). HPLC chromatograms of ciprofloxacin at the day of preparation of the formulations (T_0) and after 30 days (T_{30}) of storage at 25 °C. Ciprofloxacin's peak retained its shape and retention time after 30 days. Solvent stability during long-term storage. FTIR spectra of 40 (w/w) % of (c) [Ch]Cl:U:MA, (d) Pro:U:MA and (e) CA:Xyl in aqueous media at the first (T_0) and last day of storage (T_{30}) at 25 °C.

The results obtained here for the drug content in pure water, after 30 days, show a decrease in the concentration of ciprofloxacin to 52.3%, reinforcing the reported instability of this antibiotic in water and the need to develop improved formulations. The chromatograms shown in Figure 20b demonstrate that no significant degradation peaks of ciprofloxacin appear and only a slight decrease in drug concentration was observed after 30 days. More specifically, the DES aqueous solutions used here allowed to preserve 98.4% and 94.7% of ciprofloxacin in aqueous media, using only 40% (w/w) of Pro:U:MA and CA:Xyl, respectively, well above the required 90% as reported in the literature.[303]

The stability values are similar to ones achieved by the formulation of the antibiotic in lipidic- nanoparticles and nanoemulsions, designed to protect the drug from aqueous media and avoid the hydrolysis of APIs.[304,305] In the case of [Ch]Cl:U:MA aqueous solution only 80.7% of the drug was found in the solution at day 30, highlighting the importance of the nature of the DES in the stability of the drug. Furthermore, the stability of the studied DES aqueous solutions was analyzed by FTIR-ATR after the end of 30 days (Figure 20c, 20d and 20e), and as far as the technique can ascertain, no significant changes in the DES functional groups vibrations specific were verified at the end of this period.

2.4.4 Susceptibility of bacteria to formulations of ciprofloxacin in DES aqueous solutions

The antimicrobial activity of ciprofloxacin formulated in DES aqueous solutions was evaluated towards Gram-negative bacteria, *E. coli* ATCC 25922 and *P. aeruginosa* ATCC 27853, and Gram-positive bacteria, S. *aureus* ATCC 6538. The results achieved were compared to the antibiotic in water at the same concentration. For all the antimicrobial assays, the potential pH interference was eliminated by adjusting the pH of all solutions to more suitable values for bacterial growth, namely to pH= 6.8. The study involved firstly the determination of the MIC by the dilution method, whose results are shown in Table 6. The strains used in this work can be classified as susceptible to ciprofloxacin and the drug susceptibility results are in agreement with the EUCAST classification.[291] As expected, these bacteria are not susceptible to the pure DES solutions in the range of the studied concentrations.

Table 6. Minimal inhibitory concentrations of ciprofloxacin in water and in DES aqueous solutions for *E. coli* ATCC-25922, *P. aeruginosa* ATCC-27853 and *S. aureus* ATCC 6538. Results obtained for DES aqueous solutions (results without ciprofloxacin are also included for comparative purposes). Results are of three independent concordant experiments for each formulation and for each strain.

Minimum Inhibitory Concentration ($\mu g \cdot mL^{-1}$)			
	E. coli	*P. aeruginosa*	*S. aureus*
Ciprofloxacin	0.00488	0.00488	0.00977
[Ch]Cl:U:MA+ Ciprofloxacin	0.00488	0.00488	0.00244
Pro:U:MA+ Ciprofloxacin	0.00488	0.00244	0.00244
CA:Xyl + Ciprofloxacin	0.00488	0.00244	0.00244
[Ch]Cl:U:MA	-	-	-
Pro:U:MA	-	-	-
CA:Xyl	-	-	-

For *E. coli*, the results obtained show that the MIC values of the formulations of ciprofloxacin in DES aqueous solutions are similar to those observed for the antibiotic in water. This fact demonstrates that the solubilization of ciprofloxacin in DES aqueous solutions does not affect the efficacy of the drug towards this bacterium. In what concerns the *P. aeruginosa* and *S. aureus* bacteria, an increase in growth inhibition was observed with ciprofloxacin formulated in the DES aqueous solutions comparing to the antibiotic in water at the same pH. Furthermore, it is noticeable that Pro:U:MA and CA:Xyl aqueous solutions present higher ability to improve the antimicrobial activity against *P. aeruginosa* than [Ch]Cl:U:MA.

Table 7 and Figure 21 show the results of the antibiotic´ susceptibility in the three DES aqueous solutions and in water on the studied bacteria. Overall, the diffusion of the drug into the media is not affected by DES aqueous solutions and can match or even increase the growth inhibition zones of the pure antibiotic when compared to ciprofloxacin in water. As expected, aqueous solutions of DES (without ciprofloxacin) do not present antimicrobial activity in the concentrations used for ciprofloxacin's solubilization, being in accordance with the results obtained for the MIC analysis.

Table 7. Results on antimicrobial susceptibility of *E. coli* ATCC-25922, *P. aeruginosa* ATCC-27853 and *S. aureus* ATCC 6538 to ciprofloxacin in water and to the antibiotic formulated in DES aqueous solutions at different concentrations.

[Cipro] (µg·mL^{-1})	Inhibition zone diameter (mm)			
	Ciprofloxacin	[Ch]Cl:U:MA + Ciprofloxacin	Pro:U:MA + Ciprofloxacin	CA:Xyl + Ciprofloxacin
E.coli				
0.5	26	26	28	26
5.0	31	32	35	32
P.aeruginosa				
0.5	-	2	5	6
5.0	15	14	18	23
S.aureus				
5.0	4	3	7	6
10.0	13	12	17	14

All bacteria are susceptible to ciprofloxacin and to the antibiotic formulated in the DES aqueous solutions according with EUCAST classifications, and at the same (5.0 µg·mL^{-1}) and even at lower (0.5 µg·mL^{-1}) concentrations. The only exception to this trend occurs with *S. aureus* where higher doses are required to observe bacteria susceptibility (Figure 21e and 21d). Similarly, at lower drug concentrations (0.5 µg·mL^{-1}) *P. aeruginosa* seems to be resistant to the antibiotic solubilized in water. However, a noticeable enhanced effect is observed when the DES solutions are combined with the antibiotic. Considering the results obtained for *P. aeruginosa* (Figure 21b and 21c), a higher impact on the antibiotic's growth inhibition activity is noticed with the formulations comprising Pro:U:MA and CA:Xyl, at both concentrations (0.5 and 5.0 µg·mL^{-1} for *P. aeruginosa*). In this case, a prominent increase on the susceptibility of the bacteria to the antibiotic occurs when using aqueous solutions of Pro:U:MA acid and CA:Xyl (5 ± 2 mm and 7 ± 2 mm, respectively, comparatively with the antibiotic in water that has no activity).

Figure 21. Antimicrobial susceptibility to ciprofloxacin formulated in DES aqueous solutions. Representative inhibition zone assay on cultures using disks impregnated with ciprofloxacin's aqueous solutions with [Ch]Cl:U:MA, Pro:U:MA, CA:Xyl on TSA plates. (a) and (b) for *E. coli* ATCC-25922, the antibiotic was tested at 0.5 (a) and 5.0 (b) µg·mL^{-1}, respectively. (c) and (d) show the representative inhibition zone assays on *P. aeruginosa* ATCC-27853 cultures using disks impregnated with ciprofloxacin's formulations with the same DES in the same concentrations. (e) and (f) demonstrate the antimicrobial susceptibility of *S. aureus* ATCC 6538 to these solutions with the antibiotic at concentrations of 5.0 (e) and 10 (f) µg·mL^{-1}, respectively. Ciprofloxacin in water and the DES aqueous solutions (without ciprofloxacin) were evaluated in the same concentrations.

For *E. coli* and *S. aureus*, the effect of the antibiotic in DES aqueous solutions is less pronounced. For E. coli the susceptibility to the antibiotic is similar when solubilized in water or in DES aqueous solutions, with the exception of the formulation with Pro:U:MA in which a slight effect is denoted (35 ± 2 mm *vs.* 31 ± 2 mm for ciprofloxacin in water at 5.0 µg·mL^{-1}, in Figure 21b). Regarding *S. aureus*, and despite the higher dosages required, the formulations with Pro:U:MA and CA:Xyl are also slightly more effective than the ones with the antibiotic in water (7 ± 2 mm and 6 ± 2 mm *vs.* 4 ± 2 mm for ciprofloxacin in water at 5.0 µg·mL^{-1} – cf. in Figure 21e). Accordingly, for all strains, the antibiotic formulation with [Ch]Cl:U:MA has equal or lower effect than the antibiotic in water.

It is always relevant to address different DES combinations since, as demonstrated in this work, each DES presents a different impact in the therapeutic efficacy of the antibiotic. This trend is specially observed for the antimicrobial activity of the antibiotic formulated in [Ch]Cl:U. [Ch]Cl:U is amongst the most studied DES, with antimicrobial activity studies against similar microorganisms in the absence of APIs already reported.[151] Nonetheless, this DES does not represent an effective alternative to improve ciprofloxacin performance, has seen for its effect on the studied bacteria in comparison to the remaining formulations, and additionally for its higher toxicity.[306] Thereby, the two best formulations correspond to ciprofloxacin in aqueous solutions of Pro:U:MA and CA:xyl, which were selected for further experiments. Also, 0.5 µg·mL^{-1} was the concentration selected for further studies since it corresponds to the lowest one presenting antimicrobial activity against the bacteria, while envisaging the reduction of the antibiotic dosage.

The inactivation efficiency was evaluated by exposure of the three bacteria strains, *E. coli* (Figure 22a), *P. aeruginosa* (Figure 22b) and *S. aureus* (Figure 22c) to 0.5 µg·mL^{-1} of the antibiotic in water and to the antibiotic formulated in the selected DES aqueous solutions during 24 h. Bacterial controls without these formulations were also evaluated to guarantee the bacterial viability during the time and conditions of the experimental procedure. As previously described, the results of the new formulations were compared with the activity of ciprofloxacin in water at the same concentration and pH in aqueous media. The DES formulations were tested in the same concentrations present in the formulations with ciprofloxacin. The

gathered results (Figure 22) demonstrate different profiles according to the formulation type and strain considered.
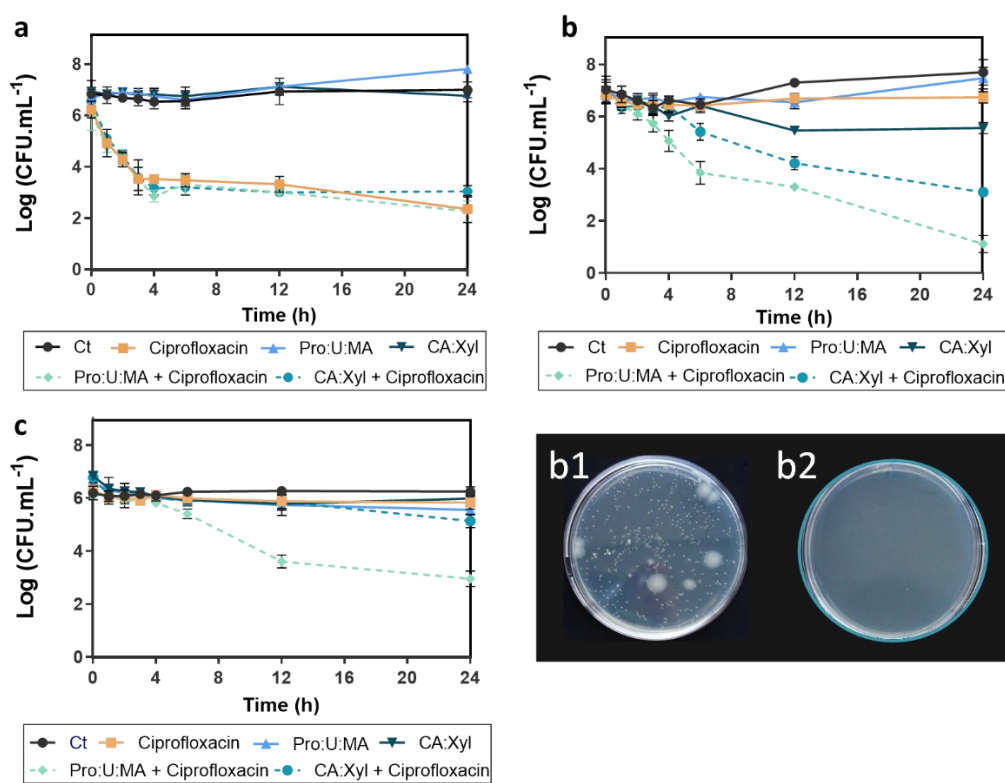
Figure 22. Effect of different times of exposure of bacteria to ciprofloxacin in water, to DES solutions (without ciprofloxacin) and to the formulations of ciprofloxacin in DES solutions in the inactivation efficiency bacteria. Inactivation profiles were determined for (a) *E. coli*, (b) *P. aeruginosa* and (c) *S. aureus* strains on PBS at 37 °C. The number of Colony Forming Units per mililiter (CFU·mL^{-1}) from samples collected over 24 h are shown. An antibiotic dose of 0.5 µg·mL^{-1} was used in all experiments. (b1) and (b2) demonstrate the difference between ciprofloxacin's ability to inactivate P. aeruginosa in water and formulated in an aqueous solution of Pro:U:MA, respectively, after 24 h. Data are presented as mean ± SD values of three independent studies for each sample and for each strain.

The results obtained for the inactivation of *E. coli* (Figure 22a) with Pro:U:MA and CA:Xyl demonstrate that there is no influence or efficacy of the DES aqueous solutions (without ciprofloxacin) in the inactivation of this bacterium. Nevertheless, the antibiotic in water and the ciprofloxacin formulated in the DES aqueous solutions (Pro:U:MA and CA:Xyl) are effective on the inactivation of *E. coli*. These formulations cause a decrease of 3.9 Log$_{10}$ (ANOVA, p < 0.0001) in the viability of the bacterium after 24 h of incubation. In all cases, the bacterial viability decreased with the exposure time. However, no significant differences in the activities are observed between the two ciprofloxacin DES formulations tested and the antibiotic in water. The marked decrease in the bacteria's viability after 4 h of incubation is in

agreement with previous antimicrobial studies for *E. coli* response to ciprofloxacin.[307,308]

Regarding the effect of ciprofloxacin DES formulations in the inactivation of *P. aeruginosa* (Figure 22b), a completely different profile was achieved. While aqueous solutions of Pro:U:MA had no influence on the bacterial viability, the aqueous solution of CA:Xyl without ciprofloxacin showed a small effect on *P. aeruginosa* inactivation. This is in accordance with the antimicrobial activity of citric acid and xylitol,[292,293,309] causing a decrease of 2.1 Log_{10} (ANOVA, p<0.0001) in the bacterium viability after 24 h of incubation. However, when the antibiotic is formulated in DES aqueous solutions of Pro:U:MA and CA:Xyl, the inactivation of *P. aeruginosa* has a distinct profile when compared to the antibiotic in water. Such differences highlight the improved efficacy of the inactivation rates of the antibiotic when formulated in DES aqueous solutions. In fact, ciprofloxacin alone was not able to inactivate *P. aeruginosa* after 24 h of incubation (Figure b1).

Nevertheless, when formulated with the selected DES aqueous solutions the antibiotic's effect is enhanced. This potentiated effect is verified only after 6 h of incubation, where a decrease in the viability of *P. aeruginosa* of 1.0 and 2.6 Log_{10} (ANOVA, p<0.0001) was achieved for ciprofloxacin formulated in aqueous solutions of Pro:U:MA and CA:Xyl, respectively. After 24 h of incubation, the pronounced effect of the DES formulations with ciprofloxacin is more notorious (Figure b2), achieving *P. aeruginosa* inactivation values of 5.6 and 3.6 Log_{10} (ANOVA, p<0.0001) for formulations of Pro:U:MA and CA:Xyl with ciprofloxacin, respectively.

Interestingly, for the Gram-positive bacteria *S. aureus*, the effect of ciprofloxacin formulated in CA:Xyl is in contrast with the one obtained for Pro:U:MA. Both the antibiotic in aqueous solution and the ciprofloxacin formulated in CA:Xyl have no significant effect on the inactivation of the bacterium for an incubation period of 24 h. However, after 12 h of exposure to the antibiotic formulated in Pro:U:MA, a decrease in the viability of 2.4 Log_{10} (ANOVA, p<0.0001) was achieved. The exposure of the bacterium to this formulation was more effective than to the aqueous solution of the antibiotic and the antibiotic formulated in aqueous solution of CA:Xyl, causing a decrease of 3.1 Log_{10} (ANOVA, p<0.0001) in the inactivation of *S. aureus* after 24 h.

2.4.5 Ciprofloxacin activity after storage in DES formulations.

The drug activity was assessed based on the results for the MIC value and inactivation efficiency. To evaluate the stability of the drug in the DES formulations after storage, the assays were carried out on the day of preparation (T_0) and after a month (T_{30}) period, stored at 25 °C and 75−80% relative humidity. An antibiotic dosage of 0.5 µg·mL^{-1} was used for the inactivation efficiency experiments and for all the bacteria studied (Figure 23). The MIC values of ciprofloxacin at T_0 and after 1 month are similar, showing a maintenance of the antimicrobial activity of the drug after storage (see Table 8). The bacterial inactivation for *E. coli* (Figure 23a), *P. aeruginosa* (Figure 23b) and *S. aureus* (Figure 23c) was analyzed for the results obtained after 24 h of incubation. The obtained data show that the inactivation efficiencies for ciprofloxacin formulated in the DES aqueous solutions after 1 month storage are comparable to those obtained with freshly prepared formulations
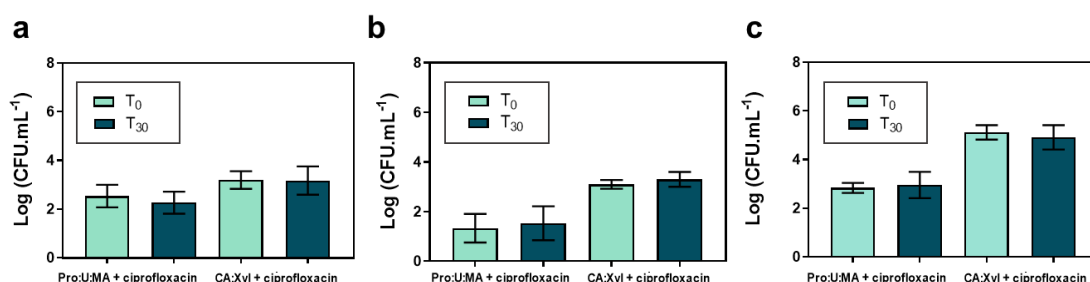
Figure 23. Activity of ciprofloxacin after 1 month storage in DES formulation. The antibiotic activity in the DES formulations was evaluated at the day of preparation (T_0) and after 1 month storage at 25 °C (T_{30}). The inactivation efficiency was studied in (a) *E. coli*, (b) *P. aeruginosa* and (c) *S. aureus* strains in PBS at 37 °C. Activity was evaluated in 3 independent experiments.

Table 8. Minimal inhibitory concentrations of ciprofloxacin in DES aqueous solutions for *E. coli* ATCC-25922, *P. aeruginosa* ATCC-27853 and *S. aureus* ATCC 6538. Results obtained for ciprofloxacin in DES aqueous solutions at preparation day and after 30 days in storage conditions at 25 °C.

	Minimum Inhibitory Concentration (µg·mL^{-1})		
	E. coli	*P. aeruginosa*	*S. aureus*
Pro:U:MA+ ciprofloxacin (T_0)	0.00488	0.00488	0.00244
Pro:U:MA+ ciprofloxacin (T_{30})	0.00488	0.00488	0.00244
CA:Xyl + ciprofloxacin (T_0)	0.00488	0.00244	0.00244
CA:Xyl + ciprofloxacin (T_{30})	0.00488	0.00244	0.00244

2.4.6 Evaluation of the development of bacterial tolerance to ciprofloxacin in DES formulations

The effective eradication of bacteria has become challenging due to their remarkable ability to resist antibiotics, as seen for ciprofloxacin.[310,311] Given the medical prescription of this antibiotic to tackle infection conditions caused by Gram-negative bacteria,[312] it is demonstrated the relevance of ciprofloxacin DES formulations. To evaluate the potential development of bacterial resistance to ciprofloxacin formulated in the DES aqueous solutions, is simulated a 7-day treatment with specific dosages (0.5 µg·mL^{-1}) administered at each 4 h (*E. coli* (Figure 24a)) and 6 h (*P. aeruginosa* (Figure 24b)). This behavior was monitored in both strains and selected the administration intervals according to the inactivation profiles previously presented. Bacterial controls were also conducted in the same conditions, being subcultured in the same number of cycles but in the absence of the antibiotic and DES.
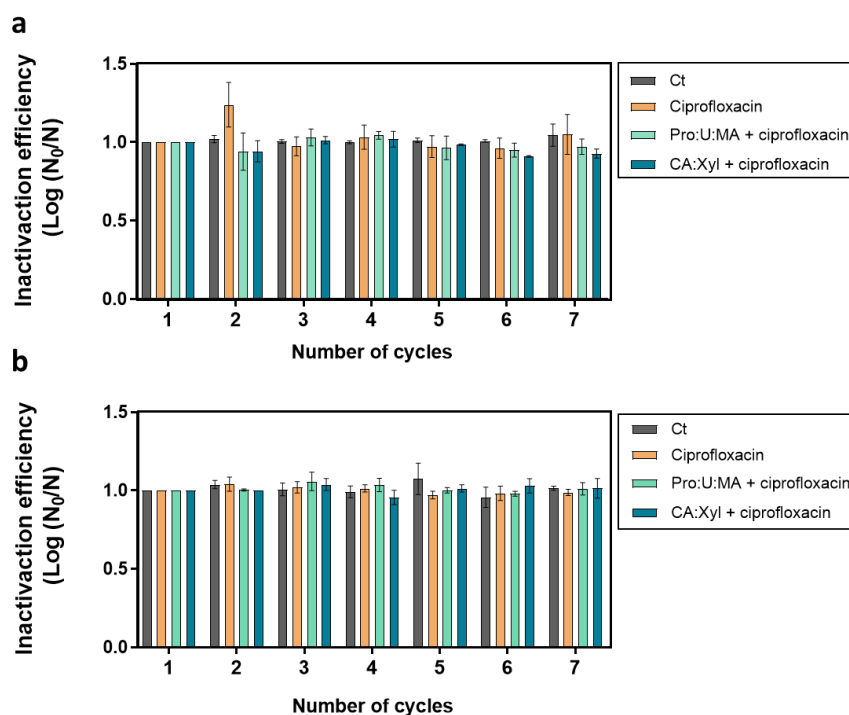
Figure 24. Inactivation efficiency of seven consecutive cycles of exposure to ciprofloxacin in water and in DES formulations. Data on (a) *E. coli*, and (b) *P. aeruginosa*. Efficiency was determined after 4 and 6 h of incubation in PBS at 37 °C, respectively, with ciprofloxacin in water and ciprofloxacin formulated in the DES solutions at 0.5 µg.mL^{-1}. N_0 and N represent, respectively, the number of Colony Forming Units per mililiter (CFU·mL^{-1}) for the first treatment with each formulation and the values after the respective cycle. The results are expressed as mean ± SD of three independent experiments for each formulation and for each strain.

According to the results depicted in Figure 24a, there is no significant increase in resistance of *E. coli* to ciprofloxacin in water or to the antibiotic formulated in DES aqueous solutions after 7 days of consecutive administrations at each 4 h treatment. A similar behavior is seen with *P. aeruginosa* (Figure 24b) since no significant increase in the inactivation efficiency was detected after 7 cycles of administration at each 6 h using the antibiotic formulated in the DES aqueous solutions at the same concentration.

Ciprofloxacin's resistance in *P. aeruginosa* is of complex and multifactorial nature still, it has been mostly attributed to target-site modifications and upregulation of efflux pumps.[313–316] In addition to numerous gyrAB and parCE genes mutations, this bacterium stand out for their low permeable outer membrane (1/100 of the permeability of *E. coli*'s).[317] Usually drug combinatory therapies are selected, attempting to avoid drug resistance and improve the treatment success rate.[318] However, due to ciprofloxacin's resistance mechanisms, the resistance to other antibiotics might also be increased, being this one of the major disadvantages of the use of such strategy.[319] The reduced susceptibility of ciprofloxacin is usually associated with mutations in regulatory genes of efflux pumps and their resulting overexpression, which increases the ciprofloxacin's expulsion from the bacteria cells, decreasing the intracellular concentration.[320,321] In this work, the possibility not only of the DES' ability to enhance antibiotic's solubility in several orders of magnitude but also its capacity to promote variations in the cellular envelope permeability[322] and manipulated the concentration as an advantage to improve the efficacy of ciprofloxacin was explored. By increasing the bacterial cell permeability, and the ciprofloxacin concentration in the media, is not only possible to increase the intracellular concentration of antibiotic, as well as to compromise the bacterial integrity improving the susceptibility of the bacterium to this formulation.

In general, and as seen for the inactivation efficiency rates depicted in Figure 24, the formulation of ciprofloxacin in DES aqueous solutions do not induce the development of tolerance to the treatment or potentiate resistance mechanisms of these bacteria to the antibiotic. The use of DES formulations in combination with ciprofloxacin can maintain an enhanced efficacy of bacterial inactivation during 7 days of treatment of infections with both strains.

2.4.7 Cytotoxicity of DES formulations

Envisaging the application of the novel DES formulations comprising ciprofloxacin for human use, the cytotoxicity of ciprofloxacin and of ciprofloxacin formulated in DES solutions was in HaCat cells after 72 h of exposure. The respective results are given in Figure 25.

Since anti-topoisomerase drugs like ciprofloxacin can inhibit the expression of topoisomerase I,[323] some toxicity is expected for HaCat cells at high concentrations. In fact, the pure ciprofloxacin was found to be slightly toxic for these cells at concentrations higher than 0.5 $\mu g \cdot mL^{-1}$. On the other hand, both DES aqueous solutions used, namely Pro:U:MA and CA:Xyl, exhibit an increase of more than 20% in cell viability in the range of concentrations studied (ANOVA, p<0.0002). Notwithstanding, when the antibiotic is formulated in DES aqueous solutions, its toxicity is reduced, even at higher concentrations. Although, at the concentration of 0.5 $\mu g \cdot mL^{-1}$, ciprofloxacin presents slight toxicity (<75% cell viability), a significant increase of more than 25% in cell viability can be noticed when the antibiotic is formulated in both DES aqueous solutions (ANOVA, p<0.025, p<0.0002).
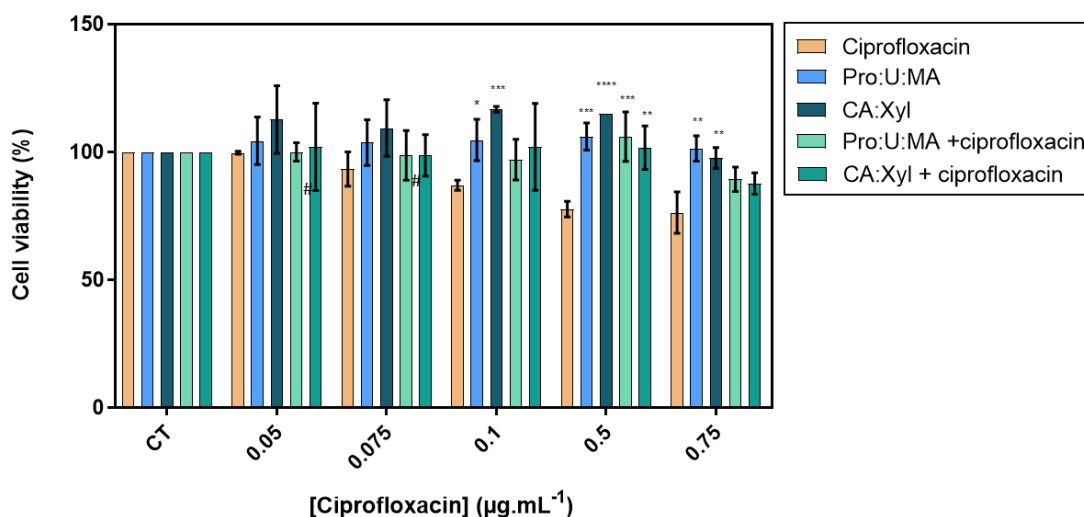
Figure 25. Effect of ciprofloxacin and DES formulations on the viability of HaCaT cells in DMEM medium. Cytotoxicity profile at 37 °C after 72 h of exposure vs control cells (CT). Results are expressed as mean ± SD of three independent experiments. *p<0.05, **p<0.025, ***p<0.0002, ****p<0.0001 viability increase compared to ciprofloxacin's effect on HaCat cells.

Conclusions

In the current study, DES formulations comprising ciprofloxacin were designed to tackle antibiotic's drawbacks. It has been demonstrated how the rational selection of the DES components can go further from their common solvent applications to the simultaneous improvement of solubility, stability, and therapeutic efficacy of antibiotics, such as ciprofloxacin, without tolerance development or cell toxicity. Our findings demonstrate that the studied DES in aqueous media can be successfully used as common pharmaceutical co-solvents and hydrotropes in antibiotics solubilization, allowing to achieve solubility enhancements up to 430-fold. While being capable of enhancing ciprofloxacin's solubility, these formulations are also able to improve the stability of the antibiotic solutions by almost 50% in comparison to its formulation in water at a similar pH. Our results reveal the long-term stability (up to 1 month) of the aqueous DES solutions as well as of the antibiotic in this novel media. The DES formulations not only preserve the fluoroquinolone's activity but are capable of increasing the antibiotic's action against both Gram-negative (*E. coli* and *P. aeruginosa*) and Gram-positive (*S. aureus*) strains. The possibility to produce a higher effect on the antimicrobial activity than ciprofloxacin in water (up to 2-fold for *P. aeruginosa* and 4-fold for *S. aureus*) might allow to decrease the drug dosage required to achieve the same therapeutic efficacy, thus decreasing the associated side-effects upon administration of higher doses. Additionally, the bacterial susceptibility to the antibiotic is enhanced by the formulation of the antibiotic in DES aqueous solutions, allowing to even produce effect in concentrations where the pure API in water presents no antimicrobial activity (0.5 $\mu g \cdot mL^{-1}$). This effect can be mainly attributed not only to an improvement in the solubility of the antibiotic, but also to the ability of DES formulations to increase bacterial cell wall permeation, allowing a higher drug content available intracellularly to exert antimicrobial action. Such an effect can be achieved by the proper design of DES and the careful selection of drug and DES concentrations to the final formulation. To the best of our knowledge, this is the first report on DES aqueous solutions where insights on the therapeutic efficacy of DES formulations with fluoroquinolones are addressed. These results reveal the pioneering use of including DES aqueous solutions in antibiotic-based formulations and their remarkable impact on improving

fluoroquinolones solubility, stability and therapeutic action and on lowering bacteria resistance with low cytotoxicity associated. Given the versatility of DES formulations comprising antibiotics, they can be directly incorporated in a vast number of materials to develop a wide range of drug delivery systems.

Chapter 3. Impact of DES Formulations in the Development of Aqueous Thermo-Responsive Drug Delivery Systems
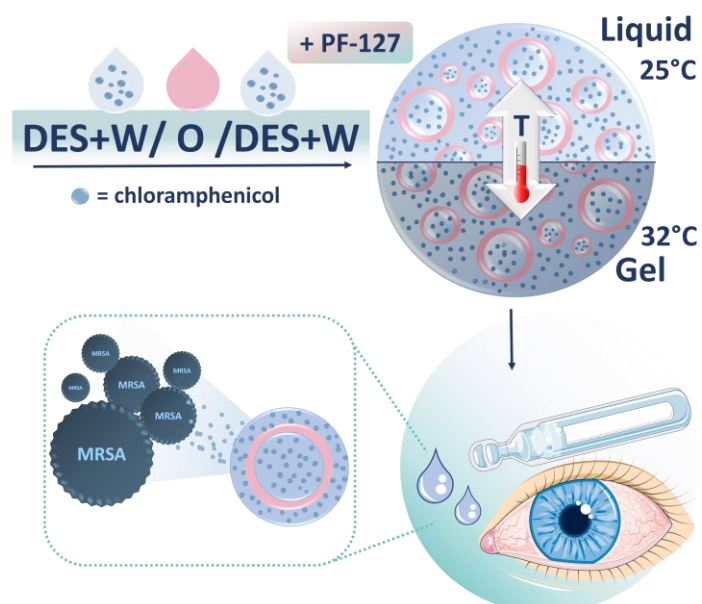
3.1 Abstract

The rise of antibiotic resistant strains, such as methicillin-resistant *Staphylococcus aureus* (MRSA), challenges the current treatment of infections. In the case of ocular infections, antibiotic eye drops are commonly prescribed. However, their efficacy is usually compromised by the low viscosity of these formulations and the eye drainage. To overcome these drawbacks, DES-based microemulsions with thermo-responsive character that increase their viscosity upon contact with the eye have been developed. Using betaine-based DES aqueous solutions, it is possible to increase up to 140-fold the water solubility of the antibiotic chloramphenicol, typically used in ocular infections. The DES solutions containing the antibiotic were applied as water phases in water-in-oil-in-water (w/o/w) microemulsions, being stable up to 3 months. Furthermore, a sustained-release and a higher permeation of the antibiotic through the cornea than that of commercialized eye drops was achieved, while presenting comparable cytotoxicity profiles (cell viabilities > 88%). Higher antimicrobial activity and faster action of the antibiotic in case of infection with MRSA was observed compared to the commercialized formulations (7 $\log_{10}$ of inactivation in 48 h *vs*. 72 h). Overall, these microemulsions comprising DES are a promising strategy to achieve higher antibiotic effectiveness in the treatment of resistant bacterial infections.

3.2 Introduction

Ocular infections affect people of all ages and genders and are associated with a high degree of visual morbidity and blindness worldwide.[324] Bacteria are the major responsible for these infections, particularly Gram-positive bacteria, such as *S. aureus*, which usually cause, among many other complications, conjunctivitis.[325,326] Despite the constant demand for new treatments and novel antimicrobial agents, antibiotic research, development and industrialization has decelerated in recent years.[327] Simultaneously, an increase in bacterial resistant strains, such as methicillin-resistant *S. aureus* (MRSA), has been globally observed boosting the search for alternative therapeutic options.[328] One of the possible solutions to this challenge is to consider the re-emerging of old antibiotics, that are no longer first-selection in clinical practice, to treat complicated infection cases.[329] In this context, in the present study, the antibacterial potential of chloramphenicol, which remains an alternative in the fight against multidrug resistant pathogens, is explored.

Chloramphenicol presents a bacteriostatic action against *Staphylococcus* species, being used in the treatment of bacterial eye infections.[330,331] One of the main disadvantages of this drug, when in an ophthalmic solution, is its low water-solubility, that only allows concentrations up to 0.25% (w/v) (pH = 4.5 to 7.5), which is below the usually recommended dosage.[332] In addition to its low water-solubility, chloramphenicol also presents stability issues in aqueous media, since it easily hydrolyzes into glycols. Since most of the ophthalmic formulations are generally available as solutions, the improvement of these formulations has focused on increasing the drug content, by using co-solvents and cyclodextrin complexes.[333] Such efforts intend to overcome the limited drug concentration in the conjunctival sac and the decreasing therapeutic response; however, such approach also increases the toxicity associated with the drug administration due to the exposure to higher drug dosages.[331,334] Therefore, the new generation of ophthalmic formulations must focus on enhancing the drug aqueous solubility, the drug concentrations at the site of infection, and extend its residence time in the ocular environment to achieve a higher therapeutic efficacy while lowering the administrated dosage.

In this vein, DES have recently arisen as promising options to improve solubility[134] and stability[110] of APIs. Furthermore, they can be advantageously designed for different administration routes. These solvents have been studied in the solubilization of antifungal APIs[134] and applied to improve the chemical stability of β-lactam antibiotics.[141] Due to their design and application versatility, DES and DES comprising active ingredients have been incorporated in different drug delivery systems, such as ion gels,[335] hydrogels[221,223] eutectogels,[222] particles[224] and nanofibers,[228] aiming at different administration routes. However, and to the best of our knowledge, their application in ocular drug delivery systems is still unexplored.

In the field of ocular drug delivery, microemulsions and gels have been considered as strategies that intend to overcome the drawbacks associated with conventional eye drops.[336] Although DES have also been applied as oil phases in microemulsions,[337,338] their study towards the development of drug delivery systems has not been pondered. Since some of these dispersions still present low viscosity, additional approaches, namely the use of *in situ* gelling polymers, can be an appealing solution. Gelling polymers allow an easy, safe and reproducible administration of the system as a liquid drop, while presenting a sol-gel transition in contact with the ocular surface as a result of changes in temperature, pH or ionic strength.[339] An example of a thermo-responsive nonionic *in situ* gelling polymer that can be used for this purpose is Pluronic® F-127 (PF-127), a polymer based on triblock copolymers of PEG and poly(propylene glycol) (PPG).[340] The colorless and transparent character of PF-127 solutions, along with its reversible gelation properties occurring at body's temperature, makes it optimal for the development of ophthalmic formulations.

Based on the exposed, in the present work, DES aqueous solutions were investigated to improve the solubility of chloramphenicol and then used to prepare thermo-responsive microemulsions. Particularly, is demonstrated how DES aqueous solutions comprising chloramphenicol can be applied as water phases of w/o/w microemulsions and how these formulations can be designed to present a thermo-responsive character, thus increasing viscosity upon contact with the ocular environment and enhancing the therapeutic efficacy of the drug towards ocular infections caused by resistant bacteria, namely MRSA. These novel DES-based

microemulsions lead to a significant improvement in the drug stability and are capable of effectively eradicating resistant ocular infections in comparison to commercial eye drops, with low cytotoxicity and in a controlled manner.

3.3 Experimental section

3.3.1 Materials

The DES studied in this work were prepared using betaine anhydrous (98%, Alfa Aesar, Germany), xylitol (≥ 99%, Acros Organics, Thermo Scientific, New Jersey, USA) and glycerol (≥ 99%, Sigma-Aldrich, St. Louis, MO, USA). Chloramphenicol (≥ 98%) was purchased from Sigma-Aldrich (St. Louis, Missouri, USA). The preparation of the microemulsions required the use of Tween® 80 and Pluronic® F-127 (≥ 98%), both provided by Sigma-Aldrich (St. Louis, MO, USA), while Span® 80 and isopropyl myristate were purchased from Acofarma (Madrid, Spain). MTT was purchased from Sigma-Aldrich (St. Louis, MO, USA) and fluorescein from Thermo Scientific (New Jersey, USA). PBS (pH 7.4) was acquired from Sigma-Aldrich (St. Louis, MO, USA) in the form of tablets. TSA and TSB from Liofilchem (Italy) were used in the antimicrobial studies. All other solvents and reagents were from HPLC grades.

3.3.2 DES preparation and characterization

The DES were prepared by mixing the respective precursors (betaine and xylitol or glycerol) in sealed glass vials with constant heating and stirring, until a homogeneous transparent liquid was formed (at a maximum temperature of 85 °C). DES were prepared at 1:2 and 1:1 molar ratio for betaine:glycerol (Bet:gly) and betaine:xylitol (Bet:xyl), respectively. The mixtures were then kept for 1 h at this maximum temperature and then allowed to return to room temperature. The DES composition was confirmed by NMR spectroscopy. The ^{1}H NMR and ^{13}C NMR spectra were recorded using a Bruker Avance 300 at 300.13 MHz and 75.47 MHz, respectively. The DES were analyzed in deuterated water and using TMSP as an internal reference.

Betaine:glycerol: ^{1}H NMR (300.13 MHz, D_2O): δ 3.11 (9H, s, $N(CH_3)_3$); 3.48 (4H, dd, H-1',3'); 3.60 (1H, m, H-2'); 3.74 (2H, s, H-2); 4.68 (solvent(D_2O)) ppm. ^{13}C NMR (75.47 MHz, D_2O): δ 53.24 ($N(CH_3)_3$); 62.44 (C-1',3'); 66.05 (C-2); 72.02 (C-2'); 168.96 (C-1) ppm.

Betaine:xylitol: ^{1}H NMR (300.13 MHz, D_2O): δ 3.14 (9H, s, $N(CH_3)_3$); 3.52 - 3.66 (1H, m, H-3', 2H, m, H-2',4', 4H, m, H-1',5'); 3.77 (2H, s, H-2); 4.69 (solvent(D_2O)) ppm. ^{13}C NMR (75.47 MHz, D_2O): δ 53.28 ($N(CH_3)_3$); 62.58 (C-1',5'); 66.04 (C-2); 70.73 (C-3'); 71.89 (C-2',4'); 169.07 (C-1) ppm.

3.3.3 Solubility assays of chloramphenicol

Chloramphenicol solubility in water and in aqueous solutions of DES was determined by adding the drug in excess to water and to 2.0 g of each DES aqueous solution (0—90% (w/w) of DES). These mixtures were placed in sealed glass vials with a stirring bar and allowed to equilibrate in a specific aluminum disk with a stirring plate at 900 rpm and at constant temperature (25 and 32 °C) during 72 h. After achieving saturation, the samples were removed and then centrifuged. An aliquot of the supernatant was taken and diluted in water. After this, the samples were carefully filtered with a 0.20 µm syringe filter to remove any solid from the liquid phase and subsequently quantified by HPLC-DAD, on a PROMINENCE model (Shimadzu, Kyoto, Japan), equipped with an analytical Kinetex 5 µm C18 100 Å reversed-phase column (250 × 4.60 mm), from Phenomenex, using similar conditions to those described in the method presented in Section 2.3.3. The wavelength was set at 277 nm.

3.3.4 Preparation of thermo-responsive microemulsions

Two DES-based microemulsions comprising a final concentration of 4 mg·mL^{-1} of chloramphenicol were prepared by emulsification and ultrasonication technique via a three-step approach. Initially, water phase I of each microemulsion was prepared by solubilization of chloramphenicol in the aqueous solutions of each DES (70% (w/w)). Then, these DES aqueous solutions were dispersed into an oil phase based on isopropyl myristate (75.5% (w/w)) stabilized with Span® 80 (12% (w/w)). To guarantee homogeneity and to generate the water-in-oil pre-emulsion, the

samples were stirred at high-speed using an Ultra-Turrax T25 equipment (Janke & Kunkel IKA Labortechnik, Staufen, Germany) at 7000 rpm during 5 min. Table 9 presents the composition of each DES-based pre-emulsion. Secondly, 40% of each water-in-oil pre-emulsion was added to the water phase II, an aqueous solution composed of a 2:9 mixture of the aqueous solutions of DES (70% (w/w)) comprising chloramphenicol and an aqueous solution of Tween® 80 (5% (w/w)). For better homogenization of the resulting water-in-oil-in-water (w/o/w) emulsions, stirring using an Ultra-Turrax under the previous conditions was carried out, followed by sonication at 70% amplitude for 10 mins using a probe sonicator (Sonics & Materials Inc. Vibra Cell VCX 130 Model CV 18, Newtown, CT). The resultant microemulsions were allowed to equilibrate at room temperature and were then stored at 4 °C. Finally, after cooling, the last step consisted in adding PF-127 to each DES-based microemulsion using the cold method and under constant stirring. Upon complete dispersion of the polymer, DES-based microemulsions with PF-127 (5% (w/w)) were obtained and stored at 4 °C. Table 10 presents the full composition of the DES-based thermoresponsive microemulsions investigated.

Table 9. Composition of each water-in-oil pre-emulsion prepared for a final mass of 25 g.

| Sample | Water phase I | | Oil phase | |
	DES aqueous solution (%)	Drug (%)	Span® 80 (%)	Isopropyl myristate (%)
Bet:gly ME	10.5	-	12.0	77.5
Bet:gly + chloramphenicol ME	10.0	0.5	12.0	77.5
Bet:xyl ME	10.5	-	12.0	77.5
Bet:xyl + chloramphenicol ME	10.0	0.5	12.0	77.5

Table 10. Composition of each DES-based microemulsion (ME) prepared for a final mass of 25 g of emulsion.

| Sample | Water phase II | | | | |
	Pre-emulsion (%)	Tween® 80 (%)	DES aqueous solution (%)	Drug (%)	Water (%)
Bet:gly ME	40.0	5.0	10.0	-	45.0
Bet:gly + chloramphenicol ME	40.0	5.0	10.0	0.5	45.0
Bet:xyl ME	40.0	5.0	10.0	-	45.0
Bet:xyl + chloramphenicol ME	40.0	5.0	10.0	0.5	45.0

3.3.5 pH and droplet size

The pH of the different DES-based microemulsions was determined at room temperature using a HI 2550 multiparameter meter (Hanna Instruments, Woonsocket, Rhode Island, USA). The droplet size of the oil phase of the w/o/w microemulsions was assessed by dynamic light scattering using a Mastersizer 3000 (Malvern Instruments, Malvern, UK). To avoid multiple light scatterings due to high droplet concentration, the microemulsions were diluted with ultrapure water (1:100). Aiming to evaluate the stability of the prepared microemulsions, both parameters were analyzed immediately after preparation and at day 90. All measurements were reported as mean values ± standard deviations of triplicates for each microemulsion.

3.3.6 Rheological measurements

Initially PF-127 was dispersed at 15% (w/w) in both Bet:gly-based and Bet:xyl-based aqueous solutions (10 and 30% (w/w) of DES in water). This was carried out at low temperature (4 °C) to facilitate the polymer dispersion. Posteriorly, the viscosity of these DES-based solutions with PF-127 was evaluated at ocular temperature (32 ± 0.5 °C) using a Thermo Haake VT-550 (Thermo Fisher Scientific, Waltham, Massachusetts, EUA) rotational viscometer equipped with an SV-DIN coaxial cylinder sensor. The rheological analysis was performed with a stabilization time of 900 s and with a variation on the shear rate from 0.1 to 500 s^{-1} (ascending curve) and from 500 to 0.1 s^{-1} (descending curve). After selection of the best DES concentration and preparation of each DES-based microemulsion, the viscosity of these formulations was also appraised on the day of preparation and after 90 days using the same conditions described.

3.3.7 Drug stability

To evaluate the stability of the drug in the novel formulations upon storage, thermo-responsive DES-based microemulsions with 4.0 mg·mL^{-1} of chloramphenicol were prepared as previously described and kept in the dark at 4 °C, for 30 days. A sample of a commercial formulation of the same drug with the same concentration was also stored according with the manufacturer instructions

for 30 days. Since the shelf-life of the commercial formulation after opening is 28 days, we performed the experiments during the same period to allow the comparison between formulations. An aliquot of each formulation was collected and analyzed by HPLC-DAD according to the previously described protocol (Section 2.3.3), at given time points (7, 15 and 30 days).

3.3.8 *In vitro* cytotoxicity assay

The cytotoxic effect of the DES-based microemulsions containing chloramphenicol was assessed on human adult retinal pigment epithelial cells (ARPE-19) by the colorimetric MTT assay. The cells were seeded in 96-well plates at a density of 30 000 cells/well in 200 mL Dulbecco's Modified Eagle Medium/Nutrient Mixture F-12 (DMEM/F-12) medium (Gibco) supplemented with 10% (v/v) of FBS (Life Technologies, Carlsbad, California, USA) and antibiotic/antimicotic containing 100 units·mL^{-1} penicillin, 100 µg·mL^{-1} streptomycin and 0.25 µg·mL^{-1} amphotericin B (Sigma). Twenty-four hours after plating, cells were exposed to a range of four concentrations, 12.5–100.0 µg·mL^{-1}, of chloramphenicol diluted in sterile PBS. These were then incubated for 24 h at 37 °C in a 5% CO_2 atmosphere. After this, the wells were washed with PBS, and 50 µL of fresh medium and 10 µL of MTT solution of 3 mg·mL^{-1} was added to each well. After 4 h of incubation, 150 µL of isopronanol (with HCl 0.04 M) were added to dissolve the formazan crystals. Cell viability was measured at 570 nm using a microplate reader (Synergy HT from BioTeK Instruments Inc., Winooski, Vermont, EUA) and the percentage of viable cells was calculated as the ratio between the absorbance of treated versus control cells.

3.3.9 *In vitro* drug release

For the drug release performance, dialysis bags with 5 mL of each microemulsion containing 4 mg·mL^{-1} of chloramphenicol were used. Each bag was completely immersed in 200 mL of PBS as dissolution medium (pH 7.4) and was maintained under continuous stirring at 150 rpm and a temperature of 32.0 ± 1 °C. An aliquot (1 mL) from each container was collected at specific time points (5, 15, 30, 45, 60, 120 and 180 min). Each sample was diluted 1:1 in running buffer, filtered

94

and analyzed by the sane HPLC-DAD method (Section 2.3.3). For each release profile, three different samples were tested, and for each time point, the aliquots were measured two times at 277 nm.

3.3.10 *Ex vivo* corneal permeation studies

The permeation of chloramphenicol through corneal tissue was performed using static Franz diffusion cells (PermeGear, Inc., Hellertown, Pennsylvania, USA) with a diffusion area of 0.636 cm^2 and a receptor compartment of 5 mL. To this purpose, fresh porcine corneal epithelium was provided by a local slaughterhouse. Briefly, on the experimental day, corneal tissue was carefully harvested from porcine eye, and immersed in PBS. After that, the tissue was cut to appropriate size and clamped between the donor and receptor compartments faced up. A PBS solution was used as receptor media stirred at 600 rpm. The receptor solution was maintained at 37 ± 0.5 °C by a thermostatic water pump, thus, the human eye conditions were mimicked, since the temperature at the ocular surface (32 °C) was assured. An aliquot of 500 µL (with *ca*. 100 mg·mL^{-1} of chloramphenicol) for each formulation was placed in the donor compartment. Then, 300 µL of the receptor medium were removed at designated time points (15, 30, 45, 60, 90, 120, 240, 360, 480 min) and immediately replaced with the same volume of fresh solution. Each collected sample was diluted to 1:3 in acetonitrile, filtered and analyzed by HPLC-DAD (conditions as presented in Section 2.3.3). The release studies were conducted in three independent studies and expressed as average of permeated drug ± standard error of mean. Permeation profiles were obtained by plotting the cumulative amount of chloramphenicol permeated per surface area against time.

3.3.11 Corneal morphology and integrity

The apical surface of the corneas treated with the different formulations were observed by scanning electron microscopy (SEM) to study their morphology and topography. Before the analysis, the samples were dried under vacuum and properly spread on a double-sided carbon tape mounted onto an aluminum stud. SEM micrographs were registered using a tungsten cathode scanning electron microscope JSM 6010LV/6010LA, (Jeol, Tokyo, Japan) Secondary electron mode,

an acceleration voltage of 1 kV, a spot size of 30, and a working distance of 10 mm, were selected as the operational conditions.

3.3.12 Bacterial culture conditions

The strain of methicillin-resistance *Staphylococcus aureus* (MRSA) DSM 25693, positive for SE A, C, H, G, and I enterotoxins, was grown on solid medium, TSA, at 37 °C, for 24 h and was posteriorly stored at 4 °C. Prior to each assay, the bacterium strain was inoculated in liquid medium, TSB, and grown aerobically at 37 °C under stirring (up to 100 rpm) for 24 h. For each assay, a 300 µL aliquot of the referred culture was transferred into a new fresh TSB medium (subcultured in 30 mL twice) and grew under constant stirring overnight at 37 °C.

3.3.13 Antimicrobial efficacy of chloramphenicol in the DES-based microemulsions

The drug efficacy was first evaluated by testing the antimicrobial susceptibility by a modified Kirby-Bauer disk diffusion method. The bacterial suspension in PBS was set for a turbidity of 0.5 on the McFarland scale, prepared by peaking up 1–2 colonies from the pure culture. The suspension was spread plated using a swab on Mueller-Hinton Agar plate. Disks containing 100 µg·mL^{-1} of the drug from each formulation were used for MRSA evaluation. The DES-based microemulsions without the drug were also assessed as the respective controls to determine its impact on the antimicrobial susceptibility. The agar plates with all samples were incubated at 37 °C for 18–24 h. Following this, the susceptibility of each formulation was determined by measuring the diameter of the inhibition zones and comparing it to the breakpoint established by the EUCAST and according to the CLSI.[290,291]

The antimicrobial efficacy was determined based on the continuous exposure of the bacterium to the DES-based microemulsions with chloramphenicol and the respective commercial formulation containing the same drug for comparison purposes. The bacterial culture was grown overnight. After dilution and adjustment to 0.5 MacFarland scale using liquid medium TSB, the bacterial suspensions were distributed equally in 5 mL tubes. Subsequently, a drug dosage of 100 µg·mL^{-1} of each DES-based microemulsion comprising chloramphenicol and of the tested

commercial eye drops were added to the bacterial suspensions at specific time points. A positive bacterium control (Ct) containing only the bacterial inoculum in TSB and the DES-based microemulsions without the drug were additionally carried out. Time points were selected according to the clinical prescription of the drug for severe skin infections: first applications every 2 h for 48 h, and then every 4 h up to 5 days. Aliquots of each bacterial suspension were taken after each dosage application. Each aliquot was serially diluted in PBS and each sample dilution was pour-plated TSA being posteriorly incubated at 37 °C for 24 h. The growth inhibition ability of chloramphenicol in both DES-based microemulsions and in the commercial eye drops was evaluated by quantifying the number of colonies forming units per milliliter ($CFU \cdot mL^{-1}$). Experiments were carried out in duplicate with three replicates for each sample.

3.3.14 Statistical analysis

The results obtained were expressed as mean ± SD of independent experiments. In the case of cell viabilities, at least four independent studies were conducted, analyzing 6 different replicas for each measurement. For the permeation profiles, three independent studies were performed using a total of 6 different corneal samples for each formulation. The statistical analysis of all data was done using a two-way ANOVA, with multiple comparisons. The levels of significance were set at probabilities of **$p<0.0043$, ***$p<0.0003$, ****$p<0.0001$ cell viability for cell viability and of *$p<0.03$, ***$p<0.003$, ****$p<0.0001$ for the amount of chloramphenicol permeated from each ME, all analyzed with Graphpad Prism 8.0.1 software (GraphPad Software, San Diego, CA, USA).

3.4 Results and discussion

This work explores an innovative approach to improve antibiotic based ophthalmic formulations by using DES-based microemulsions comprising chloramphenicol with a thermo-responsive character for the treatment of ocular infections. The DES components were selected to ensure biocompatibility for ocular administration. In this context, betaine was selected as a hydrogen-bond acceptor, and glycerol and xylitol were considered as hydrogen-bond donors. All these components present osmoprotectant properties and are suitable to be applied in eye drops.[341,342] Betaine:glycerol (Bet:gly) and betaine:xylitol (Bet:xyl) DES were prepared in 1:2 and 1:1 molar ratio, respectively, based on previous solubility studies (data not shown). The composition of the DES and the integrity of the single components was confirmed by ^{1}H and ^{13}C NMRspectroscopy.

The ^{1}H NMR spectrum for Bet:gly (Figure 26a) shows first the proton resonances of the $N(CH_3)_3$ in betaine's structure at 3.11 ppm, and of the H-2 at 3.74 ppm. Likewise, the resonances of the protons associated with CH_2 groups (H-1',3') and of the CH (H-2') of glycerol appear at 3.48 ppm and 3.60 ppm, respectively. Figure 26b depicts the ^{13}C NMR spectrum of this DES, where the carbon resonance of the $N(CH_3)_3$ in betaine's structure and the respective C-2 and C-1 can be respectively observed at 53.24 ppm, 72.02 ppm and at 168.96 ppm. Regarding glycerol's structure, the carbon resonances from the C-1',3' and C-2' can be seen at 62.44 ppm and 66.05 ppm, respectively. For Bet:xyl, concerning the ^{1}H NMR spectrum (Figure 27a) similar proton resonances can be found for betaine where $N(CH_3)_3$ and the H-2 appear at chemical shifts at 3.14 ppm and 3.77 ppm, respectively. The proton resonances on xylitol's structure (H-3', H-2',4' and H-1',5') can be observed as multiplets in the region between 3.52 to 3.66 ppm.

The ^{13}C NMR spectrum (Figure 27b) also displays similar carbon resonances regarding the betaine's structure ($N(CH_3)_3$ at 53.28 ppm, C-2 at 66.04 ppm and C-1 at 169.07 ppm) to those observed in the Bet:gly spectrum. The carbon resonances associated with xylitol's structure can be found at 62.58 ppm (C-1',5'), 70.73 ppm (C-3') and 71.89 ppm (C-2',4'), respectively.
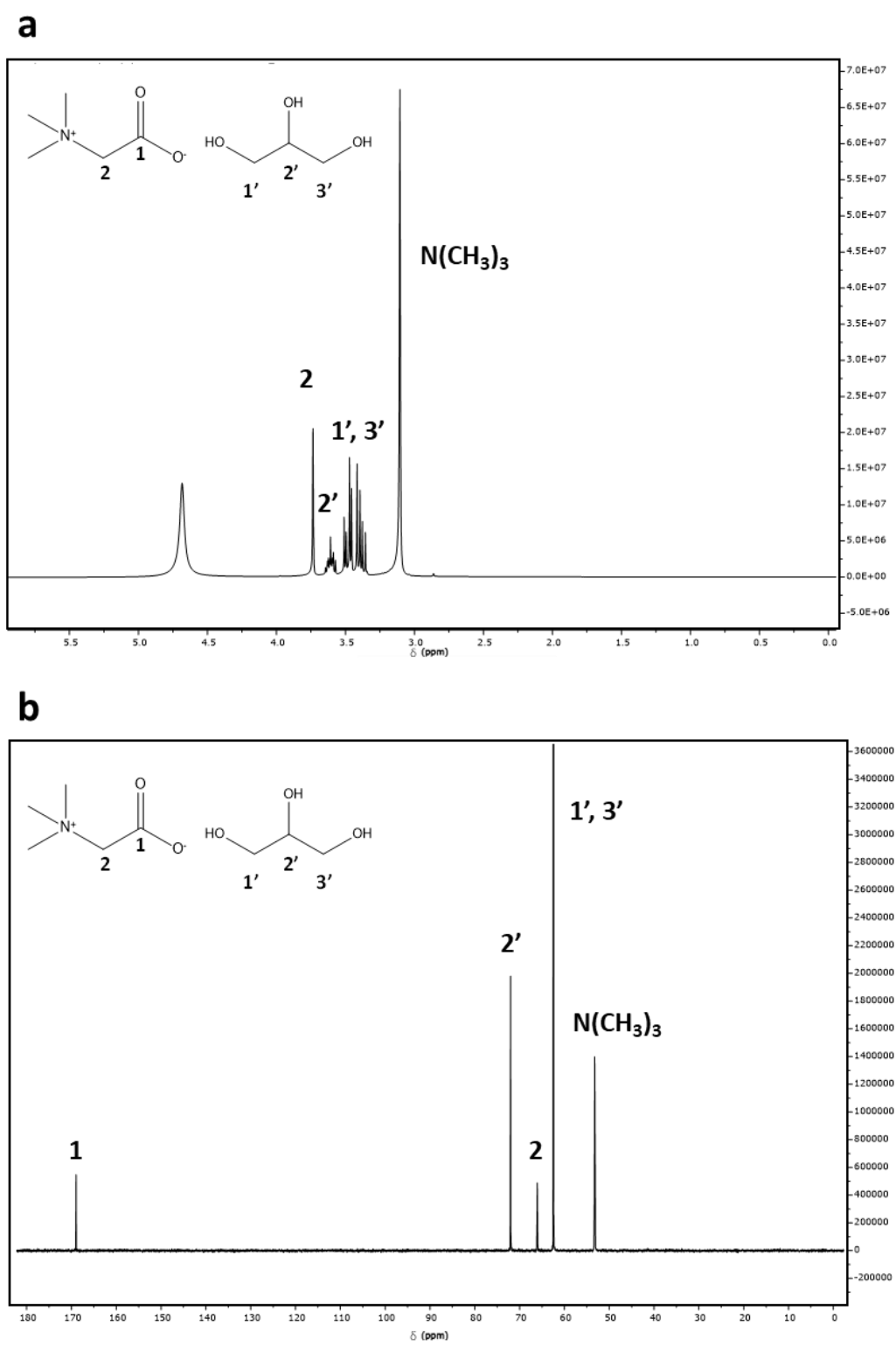
Figure 26. ^{1}H NMR (a) and ^{13}C NMR spectra (b) spectra of Bet:gly in D_2O.
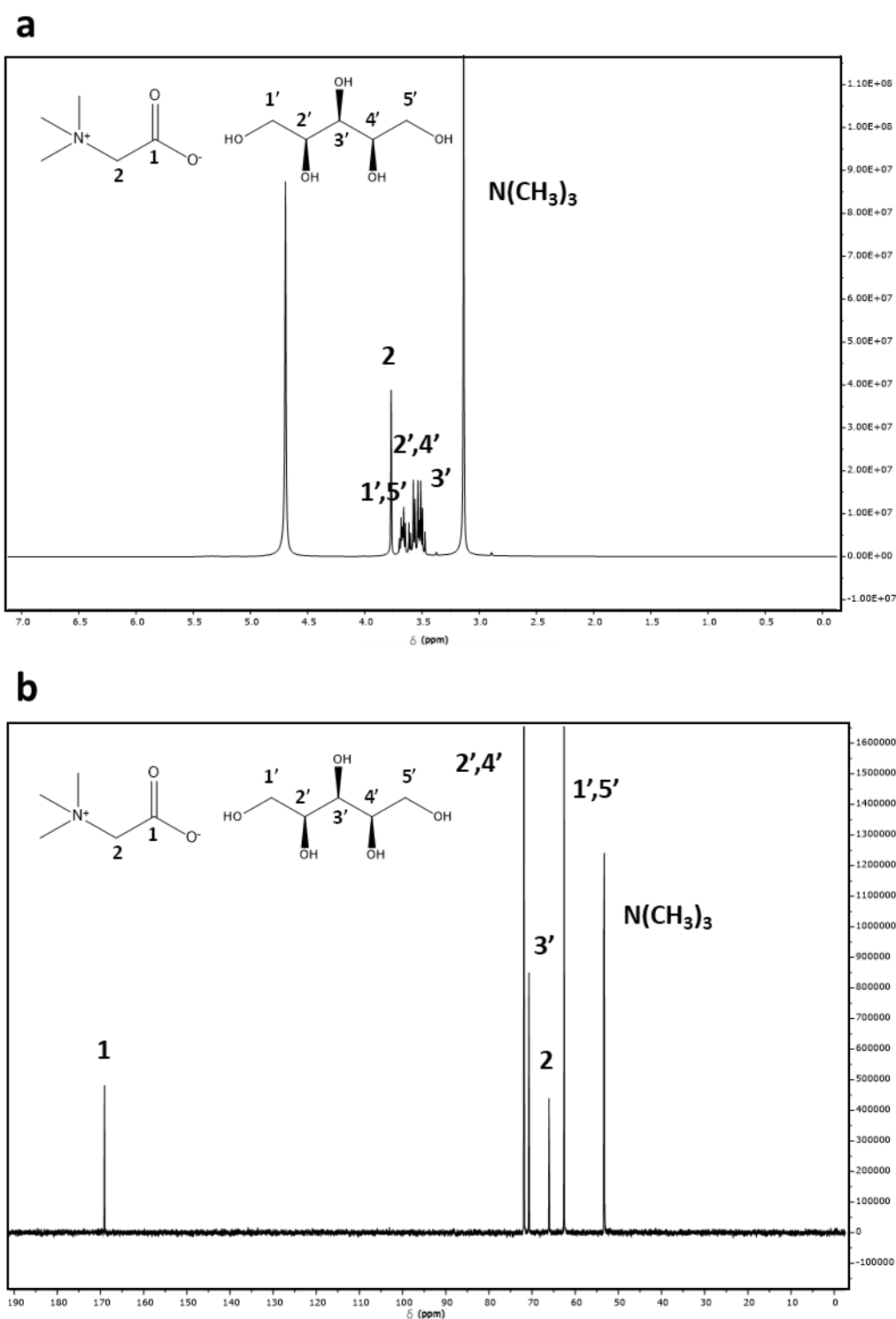
Figure 27. ^{1}H NMR (a) and ^{13}C NMR spectra (b) spectra of Bet:xyl in D$_2$O.

These DES were used in aqueous solutions and studied for the solubilization of chloramphenicol, and then used in the preparation of microemulsions (Figure 28a). The DES-based microemulsions were characterized in terms of pH, droplet

size and viscosity. The stability of these parameters and of the antibiotic in the microemulsions were also assessed. The *in vitro* cytotoxicity in retinal cells, the *in vitro* drug release and the permeation across corneal tissue were conducted to evaluate the effect of the thermo-responsive character of these microemulsions in the overall drug delivery and its influence on the therapeutic action of the antibiotic. Finally, the antimicrobial efficacy was evaluated against MRSA to assess the potential of these formulations to improve the antibiotic capacity to eradicate ocular infections caused by multidrug-resistant bacteria (Figure 28b).
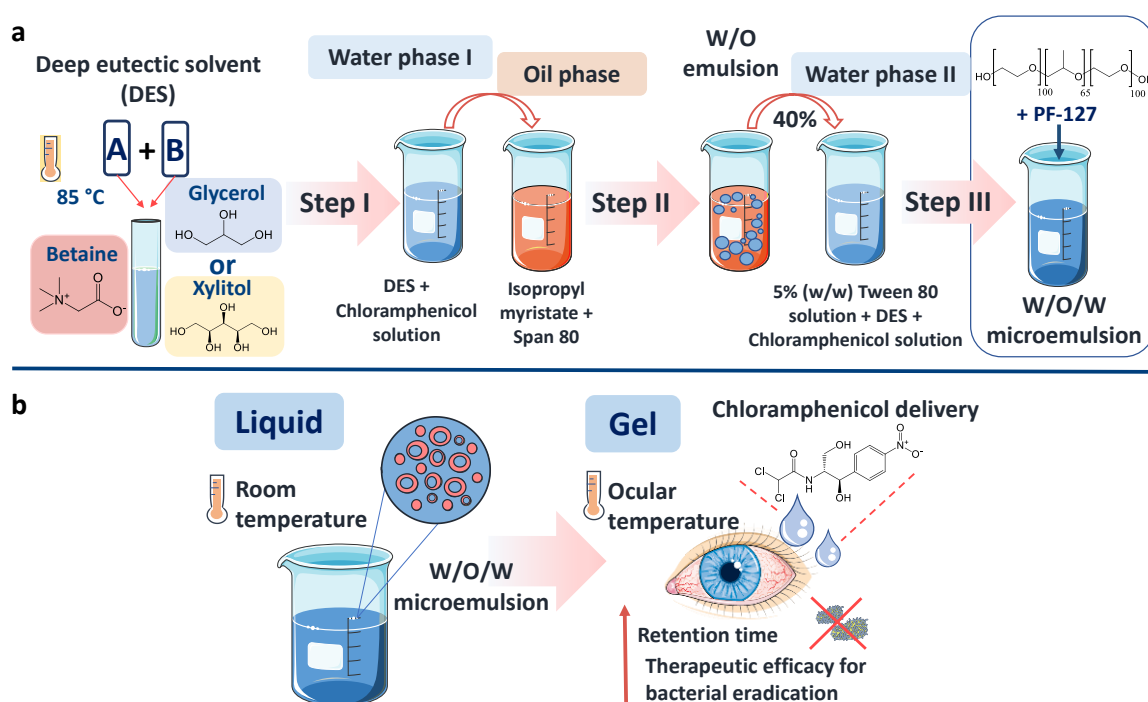
Figure 28. a) Schematic representation of the preparation procedure of the thermo-responsive DES-based microemulsions containing chloramphenicol. b) Thermo-responsive behavior of the w/o/w microemulsions: the ophthalmic formulations are liquid at room temperature increasing the viscosity upon contact with ocular environment, improving the drug retention time and therapeutic efficacy in the treatment of ocular infections. Image made with Servier Medical Art and adapted by the authors according with Servier under the CC-BY 3.0 License (at https://smart.servier.com/).

3.4.1 Chloramphenicol solubility in DES aqueous solutions

The solubility of chloramphenicol in aqueous solutions of Bet:gly and Bet:xyl, in the range of 0-90% (w/w) of DES, was initially evaluated. For a better prediction of the solubility while considering the intended ophthalmic application, chloramphenicol's solubility was studied at room (25 °C) and ocular surface (32 °C) temperatures. Figure 29 depicts the solubility curves (Figure 29a and 29b) the

respective solubility enhancements achieved by the two types of DES solutions at both temperature (Figure 29c and 29d) (S/S$_0$, where S corresponds to the solubility of chloramphenicol in the DES aqueous solution and S$_0$ to its in water).
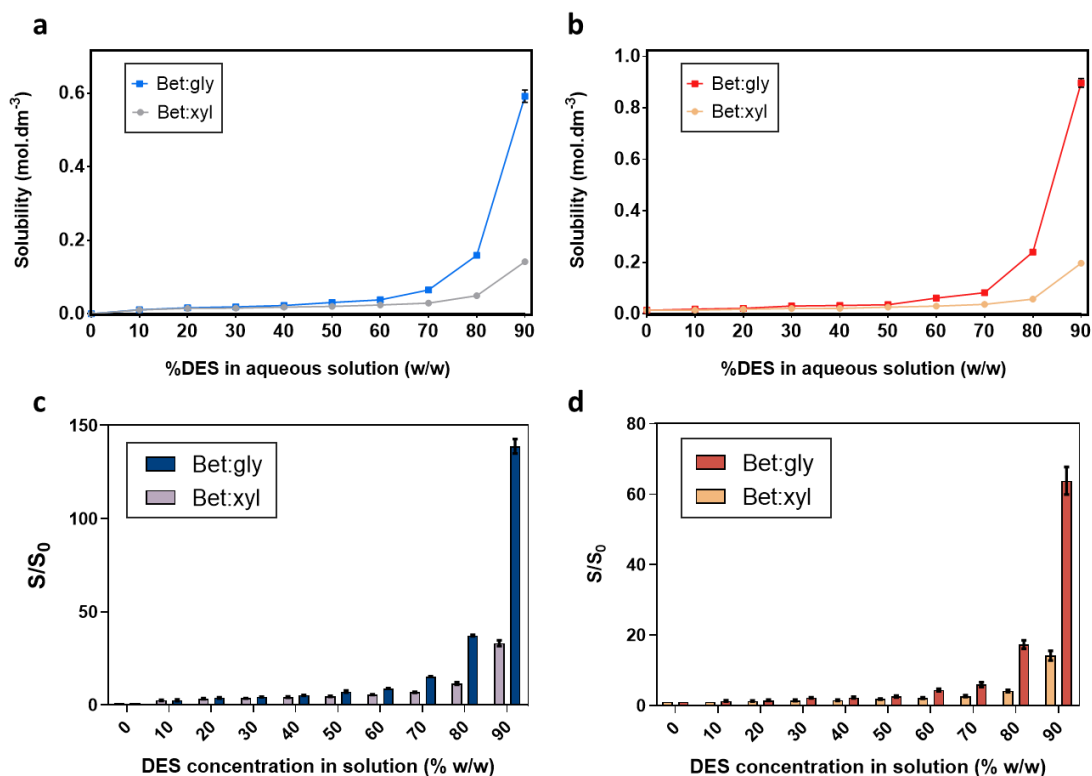
Figure 29. Solubility behavior of the chloramphenicol in Bet:gly and Bet:xyl aqueous solutions. Solubility studies at (a) room (25 °C) and (b) ocular (32 °C) temperatures. The solubility values were determined after 72 h of equilibrium. The effect of the studied DES and their concentrations in solubility enhancement (S/S$_0$) of chloramphenicol are provided at (c) 25 °C and (d) 32 °C. The results are expressed as the mean ± SD of two independent experiments and three independent measurements for each sample.

The solubility of chloramphenicol was found to be $(4.26 \pm 0.10) \times 10^{-3}$ mol·L^{-1} and $(1.45 \pm 0.06) \times 10^{-2}$ mol·L^{-1} in water at room and ocular surface temperatures, respectively. The DES aqueous solutions investigated in this work allowed to considerably enhance the aqueous solubility of chloramphenicol. Both types of DES provide a monotonic increase in the solubility with the increment of the percentage of DES, in agreement with a co-solvency mechanism.[300]

The use of 90% (w/w) of Bet:gly DES should be highlighted since it allows a remarkable 140-fold increase in the chloramphenicol solubility at room temperature (Figure 29c) and a 65-fold increase at ocular's surface temperature (Figure 29d) when compared to the antibiotic's water solubility. This corresponds to formulations

with 180 to 280 mg·mL^{-1} of chloramphenicol solubilized at room and body's temperature. The solubility of chloramphenicol in the Bet:gly aqueous solution at room temperature ($(6.20 \pm 0.12) \times 10^{-1}$ mol·L^{-1}) is even more promising when compared to its solubility in ethanol, $(6.05 \pm 0.08) \times 10^{-1}$ mol·L^{-1} (data not shown), a common organic solvent used for the solubilization of this drug. The use of 90% (w/w) of Bet:xyl, even though not as effective as the previous DES solution, also enables to enhance the water solubility of the drug by 30-fold at room temperature (Figure 29c) and by 15-fold at ocular temperature (Figure 29d).

The described solubility enhancements greatly surpass the solubilities achieved with existing commercial strategies, which enable formulations with 4 to 10 mg·mL^{-1} of chloramphenicol.[343] The high solubilization ability of the DES aqueous solutions proposed herein allows easy manipulation of the DES concentrations and the drug content according to the intended application. Moreover, these DES present higher solubilization capacity than the strategies already commercialized, such as the use of β-cyclodextrin complexes.[333] Although 90% (w/w) of aqueous DES provided the best result in terms of solubility enhancement, due to the intended application of the DES aqueous solutions as water phases in the preparation of microemulsion, solutions with 70% (w/w) of DES in water were used in the subsequent experiments with the goal of increasing the water content. At this DES concentration, solubility enhancements ranging from 7- to 15-fold can be obtained using Bet:xyl and Bet:gly aqueous solutions, still enabling the preparation of delivery systems with high drug content.

3.4.2 Characterization and stability of the aqueous DES-based microemulsions

Aiming to obtain systems that can be compared with commercial formulations, DES-based microemulsions comprising 4 mg·mL^{-1} of chloramphenicol were prepared and characterized in terms in terms of rheological and physicochemical properties. Microemulsions without the drug were equally prepared and characterized to infer the DES influence on the properties of these systems. The visual aspect of both microemulsions comprising the DES and chloramphenicol is depicted in Figure 30a, and their thermo-responsive behavior portrayed in Figure

30b. For this purpose, the viscosity, pH and particle size of the microemulsions, stored at 4 °C and protected from light to avoid degradation, were evaluated on the day of preparation (day 0) and after 90 days of storage.

Tear fluid has extremely low buffering ability since pH fluctuations depend mostly on the opening time of the eyelids; therefore, the formulations should be in the range of the tears' pH (6.5—7.6) to avoid ocular damage.[344] Following this notion, the pH of the microemulsions was monitored to evaluate the need for additional excipients to control pH variations. As depicted in Figure 30c, all DES-based microemulsions have suitable pH values for ophthalmic administration, namely 7.62 ± 0.02 for Bet:gly and 7.55 ± 0.02 for Bet:xyl. A slight decrease in pH of the microemulsions comprising chloramphenicol (7.38 ± 0.02 *vs.* 7.26 ± 0.01, respectively) was verified, especially after 90 days of storage at 4 °C in the dark (Figure 30c). However, these values are still in the ocular tolerable range.[345]

Regarding the droplet size of the internal oily phase of the multiple (w/o/w) microemulsion, the DES-based microemulsions presented a droplet diameter of 86.1—112.5 nm after their preparation, as shown in Figure 30d. The droplet size of the Bet:xyl-based microemulsions was slightly lower than that of Bet:gly ones (approximately 86.1 ± 1.2 and 101.7 ± 3.8 nm, respectively). A slight increase in the droplet size of both microemulsions was verified with the addition of chloramphenicol with values up to 110.0—111.0 nm, confirming its incorporation inside the droplets of the internal phase (Figure 30d). After 90 days of storage, the microemulsions presented a homogeneous appearance without phase separation and no significant differences in the droplet size of the internal oily phase. The droplet size influences not only the permeation process, but also the stability of the product. Microemulsions in a size range from 20 nm to 200 nm present good thermodynamic stability and low surface tension, promote mucoadhesion and are suitable for ocular administration.[346] Therefore, the DES-based microemulsions developed in this work not only have internal oily phase dimensions appropriate for ocular delivery, but also have good size stability under long-term storage conditions.
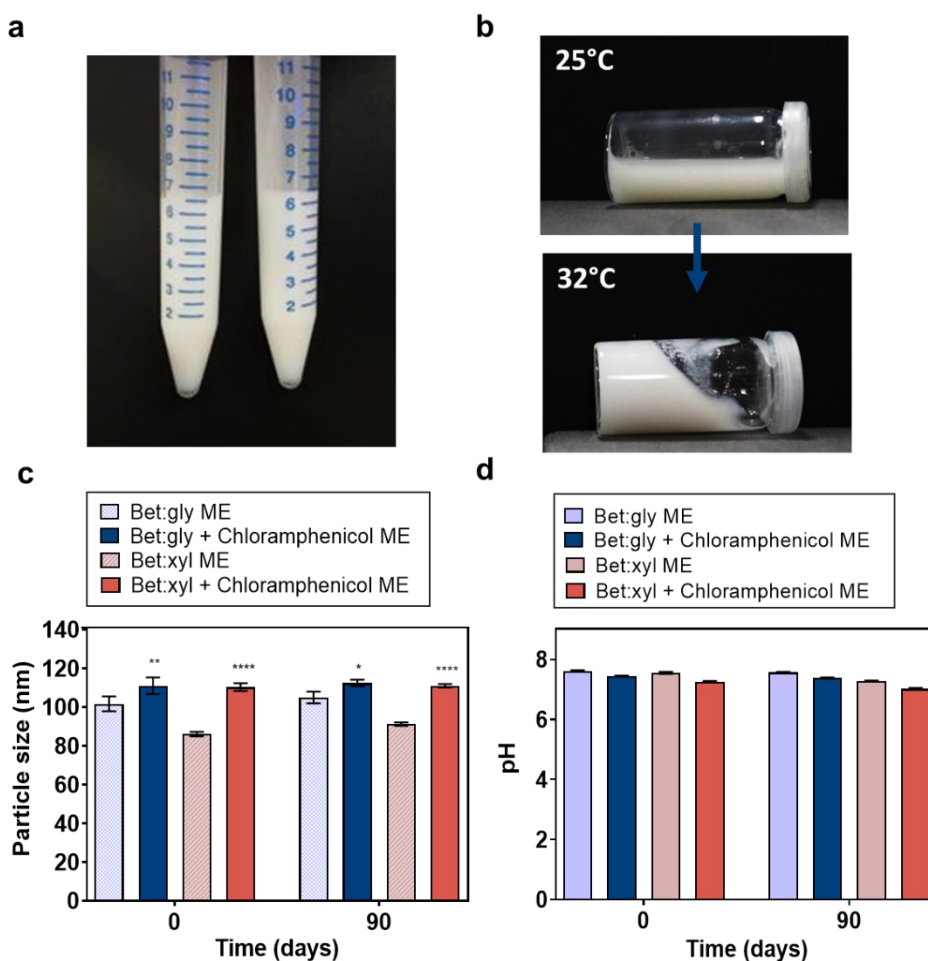
Figure 30. (a) Photographs of the Bet:gly and Bet:xyl based microemulsions comprising chloramphenicol at the day of their preparation (b) effect of temperature in the viscosity (visual appearance) of a microemulsion (c) droplet size and (d) pH of DES-based microemulsions (ME) with and without chloramphenicol upon 90 days of storage at 4 °C. *p< 0.0115, **p<0.0020, ****p<0.0001 particle size of DES-based ME comprising the antibiotic in comparison to the respective DES-based MEs without the drug. Data points represent mean ± standard deviation (n= 3).

The DES-based microemulsions were formulated to present a thermo-responsive character, which will translate into an increase in the viscosity upon contact with the ocular media, as ocular surface temperature (32 °C) is higher than the room temperature (25 °C). To study the viscosity response of these systems, the influence of the DES concentration and of the responsive polymer, that was PF-127, was tested by dispersing the polymer in DES aqueous solutions (at 10 and 30% (w/w)) (Figure 31a and 31b). Since dispersions with concentrations of PF-127 above 15% (w/w) have been reported to present adequate viscosities for ophthalmic application and a sol-gel transition below 35 °C,[347] we started by testing this polymer concentration. DES aqueous solutions with PF-127 dispersed at 15% (w/w) were

initially evaluated, showing an increased viscosity at ocular temperature; however, the DES concentration affected the two systems differently. At lower DES aqueous concentrations (10% (w/w)), the viscosity of both DES aqueous solutions with PF-127 is similar. Nevertheless, while the increase in Bet:gly concentration (up to 30% (w/w)) led to an increase in the viscosity, the increase in Bet:xyl concentration (up to 30% (w/w)) led to a decrease in the viscosity of the system (as observed Figure 31a). On the other hand, the viscosity of both DES aqueous solutions with PF-127 becomes comparable when chloramphenicol is solubilized in the media at similar concentrations to those used in eye drops, namely at 4% (w/w), independently of the DES concentration (Figure 31b).

Based on the described results, the 10% (w/w) of DES aqueous solution was selected as final concentration in each water phase of w/o/w microemulsions, to be applied in further studies. The viscosity of these DES-based microemulsions with PF-127 displayed similar tendencies to those observed for the respective DES aqueous solutions with PF-127, as illustrated in Figure 31c and 31d. This was particularly assessed by determination of an ascending and descending curve of the variation on the shear rate, to conclude about the behavior of these fluids. For both DES-based microemulsions, viscosity decreases with the increase of the shear rate (consistent with the pseudoplastic or shear thinning behavior), which in accordance with the behavior of natural tears, also categorized as a non-Newtonian, shear thinning fluid.[348] Interestingly, these formulations enhance the viscosity, even at lower concentrations of PF-127 (5% w/w), which is comparable to the results reported for other microemulsions with higher polymer concentration (15% w/w).[191] For this reason, the polymer concentration selected for the final microemulsions was 5% w/w of PF-127.

Similar to the DES aqueous solutions with PF-127 (Figure 31a and 31b), the corresponding Bet:gly-based microemulsions have also higher viscosity values than the ones with Bet:xyl (Figure 31c and 31d, respectively). This can be attributed to the effect of the co-solvents on the gelation ability of PF-127. Glycerol has shown to promote the formation of strong hydrogen-bonds with poloxamers such as PF-127, causing a slight decrease in the gelation temperature and therefore stronger gels.[349] Conversely, the use of alcohols such as ethanol or propylene glycol has proven to

106

increase the sol-gel transition temperature, decreasing the viscosity of the resulting systems, which might resemble the behavior observed for xylitol.[350]
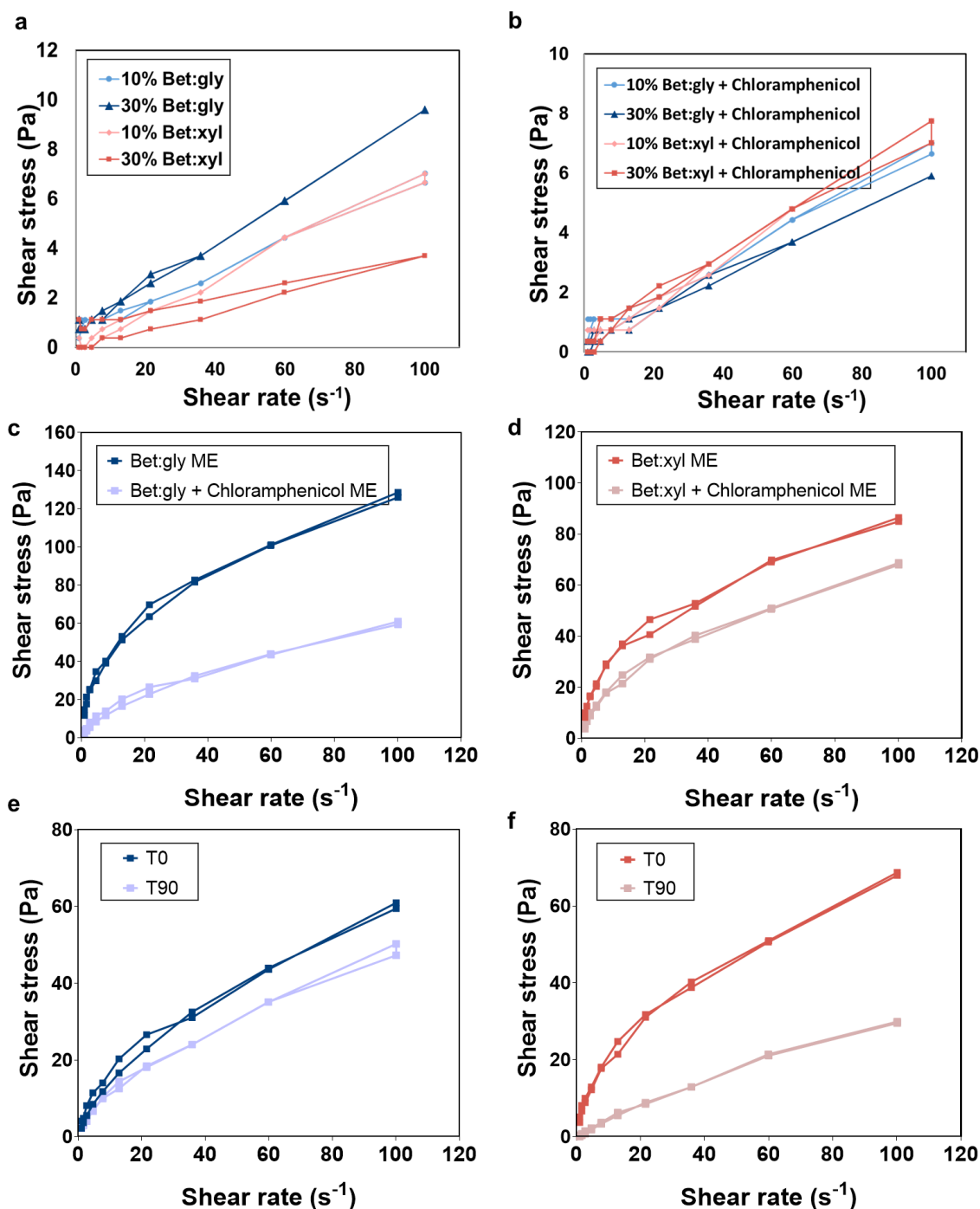
Figure 31. Rheograms of the effect of the different DES concentrations in aqueous media (10 and 30% (w/w)) with PF-127. This behavior was also studied in (a) the absence and in (b) the presence of the drug in the different DES aqueous solutions with PF-127. Rheograms of the DES-based microemulsions before and after the incorporation of chloramphenicol on (c) Bet:gly-based systems and (d) Bet:xyl-based systems and their respective stability (e) and (f) when comprising the antibiotic after 90 days of storage at 4 °C.

After the incorporation of the antibiotic in the DES-based microemulsions, the viscosity decreases for both formulations. In fact, the incorporation of drugs in PF-127 formulations or the inclusion of several additives has been stated to greatly modify the sol-gel transition boundaries of this polymer,[351,352] since it might increase the gelation temperature and decrease the adhesive forces. Other active ingredients, like diclofenac, have shown the ability to reduce the gel strength of PF-127 formulations.[353]

The stability of the DES-based microemulsions comprising chloramphenicol over 90 days stored at 4 °C was also studied (Figure 31e and 31f). After 90 days, the Bet:gly-based microemulsions comprising the antibiotic present only a slight decrease in the shear stress, and thereby in the systems' viscosity ($\approx 10\%$) (Figure 31e), maintaining the characteristics suitable for ocular application. Bet:xyl-based microemulsions comprising chloramphenicol present about a 2-fold reduction in their overall viscosity (Figure 31f). However, no visual changes or evidence of flocculation in both microemulsions were observed during the storage period.

Based on all the discussed results, generally, both DES-based microemulsions present a long-term shelf-life stability for the evaluated parameters. Furthermore, the advantageous use of the selected DES should be highlighted for this purpose since it avoids the addition of further excipients to control changes in these parameters in pharmaceutical formulations.

3.4.3 Drug stability in DES-based microemulsions

The stability of chloramphenicol in the DES-based microemulsions was assessed by measuring the drug concentration by HPLC-DAD. This parameter was evaluated over a month to allow its comparison with a commercial formulation of eye drops containing chloramphenicol, whose shelf-life is up to 28 days after opening. For this purpose, the commercial eye drops were stored following the manufacturer's recommendations (T $\leq$ 25 °C in the dark) and the DES-based microemulsions followed the storage conditions previously screened (4 °C in the dark). Figure 32a shows the chloramphenicol content at each time point relative to

the initial drug concentration. For both DES-based microemulsions, for at least 15 days of storage, the amount of the drug was kept constant.
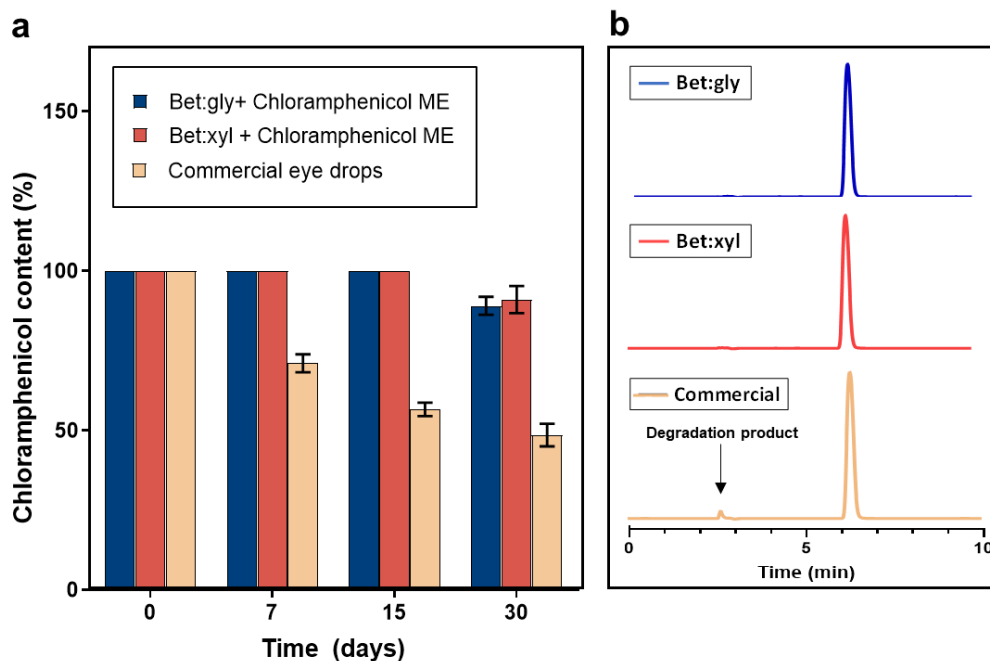
Figure 32. (a) Chloramphenicol content of each DES-based microemulsion (ME) and in commercial eye drops, quantified regularly over a month period. Each value is the respective mean ± SD. (b) HPLC chromatograms of chloramphenicol in each formulation 30 days (T_{30}) after preparation.

At the end of one month, the drug content was found to be 89% of the initial value for the Bet:gly-based microemulsion and 91% for the Bet:xyl-based one. For the commercial formulation the decrease in the drug concentration was more evident. In the commercial formulation, after 7 days, only 71% of chloramphenicol was detected, and, after one month, the drug concentration decreased to 48%, highlighting the low stability of the antibiotic in the commercial aqueous eye drops.[354] In fact, a peak of a degradation product was observed in the HPLC chromatogram of the commercial eye drops after 30 days of storage (Figure 32b). This has been already described for other commercial eye drops,[354] and happens due to the common degradation of chloramphenicol by hydrolysis of the amide group in aqueous media.[355] Remarkably, this is not verified in the DES-based microemulsions developed in this work, which not only allows us to significantly enhance the drug stability but also prevented the formation of hydrolysis products after storage, which is certainly due to the entrapping of chloramphenicol in the microemulsion droplet interface. The DES-based microemulsions have also shown the possibility to increase the stability over other microemulsions reported in the

literature to this purpose,[354] while offering a higher shelf-life for the drug over commercial formulations.

3.4.4 Cytotoxicity of the DES-based formulations

The *in vitro* cytotoxicity of chloramphenicol was studied in aqueous solution and in the DES-based microemulsions towards ARPE-19 by exposure for 24 h. Each formulation comprising chloramphenicol was evaluated in concentrations ranging from 12.5 to 100.0 $\mu g \cdot mL^{-1}$. For comparison purposes the commercial eye drops were also tested in the same range of concentrations. These concentrations were selected considering the limited amount of drug that crosses the protective mechanisms of the eye and that becomes in contact with the cells.[356] Initially, the effect of chloramphenicol in aqueous solution in ARPE-19 cells viability was appraised. This antibiotic seems to present low cytotoxicity in the studied range of concentrations since all cell viability was above 90% (Figure 33a). When formulated as eye drops, the effect of chloramphenicol and the respective excipients demonstrates dosage-dependent toxicity, which decreases in the studied range of concentrations up to 80% for a drug dosage of 100.0 $\mu g \cdot mL^{-1}$ (Figure 33b). Similar values have been found for the cell viability of human keratinocytes cells, when exposed to diluted commercial eye drops in the same range of drug concentrations here explored.[357] Therefore, the possible decrease in cell viability might be attributed to the formulation excipients commonly found in commercialized eye drops.

Following this, the cytotoxicity of both microemulsions, with and without the drug, was investigated. The DES-based microemulsions without the antibiotic exhibit non-cytotoxicity towards ARPE-19 cells with cell viabilities always above 85% (Figure 33c and 33d).

The incorporation of the antibiotic in both DES-based microemulsions does not significantly impact the cytotoxicity of the resultant formulations (Figure 33c and 33d). These exhibit similar profiles with comparable cell viability values within the studied range of concentrations. At higher concentrations, namely 100 $\mu g \cdot mL^{-1}$, the cell viability decreases to 88% for the Bet:gly-based microemulsion when containing chloramphenicol (Figure 33c) and to 91% for the Bet:xyl-based containing the same

drug (Figure 33d). Such values are comparable to those observed for aqueous solution containing the same chloramphenicol concentration (100 µg·mL^{-1}).
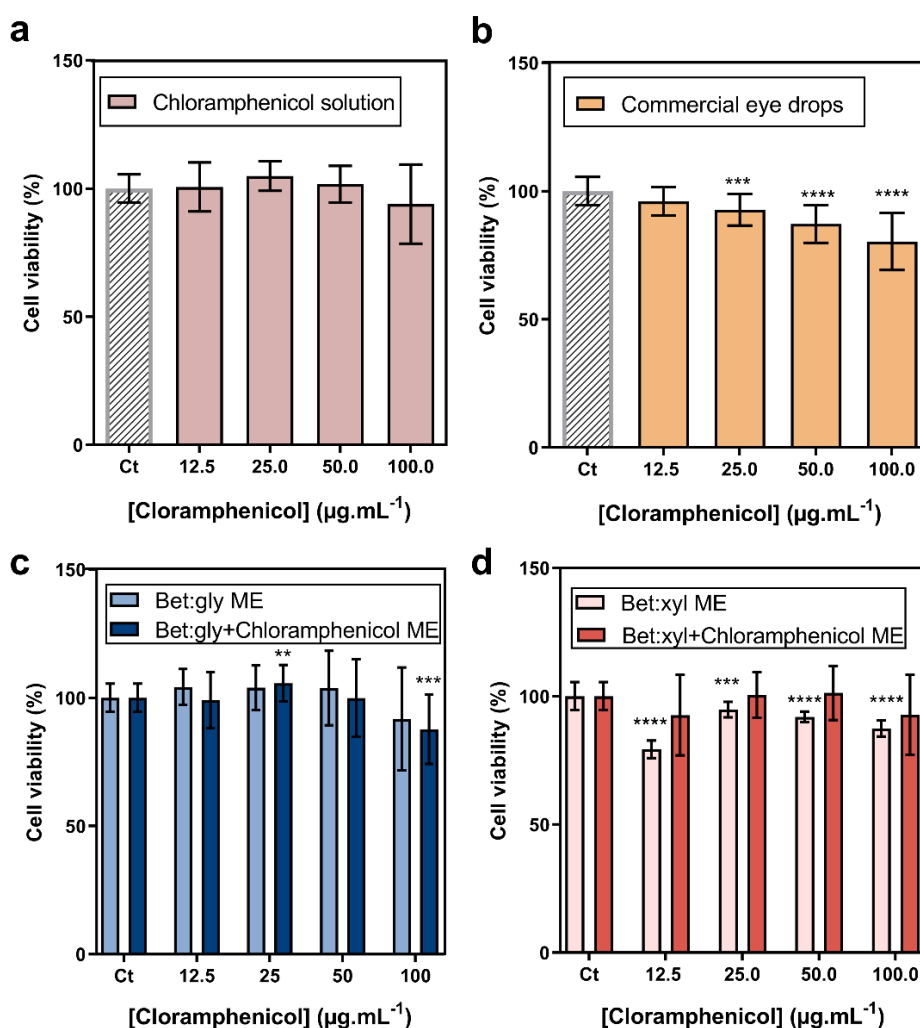
Figure 33. Cytotoxicity values after 24 h of exposure *vs.* control ARPE-19 cells (Ct) determined for (a) chloramphenicol in aqueous solution, (b) commercial eye drops, (c) Bet:gly microemulsions (ME) with and without chloramphenicol and (d) Bet:xyl MEs with and without chloramphenicol incorporated, at 37 °C. Results are expressed as mean ± SD of four independent experiments. **$p < 0.0043$, ***$p < 0.0003$, ****$p < 0.0001$ cell viability in comparison to the control cells.

These findings highlight that safe chloramphenicol concentrations were used in the present work and that the incorporation of this drug in the DES-based microemulsions does not create a more toxic ophthalmic formulation. Overall, the two developed DES-based microemulsions present comparable cytotoxicity values to already commercialized eye drops. Therefore, for the next experiments, the highest chloramphenicol concentration tested (100 µg·mL^{-1}) was considered.

3.4.5 *In vitro* and *ex vivo* drug permeation studies

The *in vitro* release profile of chloramphenicol from both DES-based microemulsions was investigated in PBS (pH 7.4) at 32 °C for 3 h, to simulate ocular physiological conditions (Figure 34a). Contrarily to commercial eye drops, in which the drug release into the ocular media is instantaneous, and for that reason is not here presented, the results of this study revealed a sustained release of the antibiotic from DES-based microemulsions. Furthermore, these microemulsions present similar release profiles over the assay period. After 1 h, 34.7% and 32.6% of chloramphenicol were released from Bet:gly and Bet:xyl-based microemulsions, respectively (Figure 34a). At the end of the total assay period (3 h), 79.8% of the drug was released from the Bet:gly-based microemulsion and 80.2% from the Bet:xyl-based one. These results are quite relevant since due to the low solubility of chloramphenicol, its release into aqueous media can be as low as 37%, even after 7 days, without the application of any solubilization strategy.[358]

Studies have reported the use of bi-layered polymer-based films,[359] nanoparticles[358] and other microemulsions[360] to offer an improvement in drug delivery over commercial eye drops. Although these can achieve high amounts of drug released, most still present a slow-release rate, which delays the therapeutic onset of the drug. The DES-based microemulsions herein prepared allow a sustained release of the drug, achieving a high drug content release within only 3 h. In fact, after only 5 min, both DES-based microemulsions could deliver chloramphenicol concentrations far above the MIC for *Staphylococcus* species (>30% the MIC value for *S. aureus*[291]).

To infer the impact of the formulations on the permeation of chloramphenicol, *ex vivo* studies through corneal tissue were conducted over 3 h at 32 °C, using Franz diffusion cells. Figure 34b presents the results obtained for each DES-based microemulsion and for the commercial formulation. As observed in the *in vitro* release assays, the permeation of chloramphenicol across the corneal tissue follows a sustained permeation pattern. This sustained drug delivery is attributed to the fact that DES-based microemulsions were designed to comprise chloramphenicol in in both external and internal DES:water phases, providing an immediate therapeutic effect from the external phase of the microemulsion and a more sustained release

of the drug from the internal phase, as depicted in Figure 34c. These release abilities associated with an increase in the viscosity under temperatures closer to the ocular environment result in a successful continuous delivery of chloramphenicol and, thereby, a sustained release of the drug.
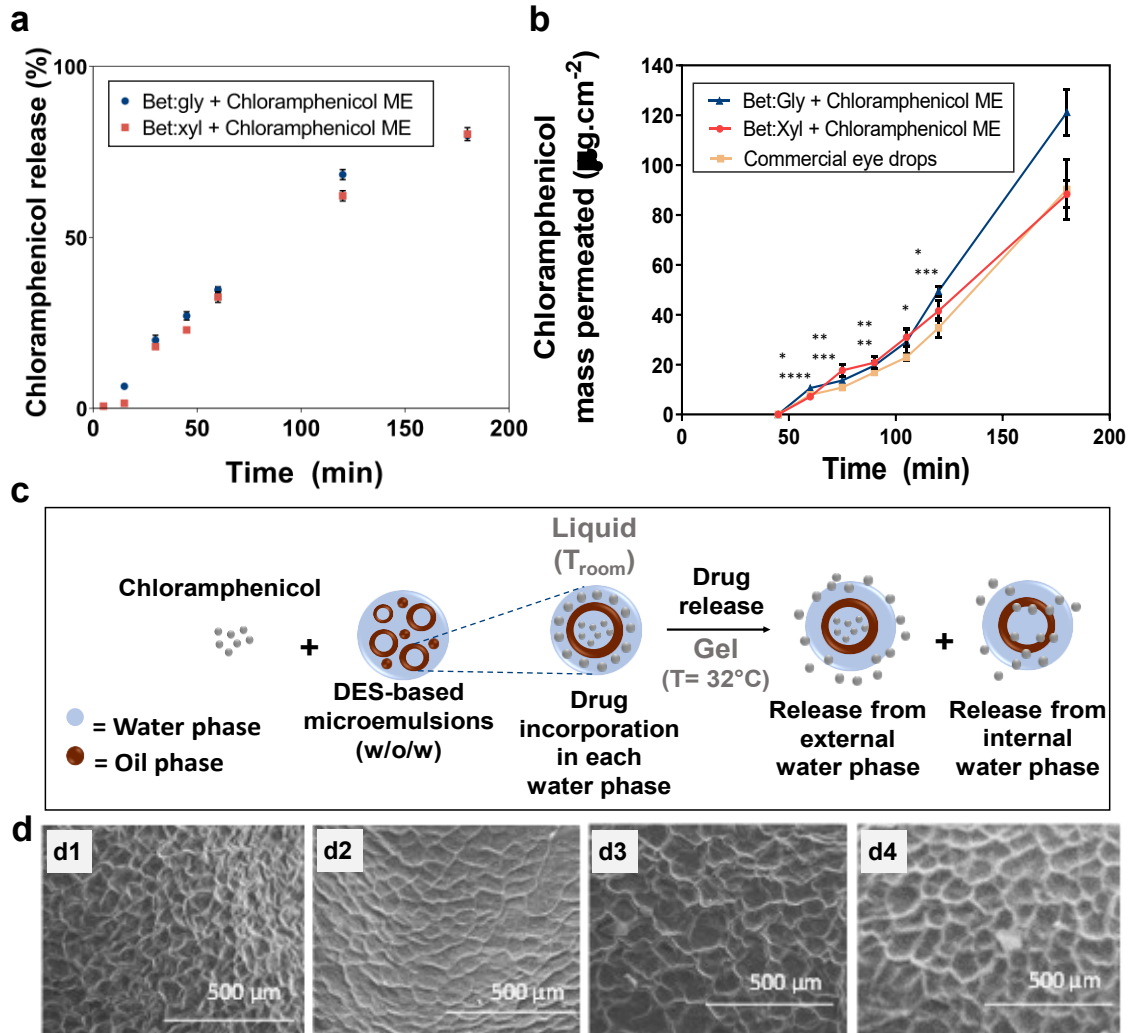
Figure 34. (a) *In vitro* release profile of chloramphenicol from Bet:gly and Bet:xyl-based microemulsions (ME) over 3 h in PBS at 32°C. (b) cumulative amount of chloramphenicol permeated across corneal tissue during 3 h for chloramphenicol from Bet:gly and Bet:xyl-based MEs and for commercial eye drops. All profile data represented as mean ± standard deviation of three independent experiments. *p<0.03, ***p<0.003, ****p<0.0001 amount of chloramphenicol permeated from each ME in comparison to the commercial eye drops. (c) Schematic representation of chloramphenicol loading into the water phases of both DES-based microemulsions and the two-phase drug release at ocular temperature. (d) SEM micrographs of the corneal tissue after 3 h of exposure to (d1) Bet:gly and (d2) Bet:xyl- based MEs comprising chloramphenicol, (d3) commercial eye drops and of (d4) control.

Both DES-based microemulsions present similar permeation profiles within the first 120 min, with permeated amounts of chloramphenicol up to *ca*. 49.4 µg·cm^{-2}. After this time, the Bet:gly-based microemulsion enabled a higher permeation of the

antibiotic across the corneal tissue than the Bet:xyl-based one. Such an effect can be expected since glycerol has been used as a permeation enhancer to improve the penetration of active ingredients across biological membranes.[361] The two DES-based microemulsions promote the permeation of higher amounts of the drug across the corneal membrane than commercial eye drops, during the assay period. This can also be anticipated as DES are known to facilitate the permeation of solubilized active ingredients across membranes without negatively affecting the cells.[137] These values reflect an amount of 44.0—46.1 $\mu g \cdot mL^{-1}$ of chloramphenicol permeated 120 min after application, which is in accordance with previous values reported for chloramphenicol permeation from ointment formulations.[362] Since these formulations allow reducing the initial drug concentration while distributing similar amounts to commercial eye drops through the corneal tissue with comparable safety, it is possible to model the amount of drug to be incorporated into DES-based microemulsions.

We have further extended the assay period for 180 min to understand the influence of the developed formulations on the corneal tissue during longer periods of exposure. Interestingly, the microemulsions, and more particularly the Bet:xyl-based microemulsion (Figure 34d2), did not induce higher structural changes than the eye drops (Figure 34d3) for the same period of exposure (180 min), demonstrating that their effect on the morphology of the corneal tissue is comparable to the commercial formulation under similar conditions. The most sustained drug release and permeation in the DES-based microemulsions are, in this sense, advantageous as these formulations allow a higher drug accumulation in contact with the cornea, which can locally prolong the therapeutic effect comparatively to the commercialized eye drops formulations.

3.4.6 Antimicrobial efficacy

Based on the chloramphenicol's action and the sustained release ability of the DES-based microemulsions, their antimicrobial activity in the treatment of multidrug-resistant infections was finally evaluated. For this purpose, the efficacy of these formulations was studied in the eradication of Gram-positive bacteria, namely

MRSA. The commercial chloramphenicol eye drops were also used in the same drug concentration for comparison purposes.

Firstly, the determination of the antimicrobial susceptibility to the DES-based microemulsions, with and without chloramphenicol and to eye drops, was performed (Figure 35a). It is possible to verify that the DES-based microemulsions without the drug do not present antimicrobial activity. The composition of the DES-based microemulsions differs only in the hydrogen-bond donor. Glycerol does not present relevant antimicrobial activity but is used in commercial antibiotic formulations and xylitol presents only a slight ability to interfere in biofilm formation, by inhibiting the bacterial adherence of *S. aureus*.[363] Overall, the bacteria seem to be susceptible to chloramphenicol in all the tested formulations comprising the drug, according to EUCAST classifications.[291] The Bet:gly and Bet:xyl-based microemulsions containing chloramphenicol exhibited growth inhibition zones of 28 ± 2 mm and 27.5 ± 2 mm, respectively, whereas eye drops commercialized formulation showed one with 25 ± 2 mm (Figure 35a).

When considering the treatment of infections caused by resistant bacteria to systemic antibiotics, topical treatment can be a more effective alternative due to the higher local concentrations. Generally, two drops of chloramphenicol formulation are prescribed every 2 to 3 h in the first 48 h, reducing afterwards to 4 to 6 h. The drug should be administered for a further 48 h after the eye appears to be normal. Based on the clinical prescription of this antibiotic, a severe eye infection caused by a resistant bacterium (MRSA) was simulated, treating it with specific drug dosages (100 $\mu g \cdot mL^{-1}$) initially administered at each 2 h for 48 h, and then each 4 h up to 5 days to guarantee complete bacterial eradication (results depicted in Figure 35c). The drug action in both DES-based microemulsions comprising chloramphenicol and the respective commercial eye drops in this strain was monitored. A bacterium positive control (Ct) containing only the bacterial inoculum in PBS was also carried out, being cultured at the same time points but in the absence of the antibiotic or the DES-based microemulsions.

In the absence of the antibiotic and DES-based microemulsions, the bacterium growth increases in the first 48 h (1.9 $\log_{10}$, $p < 0.0001$), remaining stable during the rest of the assay period at high bacterial concentrations. When the bacterium was

exposed to the antibiotic formulations, the decrease in the bacterium growth seems to be not only time-dependent but also reliant on the number of drug applications, reflecting the growth inhibition capability of the formulations studied. The DES-based microemulsions containing chloramphenicol present a similar profile of eradication of MRSA infection without statistical differences between both microemulsions, being more effective in the eradication of MRSA infections than the commercial eye drops, as presented in Figure 35c. The growth inhibition of the drug is comparable between all the studied formulations up to 24 h after the treatments' start, presenting a 2.4 $\log_{10}$ reduction of the bacterium growth (p < 0.0001).

However, at the end of the second day of dosage applications, the differences between the DES-based microemulsions and the commercial eye drops start to become obvious. While 4.5 and 4.1 $\log_{10}$ reductions in the bacterium growth (p < 0.0001) were verified for Bet:gly-based and Bet:xyl-based microemulsions, the eye drops enable only a 3.4 $\log_{10}$ decrease (p < 0.0001). After 48 h, the commercial eye drops only allowed a 3.8 $\log_{10}$ reduction in the bacterium growth (p < 0.0001) (Figure 35c and 35d1), while both DES-based microemulsions were capable of fully eradicating the MRSA bacteria (Figure 35c, 35d2 and 35d3). In fact, the commercial eye drops took 72 h to eradicate the MRSA bacteria till the detection limit of the methodology, i.e., more 24 h than the DES-based microemulsions. Considering that low drug concentrations were tested, it is expected that with the application of one drop of each DES-based microemulsion (4.0 mg·mL^{-1}) the drug efficacy would be even better than the eye drops with similar drug concentration, requiring fewer applications to fully eradicate the MRSA infection.
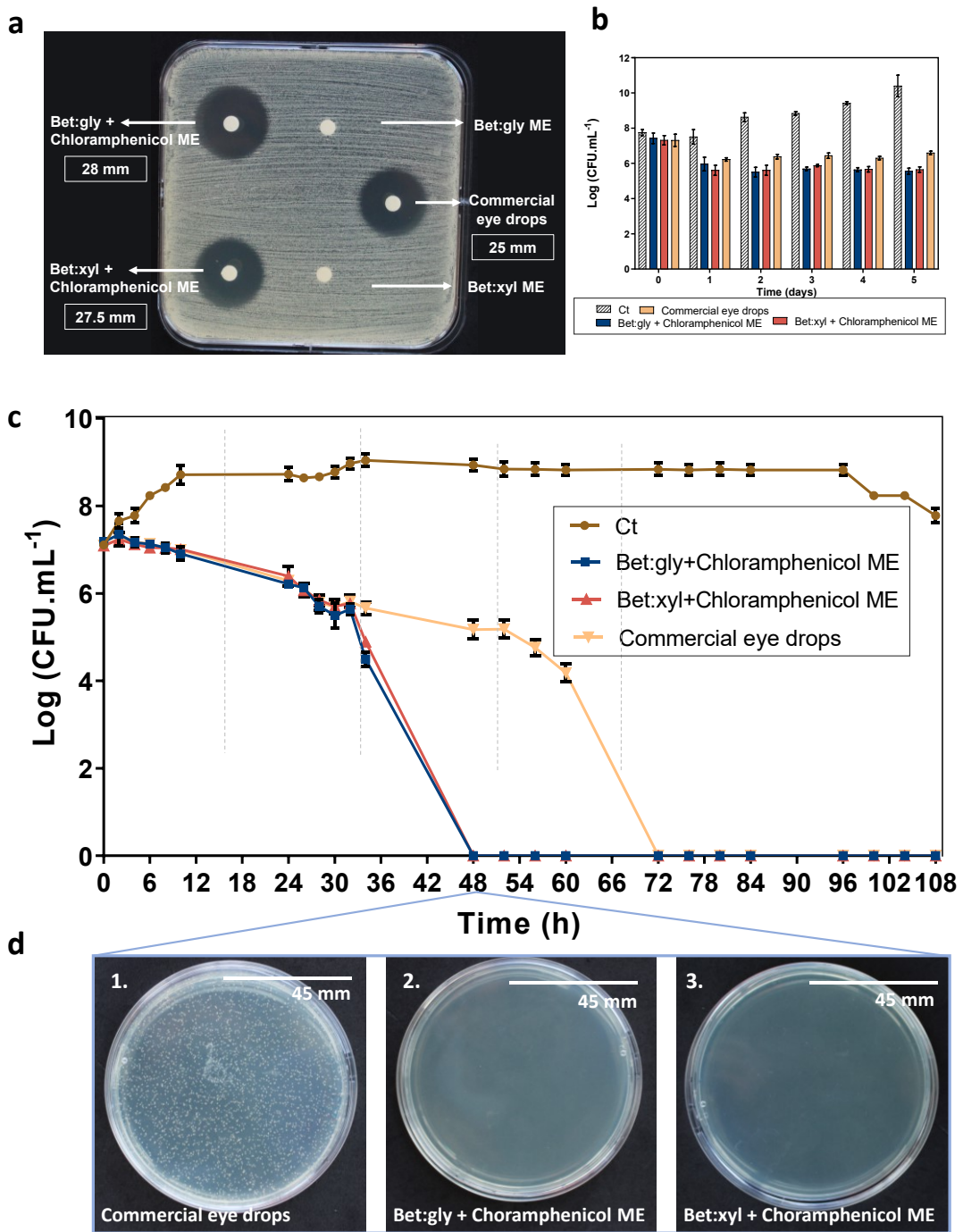
Figure 35. (a) Antimicrobial susceptibility of *Staphylococcus aureus* (MRSA) DSM 25693 to Bet:gly-based ME and Bet:xyl-based ME with and without chloramphenicol and to the commercial eye drops (disks with 100 µg·mL^{-1} of antibiotic). (b) MRSA viability after exposure to the DES-based microemulsions and to the commercial eye drops in PBS media at 37 °C. A positive control (Ct) bacterium was also conducted over the same period for comparison purposes. (c) Growth inhibition profiles, in liquid medium TSB at 37°C, of Bet:gly-based ME and Bet:xyl-based ME and commercial eye drops determined based on the Colony Forming Units per mililiter (CFU·mL^{-1}) from the samples collected over each time point after administration of an antibiotic dose of 100 µg·mL^{-1} and of the bacterium without being submitted to any formulation (Ct). Dashed lines represent the different days of drug administration. Data are presented as mean ± SD values of three independent studies for each sample. (d) Plate photographs of the colonies formed in agar after 48 h of treatment with each formulation.

117

In parallel, the toxicity of the DES-based microemulsions towards the bacterial cells has been also evaluated, performing a cell viability test after exposure to a single chloramphenicol dosage of 100 µg·mL^{-1} (data shown in Figure 35b). Such study indicated that the two DES-based microemulsions and the commercial eye drops do not present toxicity towards MRSA, and that the effective bacterium eradication by chloramphenicol in the microemulsions is due to an enhanced bactericidal action. Therefore, the behavior observed can be possibly attributed to a synergetic effect of both the DES aqueous solutions comprising chloramphenicol and the microemulsion formulation. The thermo-responsive microemulsions might act as more effective carriers to deliver the drug into the bacterial cells. In fact, both DES and microemulsions have been reported to enhance the cellular permeability of bacteria, enabling an increase in intracellular concentrations of certain compounds.[322,364] This effect might explain the improved activity of the DES-based microemulsions, since chloramphenicol is more readily available inside the bacterial cell to exert its action, to bind to the bacterial ribosome structure and inhibit protein synthesis.[330]

3.5 Conclusions

Bet:gly and Bet:xyl-based microemulsions with thermo-responsive character were developed and characterized aiming to improve the therapeutic action of the antibiotic chloramphenicol typically used to treat ocular infections. The use of aqueous solutions of DES proved to be a promising strategy to improve the drug water solubility of the antibiotic up to 140-fold, while avoiding the use of common organic solvents. Furthermore, their incorporation as water-phases in the development of w/o/w microemulsions enabled the design of thermo-responsive microemulsions with a final drug concentration of 4 mg·mL^{-1}. The investigated DES-based microemulsions present pH, droplet size and viscosity values adequate for ophthalmic administration. The use of DES in these formulations allowed to overcome the use of further preserving excipients, resulting in formulations that are stable over, at least, 3 months. Furthermore, the use of DES improved the gelling properties of the system requiring the use of a lower percentage of the *in situ* gelling polymer (PF-127) to achieve a higher viscosity at ocular temperature. Additionally, when containing chloramphenicol, the DES-based microemulsions improved the preservation of the drug stability compared to the commercial eye drops.

The microemulsions developed herein are non-cytotoxic to ARPE-19 cells (cell viability >88%), presenting similar cytotoxic values to those achieved for commercial formulations. The incorporation of chloramphenicol in the outer and inner phase of the w/o/w microemulsions and the thermo-responsive character of these systems allowed to obtain a sustained-release of the antibiotic from the Bet:gly- and Bet:xyl-based microemulsions, reaching a drug release of 79.8% and 80.2% within 3 h, respectively. These profiles translate into an *ex vivo* sustained permeation of the drug through the corneal tissue with higher amounts of permeated drug.

The use of the DES-based microemulsions shortened the treatment period from 72 h to 48 h, when compared to a commercial eye drops formulation. These results might translate into a decrease in the chloramphenicol concentration needed for the development of future ophthalmic formulations containing this antibiotic.

In summary, the developed DES-based microemulsions can enhance the efficacy of chloramphenicol ophthalmic application by improving its retention in the ocular mucosa, allowing a higher drug contact with the affected area. This results in

an enhancement in the treatment of ocular infections caused by resistant bacteria, such as MRSA. The results here reported pave the way for the use of DES in the development of drug delivery systems with improved performance, deserving to be further investigated towards their recurrent application.

Chapter 4. Incorporation of DES Formulations in Biopolymer-Based Drug Delivery Systems for Antimicrobial Photodynamic Therapy
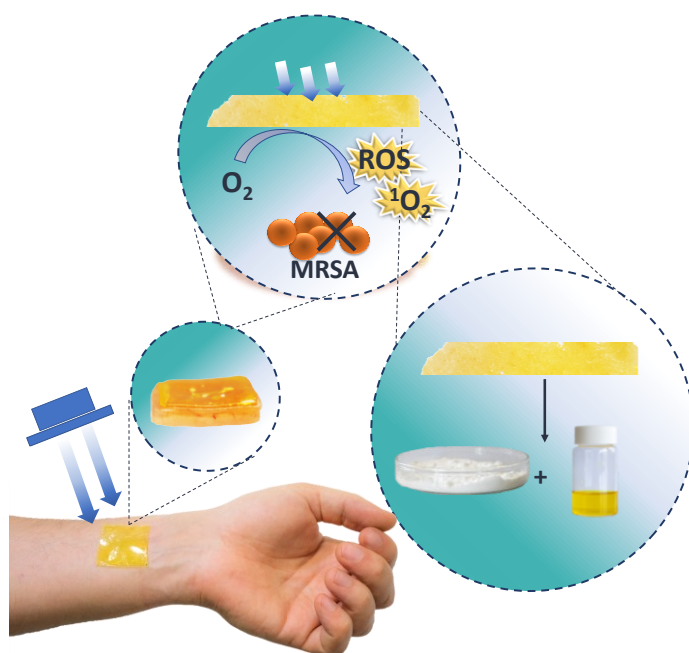
---

4.1 Abstract

Antimicrobial photodynamic therapy (aPDT) is a potent tool to surpass the global rise of antimicrobial resistance; still, the effective topical administration of photosensitizers remains a challenge. Biopolymer-based adhesive films can safely extend the residence time of photosensitizers. However, their wide application is narrowed by their limited water absorption capacity and gel strength. In this study, pullulan-based films with a switchable character (from a solid film to an adhesive hydrogel) were developed. This was accomplished by the incorporation of a betaine-based DES containing curcumin ($4.4\ \mu g \cdot cm^{-2}$) into the pullulan films, which tune the skin moisture absorption ability of the films, and therefore their switch into an adhesive hydrogel capable of delivering the photosensitizer. The obtained transparent films presented higher extensibility (elongation at break of 68.2%) than the pullulan counterparts (1.81%), and the corresponding hydrogels a 4-fold higher adhesiveness than commercial hydrogels used for skin applications. These non-cytotoxic adhesives allowed the inactivation (~ 5 log), down to the detection limit of the method of eradication, of multi-resistant strains of Staphylococcus aureus in *ex vivo* skin samples. Overall, these materials are promising for aPDT in the treatment of resistant skin infections, while being easily removed from the skin.

4.2 Introduction

Antimicrobial resistance has challenged the global healthcare system, becoming a threat during recent decades to treat antibiotic-resistant infections.[11,365] Particularly, the migration of MRSA from its hospital confinement and long-term care facilities to community-acquired infections has narrowed the number of antibiotics that are still effective to tackle this critical health concern.[366] In the search for alternative strategies to treat multidrug-resistant skin infections, antimicrobial photodynamic therapy (aPDT) has proven to be a promising option.[367] This approach uses light with appropriate wavelengths, along with a photosensitizing agent, which in the presence of molecular oxygen generates oxidant species [ROS like superoxide and singlet oxygen, ($^1O_2$), that kill pathogens.[368] Attempting to inactivate MRSA infections, several aPDT approaches and photosensitizers have been reported.[213] However, a high number of photosensitizers display low water solubility, adverse toxicity, severe self-quenching effect and even some might present photostability concerns.[213,369] A challenge to be tackled in the application of aPDT to skin infections and wounds is the selection of more benign photosensitizers and the development of carrier systems capable to release these compounds, while being transparent for light activating purposes.[370]

Hydrogels have been recently considered in aPDT treatments for wound therapy.[371] The advantage of these systems is the dual capacity for being used as both bandage material and delivery system, while providing a moist healing environment.[370,372] Hydrogels originating from natural polymers, such as alginate,[373] keratin [373] and chitosan,[374,375] have been applied for aPDT purposes. Adhesive hydrogel films have the advantage of extending the residence time, allowing to prolong the local therapeutic action.[376] These delivery systems are usually designed as flexible systems that can easily adapt to the site of application, being more comfortable to use from the patient's perspective.[377] Among these, biopolymers with hydrophilic groups are commonly used due to their high potential for adhesiveness by electrostatic interactions or hydrogen bonding.[378] Biopolymers like silk[379] and chitosan[374,375] have been applied in the production of adhesives aiming to be applied in aPDT for tissue repair and oral and skin application purposes. The use of natural polymers in this area has shown to enhance cell proliferation and tissue

differentiation, allowing to inhibit wound infection while promoting wound repair, which would be desirable in the treatment of skin infections.[380,381] Yet, some of these biopolymers still display low water absorption capacity and gel strength, which need to be ideally targeted to develop appropriate biopolymer-based systems for aPDT therapy.[382,383]

Pullulan is a polysaccharide that originates from highly transparent films, which is an appealing feature for application as supports on aPDT. Additionally, this polysaccharide possesses good mechanical performance, thermal stability and excellent water solubility.[229,384] Pullulan has also been reported for its ability to improve wounds re-epithelialization, dermal regeneration, blood vessels formation and collagen synthesis, proving that pullulan gels could be potential wound healing agents.[243] The mentioned characteristics might be advantageous for the development of target delivery systems that aim to treat topical diseases with sensitized areas, such as skin infections. However, so far, the application of pullulan-based films in this domain is limited and is mostly focused on mucoadhesive-based systems for oral administration,[385] and to a smaller extent, to produce nanoparticles and nanogels for the photodynamic therapy of cancer.[234,386]

Herein, we aimed to develop a biopolymer-based adhesive film loaded with a photosensitizer that could present enhanced mechanical and adhesive properties, as well as superior photodynamic action, for topical application. To this purpose, the application of pullulan and a natural and low toxicity photosensitizer, viz. curcumin, in the development of a delivery system to be used as aPDT towards skin infections was explored. Furthermore, this system presents a switchable character when in contact with skin moisture by transitioning from a solid film into a highly adhesive hydrogel, achieved by the incorporation of an aqueous solution of DES. The system can simultaneously adhere to skin and deliver the photosensitizer in an infected area using the single film layer, and thus enhance the photodynamic action of curcumin. All films were characterized in terms of optical, thermal and mechanical properties, and the adhesiveness of the final films was tested on *ex vivo* skin samples. The photodynamic antimicrobial action was initially studied in *S. aureus* ATCC 6538 in solution and then, as a proof-of-concept, was tested against MRSA on *ex vivo* skin samples.

4.3 Experimental section

4.3.1 Materials and culture conditions

The DES studied herein was prepared by combining betaine anhydrous (98%, Alfa Aesar, Germany) and levulinic acid (≥ 98%, Sigma-Aldrich, St. Louis, Missouri, USA). The photosensitizer used was curcumin (≥ 95, Sigma-Aldrich, St. Louis, Missouri, USA). Pullulan powder (98%, MW 272 kDa) was supplied by B&K Technology Group (Xiamen, China). MTT was purchased from Sigma-Aldrich (St. Louis, Missouri, USA). Other reagents and solvents were from HPLC grades. For the bacterial cultures, TSA and TSB were used and supplied by Liofilchem (TE, Italy). The PBS (pH 7.4) was prepared by dissolution of tablets acquired from Sigma-Aldrich (St. Louis, Missouri, USA). HaCaT cells obtained from Cell Lines Services (Eppelheim, Germany) were cultured in DMEM supplemented with 10% of FBS and 1% of L-glutamine, penicillin– streptomycin and fungizone (Life Technologies, Grand Island, NY, USA) and incubated with 5% CO_2 in a humidified atmosphere at 37 ºC.

4.3.2 DES composition and preparation

The DES investigated in this work was prepared by the heating method by mixing the respective precursors (betaine and levulinic acid, Bet:Lev) in sealed glass vials at 1:1 molar ratio. These vials were placed under constant heating and stirring until a homogeneous transparent liquid was obtained (maximum temperature of 85 °C). The DES was then allowed to return to room temperature. The respective DES components' integrity was confirmed by ^{1}H NMR and ^{13}C NMR spectroscopy. The referred spectra were recorded using a Bruker Avance 300 at 300.13 MHz and 75.47 MHz, respectively, in deuterated water and using TMSP as an internal reference.

Betaine:levulinic acid: ^{1}H NMR (300.13 MHz, D_2O): δ 2.06 (3H, s, H-5'); 2.42 (2H, m, H-2'); 2.70 (2H, m, H-3'); 3.10 (9H, s, $N(CH_3)_3$); 3.74 (2H, s, H-2); 4.71 (solvent, (D_2O)) ppm. ^{13}C NMR (75.47 MHz, D_2O): δ 27.84 (C-5'); 29.82 (C-2'); 37.87 (C-3'); 53,25 ($N(CH_3)_3$); 65.93 (C-2); 168.84 (C-1); 177.12 C-1'); 213.34 (C-4') ppm.

4.3.3 Curcumin's solubility assay

The determination of the solubility of curcumin in water and in the aqueous solutions of Bet:Lev followed a previously reported procedure in Section 2.3.3. Briefly, the solubility was determined by saturation of 2.0 g of pure water or of each DES aqueous solution (0—90% (w/w) of DES) with curcumin at both room (25 °C) and human body (37 °C) temperatures. A measured aliquot of each saturated solution was diluted to a well-defined final total v/v, carefully filtered with a 0.45 μm syringe filter to remove any solid and subsequently quantified by HPLC-DAD (Shimadzu, model PROMINENCE, Kyoto, Japan) to determine the curcumin solubility. HPLC analyses were performed with an analytical C18 reversed-phase column (250 × 4.60 mm^2), Kinetex 5 μm C18 100 Å, from Phenomenex conducted in isocratic mode under a flow rate of 1 mL·min^{-1} and operated at 35 °C. The mobile phase contained 40% (v/v) of methanol, 15% (v/v) of acetonitrile and 45% (v/v) of ultra-pure water with 0.3% (v/v) of ortho-phosphoric acid. Samples were analyzed at 377 nm in duplicates and using an injection volume of 10 μL.

4.3.4 Photostability of curcumin in the Bet:Lev solution

Photostability was evaluated by placing the samples in 6-well plates filled with a final volume of 5 mL of PBS and under stirring. DES aqueous solutions (50% w/w) comprising curcumin and aqueous solutions of curcumin solubilized in acetone (50% w/w) were added to each well to obtain specific curcumin concentrations in the range of 5 to 200 μM. After 15 min of incubation in the dark, the samples were exposed to a light source with an irradiance of 50 mW·cm^{-2} for 60 min. Aliquots (100 μL) of each well were collected at each 15 min and curcumin was quantified by HPLC-DAD using the previously described method. Three independent studies for each curcumin concentration were conducted, and each sample was analyzed at least in duplicate.

4.3.5 Preparation of the Pullulan-based films

Four different pullulan-based films were prepared using an aqueous solution of 6.0% (w/v) of pullulan, i.e., films without the photosensitizer (PL), with curcumin

solubilized in aqueous solution with acetone (PL-C) (4.4 µg·cm^{-2} dose), with the Bet:Lev aqueous solution (PL-DES) and with curcumin solution in aqueous Bet:Lev (PL-(DES+C) (4.4 µg·cm^{-2} dose). For the films with curcumin in aqueous Bet:Lev solution and the ones only with Bet:Lev aqueous solution, the DES was added to present the same concentration of the biopolymer (1:1 mass ratio). For the PL-C films, due to the low solubility of curcumin in water, the DES amount was replaced by aqueous acetone (both 50% w/w). Finally, films were obtained by casting the solutions in silicone plates with dimensions of 5 × 15 cm^2, placed at 40 °C in a ventilated oven overnight. All films were produced in triplicates.

4.3.5 UV-Vis Spectroscopy

Transmittance spectra of the films were recorded at room temperature (200-800 nm). Acquisition was made with a Shimadzu UV-1800 UV-Vis spectrophotometer (Shimadzu Corp.,Kyoto, Japan) equipped with a quartz window plate, bearing the holder in the vertical position. For better comprehension of the UV-Vis spectra in transmittance mode behavior of the films comprising the photosensitizer, curcumin absorption spectrum was also recorded in the same conditions.

4.3.6 FTIR-ATR Spectroscopy

FTIR-ATR spectra were collected for all pullulan-based films and for the Bet:Lev and for the curcumin used (for comparison purposes). With this aim, a FTIR system Spectrum BX (Perkin-Elmer Inc., Waltham, Massachusetts, USA) equipped with a diamond crystal and a single horizontal Golden Gate ATR cell was used. All analyses were performed at room temperature with controlled relative humidity (75–80%) in the range of 4000–400 cm^{-1} with a resolution of 4 cm^{-1} and by accumulating 64 scans with an interval of 1 cm^{-1}. A background air spectrum was subtracted in all the spectra acquired, and the results were recorded as transmittance values.

4.3.7 Thermogravimetric analysis

Samples were heated at a constant rate of 10 °C·min^{-1} from room temperature up to 800 °C under a nitrogen flow of 20 mL·min^{-1}. The assays were carried out with a SETSYS Setaram TGA analyzer (SETARAM Instrumentation, France) equipped with a platinum cell.

4.3.8 Mechanical tests

The mechanical properties of the pullulan-based films were evaluated through tensile tests performed on an Instron 5966 Series machine (Instron Corporation, Norwood, Massachusetts, USA). Analyses were conducted in traction mode at a crosshead velocity of 10 mm·min^{-1} and using a static load cell of 500 N and at room temperature. Rectangular specimens (5 × 1 cm^2) were used, and at least 5 replicates were tested for each sample, with final values expressed as the average ± SD. The Young's modulus, the tensile stress and the elongation at break were calculated using the Bluehill 3 material testing software. Multiple group comparisons were executed by One-Way ANOVA analysis using GraphPad Prism, version 6.01 (GraphPad Software, San Diego, California, USA).

4.3.9 Adhesive properties

Tissue adhesiveness was determined by following the 180-degree peel and lap-shear standard protocols with slight modifications (ASTM F2256 and ASTM F2255 respectively). Briefly, fresh porcine skin pieces obtained from a local butcher (7 × 2.5 cm^2) were washed with PBS to clean the skin surface. Glass films, with 1 mm of thickness were applied using ethyl cyanoacrylate super glue (Loctite$^®$) as a stiff backing for the skin pieces. Unless otherwise indicated, all adhesives were tested upon an adhesion area of 2.5 cm width and 2.5 cm length and adhere to the skin samples under gentle pressing; mechanical tests were performed 3 min after initial pressing to ensure moisturizing equilibrium of the adhered samples. The commercial adhesive tested (Hydrocoll$^®$) was applied to the skin following the conditions provided in the manufacture's manual. Since these do not possess double adhesive properties, they were unable to be used in lap-shear tests. All tests

were performed in an Instron 5966 Series (Instron Corporation, Norwood, Massachusetts, USA) testing machine, equipped with a load cell of 50 kN and conducted with a constant speed of 10 mm·min^{-1}. Interfacial toughness was calculated by measuring the peeling force until a plateau was achieved and then determined by dividing the resulting force two times by the width of the tested sample. Shear strength resulted from the ratio of the maximum force by the adhesion area (0.25 mm^2). Maximum adhesion force was distinguished as the point at which the two skin pieces started to detach.

4.3.10 Cell viability

Cell culturing followed the protocol previously described in Section 2.3.10. The cytotoxic effect of the Bet:Lev formulations without the curcumin (20─50% (w/w) of DES), the curcumin formulated in Bet:Lev aqueous solutions (in a range of 0–25 μM of curcumin), and the pullulan film containing the Bet:Lev aqueous solution comprising curcumin (20 μM) was evaluated. HaCaT cells were seeded in 96-well plates at a concentration of 5 000 cells·mL^{-1} and allowed to adhere for 24 h. After adhesion, cells were exposed to each formulation diluted in DMEM medium and incubated for 24 h at 37 °C in 5% of CO_2. After this period, the wells were washed with PBS, and the cell viability was evaluated by the colorimetric MTT assay (1 mg·mL^{-1} in PBS, pH 7.2), according to the protocol followed in Section 2.3.10. The percentage of viable cells was calculated as the ratio between the absorbance of treated versus the control cells (Ct).

4.3.11 Bacterial strains and culture conditions

S. aureus ATCC 6538, *S. aureus* DSM 25693, a methicillin-resistant (MRSA) strain, positive for SE A, C, H, G, and I;[387] and MRSA M98070 strain isolated from a hospitalized patient at Hospital de Coimbra, possessing the mec*A* gene, were used in this work. These strains were grown on TSA medium at 37 °C for 24 h and posteriorly maintained at 4 °C. Each bacterium strain was inoculated whenever necessary in liquid medium TSB and grown aerobically under stirring (100 rpm) at 37 °C for 24 h. Prior to each aPDT assay, an aliquot of this culture (300 μL) was

transferred twice into a new fresh TSB medium (subcultured in 30 mL) and grew overnight at 37 °C also under stirring.

4.3.12 *In vitro* photodynamic assays

The photodynamic treatment was first tested *in vitro* against *S. aureus* ATCC 6538 to validate the system efficacy. The assays were performed in PBS in 6-well plates with a final volume of bacterial suspension of 5.0 mL per sample with a final bacterial concentration of ~10^7 CFU·mL^{-1}. Curcumin solutions in aqueous DES (50% w/w) and in aqueous solutions of acetone (50% w/w) were added to each well to attain a final concentration of 20 µM of curcumin. A blank of DES aqueous solution (50% w/w) (without the photosensitizer) was also tested for comparison purposes. Light and dark controls were also conducted along with the samples: in the light controls, a bacterial suspension in PBS was exposed to light without addition of photosensitizer solution in aqueous DES; for the dark controls, all samples were exposed to the same conditions (time points, stirring rate and temperature), however, protected from any light source. After the addition of the solutions to the bacterial suspension, the final solutions were incubated in the dark for 15 min under stirring to promote the binding of the photosensitizer to the bacterial cells. After dark incubation, the samples and light controls were exposed to a white light-emitting diode (LED) at an irradiance of 50 mW·cm^{-2}, for 60 min under stirring. Dark controls were analyzed over the same period. Aliquots (100 µL) of each sample and of each control were collected at specific time points (0, 15, 30, 45 and 60 min). These were serially diluted in PBS and pour-plated in TSA Petri dishes. After incorporation of the photosensitizer on pullulan-based films, the *in vitro* the efficacy of the PL, PL-C, PL-DES and PL-(DES+C) films (2.5 × 2.5 cm^2) was also tested solubilized in a *S. aureus* suspension (5.0 mL) following the previously described aPDT protocol but extending the irradiation time to 90 min.

4.3.13 Photoinactivation on skin (*ex vivo* assay)

After the *in vitro* assays, the inactivation of the collection strain of *S. aureus* and both MRSA strains in *ex vivo* models after application of novel pullulan-based films was studied. Porcine skin samples were prepared by cleaning with cold

running water and the remaining water was dried using soft filter paper. After dried, the adipose tissue was removed using a scalpel. The skin was cut under sterile conditions into 9 cm^2 pieces (3 × 3 cm^2) and placed in sterilized 6-well plates. The skin samples were sprayed with 70% ethanol, incubated for 15 min, and then placed under ultraviolet radiation, for 30 min each side. After the removal of the resident bacteria, the skin samples were subjected to bacterial contamination with *S. aureus* or MRSA strains. Each strain was grown overnight and diluted in PBS to be equally distributed over the skin, in order to obtain a concentration of ~10^7 CFU·mL^{-1}. After 1 h of bacterial incubation on the skin, PL, PL-C, PL-DES and PL-(DES+C) film samples (2.5 × 2.5 cm^2) were applied on the skin pieces, one piece of skin per sampling time for each sample and for controls. Additionally, a bacterial control (not contaminated) to which only PBS was added was used to verify the efficiency of the skin disinfection. All skin pieces were incubated for 45 min in the dark, to promote the photosensitizer binding to bacterial cells. Posteriorly, all samples and respective controls were irradiated using a light at 50 mW·cm^{-2} for 180 min for *S. aureus* ATCC 6538 and 270 minutes for both MRSA strains divided by cycles of irradiation of 90 min each. For each cycle, a new sample of pullulan-based film was applied to the skin over the initial sample and moistened with 200 µL of PBS to maintain the skin humidity at surface. Dark controls were also performed alongside the aPDT samples. After specific time points (0, 90, 180 or 270 min) of irradiation, samples were collected and the bacteria was removed from each skin portion by sterile cotton wool swabs, 30 times each. The bacteria present in the cotton wool swabs were suspended in 1.0 mL of PBS, serially diluted in PBS, and each sample dilution was pour-plated using TSA as culture medium. The plates were incubated at 37 °C for 24 h and the CFU·mL^{-1} was counted in all samples. Experiments were carried out in triplicated and repeated three times for each condition.

4.3.14 Statistical analysis

The results presented are expressed as mean ± standard deviation of at least three independent experiments with three different measurements. In the case of mechanical studies, at least 5 different specimens were used for each measurement. The statistical analysis of all data was done using a one-way

ANOVA, with multiple comparisons. The levels of significance were set at probabilities of ****$p< 0.0001$ for mechanical assays, *$p< 0.01$ and **$p< 0.002$ for interfacial toughness and adhesive strength, respectively, and of p *< 0.04 and **$p < 0.001$, for the cytotoxicity experiments, all analyzed with Graphpad Prism 8.0.1 software (GraphPad Software, San Diego, CA, USA).

4.4 Results and discussion

This work focused on the development and characterization of pullulan (PL)-based films loaded with a DES-curcumin formulation, presenting improved mechanical, adhesive and antimicrobial photodynamic properties for application in aPDT of bacterial resistant skin infections.

Pullulan adhesive films with *ca.* 353 ± 68 μm of thickness were prepared by solvent-casting of a 6% (w/v) pullulan solution containing the photosensitizer (20 μM) in the aqueous solution of Bet:Lev (Figure 36a), resulting in films PL-(DES+C) containing 4.4 μg·cm^{-2} of curcumin dose to be administered. Pullulan films loaded with curcumin solutions in aqueous acetone (PL-C) with a 4.4 μg·cm^{-2} of curcumin dose were also studied. Additionally, pure pullulan films (PL) and films only with aqueous Bet:Lev (PL-DES) were prepared for comparison purposes. All obtained films were characterized in terms of their optical properties, structure, mechanical performance, adhesiveness to skin, cytotoxicity towards HaCaT cells and antimicrobial activity against different *S. aureus*. The application of these adhesive films in the treatment of skin infections was also investigated on *ex vivo* skin samples to evaluate their ability to inactivate MRSA strains relevant in the clinical setting (Figure 36b).
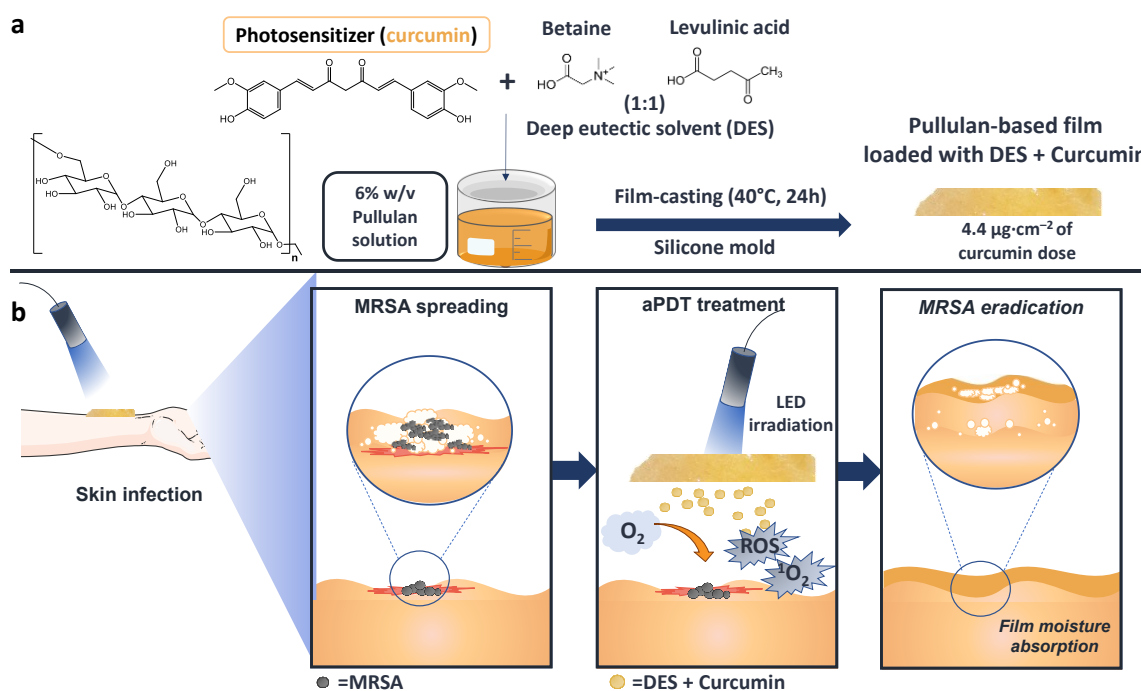
Figure 36. Schematic illustration of the (a) preparation and (b) application of pullulan-based hydrogel films loaded with Bet:Lev comprising curcumin in the treatment of skin infections using the aPDT approach. Made using arm clipart from Servier Medical Art and adapted by the authors according with Servier under the CC-BY 3.0 License (at https://smart.servier.com/, accessed on 15 June 2022).

To this purpose, the DES composed of betaine (*N,N,N*-trimethylglycine) and levulinic acid (Bet:Lev), in a 1:1 molar ratio, was selected due to the known acceptance of both components in skin care products.[341,388] The integrity of the pristine DES components in the formulation was confirmed by ^{1}H and ^{13}C NMR spectroscopy, as shown in Figure 37. The ^{1}H NMR spectrum for Bet:Lev (Figure 37a) shows first the proton resonance of H-5' (at 2.06 ppm) and two multiplets associated with H-2' (2.42 ppm) and H-3' (2.70 ppm) from levulinic acid's structure. Likewise, the proton resonances associated with $N(CH_3)_3$ and H-2 of betaine appear at 3.10 ppm and 3.74 ppm, respectively. The ^{13}C NMR spectrum (Figure 37b) displays the carbon resonances of levulinic acid's at 27.84 ppm (C-5'), 29.82 ppm (C-2') and 37.87 ppm (C-3'). The carbon resonances related to the $N(CH_3)_3$ and C-2 of betaine can be found at 53.25 ppm and 65.93 ppm, respectively. The carbon resonances of both carboxyl groups of betaine (C-1) and levulinic acid (C-1') can be observed at 168.84 ppm and 177.12 ppm, whereas the carbonyl group (C-4') of levulinic acid is found at 213.34 ppm.

134
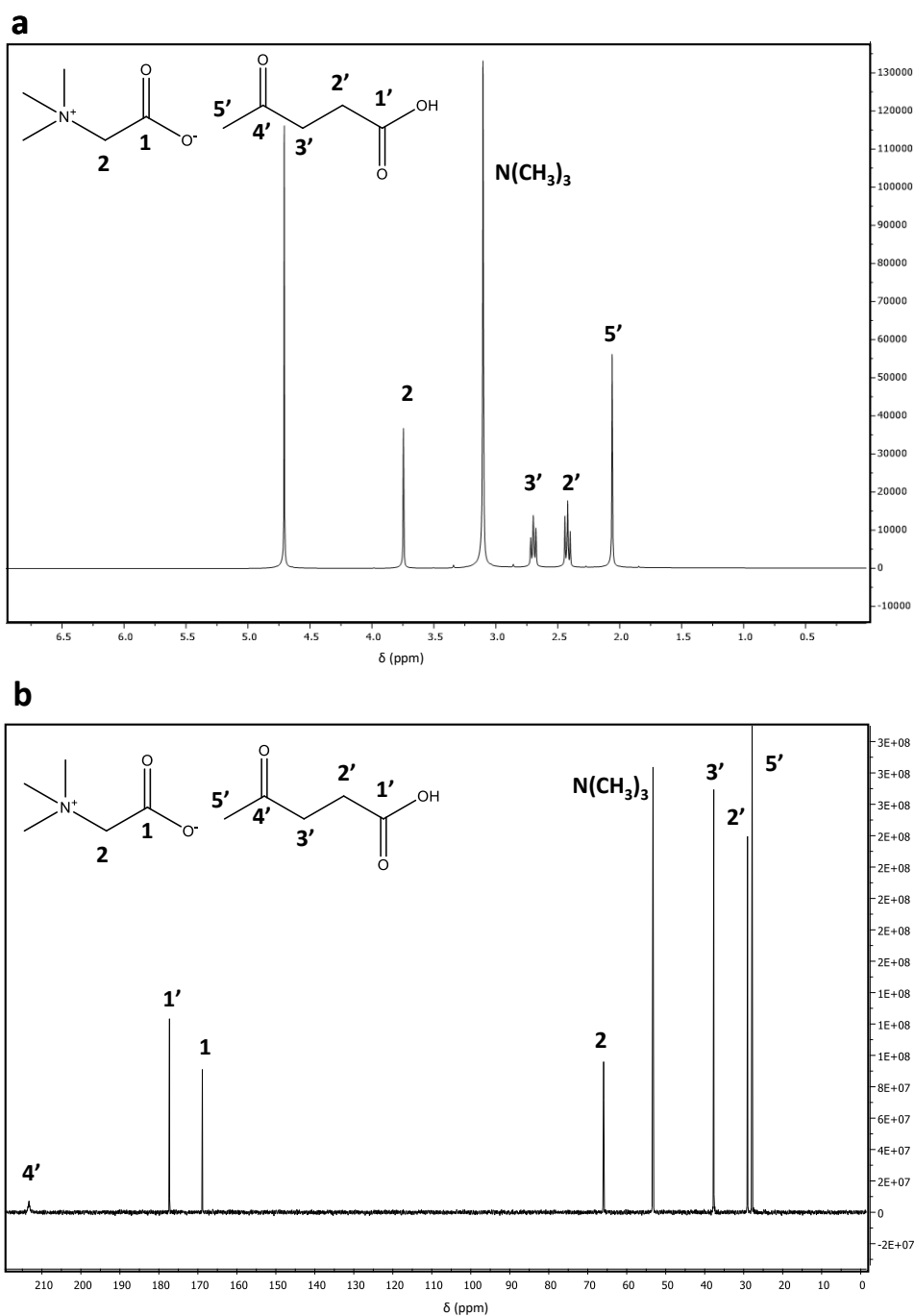
Figure 37. ^{1}H NMR (a) and ^{13}C NMR spectra (b) spectra of Bet:Lev DES in D$_2$O.

The DES was used to tune the properties of the pullulan-based films, while allowing to enhance the solubility and photostability of the photosensitizer. Curcumin was solubilized in an aqueous solution of 50% (w/w) of Bet:Lev, herein used as a co-solvent, and whose concentration was selected according with optimization studies (Figure 38a). The use of this solution allowed to achieve remarkable

concentrations of $(1.4 \pm 0.4) \times 10^3$ μM and $(2.6 \pm 0.02) \times 10^3$ μM of curcumin in aqueous media at room and body's temperature, respectively.
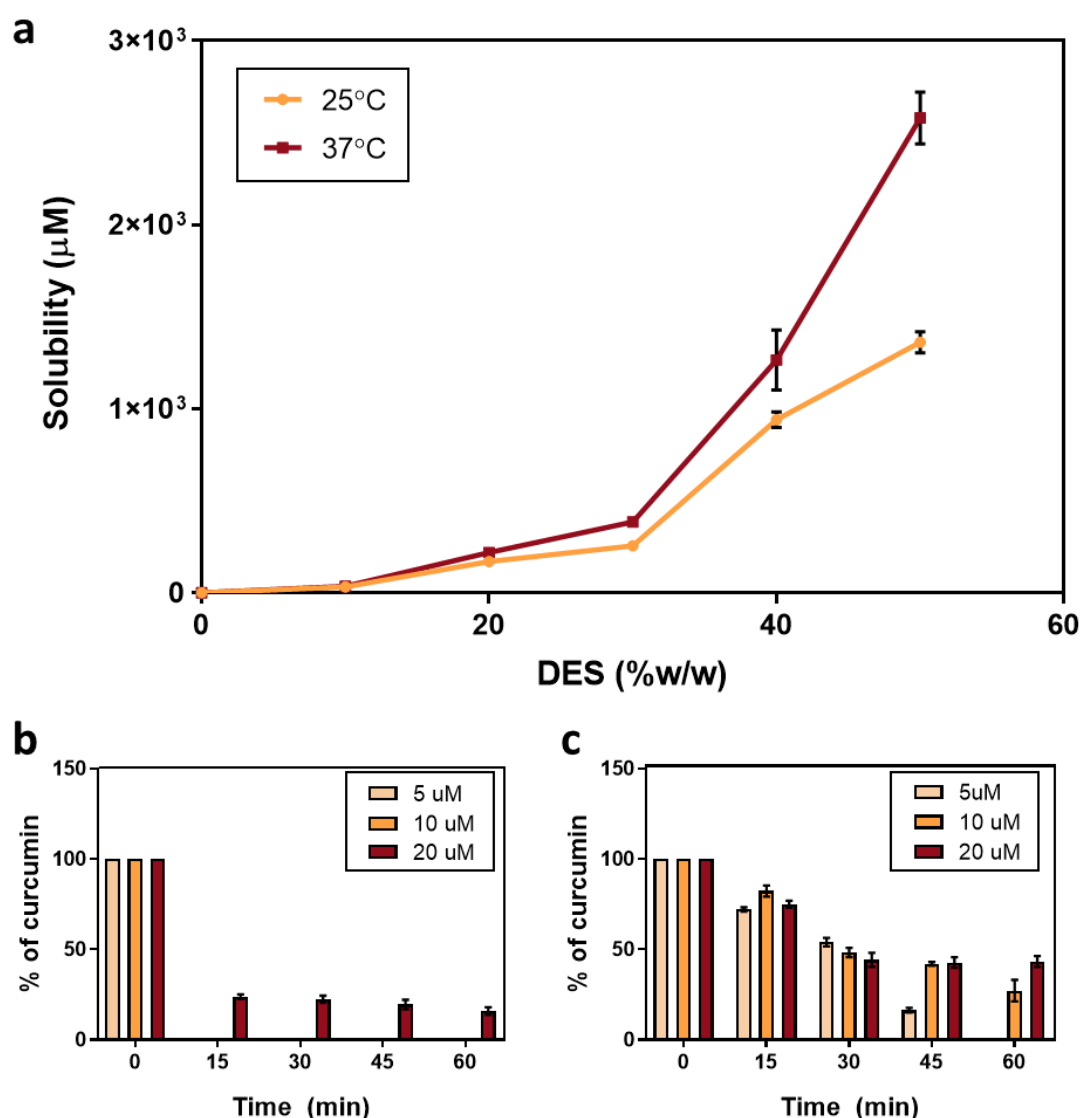
Figure 38. (a) Solubility behavior of curcumin in aqueous solutions of Bet:Lev at room (25 °C) and body (37 °C) temperatures. Photostability of curcumin in (b) acetone aqueous solutions and (c) DES aqueous solutions at 50% (w/w), exposed to 50 mW·cm^{-2} irradiation at room temperature under stirring. Values are expressed as the mean ± SD of independent experiments and independent measurements for each sample.

The solubility enhancement was accompanied by the extension of the curcumin's photostability (only 48–59% loss of the initial amount *vs* 100% loss in common solvent media like aqueous acetone in 60 min- see Figure 38b and 38c). Furthermore, the aqueous Bet:Lev studied here does not require to be removed from the final formulations and can be advantageously used in the development of the delivery system.

4.4.1 Optical properties, structural and thermal characterization

The visual aspect of the films, when topically applied on *ex vivo* skin, are depicted in Figure 39a. All the prepared films are homogeneous and without insoluble particles. While PL and PL-DES based films are colorless and transparent, PL-C and PL-(DES+C) show a uniform yellow color, which is characteristic of the photosensitizer, but are still considerably transparent.

The optical properties of the films were also accessed by measuring their transmittances in the range of 200—700 nm (Figure 39b). The spectrum of PL is in agreement with its visual aspect, indicating that the film is optically transparent, with transmittance values of 75–81% in the visible range (400−700 nm) and up to 75% in the ultraviolet range (200–400 nm), which are consistent with previously reported data.[216] The addition of Bet:Lev did not impact the film transparency, and, accordingly, the transmittance values in the visible range remained above 75% as for the pure PL films. Yet, the incorporation of curcumin slightly decreased the transparency of the films, namely PL-C to 50-80% and PL-(DES+C) to 48—76% in the visible range, due to the intense yellow color of the photosensitizer, which absorbs energy in the visible region (near 425 nm), as depicted in Figure 4b. However, the considerable preservation of transparency is particularly relevant to ensure the adequate irradiation of the photosensitizer essential for the antimicrobial action in the aPDT.

The FTIR-ATR spectrum of PL (Figure 39c) shows the characteristic absorption bands of this polysaccharide at 3280 cm^{-1}, consistent with the O–H stretching vibration of the hydroxyl groups, and at 2918 and 2900 cm^{-1} corresponding to the C–H and CH$_2$ stretching vibrations, respectively.[216,389] The C–O–C stretching of the glycosidic bridges are observed in the region of 1176 to 940 cm^{-1}, whereas the typical α-glycosidic bond stretching appears at 850 cm^{-1}. The incorporation of curcumin solubilized in acetone in the biopolymer matrix does not lead to significant differences due to the low amount of the photosensitizer used in the film preparation. However, the loading of Bet:Lev into the pullulan film leads to the appearance of some characteristic bands of the DES, particularly at 1710 cm^{-1} related to the COO$^-$ stretching vibration of both DES components.[390]
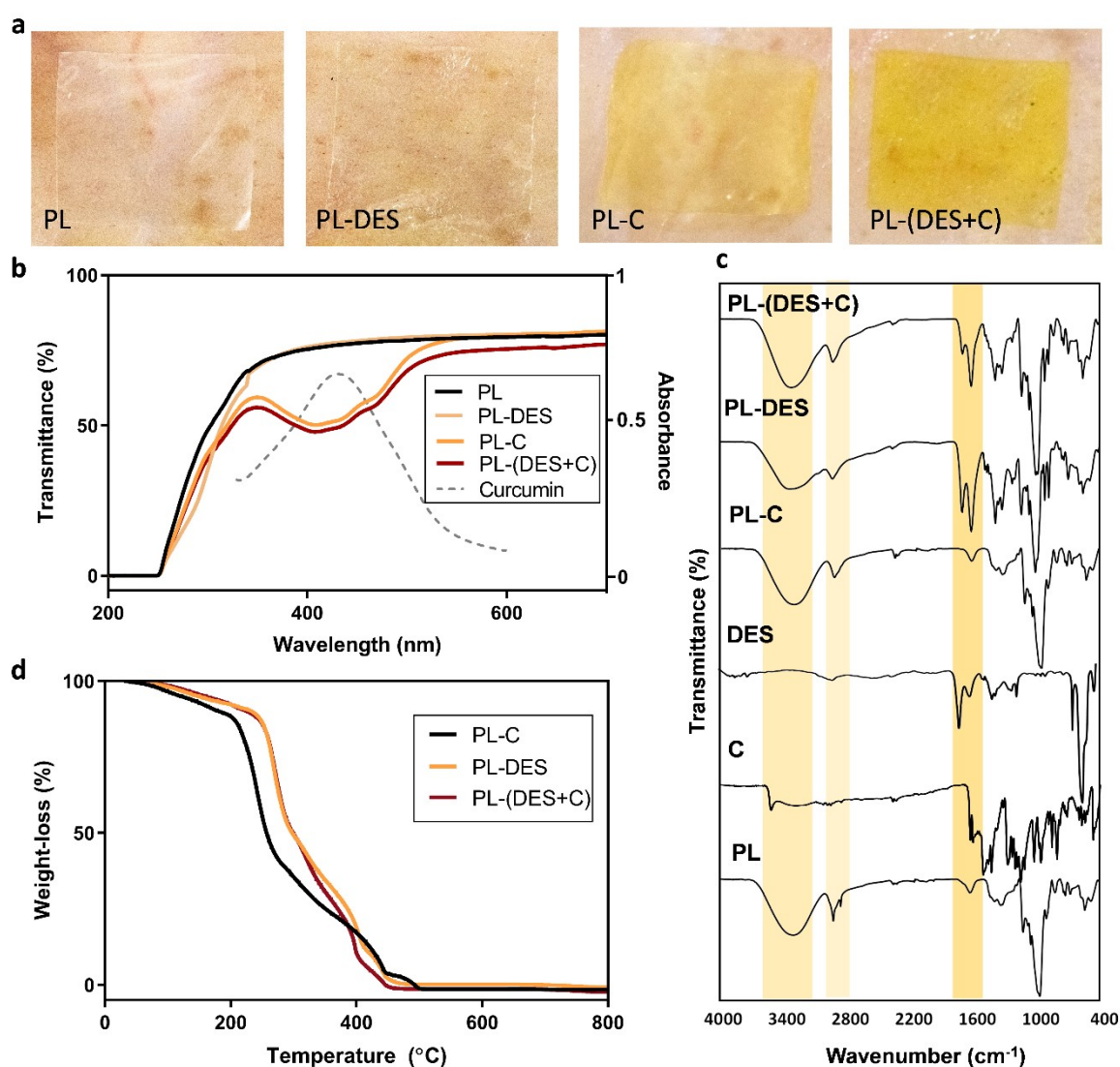
Figure 39. (a) Visual appearance of the pullulan-based films (PL) loaded with Bet:Lev (PL-DES), comprising curcumin (PL-C) and with the DES and curcumin formulation (PL-(DES+C)) placed onto *ex vivo* porcine skin. (b) UV-vis spectra of the films (solid lines) and absorption profile of curcumin (dashed line). (c) FTIR-ATR spectra of all films and of the DES and curcumin used in the Bet:Lev formulations, presented for comparison purposes. (d) Thermograms of the studied pullulan systems with different compositions.

However, when considering the spectra of the PL-DES and PL-(DES+C) films, interestingly, the most significant difference when compared with those of both PL and PL-C films is the bending motion of the adsorbed water at 1621 cm^{-1}, which is particularly increased due to the high-water sensitivity of the pullulan films with the DES.[390] This could be related with the high water affinity of the DES and in part with the decrease in the strong intramolecular interactions between the polymeric chains,

138

which are in part replaced by intermolecular hydrogen bonding between pullulan and Bet:Lev, as happens with the addition of plasticizers.[210]

TGA of the pullulan-based films was performed under a nitrogen atmosphere. The respective thermograms are provided in Figure 39d. The thermal degradation profile of pullulan follows a single weight-loss step with initial and maximum decomposition temperatures of 273 and 400 °C, respectively, leaving a residue at 800 °C corresponding to about 20% of the initial mass. This single-step degradation profile can be associated with the degradation of the PL skeleton and is in accordance with previous findings [216]. The incorporation of Bet:Lev into pullulan films led to a slight decrease in the thermal stability in comparison to the pristine polysaccharide, decreasing the maximum decomposition temperatures to 253 °C for PL-DES and 241 ºC for PL-(DES+C). This alteration can be attributed to the fact that the incorporation of Bet:Lev decreases the interactions between the pullulan chains, thereby decreasing its stability. Such modifications have been also reported for the incorporation of these co-solvents in other biopolymer matrices, like nanocellulose.[391] Despite this decrease and the thermal degradation of curcumin observed at 171 °C (both in PL-C and PL-(DES+C), these values are still above the adequate range for typical sterilization procedures, which take place around 120 °C for biomedical purposes.[392]

4.4.2 Mechanical performance and adhesive properties

The mechanical performance of the PL, PL-C, PL-DES and PL-(DES+C) films was evaluated by tensile tests. The Young's modulus, tensile stress and elongation at break were determined from the corresponding stress-strain curves (Figure 40a-c). PL films present high stiffness as confirmed by their easily breakable nature during handling, and by the high Young's modulus (2.7 ± 0.2 GPa, Figure 40a) and tensile stress (35.4 ± 2.1 MPa, Figure 40b), and low elongation at break (1.81 ± 0.34%, Figure 40c) values, which are in accordance with data previously reported for this polysaccharide.[216,393] The incorporation of curcumin (dissolved in acetone) into pullulan (4.4 µg·cm^{-2}) has only a minimal impact on the mechanical performance, slightly decreasing the Young's modulus and the tensile stress to 2.0 ± 0.1 GPa and 23.3 ± 3.1 MPa, respectively, and increasing the elongation at break

to 2.3 ± 0.4%. Therefore, these films still present low plasticity and a brittle character, being difficult to adapt to the skin irregularities and to be used for topical applications. This behavior has been described when incorporating this photosensitizer into other biopolymer-based systems, such as gelatin/chitosan[394] and carboxymethyl cellulose-based films.[395] However, the addition of the aqueous solution of Bet:Lev, on the other hand, has a remarkable effect on the mechanical performance of the prepared films, by promoting a significant decrease in the Young's modulus to around 100.3 ± 0.1 MPa and in the tensile stress to 2.4 ± MPa, along with a noticeable increase in the elongation at break to 131.4 ± 11.7%. These results clearly disclose that Bet:Lev induces a strong plasticizer effect with a considerable influence on the mechanical properties of the resultant films, in agreement with other studies where different DES have been incorporated on polymeric materials.[396,397] Furthermore, when curcumin is added to the DES aqueous solution, its impact on the corresponding films (PL-(DES+C)) is verified by a decrease in the Young's modulus and the tensile stress, as well as elongation at break values, in comparison to the PL-DES films. For the PL-(DES+C) film, a Young's modulus of 60.1 ± 0.1 MPa and a tensile stress of 1.04 ± 0.1 MPa were observed, along with values of elongation at break of 68.2 ± 11.1%. This can be attributed to the fact that the incorporation of the photosensitizer in the biopolymer matrix might create slight breaking points that allow an easier disruption of the PL-(DES+C) films than with PL-DES.[398] Yet, it must be highlighted that the effect obtained with Bet:Lev in the PL-(DES+C), particularly on the improvement of extensibility of pullulan, is higher than that observed when using common plasticizers employed in the preparation of pullulan-based films, such as glycerol.[210,216] Thus, the results obtained with PL-(DES+C) surpass these values, achieving a high degree of stretchability when handled, as portraited in Figure 40d. Since skin infections can cause clinical manifestations, such as edema and skin deformation,[399] the improvement in the film mechanical performance is advantageous since it enables the system to better adapt and keep up with the skin elasticity.

For photodynamic treatment purposes, adhesiveness might be particularly demanding, since the film loaded with the photosensitizer must be sustained at the

140

infection site during the treatment period.[400] The adhesive capacity of the pullulan films prepared in this study (PL, PL-C, PL-DES and PL-(DES+C) was evaluated through different mechanical tests, by measuring the interfacial toughness through peel tests (Figure 40e) and the adhesive strength by lap-shear tests (Figure 40f).
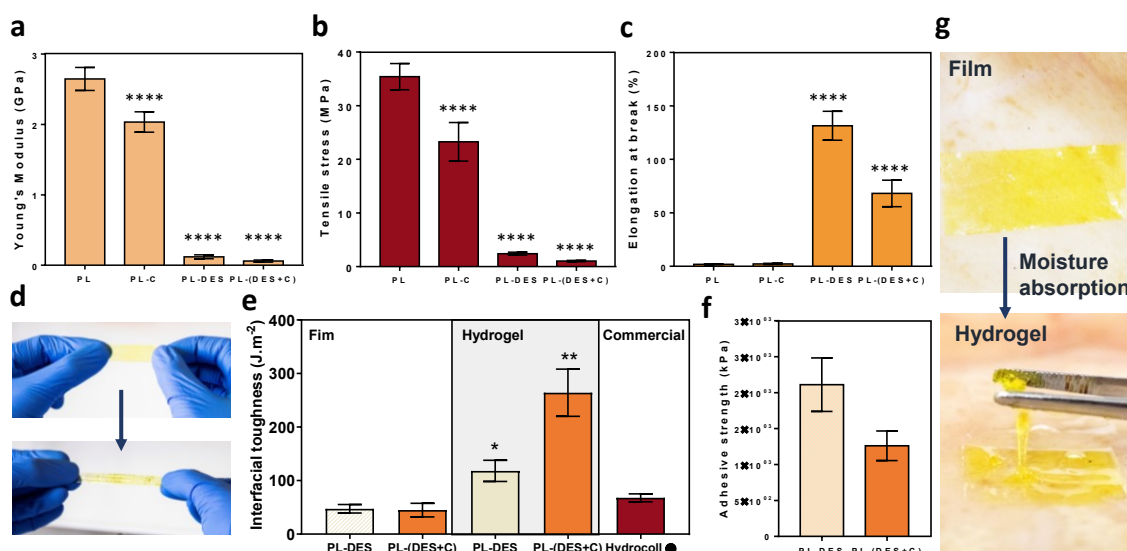
Figure 40. (a) Young's modulus (GPa), (b) tensile stress (MPa) and (c) elongation at break (%) of the pullulan-based films. The results are expressed as mean ± SD. Levels of significance were set at probabilities of ****$p < 0.0001$, calculated through one-way ANOVA and in comparison, to the PL system. (d) Graphical display of the extensibility of the PL-(DES+C) adhesive film. (e, f) Adhesion performance of PL-DES and PL-(DES+C) on porcine skin, determined by interfacial toughness and adhesive strength, respectively. *$p < 0.01$ and **$p < 0.002$ increase in interfacial toughness in comparison to commercial adhesives (Hydrocoll®). (g) Visual appearance of the transition from solid to hydrogel of the PL-(DES+C) adhesive systems upon skin moisture absorption.

Porcine skin was chosen as model tissue for this evaluation, due to its similarity to human skin.[401] After immediate application onto skin, both PL-DES and PL-(DES+C) maintain their solid film appearance and were able to establish tough adhesion with the porcine skin samples upon contact and after application of gentle pressure. However, after the application, the films with DES start to absorb the skin moisture, transiting into hydrogels, as portrayed in Figure 40g. These hydrogels, by contrast, exhibit remarkably higher interfacial toughness values in comparison to the commercial system (Figure 40e). This switchable character allows to enhance the interfacial toughness of the PL-DES film from values ranging from 47.27 ± 7.13 to 118.12 ± 17.63 J·m^{-2}, and even more notoriously from 44.87 ± 5.43 to 264.10 ± 39.5 J·m^{-2} for the PL-(DES+C) film. The interface toughness of PL-(DES+C) after switch into a hydrogel state presents a 2-fold increase in comparison to PL-DES and a 4-

fold increase than that of the commercially available hydrocolloid Hydrocoll® (67.83 ± 6.62 J·m^{-2}). This DES possess a high-water absorption capacity due to the hydrophilic nature of its components;[402] therefore, Bet:Lev might enhance the removal of interfacial water from the tissue surface, while also enabling the establishment of hydrogen bonding interactions between the biopolymer system with the skin epithelium.[403] In addition to the high adhesion capacity, these films highly withstand stress after adhesion. The adhesive strength of the films towards the porcine skin was found to be $(2.11 ± 0.32) × 10^3$ kPa for PL-DES and $(1.26 ± 0.18).× 10^3$ kPa for PL-(DES+C) (Figure 40f). Hydrogels based on pullulan (10% w/v) have been reported to present adhesive strength values of only approximately 25.5 kPa,[243] which clearly highlight the positive effect of the incorporation of Bet:Lev, bringing improvements in the adhesive capacity of the material and in the local administration of the photosensitizer.

4.4.3 Biocompatibility of DES formulations and pullulan-based systems

The cytotoxicity of curcumin, curcumin in aqueous solution with Bet:Lev and of the final adhesive system to be topically applied was initially determined on human keratinocytes (HaCaT cell line) (Figure 41). Control groups were also studied cultivating them in the absence of the studied samples. Firstly, the influence of the aqueous Bet:Lev (50% (w/w)) on the overall toxicity of the formulations was appraised, after 24 h of exposure. The aqueous Bet:Lev is non-cytotoxic to HaCaT cells in the studied concentration with cell viabilities above 80%; therefore, it will not significantly impact the cytotoxicity of the studied adhesive systems. Following this, the effect of curcumin on cell viability was accessed at the concentration included in the aqueous solution of 50% (w/w) of Bet:Lev during the previous experiments (20 µM).

Curcumin is non-cytotoxic in this concentration, with cell viability higher than 75%. This is expected since curcumin affects the non-cytotoxic cells viability in a dose-dependent manner. In fact, it was reported that at concentrations higher than 20 µM, curcumin effectively inhibited the proliferation and induced apoptosis of HaCaT cells with a rate as high as 34%.[404,405] Therefore, the concentration selected

to be incorporated in the pullulan-based adhesive films is safe to be in contact with healthy skin cells. Finally, the cytotoxicity of the pullulan-based films containing curcumin (equivalent to a 4.4 µg·cm^{-2} dose) solubilized in aqueous Bet:Lev was evaluated. Our results reveal that both curcumin and aqueous Bet:Lev do not impact the overall cell viability of pullulan-based adhesive films (cell viability > 80%). This could be expected since pullulan-based materials do not seem to present cytotoxicity towards this type of cell line,[242] indicating their safeness for contact with healthy skin cells and being suitability for topical application.
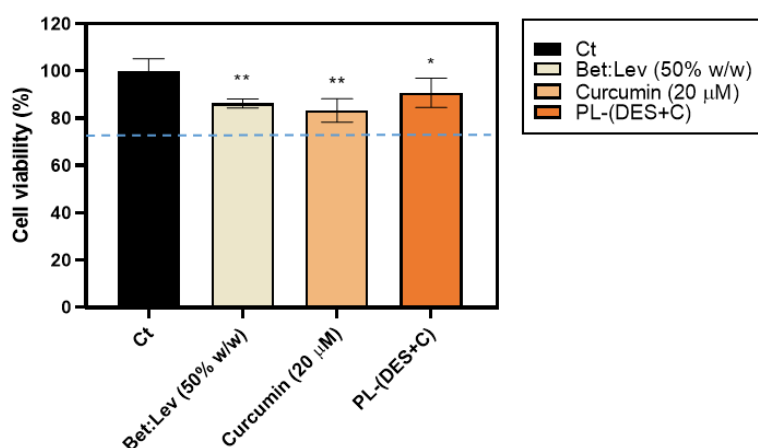
Figure 41. Effect of Bet:Lev formulation (Bet:Lev 50% w/w) curcumin concentration (20 µM) in aqueous Bet:Lev and pullulan-based films (PL-(DES+C)) in the viability of HaCaT cells in DMEM medium at 37 °C. Cytotoxicity profiles after 24 h of exposure vs control cells (Ct). Results are expressed as mean ± SD of three independent experiments. *p<0.04 and **p<0.001 cell viability compared to the control cells.

4.4.4 *In vitro* antimicrobial action towards *S. aureus*

Skin and soft tissue infections can range from uncomplicated to invasive and life-threatening situations, of which *S. aureus* is a major contributor.[406] Therefore, the *S. aureus* ATCC 6538 strain was chosen to firstly address photodynamic antimicrobial action, given that it is used as reference in standard bactericidal tests. Since the effectiveness of aPDT can decrease with the sample complexity,[407] it is particularly relevant to initially test controlled conditions. In this case, the aqueous solution of Bet:Lev comprising the photosensitizer was added directly to the bacterial suspension before testing it after incorporation in the pullulan film (Figure 42a). Initially, the antimicrobial activity of the Bet:Lev aqueous solutions and of curcumin (20 µM) solubilized in these formulations (50% (w/w) of Bet:Lev in water)

was assessed in the dark. Curcumin solution (20 µM) in an aqueous acetone (50% (w/w)) solution was also studied to infer about the curcumin's photodynamic activity in the absence of Bet:Lev. As indicated in Figure 42b, without irradiation, none of the tested solutions displayed antimicrobial activity towards *S. aureus* ATCC 6538. Then, samples were incubated in the dark for 15 min and irradiated with a light dose of 50 mW·cm^{-2}. In this case, it is possible to verify that both acetone and Bet:Lev do not affect the cell viability of the bacterium (Figure 42c).
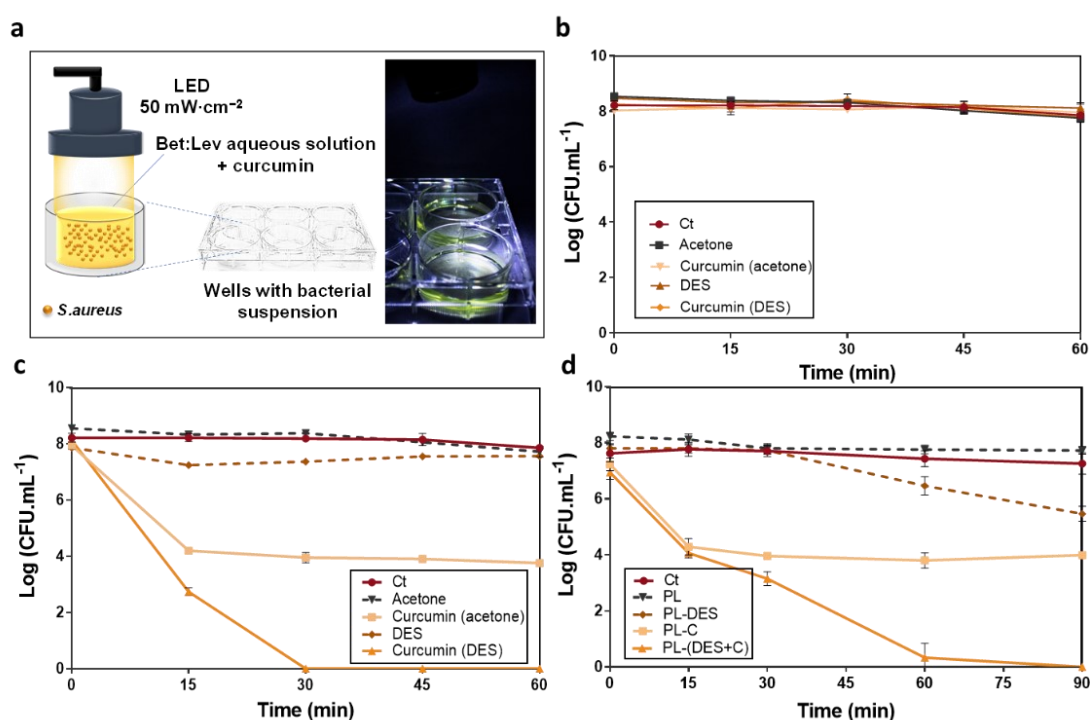
Figure 42. (a) Schematic illustration of the *in vitro* aPDT assay process for the eradication of *S. aureus*. (b) Antimicrobial activity of each solution tested initially for dark controls. (c) Photoinactivation of S. aureus ATCC 6538 incubated with each sample and irradiated with LED at an irradiance of 50 mW·cm^{-2}, using curcumin at 20µM. (d) Photoinactivation profiles of *S. aureus* treated with pullulan-based films loaded with curcumin, with the DES, Bet:Lev and with Bet:Lev comprising curcumin. Light controls (Ct) represent the exposure of the bacteria to the same conditions in the absence of the photosensitizer. All assays were conducted in PBS at 37°C. Results are expressed as mean ± SD of three independent experiments with three replicates each.

On the contrary, both curcumin aqueous solutions (20 µM) lead to successful bacterial reduction when irradiated. Thus, the bacterial reduction is owing to the photodynamic treatment. Specifically, curcumin in aqueous acetone leads to a 3.9 log$_{10}$ of inactivation (p < 0.0001) after 30 min of irradiation, decreasing to 4.2 log$_{10}$ of inactivation (p < 0.0001) after a 60 min with aPDT (Fig. 42c), while curcumin in aqueous Bet:Lev solution led to an abrupt inactivation of *S. aureus*, originated an 8.1 log$_{10}$ reduction (p < 0.0001) of the bacterium in only 30 min. The difference in

144

the bactericidal activity between both samples can be attributed to the fact that not only curcumin is more prone to precipitate in the bacterial suspensions[408] when solubilized in an acetone solution but also curcumin dissolved in aqueous acetone completely degrades after 15 min (as seen in Figure 42b). On the contrary, curcumin in aqueous Bet:Lev shows improved photostability (Figure 42c), enabling the photosensitizer to exert its effect for a longer period, being possible to fully inactivate *S. aureus* suspensions.

After the obtained promising results, the antimicrobial activity of the formulation after the incorporation in the adhesive film (4.4 µg·cm^{-2} of curcumin) was investigated. PL, PL-DES and PL-C were also tested for comparison purposes. Fig. 42d shows the photoinactivation profiles of *S. aureus* treated with all the pullulan-based films and with the control. Since the photosensitizer is loaded in the biopolymeric film, aPDT treatment was extended by an additional 30 min period to guarantee the complete release of curcumin into the media.[409] PL-C and PL-(DES+C) films exhibit a similar photoinactivation behavior in the first 15 min with a 3.2 log$_{10}$ reduction (p < 0.0001) of the viability of the bacterium. In contrast, in the PL-(DES+C), since the photosensitizer shows an enhanced photostability as previously stated, this is reflected in the complete photoinactivation of the bacteria after 60 min of the aPDT. Given the high efficacy of the tested conditions and the bactericidal enhancement of the PL-(DES+C) system in comparison to the PL-C one, we further investigated their effect on infected skin samples.

4.4.5 Bacterial photoinactivation on an *ex vivo* skin model

To better evaluate the final effectiveness of the aPDT using the developed adhesive films against *S. aureus* ATCC 6538, the aPDT conditions were first adjusted in skin. Following this, the treatments on skin samples contaminated with MRSA DSM 25693 and with MRSA M98070, a clinically isolated strain that comprehend different colonization and toxin factors, were conducted. Aiming to resemble the conditions found in *in vivo* skin infections, porcine skin samples were individually contaminated with each strain. The adhesive films were placed over the contaminated site and the photosensitizer was allowed to incubate. During the incubation period the adhesive absorbs skin moisture and switches into a hydrogel,

as previously described. After this, the samples were irradiated with a light dose of 50 mW·cm^{-2} over 90 min. Owing to the skin complexity, photoinactivation is not as simple to attain as it is *in vitro* suspension. Therefore, attempting to achieve high inactivation rates, initially two cycles of 90 min irradiation each were performed, using a new adhesive in each cycle. Figure 43a illustrates aPDT treatment cycle using the PL-(DES+C) adhesive films on infected skin for a better understanding.

The *ex vivo* experiments were first conducted for the same photosensitizer concentrations (topical application of 4.4 µg·cm^{-2} of curcumin dose) and irradiance source (50 mW·cm^{-2}), tested in the previous assays but extending the dark incubation time from 15 to 45 min. This modification was considered since it has been already shown that a prolonged incubation period is required in the transition from *ex vivo* skin model as compared to the *in vitro* circumstances.[407] This update in the aPDT did not produce relevant alterations regarding the action of PL-C on *S. aureus* ATCC 6538 (Figure 43b). Even after 2 cycles of aPDT, no inactivation of the bacterium is verified when applying PL-C, and the viability of the bacterium was not affected in the dark controls (data not shown). However, when the PL-(DES+C) adhesive was used, a 2.6 log$_{10}$ reduction (p < 0.0001) is observed over one cycle of the aPDT. Over two cycles of the aPDT it is possible to inactivate the bacterium down to the detection limit of the method (Figure 43b). In addition, the PL-DES system shows only a slight impact in the photoinactivation, allowing 1.5 log$_{10}$ reduction (p < 0.0001). Based on these results, it is possible to conclude that the efficacy of PL-(DES+C) adhesive is not only due to the photodynamic treatment, but also to a synergistic effect between Bet:Lev and curcumin.

As shown in Figure 43c, by observation of the respective agar plates used in the photodynamic experiments, the PL-C films do not exhibit any bacterial killing effect; thus, the continuous application of the PL-(DES+C) adhesives seems to be an effective strategy to treat *S. aureus* infections. Such fact prompted us to apply these adhesives in skin samples infected with MRSA strains, under the same conditions. Interestingly, these systems also show high photodynamic antimicrobial ability, enabling a similar inactivation profile for both MRSA strains over two cycles of photoinactivation (Figure 43d). However, for these two bacterial strains an additional aPDT cycle was necessary. With this addition, it is possible to inactivate

MRSA DSM 25693 (>4.7 $\log_{10}$) down to the detection limit and to obtain a reduction of 3.3 $\log_{10}$ (p < 0.0001) in the bacterial viability of the clinically isolated MRSA strain. The increase in the incubation period, where the PL-(DES+C) adhesive gradual switches from a solid film into a thick hydrogel, together with the high stability of the curcumin in this system, allows to deliver the photosensitizer in the infected area.
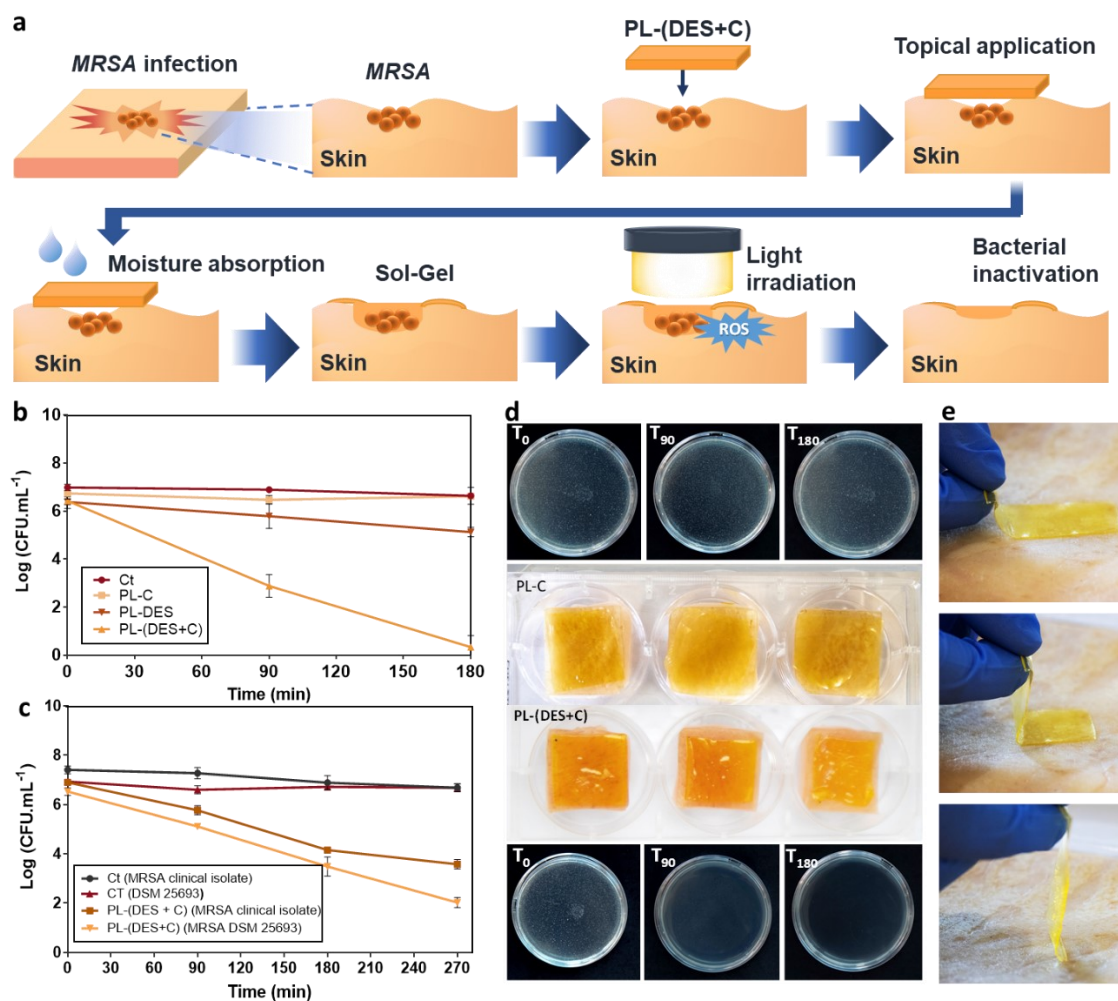
Figure 43. (a) Graphic representation of an aPDT treatment cycle using the adhesive film PL-(DES+C). (b) Photoinactivation of *S. aureus* ATCC 6538 by pullulan-based films irradiated with LED at an irradiance of 50 mW·cm^{-2}. (c) Photoinactivation of MRSA DSM 25693 and MRSA strain clinically isolated, treated with the adhesive film PL-(DES+C). (d) Visual appearance of the aPDT treatment with PL-C and PL-(DES+C) and its impact on skin samples contaminated with *S. aureus* ATCC 6538. Results are expressed as mean ± SD of three independent experiments with three replicates each; and (e) photographs of the skin application and removal of PL-(DES+C) adhesives.

As result, not only is the adhesion of the photosensitizer to the bacteria enhanced, but more importantly, the combined delivery of both Bet:Lev and the photosensitizer might improve their permeation into the bacterial cell membrane. Thus, a higher yield of ROS and free radicals is likely achieved upon the treatment.

This contrasts with the reported reduced attachment and penetration of photosensitizers in *ex vivo* and *in vivo* conditions, which lead to a lower inactivation efficacy.[410] As herein verified, the antimicrobial activity is enhanced even in situations where agglomeration and biofilm formation can be foreseen, such as verified for the results of contaminations with both MRSA strains. MRSA strains obtained from chronic wounds seem to harbor more virulent genes compared to other strains and different abilities for biofilm formation.[411] Such a fact can justify the slight difference between the photoinactivation of *S. aureus* ATCC 6538 and of both MRSA strains after four cycles of the aPDT. Furthermore, by using the adhesive film with Bet:Lev and curcumin, it is achieved a higher killing efficacy than liquid porphyrinic formulations tested *ex vivo* on skin contaminated with similar MRSA strains.[412] The application of these liquid formulations usually implies the use of water–ethanol solutions, which are not only associated with the photobleaching of the photosensitizer, but also dry the *stratum corneum* impacting the efficacy of the aPDT in skin samples.

The systems herein developed are capable of overcoming the drawbacks of liquid formulations without causing skin staining after application, particularly in the adhesive film form (as portrayed in Figure 43e) and after transition into the hydrogel. More importantly, these adhesives can be easily removed after the treatment (in hydrogel form) with water, due to the soluble character of all employed components, while being gentle to skin.

4.5 Conclusions

In this study, pullulan-based adhesive films loaded with Bet:Lev and curcumin formulations were developed. The selection and use of 50% (w/w) aqueous Bet:Lev allowed not only to solubilize curcumin in aqueous media, but also enabled to extend its photostability and the incorporation in a hydrophilic matrix like pullulan. The resultant pullulan-based films presented enhanced mechanical properties, namely higher extensibility and adhesive properties. The developed adhesive films present a switchable character, being capable of absorbing skin moisture, and thus passing from solid films to strong adhesive hydrogels with higher adhesiveness than commercial hydrogels (4-fold increase). These adhesives are capable to deliver the photosensitizer in specific skin areas, with no significant cytotoxicity associated (HaCaT cell viability >80%). More importantly, the combination of these properties provides a higher therapeutic effect than the photosensitizer solubilized in common solvents such as acetone. This translates into a higher *in vitro* photodynamic antimicrobial action against *S. aureus* ATCC 6538 during the aPDT. PL-(DES+C) adhesive films allow to decrease the viability of multidrug-resistant bacteria, such as MRSA strains, below the detection limit of the method when tested in *ex vivo* skin sample models. These results are of high relevance since the PL-C films do not present antimicrobial activity in any of the *ex vivo* assays. Overall, the developed novel switchable adhesive films loaded with curcumin solutions in aqueous Bet:Lev proved to be effective systems to eradicate skin infections caused by drug-resistant strain.

Chapter 5. Application of DES Formulations in Biopolymer-Based Drug Delivery Systems for Transdermal Delivery Improvement
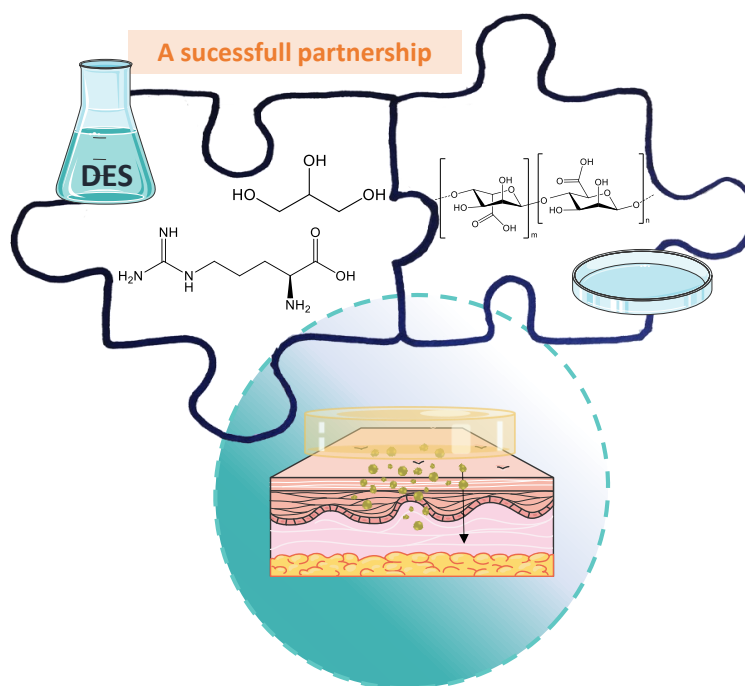
---

5.1 Abstract

The transdermal administration of nonsteroidal anti-inflammatory drugs (NSAIDs) is a valuable and safer alternative to their oral intake. However, most of these drugs display low water solubility, which makes their incorporation into hydrophilic biopolymeric drug-delivery systems difficult. To overcome this drawback, aqueous solutions of bio-based DES were investigated to enhance the solubility of ibuprofen, a widely used NSAID, leading to an increase in its solubility of up to 7917-fold when compared to its water solubility. These DES solutions were shown to be non-toxic to macrophages with cell viabilities of 97.4% (at ibuprofen concentrations of 0.25 mM), while preserving the anti-inflammatory action of the drug. Their incorporation into alginate-based hydrogels resulted in materials with a regular structure and higher flexibility. These hydrogels present a sustained release of the drug, which is able, when containing the DES aqueous solution comprising ibuprofen, to deliver 93.5% of the drug after 8 h in PBS. Furthermore, these hydrogels were able to improve the drug permeation across human skin by 8.5-fold in comparison with the hydrogel counterpart containing only ibuprofen. This work highlights the possibility to remarkably improve the transdermal administration of NSAIDs by combining new drug formulations based on DES and biopolymeric drug delivery systems.

5.2 Introduction

Nonsteroidal anti-inflammatory drugs (NSAIDs) represent one of the most prescribed medications for pain and inflammation treatment.[413] The key effect of NSAIDs is primarily linked to their ability to block specific prostaglandins synthesis by the inhibition of cyclooxygenase enzymes (COX-1 and COX-2).[413] This inhibition also plays a major role in the side-effects associated with their oral intake.[50] The inhibition of COX-2 plays a central role anti-inflammatory and analgesic effects of these drugs; however, its inhibition also impacts cardiovascular health with chronic drug usage. On the other hand, the inhibition of COX-1 is responsible for severe gastrointestinal ulceration and renal toxicity. Although the gastrointestinal safety of these drugs can be improved by association with phospholipids or the concomitant administration of gastroprotective pharmaceuticals, such as proton pump inhibitors, the cardio-nephrotoxic side-effects are still substantial.[50] Considering the chronic use of NSAIDs, the transdermal administration of these drugs can be an advantageous alternative, with considerable efficacy and safety.[414] Studies have shown that NSAIDs administered by this vein can permeate across skin.[415,416] Following this, numerous formulations of NSAIDs have become available, including creams, gels, patches and solutions (lotions), which have mainly been used for musculoskeletal pain conditions.[417] However, similarly to many antimicrobial agents, the formulation of NSAIDs in these systems is hindered by their low-water solubility, requiring the use of high contents of organic solvents, such as ethanol, to solubilize them and improve their permeation.[418]

In an attempt to avoid the use of organic solvents and to improve the delivery of low-water-soluble molecules, eutectic mixtures, and particularly DES have been explored as alternative pharmaceutical solvents and permeation enhancers.[108,137] As previously described, DES can improve the solubility of anti-inflammatory drugs (such as ibuprofen, naproxen, ketoprofen)[134] and paracetamol,[110] being particularly appealing to enhance NSAIDs' permeation across skin. Nevertheless, the use of hydrophobic DES to this purpose poses the same issues as associated with the use of organic compounds concerning the development of biopolymer-based drug delivery systems, such as hydrogels, which are typically based on hydrophilic biopolymers, such as polysaccharides.[419] Therefore, the study and application of

154

water-soluble DES needs to be further explored as an approach to the simultaneous solubilization of NSAIDs and their incorporation in hydrogel-based drug-delivery systems. Since hydrogels possess a high-water content and a 3D microstructure, they can be valuable as delivery systems for transdermal drug administration, ensuring simplicity of application, with a significant minimization of side effects.[419] One example of a biopolymer that is commonly used in these systems is alginate.[201] Furthermore, alginate-based hydrogels have been also studied for the incorporation of NSAIDs, such as ibuprofen; however, these present a low loading capacity and low homogeneity.[420] This limitation has increased the search for strategies to improve the compatibility of hydrogels and hydrophobic drugs. Even though the combination of alginate and DES is promising, it has scarcely been explored, with only one study, focused on the use of DES to favor the encapsulation of curcumin into alginate/chitosan beads for oral administration.[226] So far, there are no previous reports on the combination of alginate hydrogels and DES for the improvement in the transdermal delivery of pharmaceutical ingredients.

Taking advantage of the properties of both DES and alginate, in this study, their partnership for the transdermal administration of hydrophobic molecules, such as NSAIDs, using ibuprofen as a model drug, was explored, showing that the DES benefit in these systems can be applicable to other drug classes. Herein, we demonstrated the possibility to enhance the solubility and stability of ibuprofen by using aqueous solutions of DES, and the improvement in its skin permeation when incorporated into an alginate solid hydrogel system.

5.3 Experimental Section

5.3.1 DES preparation and characterization

In this work, the DES arginine:glycerol (Arg:Gly) was studied to solubilize ibuprofen (Alfa Aesar, Haverhill, MA, USA, 99%). This DES was prepared by mixing L-arginine (Panreac, Barcelona, Spain, 99%) with glycerol (Sigma-Aldrich, St. Louis, MO, USA, ≥99.5%) in a 1:4 molar ratio. This mixture was placed in sealed glass vials with constant stirring while heated (maximum temperature of 85 °C), until a homogeneous transparent liquid was obtained. After being kept at the maximum temperature for 1 h, the mixture was allowed to return to room temperature. Aqueous solutions (0—60% (w/w)) of Arg:Gly were prepared from this neat DES by addition of the proper water amount.

To infer the integrity of the Arg:Gly components in the DES, ^{1}H and ^{13}C NMR spectroscopy was carried out. The spectra were recorded using a Bruker Avance 300 spectrometer (Bruker Corporation, Billerica, MA, USA) operating at 300.13 MHz for ^{1}H NMR, and at 75.47 MHz for ^{13}C NMR. The mixtures were dissolved in deuterated water using TMSP as an internal reference.

Arginine:glycerol: ^{1}H NMR (300.13 MHz, D$_2$O): δ 1.41 (4H, m, H-3,4); 2.98 (2H, m, H-2); 3.05 (1H, m, H-5); 3.39 (4H, m, H-1',3'); 3.55 1H, m, H-2') ppm. ^{13}C NMR (75.47 MHz, D2O): δ 24.40 (C-3); 31.50 (C-4); 40.86 (C-2); 53.21 (C-5); 62.15 (C-1',3'); 71.97 (C-2'); 156.57 (C-1); 182.54 (C-6) ppm.

The interactions between the components of the DES were analyzed by FTIR-ATR spectroscopy. The spectra of arginine, glycerol and the Arg:Gly (1:4) were obtained on a Perkin Elmer spectrometer (Perkin-Elmer Inc., Waltham, MA, USA) equipped with a single horizontal Golden Gate ATR cell and a diamond crystal. Data were recorded by the accumulation of 32 scans performed at room temperature in the range of 4000–400 cm^{-1}, with a resolution of 4 cm^{-1} and an interval of 1 cm^{-1}. All spectra were subtracted against background air spectrum and recorded in transmittance mode.

5.3.2 Ibuprofen's solubility assay

To determine the drug solubility, ibuprofen was added in excess to 2.0 g of arginine:glycerol (1:4) aqueous solutions (0—60% (w/w) of DES) and pure water. These solutions were placed in sealed glass vials and allowed to equilibrate in a specific aluminium disk at constant temperatures (room (25 °C) and body (37 °C) temperatures) and under stirring (900 rpm) over 72 h. The solubility of ibuprofen was studied in the range of from 0 to 60% (w/w) of Arg:Gly in water, given the high viscosity of the mixtures above this concentration. After saturation of each DES aqueous solution (0—60% w/w), the samples were centrifuged, and an aliquot of the supernatant was collected and diluted in distilled water. The sample was then carefully filtered with a 0.45 µm syringe filter to remove any solid from the liquid phase and subsequently analyzed by HPLC-DAD (Shimadzu, model PROMINENCE, Kyoto, Japan). The HPLC quantifications were performed in isocratic mode with an analytical C18 reversed-phase column (250 × 4.60 mm), Kinetex 5 µm C18 100 Å, from Phenomenex. The mobile phase consisted of 45% (v/v) of acetonitrile and 55% (v/v) of ultra-pure water with 0.3% (v/v) of ortho-phosporic acid. The separation was conducted using an injection volume of 10 µL at a flow rate of 0.8 mL·min^{-1} and operated at 25 °C. The wavelength was set at 264 nm and each sample was analysed at least in triplicate. Calibration curves were obtained using ibuprofen dissolved in the mobile phase. Under the referred conditions, ibuprofen displays a retention time of 15.2 min.

5.3.3 Drug stability storage

To evaluate the stability of ibuprofen in the novel formulations, the drug was dissolved in water and in the Arg:Gly aqueous solution (60% (w/w) of DES) below the solubility limit. An initial aliquot of each solution was then analyzed by HPLC-DAD to determine the drug content in each formulation (T_0). The solutions then were kept at 25 and 37 °C and at 75—80% relative humidity for 30 days and protected from light. After this period, new aliquots were collected and quantified by HPLC-DAD using the previously described method. Two independent studies were conducted, and each sample was analyzed at least in triplicate.

5.3.4 Biological activity

5.3.4.1 Cell culture

Murine Raw 264.7 macrophages (ATCC number: TIB-71) were cultured in DMEM containing 4.5 mg·mL^{-1} glucose, 4 mM *L*-glutamine, 1.5 mg·mL^{-1} sodium bicarbonate and supplemented with 10% non-inactivated FBS, 100 IU·mL^{-1} penicillin, and 100 µg·mL^{-1} streptomycin. Cells were incubated in a humidified atmosphere of 95% of air and 5% of CO_2 at 37 °C and were used after reaching up to 80% confluence.

5.3.4.2 Cell viability assays

The impact of ibuprofen solubilized in Arg:Gly aqueous solutions on macrophage cells viability was evaluated by the resazurin assay. Firstly, 4×10^4 of Raw 264.7 cells/well were plated on a 96 well plate and let to stabilize overnight. Then, pure ibuprofen, the Arg:Gly aqueous solution (60% (w/w) of DES in water and ibuprofen solubilized in the Arg:Gly aqueous solution, in the concentrations rang of 0.01–4 mM, were added to the cell cultures for 24 h. After this, resazurin (Sigma-Aldrich, cell culture grade) was added to the cells during the last hour of incubation, achieving a final concentration of 50 µM. Lastly, the absorbance was measured at 570 and 600 nm in a BioTek Synergy HT spectrophotometer (Biotek Instruments, Winooski, VT, USA). The reported data are from three biological independent experiments conducted in duplicate for each condition and the results were expressed as the average cell viability ± SD. The aqueous solutions used in the assay were previously sterilized by filtration.

5.3.4.3 Anti-Inflammatory assays

The anti-inflammatory action of ibuprofen solubilized in water and in the Arg:Gly aqueous solution was evaluated by the ability to inhibit the LPS-induced nitric oxide (NO) production in macrophages. The NO production was measured by a colorimetric assay with the Griess reagent (0.1% (w/v) *N*-(1-naphthyl)ethylenediamine dihydrochloride (Sigma-Aldrich, ≥98) and 1% (w/v) sulfanilamide (Sigma-Aldrich, ≥98) containing 5% (w/v) H_3PO_4) (Sigma-Aldrich, ≥85

158

wt.% in H_2O), that aimed to detect the accumulation of nitrite in the culture supernatants. To this purpose, the cells were plated at 3×10^5 cells/well in 48-well culture plates, allowed to stabilize for 12 h, and then incubated as previously described with non-cytotoxic concentrations of formulations. Incubations with the culture medium (control), ibuprofen (250 µM), ibuprofen (250 µM) in the DES aqueous solution (60% (w/w) of DES in water) were performed over 24 h. After incubation, 100 µL of culture supernatants were collected and mixed with an equal volume of the Griess reagent and kept during 15 min in the dark. The absorbance of these samples was measured at 550 nm, using a standard spectrophotometer BioTek Synergy HT (Biotek Instruments, Winooski, VT, EUA). Multiple group comparisons were executed by One-Way ANOVA analysis using GraphPad Prism, version 6.01 (GraphPad Software, San Diego, CA, USA).

5.3.5 Incorporation of aqueous solutions of DES in the alginate hydrogel

5.3.5.1 Preparation of the alginate-based hydrogel

Four different solid hydrogels were prepared using an alginate aqueous solution with a concentration of 4% (w/v), namely, alginate hydrogels without the drug (Alg), with ibuprofen (Alg-Ibu), with the Arg:Gly aqueous solution (Alg-DES) (60% (w/w) of DES) and with ibuprofen solubilized in the Arg:Gly aqueous solution (Alg-(DES + Ibu)). Ibuprofen was previously solubilized in the Arg:Gly aqueous solution to obtain hydrogels loaded with 20 mg of ibuprofen. For the hydrogels containing ibuprofen solubilized in the Arg:Gly aqueous solution and the ones only solubilized with the Arg:Gly aqueous solution, the solvent represented 3% (w/v) of the totality of the hydrogel. In the Alg-Ibu hydrogels, due to the drug's low-water solubility, the DES amount was replaced by a 0.1 M aqueous NaOH solution.[421] Firstly, alginate was dissolved in water under continuous stirring (500 rpm) until a homogeneous solution was obtained. The Arg:Gly aqueous solution, ibuprofen, and ibuprofen solubilized in the Arg:Gly aqueous solution were added to the corresponding alginate solutions during the biopolymer solubilization process. These solutions were then placed in a sonication bath (ElmaSonic S 300, Singen, Germany) for removal of the entrapped air bubbles. Finally, samples were poured

into circular molds and crosslinked for 1 h at room temperature, by osmosis, using a 10% (w/w) calcium chloride ($CaCl_2$) solution.

For the hydrogels containing ibuprofen, the drug incorporation efficiency was calculated based on the total amount of ibuprofen added to the formulations and the amount retained in the hydrogels after their preparation, according to the following equation:

$$\text{Incorporation efficiency}\% = \frac{Mass\ of\ ibuprofen\ in\ the\ hydrogel}{Total\ mass\ of\ ibuprofen} \times 100\%$$

The mass of ibuprofen retained in the hydrogel was calculated by subtracting the amount of ibuprofen dissolved in the $CaCl_2$ solution during cross-linking of the hydrogel to the total amount initially added to the formulations.

5.3.5.2 Evaluation of the morphology and mechanical properties of the hydrogels

The morphological analysis of the hydrogels loaded with ibuprofen and with the DES aqueous solution comprising ibuprofen was performed by SEM. For this analysis, the hydrogel samples were first frozen in a refrigerator at −80 °C for 24 h and then freeze-dried for 72 h at −85 °C and 0.01 mbar using a freeze dryer (Telstar, LyoQuest, Tokyo, Japan). Freeze-dried samples were coated with carbon using an EMITECH K950 coating system before the analysis. The micrographs of the cross-sections of the samples (obtained by cutting with a sharp razorblade) were acquired using a high-voltage microscope (HITACHI SU 70, Tokyo, Japan) operated at 4.0 kV. For determination of the porous sizes of the hydrogels, SEM micrographs were processed with ImageJ software (version 1.53 for Windows, 64-bit, free software, National Institutes of Health, Bethesda, MD, USA) and values are expressed as mean of 50 different measurements.

Mechanical properties of the hydrogels loaded with ibuprofen, Alg-Ibu and Alg-(DES + Ibu), and of Alg and Alg-DES (for comparison purposes), were evaluated through compressive assays performed using an Instron 5564 (Instron Corporation, Norwood, MA, USA) testing machine with Bluehill 3 software in compressive mode with a 50 N load cell. Circular samples with a 2-cm diameter and 4-mm gauge length were used. At least 5 replicates were tested for each sample. The corresponding

compressive Young's modulus (MPa) and the compressive stress at 30% (MPa) values were determined and expressed as the average ± SD. Multiple group comparisons were executed by One-Way ANOVA analysis using GraphPad Prism, version 6.01 (GraphPad Software, San Diego, CA, USA).

5.3.6 Ibuprofen dissolution test

The Alg-Ibu and Alg-(DES + Ibu) solid hydrogels were immersed in 200 mL of a 0.01-M phosphate buffer (pH 7.4) solution. The dissolution was then carried out at 32.0 ± 1 °C and constant stirring (100 rpm). Aliquots of 1 mL were collected at specific timepoints (0, 5, 10, 30, 60, 90, 120, 180, 240, 300, 360, and 420 min) for a total of 8 h. The same volume of fresh buffer solution was added to maintain a constant volume. The dissolved ibuprofen in each aliquot was quantified by HPLC-DAD, at 264 nm, using the previously described method. The percentage of ibuprofen release at each time was determined based on the ratio of the amount of drug released and the total drug content in the hydrogels. Three replicates were performed for each sample.

5.3.7 Skin permeation assays

Human abdominal skin samples were used for the permeation assays. These samples were obtained from women under the ages of 25–35 who were submitted to an abdominoplasty in Centro Hospitalar São João, Portugal. All patients signed the respective informed consent. The approval of the Ethics Committee of Hospital São João was also obtained for this procedure. After collection, the skin samples were transported under refrigerated conditions. Hypodermis was removed using a scalpel, and then the skin surface was washed, dried and frozen at −20 °C. Skin biopsies were obtained using a biopsy punch (30 mm diameter) to fit the Franz diffusion cell apparatus. The skin was placed in water at 65 °C for 80 s to separate the epidermis, as previously reported in the literature.[422] The experiments with epidermal membranes were conducted on glass Franz-type diffusion cells with a receptor volume of ca. 7 mL and a diffusional area of 1.77 cm^2. A hydroalcoholic solution of PBS (pH 7.4) and ethanol (1:1) was used as the receptor media. The receptor compartment was maintained at 37 °C and under constant stirring. Alginate

hydrogels with a load of 20 mg of ibuprofen were cut to fit the surface area (1.77 cm^2) of the donor compartment and cover the entire epidermal surface. After 6 h, the receptor solution was withdrawn from the receptor compartment and the amount of permeated ibuprofen was quantified. The drug content was analyzed by HPLC-DAD, at 264 nm, using the method previously described for ibuprofen. The permeation assays were executed in triplicate, and each aliquot was measured twice. Results were expressed as the average of permeated drug ± SD.

5.4 Results and discussion

NSAIDs, such as ibuprofen, present very low water solubility at room temperature (4.3 × 10^{-5} mol·L^{-1} for ibuprofen).[423] However, this solubility not only increases with temperature, it can also be increased by adding organic co-solvents to the aqueous solutions, such as ethanol, which are commonly used in commercial topical formulations.[424,425] Due to the negative effect of ethanol on skin, such as dryness, and its association with the development of several skin disorders (e.g., eczema, psoriasis),[426] the solubilization of ibuprofen and its stability in DES aqueous solutions was studied in this work. The components of the DES used herein, viz. glycerol and arginine, were selected due to their administration route and the intended efficacy improvement. Glycerol is widely used as a humectant in skin formulations,[427] and arginine has been reported to down-regulate cytokine secretion and decrease the activity of metalloproteinases, helping to decrease inflammation.[428] This DES, Arg:Gly (1:4 molar ratio), was prepared by the heat-method and ibuprofen was added to the respective aqueous solution (Figure 44a); then, the drug solubility, stability, cytotoxicity and anti-inflammatory action were appraised. The DES formulation comprising ibuprofen (with 60% (w/w) of DES in water) was then incorporated in an alginate-based hydrogel (Figure 44b), which was characterized in terms of its morphology, mechanical properties, dissolution and permeation profiles through human skin. A hydrogel containing ibuprofen solubilized in a slightly alkaline aqueous solution was prepared and characterized for comparison. These characterizations were performed to evaluate the potentialities of the partnership between DES solutions and alginate hydrogels to improve the transdermal delivery of ibuprofen.
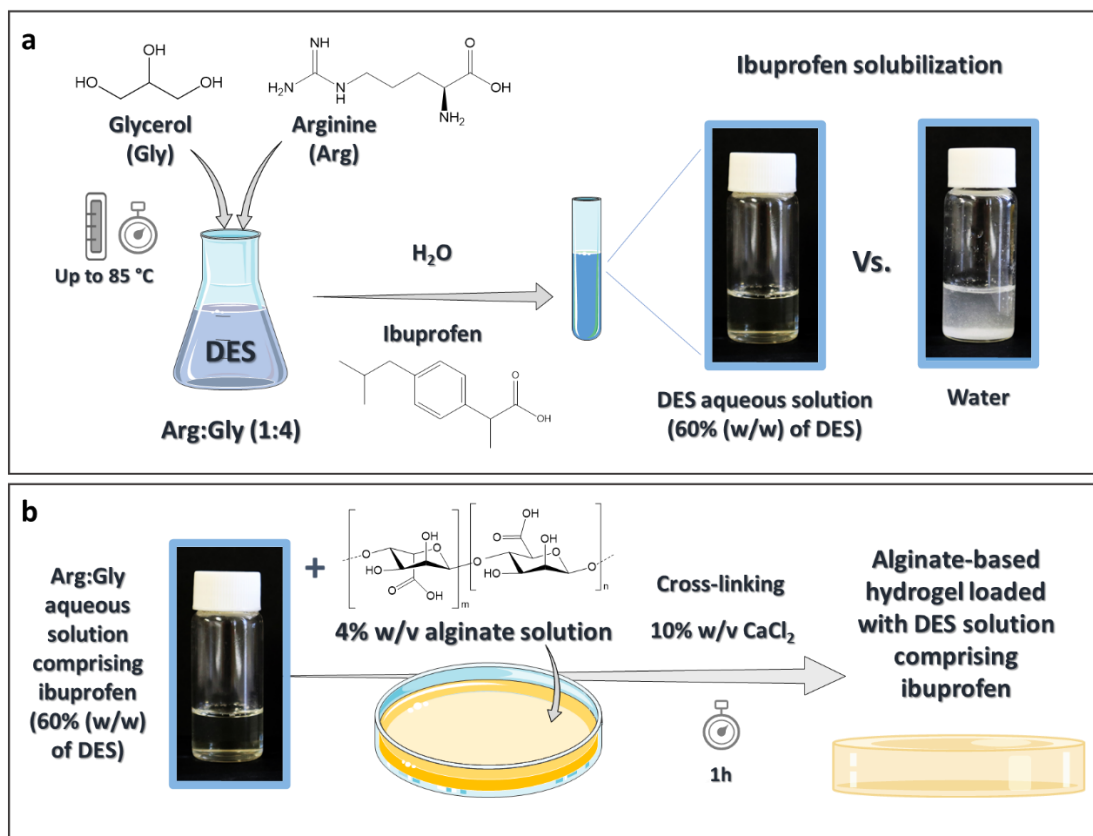
Figure 44. Schematic illustration of the preparation of a DES aqueous solution with higher solubilization ability for ibuprofen (a) and its incorporation in an alginate-based hydrogel (b) developed for the transdermal delivery of ibuprofen. Image made with Servier Medical Art and adapted by the authors according with Servier under the CC-BY 3.0 License (at https://smart.servier.com/, accessed on 23 January 2020).

5.4.1 DES characterization

Firstly, the structure of the hydrogen-bond donor/acceptors was assessed after the preparation of the DES containing Arg:Gly. This was evaluated by ^{1}H and ^{13}C NMR spectroscopy, as depicted Figure 45.

The recorded spectra show that both components maintain their structure after the DES preparation. Such conclusions can be drawn due to the similarity of the resonances observed for Arg:Gly to those predicted for the single components' spectra. The ^{1}H NMR spectrum (Figure 45a) reveals the proton resonance of H-3,4 of arginine can be found as a multiplet at 1.41 ppm, while the protons from the CH_2 (H-2) and CH (H-5) groups directly linked to the NH groups can be observed as multiplets at 2.98 ppm and 3.05 ppm, respectively. Likewise, the H-1',3' and H-2' of glycerol can be found as two multiplets at range between 3.39 ppm and 3.55 ppm. The signals in the ^{13}C NMR spectrum of this DES (Figure 45b) show the carbon

resonances from the CH$_2$ groups of arginine's backbone (at 24.40 ppm (C-3), 31.50 ppm (C-4), 40.86 ppm (C-2) and 53.21 ppm (C-5) respectively) and those expected in glycerol's structure (62.15 ppm (C-1',3') and 71.97 ppm (C-2')). Finally, the carbon resonances of C-1 and C-6 of arginine can be observed at 156.57 ppm and 182.54 ppm, respectively.
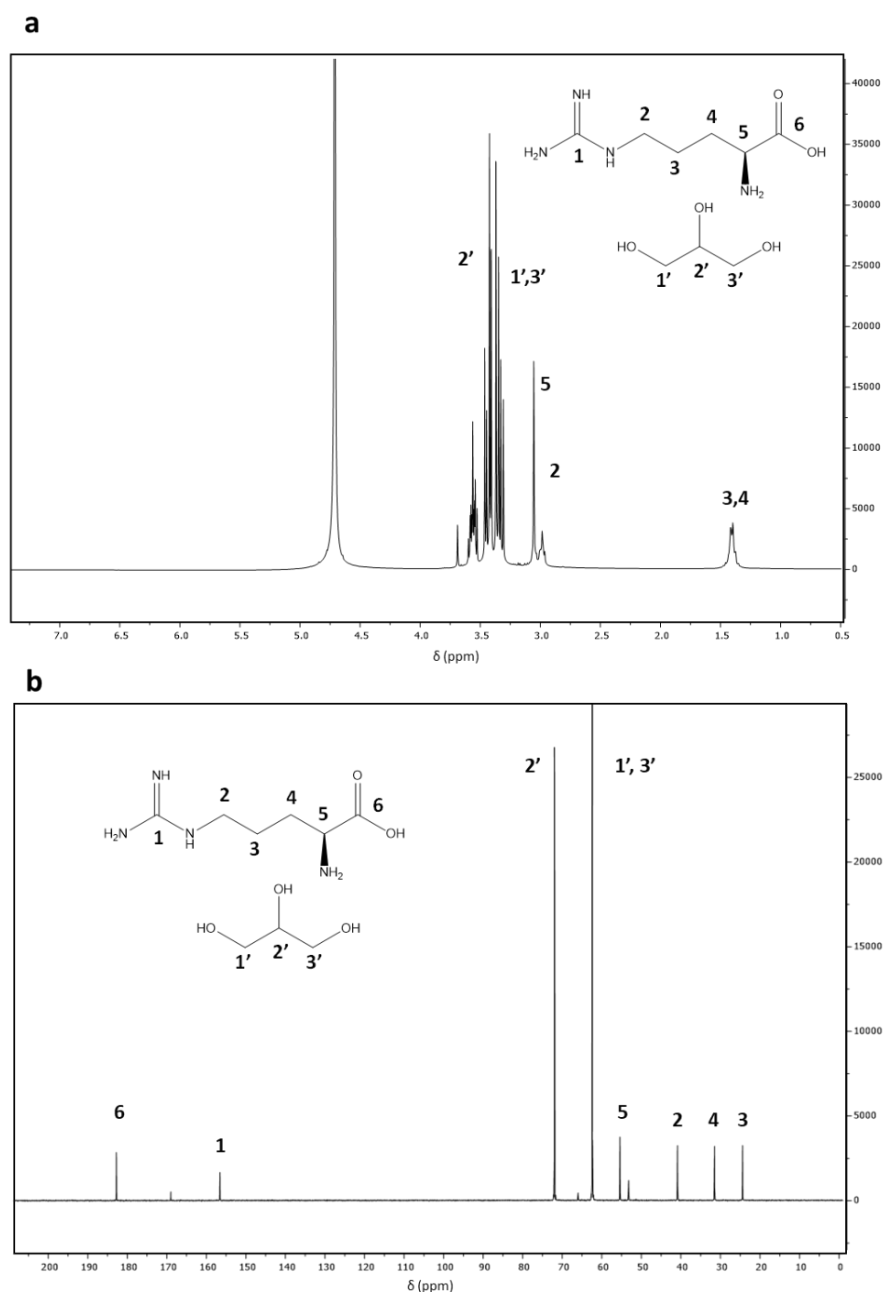
Figure 45. ^{1}H NMR (a) and ^{13}C NMR spectra (b) spectra of Arg:Gly DES in D$_2$O.

Afterwards, the DES formation and the interaction between the components was confirmed by FTIR-ATR spectroscopy (Figure 46).
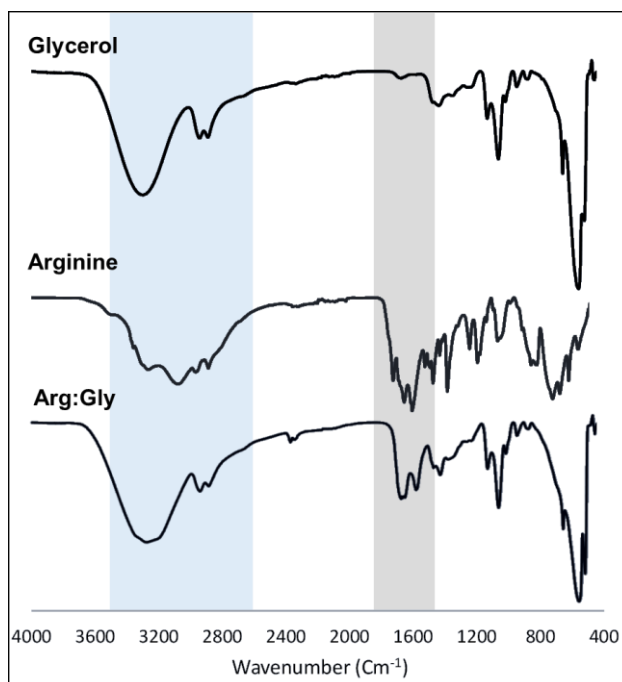
Figure 46. FTIR-ATR spectra of glycerol, arginine and the DES Arg:Gly.

By comparing the FTIR-ATR spectra of the pure compounds with that of the DES, it is possible to observe that the DES spectrum is more similar to that of glycerol. This can be expected since Arg:Gly was prepared in a 1:4 molar ratio. Specifically, it is possible to verify that, in the spectrum of glycerol, there is an absorption band at 3279 cm^{-1}, which corresponds to the hydroxyl groups' (O–H) stretching vibration and the peaks corresponding to the C–H stretching in the region of 2812–2980 cm^{-1}.[429] For arginine, O–H and N–H stretching vibrations appear at the region of 2940–3324 cm^{-1}, while the absorption bands observed at 1550 cm^{-1} and 1560 cm^{-1} correspond with the C–O vibration and the C=O stretching of the carbonyl group, respectively [430]. In the DES spectrum, the establishment of hydrogen–bond interactions, among others, between both components leads to a slight deviation in the vibration of the N–H and O–H groups to 3255 cm^{-1}, and of the peaks' corresponding to the C–H stretching to values in the region of 2838–2970 cm^{-1}. This is also verified for the C–O vibration and the C=O stretch of the carboxyl group of arginine, which are found at 1565 cm^{-1} and 1634 cm^{-1}, respectively, in the DES spectrum.

5.4.2 Ibuprofen solubility in DES aqueous solutions

Aqueous solutions of Arg:Gly (1:4) were tested up to 60% (w/w) of DES given the high viscosity of solutions above this concentration. To understand the solubilization mechanism of ibuprofen, and which Arg:Gly concentration is the most effective to the intended purpose, the solubility of the drug at both room (25 °C) and human body (37 °C) temperatures was investigated in aqueous solutions with different DES percentages (Figure 47a). The solubility enhancements presented in Figure 47b are calculated from the ratio (S/S_0) between the solubility of ibuprofen in each Arg:Gly aqueous solution (S) and its solubility in water (S_0) at the same temperature.
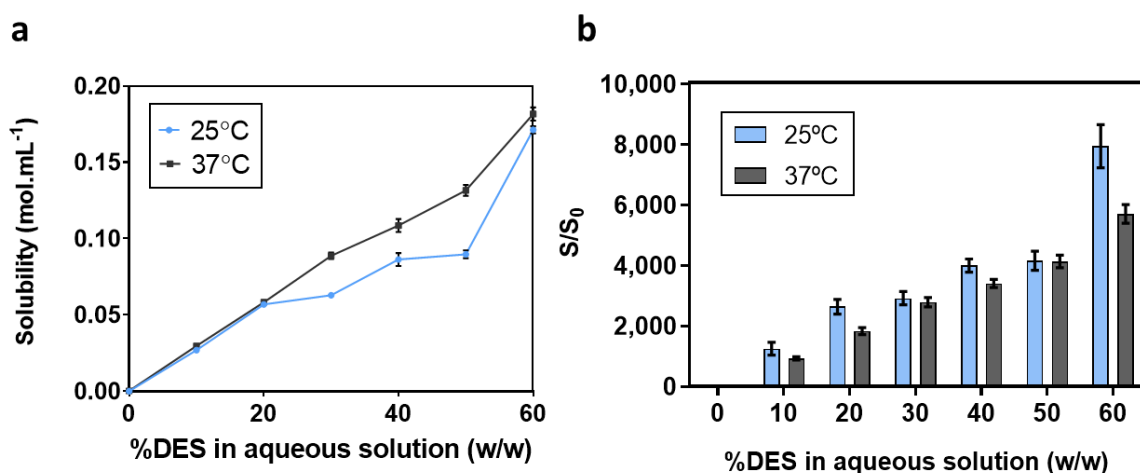
Figure 47. Solubility enhancements for ibuprofen in Arg:Gly aqueous solutions achieved at both room and body temperatures. The results are expressed as the mean ± SD of three independent experiments.

The solubility of ibuprofen in water increases from $(2.16 \pm 0.16) \times 10^{-5}$ mol·mL^{-1} up to $(3.19 \pm 0.18) \times 10^{-5}$ mol·mL^{-1} from room to body temperature. However, these concentrations are still inadequate for therapeutic purposes. The dosage of ibuprofen in common commercial formulas is generally 200 mg, administered every 6 h.[51] However, the quantity required for therapeutic purposes in an adult is only approximately 20 mg. The usually commercialized forms possess more than 10-fold this amount, not only due to their first pass metabolism and poor absorption, but also due to the poor aqueous solubility of the drug. This limited solubility and the rate of dissolution from the currently available solid forms leads to poor bioavailability; therefore, higher doses need to be administered to reach the

166

therapeutic dosage contributing to the increase in some of the unwanted adverse effects.[50]

For the Arg:Gly aqueous solutions studied here, the solubility of the drug increases proportionally to the increment of the Arg:Gly percentage (w/w) in water. This monotonic behavior reveals that the Arg:Gly solubilization ability is in agreement with a co-solvency mechanism.[300] When using 60% (w/w) of Arg:Gly in the aqueous solution, $(1.71 \pm 0.02) \times 10^{-1}$ mol·mL^{-1} of ibuprofen are solubilized (Figure 47a); this amount is equivalent to 46.92 mg, which is 2-fold the therapeutic dosage needed.[51] This represents a notable 7917-fold increase in the drug solubility when compared to its solubility in water at the same temperature (Figure 47b). At body temperature, since the drug solubility is higher, this value was increased up to $(1.82 \pm 0.03) \times 10^{-1}$ mol·mL^{-1}, meaning a 5705-fold increase in the solubility of ibuprofen when compared to its water solubility at 37 °C (Figure 47a and 47b). Since the amount of ibuprofen that can be solubilized in the Arg:Gly aqueous solutions shows a monotonic increase, maximum solubility was not fully achieved. Higher drug amounts are expected to be solubilized above 60% (w/w) of DES in water; however, these values were not determined due to the viscosity of the mixtures above these concentrations, as previously stated. Nevertheless, the solubility enhancements obtained using this DES solution surpass the increases in solubility achieved using aqueous solutions of co-solvents, such as propylene glycol and PEG 300, that allow for a 400-fold and 1500-fold increase in the water solubility of ibuprofen at room temperature, when using 80% (w/w) of each co-solvent [133]. Eutectic mixtures, and particularly DES, have also been studied to improve the solubility of ibuprofen in water and in neat DES, for transdermal applications.[110,135] For example, a 4-fold increase in water solubility was achieved with the mixture menthol:camphor (1:1).[135] However, the DES menthol:camphor presents itself as having low water solubility, presenting a problem for its application in water-rich matrices. Solubility enhancements of more than 3810-fold have also been verified for neat DES, such as cholinium chloride:propanediol (1:5); however, this enhancement is highly reduced when less than 75% (w/w) of DES is used in an aqueous solution.[110]

In sum, by applying Arg:Gly aqueous solutions, it is not only possible to obtain higher solubility enhancements than the DES previously reported in the literature[135] and the previously mentioned co-solvents,[133] but also, to use less co-solvent (in this case, DES) in the final formulation. Therefore, the aqueous solution with 60% of Arg:Gly (w/w) was selected for further studies.

5.4.3 Ibuprofen stability in the DES aqueous solutions

The stability of ibuprofen in aqueous solution containing 60% (*w/w*) of DES was investigated at 25 and 37 °C. The content of ibuprofen solubilized in the Arg:Gly aqueous solution, and in water for comparison, was analyzed each 15 days for both temperatures, as shown in Figure 48.
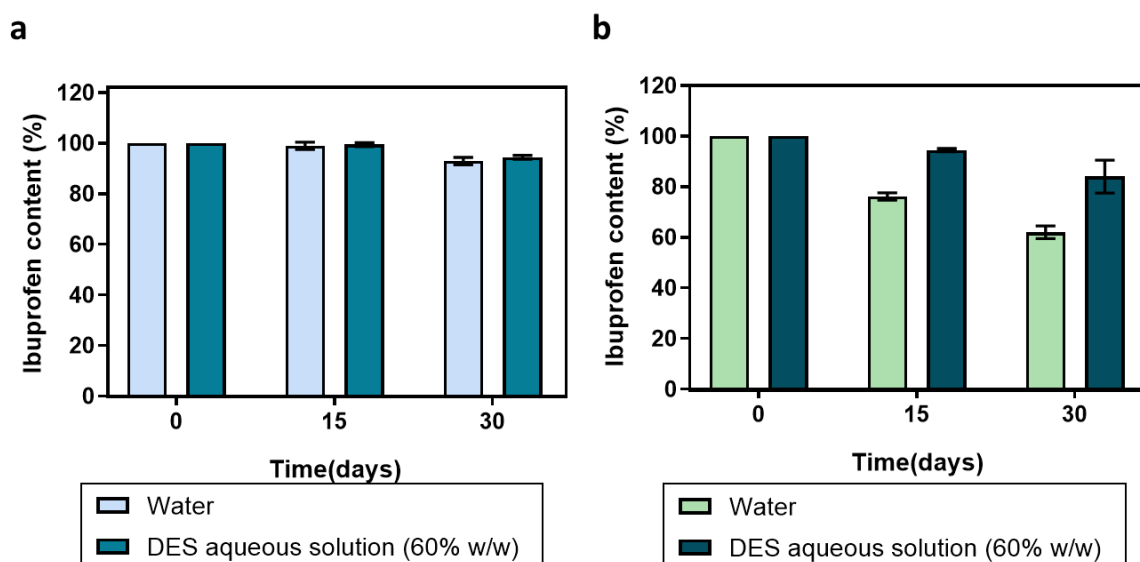
Figure 48. Effect of the solvent in the stability of ibuprofen at 25 °C (a) and 37 °C (b) over a period of 30 days. The results are expressed as the mean ± SD of three independent experiments.

When stored at 25 °C, ibuprofen presents high stability in both water and the DES aqueous solution, making it possible to quantify 93–95% of ibuprofen after 30 days of storage (Figure 48a). For higher temperatures, namely, 37 °C, the stability of ibuprofen in water decreases, with 76.2% of ibuprofen being quantified in solution after 15 days and only 62.1% after 1 month. The use of DES aqueous solutions clearly improved the stability of ibuprofen when the drug was submitted to higher temperatures, as depicted in Figure 48. After 15 days at 37 °C, the drug content was 94.5%, and there was still 84.1% of ibuprofen in the formulation after 1 month.

It has been reported [431] that when ibuprofen is solubilized in 0.9% sodium chloride or 5% dextrose aqueous solutions, more than 92% of its initial concentration is retained when stored for 14 days at 4 °C. Liposomal formulations of ibuprofen were also reported to be stable under similar conditions during the same period.[432] Thus, it was possible not only to improve the ibuprofen solubility by using the aqueous DES as a pharmaceutical co-solvent, but also to improve the stability of the drug without requiring the use of additional excipients or storage under refrigerated conditions.

5.4.4 Cytotoxicity and anti-Inflammatory activity of DES-based formulations containing ibuprofen

The cytotoxicity of ibuprofen that is solubilized in the Arg:Gly aqueous solution (60% w/w), of ibuprofen and of the Arg:Gly aqueous solution for comparison was evaluated in cells that were relevant for the intended application, namely, macrophages. In Figure 49, the cytotoxicity results obtained for a concentration range of 0.01–4.00 mM of ibuprofen are presented. The Arg:Gly aqueous solution (60% w/w) was tested in the same concentrations as the one with the Arg:Gly, comprising ibuprofen for comparison purposes.

As depicted, the Arg:Gly aqueous solution is not cytotoxic towards macrophages at concentrations up to 2.0 mM. This cytotoxicity profile is expected, since the DES' components and the initial DES concentration were carefully selected to be non-toxic, in accordance with previous findings in the literature.[342,433] Although there are no data in the literature about the cytotoxicity of the DES used in the present study, the cytotoxicity of other DES comprising several alcohols and cholinium chloride has been reported in the literature for HaCaT,[306] and, in most cases, these were shown to be harmless even at concentrations up to 500 µg·mL^{-1} (above the ones tested in this work). The cytotoxicity profile of ibuprofen solubilized in the Arg:Gly aqueous solution is generally similar to that of the aqueous solutions of ibuprofen, and non-toxic to macrophages in concentrations below 0.5 mM (Figure 49a). This dose–response profile, obtained for ibuprofen solubilized in both water and in the Arg:Gly aqueous solution (60% w/w), is in accordance with previous results for ibuprofen solubilized in water towards the same cell line and range of

concentrations.[434] Therefore, our results show that the Arg:Gly aqueous solution containing ibuprofen in concentrations up to 0.5 mM is safe to be applied in transdermal drug delivery administration.
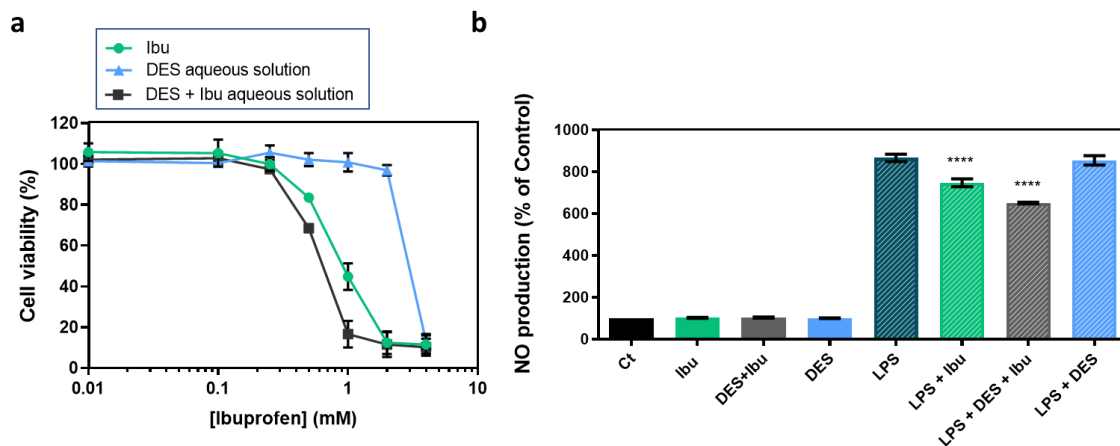
Figure 49. Effect of ibuprofen, Arg:Gly aqueous solution (60% *w/w*) and ibuprofen solubilized in Arg:Gly aqueous solution on the (a) cell viability profile of Raw 264.7 macrophages, measured by the metabolic conversion of resazurin; and on the (b) anti-inflammatory action evaluated by the NO production of Raw 264.7 macrophages. Results were expressed relative to the control as mean ± SD of three independent biological experiments. Statistically significant differences were using one-way ANOVA (**** = $p \leq 0.0001$).

To find the influence of these formulations on the anti-inflammatory activity of ibuprofen, their effect on the NO and LPS-induced production in macrophages was analyzed (Figure 49b). Macrophages can increase NO secretion after LPS stimulation *in vitro*, providing a good model to evaluate the anti-inflammatory potential of drug formulations.[435] If a given drug formulation presents anti-inflammatory action, the NO production after the LPS stimulation will decrease. Figure 49b shows that the Arg:Gly aqueous solution per se does not present the ability to inhibit NO production. Ibuprofen treatment decreased LPS-triggered NO production by macrophages. This may be attributed to its inhibition of NF-κB, a transcription factor essential for iNOS expression. However, this inhibition is relatively modest, and the anti-inflammatory activity of ibuprofen mostly relies on its inhibition of the COX-2 enzyme.[50] Surprisingly, when ibuprofen is solubilized in the Arg:Gly aqueous solution, a synergistic effect can be observed, and it is possible to obtain a statistically significant decrease in NO production when compared to both components separately. By solubilizing ibuprofen in the Arg:Gly in aqueous solution, it was verified that this formulation does not jeopardize the anti-inflammatory action

of the drug and allows for a reduction in inflammation by providing a small increase in the therapeutic activity of the drug.

5.4.5 Incorporation of aqueous solutions of DES in an alginate hydrogel

The DES aqueous solution (60% (w/w) of DES in water) has shown promising ability to enhance the solubility and stability of ibuprofen, while preserving its anti-inflammatory action without cytotoxicity towards macrophages. To deliver this formulation with improved efficacy, the incorporation of this ibuprofen formulation into an alginate-based hydrogel was investigated. The effect of the use of Arg:Gly-based DES on the morphologic and mechanical properties of the biopolymer-based system, and on ibuprofen's dissolution in a buffer solution and permeation across human skin, was evaluated.

The alginate hydrogels with ibuprofen solubilized in a slightly alkaline aqueous solution (Alg-Ibu) and ibuprofen in the Arg:Gly aqueous solution (Alg-(DES + Ibu) present distinct visual aspects and morphologies, as depicted in Figure 50.

While Alg-Ibu hydrogels exhibited a rougher and waver surface (Figure 50a), Alg-(DES + Ibu) ones showed a relatively smoother surface (Figure 50b). To corroborate these visual observations, the cross-sections of both freeze-dried hydrogels (Alg-Ibu and Alg-(DES + Ibu)) were also examined by SEM. The obtained micrographs show that both hydrogels have a porous 3D structure (Figure 50c and 50d). However, the pore shapes of the Alg-Ibu hydrogel are more irregular than those of Alg-(DES + Ibu), which present more clearly defined walls and a considerably higher homogeneity. A similar trend was reported for Basiak *et al*. [436], where the microstructure of wheat starch films also showed an increase in the homogeneity and a smoother surface when glycerol (a component of the DES used in the present study) was added to the biopolymer-based system. Moreover, Alg-(DES + Ibu) hydrogel presented slightly smaller pores (112.24 ± 8.51 µm) than the Alg-(Ibu) counterpart (138.77 ± 9.30 µm). Additionally, when considering the micrograph of the Alg-Ibu cross-section (Figure 50c), is possible to notice a mild drug precipitation, which is not observed for the Alg-(DES + Ibu) systems (Figure 50d) and which can possibly justify the mechanical properties further discussed in

this section. This observation is certainly due to the higher solubility of ibuprofen in the aqueous solutions, as previously described.
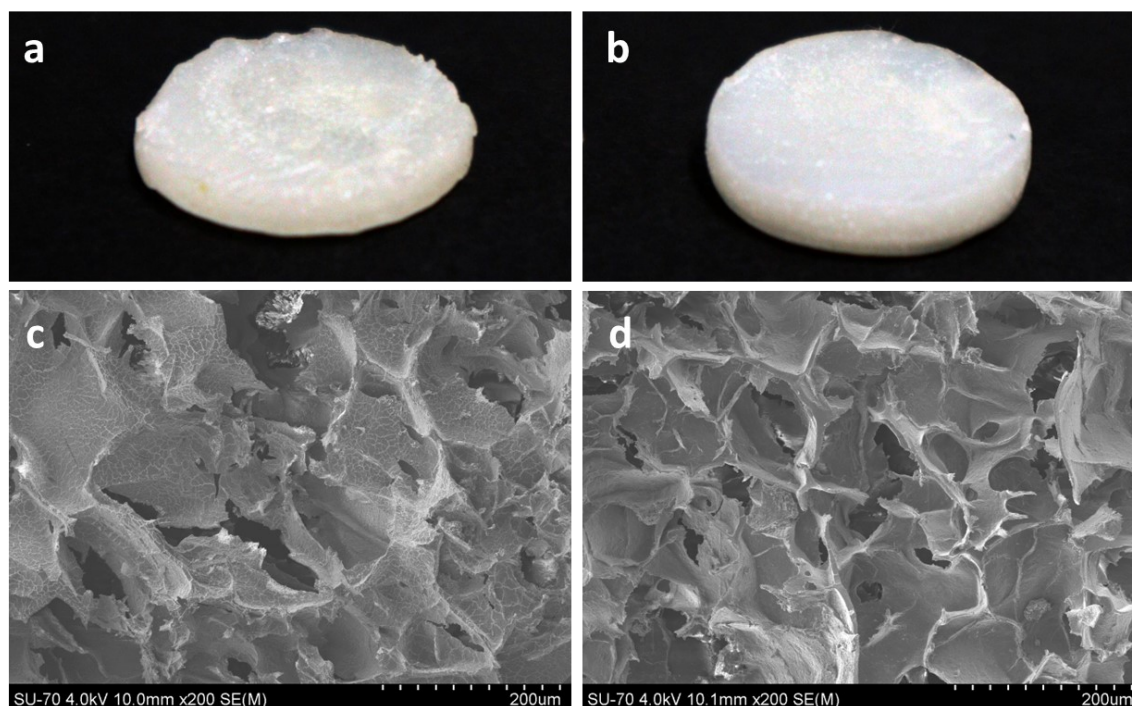
Figure 50. (a,b) Visual aspect of alginate-based hydrogels with (a) ibuprofen (Alg-Ibu) and (b) with DES aqueous solutions comprising ibuprofen (Alg-(DES + Ibu)) and (c,d) the corresponding cross-section SEM micrographs.

The mechanical performance of the two solid hydrogels were studied by compressive tests. To better understand their performance, pure alginate hydrogels (Alg) and hydrogels with the DES solution (Alg-DES) were also tested for comparison purposes. The Young's modulus (Figure 51a) and the compressive stress at 30% (Figure 51b) of the different samples were determined from the respective stress–strain curves.

The Alg hydrogel showed a Young's modulus of 580.20 ± 50.27 kPa and a compressive stress at 30% of 38.92 ± 1.56 kPa. A lower Young's modulus of 213.60 ± 13.84 kPa (Figure 51a) and a lower compressive stress at 30% of 25.63 ± 1.72 kPa (Figure 51b) was obtained for the Alg-DES hydrogel. These results reveal that the incorporation of the DES solution has a noticeable plasticizer effect, with a considerable impact on the mechanical properties of the Alg hydrogel network. This effect was previously observed for other biopolymers-based systems, for instance, for cellulose [437] and starch-based ones,[438] comprising DES, such as cholinium

chloride:glycerol and other cholinium and alcohol-based DES. In the present study, this can be obviously attributed to the effect of glycerol, which is known to present a plasticizer effect on biopolymers, and particularly on alginate hydrogels.[439] The use of glycerol-based DES not only promotes the formation of hydrogen-bonding between the biopolymer and the DES, but also decreases the biopolymer matrix's strong intramolecular attraction, thereby increasing the interchain spacing, as see in previously reported alginate-based systems plasticized with glycerol.[396,439] This reduction in the interchain interactions of alginate, which can be attributed to the effect of glycerol from Arg:Gly, results in alginate hydrogels with lower rigidity.

However, the incorporation of ibuprofen solubilized in a slightly alkaline aqueous solution in the alginate hydrogel (Alg-Ibu) promoted an increase in the Young's modulus and on the compressive stress at 30%, with values of 1283.50 ± 46.57 kPa and 45.13 ± 3.15 kPa, respectively (Figure 51a and 51b). Therefore, the incorporation of the drug in the hydrogel network turns it into a more rigid and brittle system. These findings have also been reported for the incorporation of ibuprofen into gellan gum-based hydrogels.[440]

The Alg-(DES + Ibu) displayed a Young's modulus of 559.00 ± 38.38 kPa and compressive stress values of 26.59 ± 1.35 kPa. Regarding the Young's modulus, the obtained value is similar to that observed for the Alg system and higher than the that observed for the Alg-DES hydrogel. These results are certainly due to the combined effect of both the drug incorporation, which increases the Young's modulus, and the plasticizer effect of the DES, which strongly decreases this parameter, as observed in Figure 51a. In addition, for the compressive stress at 30%, the plasticizer effect of the DES is highlighted for both the Alg-DES and Alg-(DES + Ibu), which presented similar values to each other, but lower values than those of the other systems (Figure 51b). The Alg-(DES + Ibu) hydrogel presents more appealing mechanical properties for transdermal delivery purposes, since these mechanical properties translate into a loss of stiffness, allowing for a more pliable delivery system than Alg-Ibu to be obtained, enabling the hydrogel to better adapt to the wrinkles and deformations of the skin, and consequently allowing for better contact with the skin surface for drug permeation.[268]
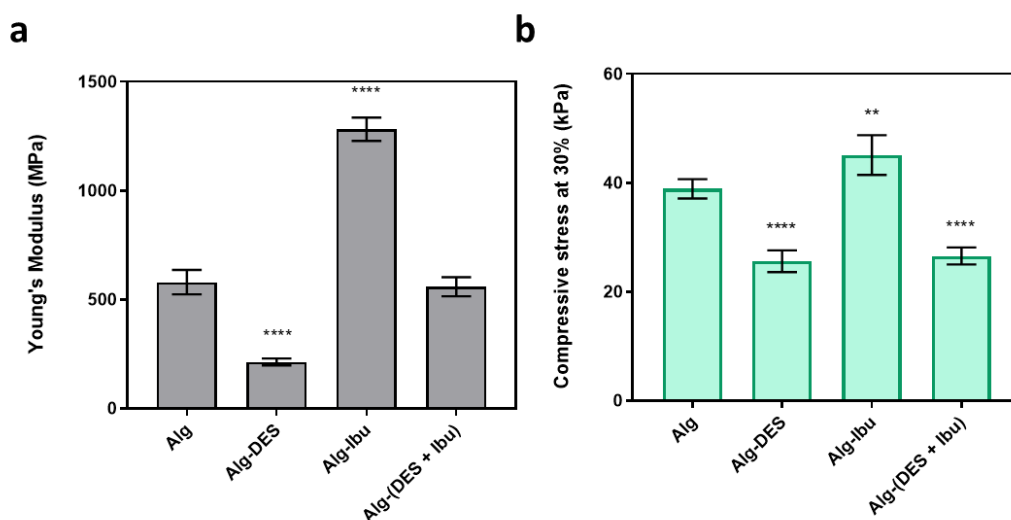
Figure 51. (a) Young's modulus and (b) compressive stress at 30% of pure alginate (Alg), and alginate with DES solution (Alg-DES), ibuprofen (Alg-Ibu) and DES solutions containing ibuprofen (Alg-(DES + Ibu)) hydrogels obtained from the compressive tests. Values are presented as mean of five replicates and respective standard deviations. ** $p < 0.0080$, **** $p < 0.0001$ compared to the Alg-based hydrogel mechanical performance results.

5.4.6 Dissolution and permeation across human skin

The *in vitro* dissolution profile of ibuprofen was determined for the hydrogels loaded with ibuprofen solubilized in a slightly alkaline aqueous solution, or in the aqueous Arg:Gly solution. Before the dissolution tests, the incorporation efficiency of the drug in the hydrogels was calculated, and it was observed that both systems presented high incorporations of ibuprofen, viz. 82.5 ± 3.9% and 77.4 ± 2.3% for Alg-(DES + Ibu) and Alg-Ibu hydrogels, respectively. Since ibuprofen is commonly administered from 6 to 8 h,[441] the dissolution assay was carried out *in vitro* for 8 h.

As depicted in Figure 5.4.6, ibuprofen shows a sustained dissolution profile for both systems; however, the dissolved amounts are higher for the hydrogels containing the DES solution with ibuprofen. After the first hour, the Alg-(DES + Ibu) hydrogel released 39.6 ± 1.5% of the total ibuprofen content, which represents a released amount that is 1.6-fold higher than that released by the Alg-Ibu system, with only 24.1 ± 1.7% released (Figure 52). After 8 h, the duration of the test, the Alg-(DES + Ibu) hydrogel released 93.5 ± 2.2% of the drug content, and the hydrogel Alg-Ibu only released 68.9 ± 2.5% (Figure 52).

174
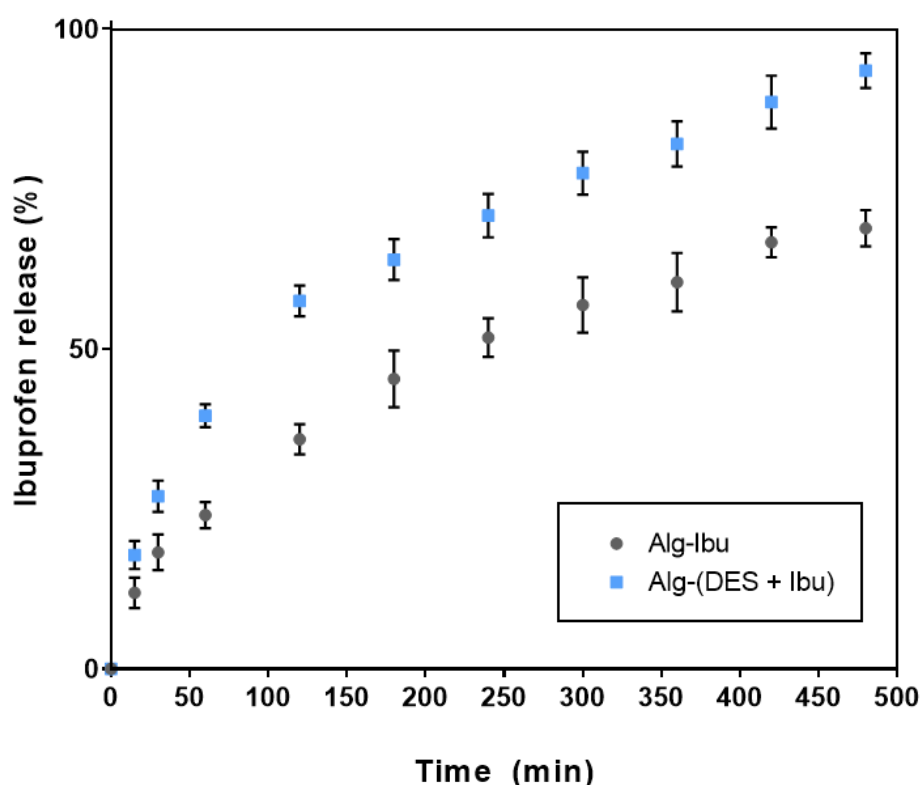
Figure 52. *In vitro* release profile of ibuprofen from alginate-based hydrogels in PBS solution. Profile data represented as mean ± SD of three independent experiments.

Indeed, for other, previously reported transdermal delivery systems[442,443] ibuprofen's incomplete delivery represents an obstacle towards a more effective therapeutic outcome. For example, membranes of synthetic polymers, such as latex, prepared for the transdermal delivery of ibuprofen, released only 60% of the drug after 96 h.[442] These values can be enhanced when considering alternative formulations, such as nanoliposomes, which showed a drug release of 81—92% over a 24 h period [444]. However, the delivery period is still lengthy. The use of biopolymer-based membranes, such as bacterial cellulose, also enables a low release of ibuprofen to the media, achieving a plateau of 25—40% of total release within the first hour.[434,443] The development of more soluble forms of ibuprofen, such as ionic liquids, namely, cholinium ibuprofenate,[434] or the drug conjugation with L-valine alkyl esters[443] can improve the drug release, especially when considering their incorporation into bacterial cellulose membranes. Cholinium ibuprofenate incorporation in bacterial cellulose allows for fast release of the drug, enabling 90% of release to be achieved within 10 min, which is beneficial for a fast therapeutic

action.[434] The drug conjugation with L-valine alkyl esters also enables a high and faster delivery of the drug content, 87—90%, from 30 to 120 min, but does not necessarily translate into a higher permeation capacity and, therefore, into faster therapeutic action.[443] In this context, the Alg-(DES + Ibu) hydrogels developed in this work present a sustained release of the drug, with a high drug release, providing a fast and increasing drug dosage over the treatment period.

To infer if the improved dissolution profile of the hydrogels containing the DES solution translated into an effective drug permeation, the cumulative amount of ibuprofen that permeated from the two solid hydrogel systems on human epidermal skin was tested using a Franz diffusion cell. The cumulative mass of the drug, which permeated through the human skin samples after 6 h at 32 °C, is presented in Table 1. In terms of absolute quantities, after 6 h, ibuprofen permeated to a higher extent from the Alg-(DES + Ibu) hydrogel than from the Alg-Ibu (382.43 ± 16.62 $\mu g \cdot cm^{-2}$ vs. 44.81 ± 15.71 $\mu g \cdot cm^{-2}$). The presence of the DES aqueous solution comprising ibuprofen in the alginate hydrogel allowed for an 8.5-fold increase in the amount of ibuprofen that permeated through human epidermis. These results are in total agreement with the previously described dissolution profiles.

Table 11. The average cumulative mass of ibuprofen after 6 h permeation from the hydrogel with ibuprofen and the hydrogel with ibuprofen solubilized in the DES aqueous solution test across human epidermis.

Sample	Cumulative Mass (μg Ibu$\cdot cm^{-2}$)
Alg-Ibu	44.81 ± 15.71
Alg-(DES + Ibu)	382.43 ± 16.62

The amount of ibuprofen that permeated from the Alg-Ibu hydrogel is in accordance with the values obtained for commercial ibuprofen gels (≈ 40 $\mu g \cdot cm^{-2}$) for 6 h of permeation.[445] The incorporation of this model drug in biopolymer-based systems, such as bacterial cellulose membranes, has been proven to enhance the transdermal delivery of the drug when compared to commercial gel formulations.[446] The amount permeated achieved using a DES solution comprising ibuprofen in alginate-based hydrogels is not only considerably higher (8.5-fold) than the amount achieved for commercial formulations (≈ 40 $\mu g \cdot cm^{-2}$) and for other biopolymer-based systems, but also comparable to the values that were observed for formulations of

ibuprofen conjugated with L-valine alkyl esters, which also display high drug solubility (382.35 ± 1.05 µg·cm^{-2}).[447] The Alg-(DES + Ibu) hydrogels reported herein enable higher permeation enhancements than those previously reported when using DES formulations that comprised the drug and a permeation enhancer, such as menthol (ibuprofen:menthol).[448] However, the previously mentioned values are commonly evaluated for a 24 h assay period. The Alg-(DES + Ibu) hydrogels presented herein provided higher permeated amounts after only 6 h, allowing for a faster therapeutic onset to be obtained than that of typical delivery systems.

5.5 Conclusions

DES aqueous solutions comprising ibuprofen were studied in this work, aiming to improve the drugs' characteristics and their transdermal delivery when using an alginate hydrogel. Herein, is demonstrate that Arg:Gly aqueous solutions are able to improve the solubility of ibuprofen up to 7917-fold (solution with 60% *w/w* of the DES) at room temperature, providing competitive pharmaceutical co-solvents to those commonly applied in pharmaceutical formulations. Furthermore, this DES aqueous solution can preserve the ibuprofen's stability even when the drug is submitted to higher room temperatures (up to 37 °C over 1 month), allowing for their storage in non-refrigerated conditions. Moreover, these formulations showed non-toxicity towards macrophages, and slightly increased the therapeutic action of the drug (namely, its anti-inflammatory activity).

The combination of these DES aqueous solutions and an alginate-based hydrogel resulted in efficient drug-delivery systems for the transdermal administration of ibuprofen. Based on the results, the plasticizer effect of the Arg:Gly DES can be highlighted, which allowed for hydrogel systems with a more homogenous and defined structure to be obtained, which are more flexible when handled. Moreover, the dissolution of the drug from the biopolymer-based system with the Arg:Gly solution shown a sustained release of the drug, achieving 93.5 ± 2.2% of drug release after 8 h. Finally, the permeation of the drug through the human skin was improved by up to 8.5-fold when the Ag:Gly aqueous solutions comprising ibuprofen was used, highlighting the successful partnership between DES and alginate hydrogels for the transdermal delivery of this drug. Moreover, this study forms a basis for future optimizations of the developed systems and additional studies using different drugs, DES and polymeric systems, with the aim of improving the transdermal administration of distinct drugs. In advanced stages of this research, *in vivo* studies will also be considered, aiming to guarantee a safe and efficient administration of these systems and confirm their potential as a strategy for use in different clinical scenarios.

Final Remarks and future work

The high number of active pharmaceutical ingredients with low water-solubility, low permeation and stability issues in the market are a driving force towards the research of more effective formulations with the goal of developing safer and more effective treatments. Drug reformulation can be seen as an appealing strategy to tackle some of the marketed drugs' limitations. In this sense, the selection of better formulation components that can improve the drug efficacy improvement, could benefit both the industry and the patient's treatment quality.

With this in mind, in this thesis, the use of DES formulations was explored to improve the properties of marketed drugs' and, ultimately, their drug delivery and therapeutic efficacy. The works herein presented are a reflex of the growing knowledge and application of DES formulations, that range from the simple use of aqueous DES formulations to their use in complex drug delivery systems.

To explore the versatility of DES in this realm, DES aqueous solutions were applied for the solubilization of antibiotics (ciprofloxacin, chloramphenicol), photosensitizers (curcumin) and non-steroidal anti-inflammatory drugs (ibuprofen). The effect of DES aqueous solutions, comprising active pharmaceutical ingredients, were studied in simple aqueous formulations, thermo-responsive microemulsions, adhesive films and hydrogels aimed for ocular, topical and transdermal delivery, respectively. It was demonstrated how the rational selection of the DES components can be adjusted to the administration route and to go further from their common solvent application, playing multiple roles as pharmaceutical excipients. In particular, in this thesis, DES aqueous solutions of cholinium chloride:urea:malonic acid ([Ch]Cl:U:MA), proline:urea:malonic acid (Pro:U:MA) and citric acid:xylitol (CA:Xyl) (used to solubilize ciprofloxacin), betaine:glycerol (Bet:gly) and betaine:xylitol (Bet:xyl) (applied for chloramphenicol solubilization), betaine:levulinic acid (Bet:Lev) (applied for curcumin solubilization) and arginine:glycerol (applied for ibuprofen solubilization) have been studied.

The findings herein presented highlight the remarkable ability of the studied DES for the solubility enhancement in aqueous media by several orders of magnitude for all the active ingredients studied (maximum enhancements ranging from 140- to 7917-fold in comparison to water). In this context, the studied DES can

be successfully used as common co-solvents and hydrotropes in pharmaceutical active ingredients solubilization.

The use of these DES also proved to be advantageous in extending and improving drug stability in aqueous media. This capability covers the improvement of the hydrolytic (ciprofloxacin and chloramphenicol), photochemical (curcumin) and thermal (ibuprofen) stability of the studied ingredients, stored from 30 days to 3 months. Furthermore, in the case of chloramphenicol formulations, it was demonstrated how the studied DES can not only improve the antibiotic stability but also the stability of the drug delivery system (a thermos-responsive microemulsion). This is particularly advantageous since the selected DES play an additional role as excipients capable to control changes in the pharmaceutical formulation (such as pH, particle size and viscosity), avoiding the addition of multiple components to this purpose.

The incorporation of DES aqueous solutions in the drug delivery systems also seemed to impact the permeation ability of the active ingredients through biological membranes. This was specifically observed in the thermo-responsive microemulsions and in the alginate hydrogel-based systems developed. These two studies explored different biological membranes, namely porcine corneal tissue and human skin. The formulation of the target drugs using DES improved the release abilities of the systems resulting on a successful sustained delivery of chloramphenicol; and with higher amounts of chloramphenicol and ibuprofen permeated across the biological membranes than the values achieved with the drug alone. Both achievements result from the higher solubility of the active pharmaceutical ingredients in the studied aqueous DES media, that allow a higher amount of drug available to be permeated, but also, from the permeation enhancer effect of the DES used.

These formulations have shown to strongly influence the properties of the delivery systems. For instance, in the development of the DES-based thermo-responsive microemulsions, it was shown that the studied DES improved the system's gelling properties. The adjustment of the DES concentration allowed to use a lower percentage of the *in situ* gelling polymer (PF-127) to achieve a higher viscosity than other microemulsions of this type, at ocular temperature. Furthermore,

it was shown that DES acted also as plasticizers of pullulan and alginate, resulting in biopolymer-based materials with improved mechanical properties, namely reducing the rigidity of the materials and allowing for flexible systems to be developed. These two systems were designed for topical and transdermal delivery purposes, in which their reduced stiffness allowed an easier adaptation to skin irregularities and maximization of the contact with the targeted area. More interestingly, the studied DES also provided additional properties to the biopolymer-based systems, notably, in the case of pullulan-based films, the studied DES provided higher adhesiveness to the material and a switchable character allowing it to change from a film to a highly adhesive hydrogel when in contact with skin moisture.

Overall, the impact of the studied DES on the drugs and on the delivery systems' properties was reflected on their performance and in the final therapeutic efficacy. DES aqueous solutions were capable of preserving the therapeutic action of the different active ingredients, but more importantly, regarding the antimicrobial agents, an increase in their action was verified. The susceptibility of Gram-negative and Gram-positive bacteria to the antibiotics is higher in the studied aqueous DES formulations than in water. The ability of these DES formulations to increase bacterial cell wall permeation allowed a higher antibiotics action. This might allow to decrease the drug dosages while providing the same therapeutic efficacy, thus decreasing the associated side-effects upon administration of higher doses. Furthermore, the DES formulations can be used without inducing the development of tolerance to the treatment or potentiate resistance mechanisms in bacteria. In fact, it was shown that when dealing with multidrug-resistant strains, delivery systems containing DES can act faster to eradicate bacterial infection than commercialized formulations (48 vs.72h). Moreover, the beneficial partnership of DES and biopolymers can even help active ingredients, such as photosensitizers, to have antimicrobial action against multidrug-resistant bacterial strains in *ex vivo* skin samples, when systems without these solvents cannot exert any effect.

All the described studies highlight the need to carefully select the DES components and their concentration to obtain a biocompatible drug delivery system. Since all the DES components were selected according with the administration

route, to minimize toxicity in the delivery site and given the selection of biocompatible biopolymers (such as pullulan and alginate), all presented low associated cytotoxicity (with cell viabilities > 80%).

The knowledge acquired with these studies also emphasizes the versatility of DES formulations, and that they can be combined with different active ingredients and directly incorporated in different material-based systems for distinct drug delivery purposes. This means a wide variety of opportunities for DES in the pharmaceutical field. Given the potential demonstrated so far, DES usage can envisage the development of more effective therapies and in the future their final approval in the pharmaceutical market.

Future work

However, there is still a significant path to follow until the complete understanding and adjustment of the use of DES in drug delivery systems. This knowledge will be fundamental for their full acceptance and pharmaceutical application.

DES application in the pharmaceutical context should be studied from simple to complex systems and, if possible, from *in vitro* to *in vivo* studies. When the gathered knowledge is sufficient, different animal models can be considered. These results will more easily prompt the pharmaceutical industry to accept these excipients and apply them in the new formulations. When considering the development of oral drug delivery systems, pharmacokinetic and pharmacodynamic studies are expected to be conducted.

In the future, more studies should be dedicated to understanding the mechanisms of solubilization in DES aqueous media, to allow the fast and easy selection of DES for a specific pharmaceutical application. Furthermore, stability studies concerning DES and active ingredients should probe for possible degradation products that can impact systemic safety.

Regarding the interaction of DES and other formulation components, insights into the molecular impact of DES should be assessed. For example, the parameters governing the influence of DES in the thermo-responsive behavior of polymers should be identified. Furthermore, the interaction of DES and biopolymers deserves

a more dedicated look, exploring the impact of the different DES in the distinct biopolymers. For this purpose, different combinations should be encouraged for the easier selection of both components in future drug delivery design.

Finally, the research of the effect of the DES in the therapeutic efficacy of active pharmaceutical ingredients should be a main goal. The different mechanisms by which DES improve the action of the different pharmacological classes of drugs must be enlightened to allow to tune and select the best mixture for the intended therapeutic purpose.

References

1. Lichtenberg, F. R. How many life-years have new drugs saved? A three-way fixed-effects analysis of 66 diseases in 27 countries, 2000-2013. *Int Health* **11,** 403–416 (2019).

2. Laermann-Nguyen, U. & Backfisch, M. Innovation crisis in the pharmaceutical industry? A survey. *SN Business & Economics* **1,** 164 (2021).

3. Scannell, J. W., Blanckley, A., Boldon, H. & Warrington, B. Diagnosing the decline in pharmaceutical R&D efficiency. *Nat Rev Drug Discov* **11,** 191–200 (2012).

4. Grabowski, H. The evolution of the pharmaceutical industry over the past 50 years: A personal reflection. *Int J Econ Bus* **18,** 161–176 (2011).

5. Sun, D., Gao, W., Hu, H. & Zhou, S. Why 90% of clinical drug development fails and how to improve it? *Acta Pharm Sin B,* **12,** 3049–3062 (2022).

6. Ayati, N., Saiyarsarai, P. & Nikfar, S. Short and long term impacts of COVID-19 on the pharmaceutical sector. *DARU J Pharm Sci*, **28,** 799-805 (2020).

7. Finding new formulas for pharma success. *Nat Rev Drug Discov* **6,** 423–423 (2007).

8. Wang, J., Peng, Y., Xu, H., Cui, Z. & Williams, R. O. The COVID-19 Vaccine Race: Challenges and Opportunities in Vaccine Formulation. *AAPS PharmSciTech* **21,** 225 (2020).

9. Sleigh, S. H. & Barton, C. L. Repurposing Strategies for Therapeutics. *Pharm Med* **24,** 151–159 (2010).

10. Al-Tawfiq, J. A., Momattin, H., Al-Ali, A. Y., Eljaaly, K., Tirupathi, R., Haradwala, M. B., Areti, S., Alhumaid, S., Rabaan, A. A., al Mutair, A. & Schlagenhauf, P. Antibiotics in the pipeline: a literature review (2017–2020). *Infection* **50,** 553–564 (2022).

11. Murray, C. J., *et al.* Global burden of bacterial antimicrobial resistance in 2019: a systematic analysis. *The Lancet* **399,** 629–655 (2022).

12. Prestinaci, F., Pezzotti, P. & Pantosti, A. Antimicrobial resistance: A global multifaceted phenomenon. *Pathog Glob Health* **109,** 309–318 (2015).

13. Butler, M. S., Blaskovich, M. A. & Cooper, M. A. Antibiotics in the clinical pipeline in 2013. *J Antibiot (Tokyo)* **66,** 571–591 (2013).

14. Smith, A. Screening for drug discovery: The leading question. *Nature* **418,** 453–455 (2002).

15. Steinmetz, K. L. & Spack, E. G. The basics of preclinical drug development for neurodegenerative disease indications. *BMC Neurol* **9,** S2 (2009).

16. Taylor, D. The pharmaceutical industry and the future of drug development. In: Issues in Environmental Science and Technology. *R Soc Chem* **41,** 1–33 (2016)

17. Brereton, N., Bodger, K., Kamm, M. A., Hodgkins, P., Yan, S. & Akehurst, R. A cost-effectiveness analysis of MMX mesalazine compared with mesalazine in the treatment of mild-to-moderate ulcerative colitis from a UK perspective. *J Med Econ* **13,** 148–161 (2010).

18. Guerrini, R. Valproate as a Mainstay of Therapy for Pediatric Epilepsy. *Pediatric Drugs* **8,** 113–129 (2006).

19. Verbaanderd, C., Rooman, I., Meheus, L. & Huys, I. On-label or off-label? overcoming regulatory and financial barriers to bring repurposed medicines to cancer patients. *Front Pharmacol* **10,** 1664 (2020).

20. Desai, M., Njoku, A. & Nimo-Sefah, L. Comparing Environmental Policies to Reduce Pharmaceutical Pollution and Address Disparities. *Int J Environ Res Public Health* **19,** 8292 (2022)

21. Sheldon, R. A. The E factor 25 years on: the rise of green chemistry and sustainability. *Green Chem* **19,** 18–43 (2017).

22. Schneider, J. L., Wilson, A. & Rosenbeck, J. M. Pharmaceutical companies and sustainability: An analysis of corporate reporting. *BIJ* **17,** 421–434 (2010).

23. Smith, E. L., Abbott, A. P. & Ryder, K. S. Deep Eutectic Solvents (DESs) and Their Applications. *Chem Rev* **114,** 11060–11082 (2014).

24. Agatemor, C., Ibsen, K. N., Tanner, E. E. L. & Mitragotri S. Ionic Liquids for Addressing Unmet Needs in Healthcare. *Bioeng Transl Med* **3,** 7–25 (2017).

25. Melo, C. I., Bogel-Łukasik, R., Nunes da Ponte, M. & Bogel-Łukasik, E. Ammonium ionic liquids as green solvents for drugs. *Fluid Phase Equilib* **338,** 209–216 (2013).

26. Silva, A. C. Q., Silvestre, A. J. D., Vilela, C. & Freire, C. S. R. Natural polymers-based materials: A contribution to a greener future. *Molecules* **27,** (2022).

27. Ayad, M. H. Rational formulation strategy from drug discovery profiling to human proof of concept. *Drug Deliv* **22,** 877–884 (2015).

28. Jones, T. M. Chapter 1. Preformulation Studies. In Pharmaceutical Formulation. *RSC Drug Discovery Series,* 1–20 (2018).

29. Kumar, V., Bansal, V., Madhavan, A., Kumar, M., Sindhu, R., Awasthi, M. K., Binod, P. & Saran, S. Active pharmaceutical ingredient (API) chemicals: a critical review of current biotechnological approaches. *Bioengineered* **13,** 4309–4327 (2022).

30. Adepu, S. & Ramakrishna, S. Controlled drug delivery systems: Current status and future directions. *Molecules* **26,** 5905 (2021)

31. van der Merwe, J., Steenekamp, J., Steyn, D. & Hamman, J. The role of functional excipients in solid oral dosage forms to overcome poor drug dissolution and bioavailability. *Pharmaceutics* **12,** 393 (2020)

32. Bhalani, D. v., Nutan, B., Kumar, A. & Singh Chandel, A. K. Bioavailability Enhancement Techniques for Poorly Aqueous Soluble Drugs and Therapeutics. *Biomedicines* **10,** 2055 (2022)

33. Nanda, K. K., Ginnetti, A. & Wuelfing, W. P. Base-Mediated Oxidative Degradation of Secondary Amides Derived from p-Amino Phenol to Primary Amides in Drug Molecules. *J Pharm Sci* **109,** 3394–3403 (2020).

34. *ICH Topic Q 1 A (R2) Stability Testing of new Drug Substances and Products*. (2003). Available at: https://www.ema.europa.eu/en/ich-q1a-r2-stability-testing-new-drug-substances-drug-products-scientific-guideline.

35. Blessy, M., Patel, R. D., Prajapati, P. N. & Agrawal, Y. K. Development of forced degradation and stability indicating studies of drugs — A review. *J Pharm Anal* **4,** 159–165 (2014).

36. Kračun, M., Kocijan, A., Bastarda, A., Grahek, R., Plavec, J. & Kocjan, D. Isolation and structure determination of oxidative degradation products of atorvastatin. *J Pharm Biomed Anal* **50,** 729–736 (2009).

37. Waterman, K. C., Adami, R. C., Alsante, K. M., Antipas, A. S., Arenson, D. R., Carrier, R., Hong, J., Landis, M. S., Lombardo, F., Shah, J. C., Shalaev, E., Smith, S. W. & Wang, H. Hydrolysis in Pharmaceutical Formulations. *Pharm Dev Technol* **7,** 113–146 (2002).

38. Lieberman, H. & Vemuri, N. M. Chemical and Physicochemical Approaches to Solve Formulation Problems. In The Practice of Medicinal Chemistry: Fourth Edition. *Academic Press*, 767–791 (2015).

39. Shamsipur, M., Pourmortazavi, S. M., Beigi, A. A. M., Heydari, R. & Khatibi, M. Thermal Stability and Decomposition Kinetic Studies of Acyclovir and Zidovudine Drug Compounds. *AAPS PharmSciTech* **14,** 287–293 (2013).

40. Ammann, C. Stability Studies Needed to Define the Handling and Transport Conditions of Sensitive Pharmaceutical or Biotechnological Products. *AAPS PharmSciTech* **12,** 1264–1275 (2011).

41. Ramos, P. & Broncel, M. Influence of Storage Conditions on the Stability of Gum Arabic and Tragacanth. *Molecules* **27,** 1510 (2022).

42. Ruggeri, G., Ghigo, G., Maurino, V., Minero, C. & Vione, D. Photochemical transformation of ibuprofen into harmful 4-isobutylacetophenone: Pathways, kinetics, and significance for surface waters. *Water Res* **47,** 6109–6121 (2013).

43. Yahya, A. M., McElnay, J. C. & D'Arcy, P. F. Photodegradation of frusemide during storage in burette administration sets. *Int J Pharm* **31,** 65–68 (1986).

44. Yamashita, S., Iguchi, K., Noguchi, Y., Sakai, C., Yokoyama, S., Ino, Y., Hayashi, H., Teramachi, H., Sako, M. & Sugiyama, T. Changes in the quality of medicines during storage under LED lighting and consideration of countermeasures. *J Pharm Health Care Sci* **4,** 12 (2018).

45. Deota, P. T., Upadhyay, P. R., Patel, K. B., Mehta, K. J., Varshney, A. K. & Mehta, M. H. Effect of Some Ultraviolet Light Absorbers on Photo-Stabilization of Azadirachtin-A. *Nat Prod Lett* **16,** 329–334 (2002).

46. Bayomi, M. A., Abanumay, K. A. & Al-Angary, A. A. *Effect of inclusion complexation with cyclodextrins on photostability of nifedipine in solid state. Int J Pharm* **243,** 107-117 (2002).

47. Ioele, G., Grande, F., de Luca, M., Occhiuzzi, M. A., Garofalo, A. & Ragno, G. Photodegradation of Anti-Inflammatory Drugs: Stability Tests and Lipid Nanocarriers for Their Photoprotection. *Molecules* **26,** 5989 (2021).

48. Gupta, S., Kesarla, R. & Omri, A. Formulation strategies to improve the bioavailability of poorly absorbed drugs with special emphasis on self-emulsifying systems. *ISRN Pharm* **2013,** 848043 (2013).

49. Savjani, K. T., Gajjar, A. K. & Savjani, J. K. Drug Solubility: Importance and Enhancement Techniques. *ISRN Pharm* **2012,** 195727 (2012).

50. Harirforoosh, S., Asghar, W. & Jamali, F. Adverse Effects of Nonsteroidal Antiinflammatory Drugs: An Update of Gastrointestinal, Cardiovascular and Renal Complications. *J Pharm & Pharm Sci* **16,** 821 (2014).

51. Irvine, J., Afrose, A. & Islam, N. Formulation and delivery strategies of ibuprofen: challenges and opportunities. *Drug Dev Ind Pharm* **44,** 173–183 (2018).

52. Chow, S. C. Bioavailability and bioequivalence in drug development. *Wiley Interdiscip Rev Comput Stat* **6,** 304–312 (2014).

53. Serajuddin, A. T. M. Salt formation to improve drug solubility. *Adv Drug Deliv Rev* **59,** 603–616 (2007).

54. Benet, T. The Role of BCS (Biopharmaceutics Classification System) and BDDCS (Biopharmaceutics Drug Disposition Classification System) in Drug Development. *J Pharm Sci* **102,** 34–42 (2014).

55. European Medicines Agency. *Committee for Medicinal Products for Human Use ICH M9 guideline on biopharmaceutics classification system-based biowaivers*. (2020). Available at: www.ema.europa.eu/contact.

56. Tsume, Y., Mudie, D. M., Langguth, P., Amidon, G. E. & Amidon, G. L. The Biopharmaceutics Classification System: Subclasses for in vivo predictive dissolution (IPD) methodology and IVIVC. *European Journal of Pharmaceutical Sciences* **57,** 152–163 (2014).

57. Markovic, M., Zur, M., Ragatsky, I., Cvijić, S. & Dahan, A. BCS Class IV Oral Drugs and Absorption Windows: Regional-Dependent Intestinal Permeability of Furosemide. *Pharmaceutics* **12,** 1175 (2020).

58. Constantinescu, T., Lungu, C. N. & Lung, I. Lipophilicity as a Central Component of Drug-Like Properties of Chalchones and Flavonoid Derivatives. *Molecules* **24,** 1505 (2019).

59. Bennion, B. J., Be, N. A., McNerney, M. W., Lao, V., Carlson, E. M., Valdez, C. A., Malfatti, M. A., Enright, H. A., Nguyen, T. H., Lightstone, F. C. & Carpenter, T. S. Predicting a Drug's Membrane Permeability: A Computational Model Validated With in Vitro Permeability Assay Data. *J Phys Chem B* **121,** 5228–5237 (2017).

60. Hopkins, A. L., Keserü, G. M., Leeson, P. D., Rees, D. C. & Reynolds, C. H. The role of ligand efficiency metrics in drug discovery. *Nat Rev Drug Discov* **13,** 105–121 (2014).

61. Arnott, J. A. & Planey, S. L. The influence of lipophilicity in drug discovery and design. *Expert Opin Drug Discov* **7,** 863–875 (2012).

62. Kokate, A., Li, X. & Jasti, B. Effect of Drug Lipophilicity and Ionization on Permeability Across the Buccal Mucosa: A Technical Note. *AAPS PharmSciTech* **9,** 501–504 (2008).

63. Alkilani, A., McCrudden, M. T. & Donnelly, R. Transdermal Drug Delivery: Innovative Pharmaceutical Developments Based on Disruption of the Barrier Properties of the Stratum Corneum. *Pharmaceutics* **7,** 438–470 (2015).

64. Dosmar, E., Walsh, J., Doyel, M., Bussett, K., Oladipupo, A., Amer, S. & Goebel, K. Targeting Ocular Drug Delivery: An Examination of Local Anatomy and Current Approaches. *Bioengineering* **9**, 41 (2022).

65. Souto, E. B., Fangueiro, J. F., Fernandes, A. R., Cano, A., Sanchez-Lopez, E., Garcia, M. L., Severino, P., Paganelli, M. O., Chaud, M. v. & Silva, A. M.

Physicochemical and biopharmaceutical aspects influencing skin permeation and role of SLN and NLC for skin drug delivery. *Heliyon* **8,** e08938 (2022).

66. Patel, A. Ocular drug delivery systems: An overview. *World J Pharmacol* **2,** 47 (2013).

67. Boddu, S. H., Gunda, S., Earla, R. & Mitra, A. K. Ocular microdialysis: a continuous sampling technique to study pharmacokinetics and pharmacodynamics in the eye. *Bioanalysis* **2,** 487–507 (2010).

68. Bachu, R. D., Chowdhury, P., Al-Saedi, Z. H. F., Karla, P. K. & Boddu, S. H. S. Ocular drug delivery barriers—role of nanocarriers in the treatment of anterior segment ocular diseases. *Pharmaceutics* **10,** 28 (2018)

69. Lallemand, F., Daull, P., Benita, S., Buggage, R. & Garrigue, J.-S. Successfully Improving Ocular Drug Delivery Using the Cationic Nanoemulsion, Novasorb. *J Drug Deliv* **2012,** 604204 (2012).

70. Zhou, Y., Li, L., Li, S., Li, S., Zhao, M., Zhou, Q., Gong, X., Yang, J. & Chang, J. Autoregenerative redox nanoparticles as an antioxidant and glycation inhibitor for palliation of diabetic cataracts. *Nanoscale* **11,** 13126–13138 (2019).

71. Nguyen, D. C. T., Dowling, J., Ryan, R., McLoughlin, P. & Fitzhenry, L. Pharmaceutical-loaded contact lenses as an ocular drug delivery system: A review of critical lens characterization methodologies with reference to ISO standards. *Contact Lens Anterior Eye* **44,** 101487 (2021).

72. van den Mooter, G. The use of amorphous solid dispersions: A formulation strategy to overcome poor solubility and dissolution rate. *Drug Discov Today Technol* **9,** e79–e85 (2012).

73. Seedher, N. & Kanojia, M. Co-solvent solubilization of some poorly-soluble antidiabetic drugs. *Pharm Dev Technol* **14,** 185–192 (2009).

74. Soares, B. P., Abranches, D. O., Sintra, T. E., Leal-Duaso, A., García, J. I., Pires, E., Shimizu, S., Pinho, S. P. & Coutinho, J. A. P. Glycerol Ethers as Hydrotropes and Their Use to Enhance the Solubility of Phenolic Acids in Water. *ACS Sustain Chem Eng* **8,** 5742–5749 (2020).

75. Bhalani, D. v., Nutan, B., Kumar, A. & Singh Chandel, A. K. Bioavailability Enhancement Techniques for Poorly Aqueous Soluble Drugs and Therapeutics. *Biomedicines* **10,** 2055 (2022).

76. Vargason, A. M., Anselmo, A. C. & Mitragotri, S. The evolution of commercial drug delivery technologies. *Nat Biomed Eng* **5,** 951–967 (2021).

77. Khan, K. U., Minhas, M. U., Badshah, S. F., Suhail, M., Ahmad, A. & Ijaz, S. Overview of nanoparticulate strategies for solubility enhancement of poorly soluble drugs. *Life Sci* **291,** 120301 (2022).

78. Jelveghari, M. & Nokhodchi, A. Development and Chemical Stability Studies of Alcohol-Free Phenobarbital Solution for Use in Pediatrics: a Technical Note. *AAPS PharmSciTech* **9,** 939 (2008).

79. Sajedi-Amin, S., Barzegar-Jalali, M., Fathi-Azarbayjani, A., Kebriaeezadeh, A., Martínez, F. & Jouyban, A. Solubilization of bosentan using ethanol as a pharmaceutical cosolvent. *J Mol Liq* **232,** 152–158 (2017).

80. Nayak, A. K. & Panigrahi, P. P. Solubility Enhancement of Etoricoxib by Cosolvency Approach. *ISRN Physical Chemistry* **2012,** 820653 (2012).

81. Baracaldo-Santamaría, D., Calderon-Ospina, C. A., Ortiz, C. P., Cardenas-Torres, R. E., Martinez, F. & Delgado, D. R. Thermodynamic Analysis of the Solubility of Isoniazid in (PEG 200 + Water) Cosolvent Mixtures from 278.15 K to 318.15 K. *Int J Mol Sci* **23,** 10190 (2022).

82. Soares, B., Silvestre, A. J. D., Rodrigues Pinto, P. C., Freire, C. S. R. & Coutinho, J. A. P. Hydrotropy and Cosolvency in Lignin Solubilization with Deep Eutectic Solvents. *ACS Sustain Chem Eng* **7,** 12485-12493 (2019).

83. Abranches, D. O., Benfica, J., Soares, B. P., Leal-Duaso, A., Sintra, T. E., Pires, E., Pinho, S. P., Shimizu, S. & Coutinho, J. A. P. Unveiling the mechanism of hydrotropy: evidence for water-mediated aggregation of hydrotropes around the solute. *Chem Comm* **56,** 7143–7146 (2020).

84. Sekiguchi, K. & Obi, N. Studies on Absorption of Eutectic Mixture. I. A Comparison of the Behavior of Eutectic Mixture of Sulfathiazole and that of Ordinary Sulfathiazole in Man. *Chem Pharm Bull (Tokyo)* **9,** 866–872 (1961).

85. Araya-Sibaja, A. M., Vega-Baudrit, J. R., Guillén-Girón, T., Navarro-Hoyos, M. & Cuffini, S. L. Drug solubility enhancement through the preparation of multicomponent organic materials: Eutectics of lovastatin with carboxylic acids. *Pharmaceutics* **11,** 112 (2019).

86. Parveen, F., Madni, A., Torchilin, V. P., Rehman, M., Jamshaid, T., Filipczak, N., Rai, N., Khan, M. M. & Khan, M. I. Investigation of Eutectic Mixtures of Fatty Acids as a Novel Construct for Temperature-Responsive Drug Delivery. *Int J Nanomedicine* **17,** 2413–2434 (2022).

87. Marwah, H., Garg, T., Goyal, A. K. & Rath, G. Permeation enhancer strategies in transdermal drug delivery. *Drug Deliv* **23,** 564–578 (2016).

88. Ahad, A., Aqil, M., Kohli, K., Sultana, Y., Mujeeb, M. & Ali, A. Role of novel terpenes in transcutaneous permeation of valsartan: effectiveness and mechanism of action. *Drug Dev Ind Pharm* **37,** 583–596 (2011).

89. Gupta, R., Badhe, Y., Rai, B. & Mitragotri, S. Molecular mechanism of the skin permeation enhancing effect of ethanol: a molecular dynamics study. *RSC Adv* **10,** 12234–12248 (2020).

90. Som, I., Bhatia, K. & Yasir, M. Status of surfactants as penetration enhancers in transdermal drug delivery. *J Pharm Bioallied Sci* **4,** 2-9 (2012).

91. Morrison, P. W. J. & Khutoryanskiy, V. v. Enhancement in corneal permeability of riboflavin using calcium sequestering compounds. *Int J Pharm* **472,** 56–64 (2014).

92. Burgalassi, S., Chetoni, P., Monti, D. & Fabrizio Saettone, M. Cytotoxicity of potential ocular permeation enhancers evaluated on rabbit and human corneal epithelial cell lines. *Toxicol Lett* **122,** 1-8 (2001).

93. Morrison, P. W. J., Connon, C. J. & Khutoryanskiy, V. v. Cyclodextrin-Mediated Enhancement of Riboflavin Solubility and Corneal Permeability. *Mol Pharm* **10,** 756–762 (2013).

94. Kikuchi, T., Suzuki, M., Kusai, A., Iseki, K. & Sasaki, H. Synergistic effect of EDTA and boric acid on corneal penetration of CS-088. *Int J Pharm* **290,** 83–89 (2005).

95. Pescina, S., Sala, M., Padula, C., Scala, M. C., Spensiero, A., Belletti, S., Gatti, R., Novellino, E., Campiglia, P., Santi, P., Nicoli, S. & Ostacolo, C. Design and Synthesis of New Cell Penetrating Peptides: Diffusion and Distribution Inside the Cornea. *Mol Pharm* **13,** 3876–3883 (2016).

96. da Fonseca Antunes, A. B., de Geest, B. G., Vervaet, C. & Remon, J. P. Gelucire 44/14 based immediate release formulations for poorly water-soluble drugs. *Drug Dev Ind Pharm* **39,** 791–798 (2013).

97. Bolla, P. K., Clark, B. A., Juluri, A., Cheruvu, H. S. & Renukuntla, J. Evaluation of Formulation Parameters on Permeation of Ibuprofen from Topical Formulations Using Strat-M® Membrane. *Pharmaceutics* **12,** 151 (2020).

98. Brodin, a., Nyqvist-Mayer, a., Broberg, F., Wadsten, T. & Forslund, B. Phase diagram and aqueous solubility of the lidocaine-prilocaine binary system. *J Pharm Sci* **73,** 481–484 (1984).

99. Ehrenström-Reiz G., Reiz S., S. O. Topical Anaesthesia with EMLA, a New Lidocaine-Prilocaine Cream and the Cusum Technique for Detection of Minimal Application Time. *Acta Anaesthesiol Scand* **27,** 510–512 (1983).

100. Ohzeki, K., Kitahara, M., Suzuki, N., Taguchi, K., Yamazaki, Y., Akiyama, S., Takahashi, K. & Kanzaki, Y. Local anesthetic cream prepared from lidocaine-tetracaine eutectic mixture. *Yakugaku Zasshi* **128,** 611–616 (2008).

101. Gala, U., Chuong, M. C., Varanasi, R. & Chauhan, H. Characterization and Comparison of Lidocaine-Tetracaine and Lidocaine-Camphor Eutectic Mixtures Based on Their Crystallization and Hydrogen-Bonding Abilities. *AAPS PharmSciTech* **16,** 528–536 (2015).

102. Wang, W., Cai, Y., Liu, Y., Zhao, Y., Feng, J. & Liu, C. Microemulsions based on paeonol-menthol eutectic mixture for enhanced transdermal delivery: formulation development and in vitro evaluation. *Artif Cells Nanomed Biotechnol* **45,** 1241–1246 (2017).

103. Martins, M. A. R., Pinho, S. P. & Coutinho, J. A. P. Insights into the Nature of Eutectic and Deep Eutectic Mixtures. *J Solution Chem* 48, 962-982 (2018).

104. Abbott, A. P., Capper, G., Davies, D. L., Rasheed, R. K. & Tambyrajah, V. Novel solvent properties of choline chloride/urea mixtures. *Chem Comm* 70–71 (2003).

105. Peng, Y., Lu, X., Liu, B. & Zhu, J. Separation of azeotropic mixtures (ethanol and water) enhanced by deep eutectic solvents. *Fluid Phase Equilib* **448,** 128–134 (2017).

106. Abranches, D. O. & Coutinho, J. A. P. Type V deep eutectic solvents: Design and applications. *Curr Opin Green Sustain Chem* **35,** 100612 (2022).

107. Wang, J., Li, M., Duan, L., Lin, Y., Cui, X., Yang, Y. & Wang, C. Deep Eutectic Systems as Novel Vehicles for Assisting Drug Transdermal Delivery. *Pharmaceutics* **14,** 2265 (2022).

108. Aroso, I. M., Craveiro, R., Rocha, Â., Dionísio, M., Barreiros, S., Reis, R. L., Paiva, A. & Duarte, A. R. C. Design of controlled release systems for THEDES - Therapeutic deep eutectic solvents, using supercritical fluid technology. *Int J Pharm* **492,** 73–79 (2015).

109. Mokhtarpour, M., Shekaari, H., Zafarani-moattar, M. T. & Golgoun, S. Solubility and solvation behavior of some drugs in choline based deep eutectic solvents at different temperatures. *J Mol Liq* 111799 (2019).

110. Lu, C., Cao, J., Wang, N. & Su, E. Significantly improving the solubility of non-steroidal anti-inflammatory drugs in deep eutectic solvents for potential non-aqueous liquid administration. *MedChemComm* **7,** 955–959 (2016).

111. Abbott, A. P., Ahmed, E. I., Prasad, K., Qader, I. B. & Ryder, K. S. Liquid pharmaceuticals formulation by eutectic formation. *Fluid Phase Equilib* **448,** 2–8 (2017).

112. Aroso, I. M., Silva, J. C., Mano, F., Ferreira, A. S. D., Dionísio, M., Sá-Nogueira, I., Barreiros, S., Reis, R. L., Paiva, A. & Duarte, A. R. C. Dissolution enhancement of active pharmaceutical ingredients by therapeutic deep eutectic systems. *Eur J Pharma and Biopharma* **98,** 57–66 (2016).

113. Silva, J. M. M., Reis, R. L., Paiva, A., Rita, A. & Duarte, C. Design of functional therapeutic deep eutectic solvents based on choline chloride and ascorbic acid. *ACS Sustainable Chem Eng.* **6**, 10355-10363 (2018).

114. Mota-Morales, J. D., Gutiérrez, M. C., Ferrer, M. L., Sanchez, I. C., Elizalde-Peña, E. a., Pojman, J. a., Monte, F. del & Luna-Bárcenas, G. Deep eutectic solvents as both active fillers and monomers for frontal polymerization. *J Polym Sci A Polym Chem* **51,** 1767–1773 (2013).

115. Palmelund, H., Andersson, M. P., Asgreen, C. J., Boyd, B. J. & Rantanen, J. Tailor-made solvents for pharmaceutical use? Experimental and computational approach for determining solubility in deep eutectic solvents. *Int J Pharm X* **1,** 100034 (2019).

116. Abbott, A. P., Boothby, D., Capper, G., Davies, D. L. & Rasheed, R. K. Deep Eutectic Solvents formed between choline chloride and carboxylic acids: Versatile alternatives to ionic liquids. *J Am Chem Soc* **126,** 9142–9147 (2004).

117. Wang, H., Liu, S., Zhao, Y., Wang, J. & Yu, Z. Insights into the Hydrogen Bond Interactions in Deep Eutectic Solvents Composed of Choline Chloride and Polyols. *ACS Sustain Chem Eng* **7,** 7760–7767 (2019).

118. Farooq, M. Q., Abbasi, N. M. & Anderson, J. L. Deep eutectic solvents in separations: Methods of preparation, polarity, and applications in extractions and capillary electrochromatography. *J Chromatogr A* **1633,** 461613 (2020).

119. Alhadid, A., Mokrushina, L. & Minceva, M. Influence of the molecular structure of constituents and liquid phase non-ideality on the viscosity of deep eutectic solvents. *Molecules* **26,** 4208 (2021).

120. Cunha, S. C. & Fernandes, J. O. Extraction techniques with deep eutectic solvents. *TrAC Trends in Anal Chem* **105,** 225–239 (2018).

121. Sarmad, S., Xie, Y., Mikkolab, J., & Ji, X. Screening of Deep Eutectic Solvents (DESs) as green CO2 sorbents: from solubility to viscosity. *New J Chem* 41, 290–301 (2017).

122. Grodowska, K. Parczewski, A. Organic Solvents in the Pharmaceutcal Industry. *Polish Pharmaceutical Society* **67,** 3–12 (2010).

123. Sousa, A. M. M., Souza, H. K. S., Uknalis, J., Liu, S. C., Gonçalves, M. P. & Liu, L. S. Improving agar electrospinnability with choline-based deep eutectic solvents. *Int J Biol Macromol* **80,** 139–148 (2015).

124. Sharma, M., Mukesh, C., Mondal, D. & Prasad, K. Dissolution of α-chitin in deep eutectic solvents. *RSC Adv* **39,** 18149 (2013).

125. Pontillo, A. R. N., Koutsoukos, S., Welton, T. & Detsi, A. Investigation of the influence of natural deep eutectic solvents (NaDES) in the properties of chitosan-stabilised films. *Mater Adv* **2,** 3954–3964 (2021).

126. Emami, S. & Shayanfar, A. Deep eutectic solvents for pharmaceutical formulation and drug delivery applications. *Pharm Dev Technol* **25,** 779–796 (2020).

127. Abranches, D. O., Larriba, M., Silva, L. P., Melle-Franco, M., Palomar, J. F., Pinho, S. P. & Coutinho, J. A. P. Using COSMO-RS to design choline chloride pharmaceutical eutectic solvents. *Fluid Phase Equilib* **497,** 71–78 (2019).

128. Morrison, H. G., Sun, C. C. & Neervannan, S. Characterization of thermal behavior of deep eutectic solvents and their potential as drug solubilization vehicles. *Int J Pharm* **378,** 136–139 (2009).

129. Trombino, S., Siciliano, C., Procopio, D., Curcio, F., Laganà, A. S., di Gioia, M. L. & Cassano, R. Deep Eutectic Solvents for Improving the Solubilization and Delivery of Dapsone. *Pharmaceutics* **14,** 333 (2022).

130. Pascual-Fernández, L., Giner, B. & San Jorge, U. Enhancing the Solubility of Active Pharmaceutical Ingredients using Deep Eutectic Solvents to Develop Liquid Oral Formulations. (2022).

131. Faggian, M., Sut, S., Perissutti, B., Baldan, V., Grabnar, I. & Dall'Acqua, S. Natural Deep Eutectic Solvents (NADES) as a tool for bioavailability improvement: Pharmacokinetics of rutin dissolved in proline/glycine after oral administration in rats: Possible application in nutraceuticals. *Molecules* **21,** 1531 (2016).

132. Sut, S., Faggian, M., Baldan, V., Poloniato, G., Castagliuolo, I., Grabnar, I., Perissutti, B., Brun, P., Maggi, F., Voinovich, D., Peron, G. & Dall'Acqua, S. Natural Deep Eutectic Solvents (NADES) to Enhance Berberine Absorption: An In Vivo Pharmacokinetic Study. *Molecules* **22,** 1921 (2017).

133. Nerurkar, J., Beach, J. W., Park, M. O. & Jun, H. W. Solubility of (±)-Ibuprofen and S (+)-Ibuprofen in the Presence of Cosolvents and Cyclodextrins. *Pharm Dev Technol* **10,** 413–421 (2005).

134. Li, Z. & Lee, P. I. Investigation on drug solubility enhancement using deep eutectic solvents and their derivatives. *Int J Pharm* **505,** 283–288 (2016).

135. Phaechamud, T., Tuntarawongsa, S. & Charoensuksai, P. Evaporation Behavior and Characterization of Eutectic Solvent and Ibuprofen Eutectic Solution. *AAPS PharmSciTech* **17,** 1213–1220 (2016).

136. Jeliński, T., Przybyłek, M. & Cysewski, P. Natural Deep Eutectic Solvents as Agents for Improving Solubility, Stability and Delivery of Curcumin. *Pharm Res* **36,** 116 (2019).

137. Stott, P. W., Williams, A. C. & Barry, B. W. Transdermal delivery from eutectic systems: Enhanced permeation of a model drug, ibuprofen. *J Control Release* **50,** 297–308 (1998).

138. Silva, J. M., Silva, E., Reis, R. L. & Duarte, A. R. C. A closer look in the antimicrobial properties of deep eutectic solvents based on fatty acids. *Sustain Chem Pharm* **14,** 100192 (2019).

139. Chang, P. C., Goresky, G. v., O'Connor, G., Pyesmany, D. A., Rogers, P. C. J., Steward, D. J. & Stewart, J. A. A multicentre randomized study of single-unit dose package of EMLA patch vs EMLA 5% cream for venepuncture in children. *Can J Anaesth* **41,** 59–63 (1994).

140. Al-akayleh, F., Hani, H., Ali, M., Ghareeb, M. M. & Al-remawi, M. Therapeutic deep eutectic system of capric acid and menthol: Characterization and pharmaceutical application. *J Drug Deliv Sci Technol* **53,** 101159 (2019).

141. Olivares, B., Martínez, F., Rivas, L., Calde, C., Munita, J. M. & Campodonico, P. R. A Natural Deep Eutectic Solvent Formulated to Stabilize β -Lactam Antibiotics. *Sci Rep* **8**, 14900 (2018).

142. Wikene, K. O., Bruzell, E. & Tonnesen, H. H. Improved antibacterial phototoxicity of a neutral porphyrin in natural deep eutectic solvents. *J Photochem Photobiol B* **148,** 188–196 (2015).

143. Daneshjou, S., Khodaverdian, S., Dabirmanesh, B., Rahimi, F., Daneshjoo, S., Ghazi, F. & Khajeh, K. Improvement of chondroitinases ABCI stability in natural deep eutectic solvents. *J Mol Liq* **227,** 21–25 (2017).

144. Min, A., Lee, S., Lee, K., Nam, M. W., Jeong, M., Lee, J. E., Kim, N. W., Yin, Y. & Yeon, S. Natural deep eutectic solvents as a storage medium for human interferon-α2: a green and improved strategy for room-temperature biologics Authors: *J Ind Eng Chem* **65,** 343–348 (2018).

145. Ladeira, B. M. F., Dias, C. J., Gomes, A. T. P. C., Tom, A. C., Neves, M. G. P. M. S., Moura, N. M. M., Almeida, A. & Faustino, M. A. F. Cationic Pyrrolidine/Pyrroline-Substituted Porphyrins as Efficient Photosensitizers against E. coli. *Molecules* **26,** 464 (2021).

146. Alejandra, D., Méndez, C., Gutierres, E., Dionisio, E. J., Afonso, M., Buzalaf, R., Oliveira, R. C., Aparecida, M., Moreira, A. & Cruvinel, T. Curcumin-mediated Antimicrobial Photodynamic Therapy reduces the viability and vitality of infected dentin caries microcosms. *Photodiagnosis Photodyn Ther* **24,** 102–108 (2018).

147. Leader, B., Baca, Q. J. & Golan, D. E. Protein therapeutics: a summary and pharmacological classification. *Nat Rev Drug Discov* **7,** 21–39 (2008).

148. Halder, A. K. & Cordeiro, M. N. D. S. Probing the Environmental Toxicity of Deep Eutectic Solvents and Their Components: An In Silico Modeling Approach. *ACS Sustain Chem Eng* **7,** 10649–10660 (2019).

149. Lapeña, D., Errazquin, D., Lomba, L., Lafuente, C. & Giner, B. Ecotoxicity and biodegradability of pure and aqueous mixtures of deep eutectic solvents: glyceline, ethaline, and reline. *Environ Sci Pollut Res* **28,** 8812–8821 (2021).

150. Zhao, B. Y., Xu, P., Yang, F. X., Wu, H., Zong, M. H. & Lou, W. Y. Biocompatible Deep Eutectic Solvents Based on Choline Chloride: Characterization and Application to the Extraction of Rutin from Sophora japonica. *ACS Sustain Chem Eng* **3,** 2746–2755 (2015).

151. Radošević, K., Čanak, I., Panić, M., Markov, K., Bubalo, M. C., Frece, J., Screk, V. G. & Redovniković, R. Antimicrobial, cytotoxic and antioxidative evaluation of natural deep eutectic solvents. *Environmental Science and Pollution Research* **25,** 14188–14196 (2018).

152. Juneidi, I., Hayyan, M. & Mohd Ali, O. Toxicity profile of choline chloride-based deep eutectic solvents for fungi and Cyprinus carpio fish. *Environ Sci Pollut Res* **23,** 7648–7659 (2016).

153. Hayyan, M., Looi, C. Y., Hayyan, A. & Wong, W. F. In Vitro and In Vivo Toxicity Profiling of Ammonium-Based Deep Eutectic Solvents. *PLoS One* **10,** 1–18 (2015).

154. Hayyan, M., Mbous, Y. P., Looi, C. Y., Wong, W. F., Hayyan, A., Salleh, Z. & Mohd-Ali, O. Natural deep eutectic solvents: cytotoxic profile. *Springerplus* **5,** 913 (2016).

155. Mbous, Y. P., Hayyan, M., Wong, W. F., Looi, C. Y. & Hashim, M. A. Unraveling the cytotoxicity and metabolic pathways of binary natural deep eutectic solvent systems. *Sci Rep* **7,** 41257 (2017).

156. Ferreira, I. J., Meneses, L., Paiva, A., Diniz, M. & Duarte, A. R. C. Assessment of deep eutectic solvents toxicity in zebrafish (Danio rerio). *Chemosphere* **299,** 134415 (2022).

157. Jung, D., Jung, J. B., Kang, S., Li, K., Hwang, I., Jeong, J. H., Kim, H. S. & Lee, J. Toxico-metabolomics study of a deep eutectic solvent comprising choline chloride and urea suggests in vivo toxicity involving oxidative stress and ammonia stress. *Green Chem* **23,** 1300–1311 (2021).

158. Radošević, K., Čurko, N., Screk, V. G., Bubalo, M. C., Tomašević, M., Ganić, K. K., Redovniković, I. R. Natural deep eutectic solvents as beneficial extractants for enhancement of plant extracts bioactivity. *LWT* **73,** 45–51 (2016).

159. Torregrosa-Crespo, J., Marset, X., Guillena, G., Ramón, D. J. & María Martínez-Espinosa, R. New guidelines for testing "Deep eutectic solvents" toxicity and their effects on the environment and living beings. *Scie Total Environ* **704,** 135382 (2020).

160. Vargason, A. M., Anselmo, A. C. & Mitragotri, S. The evolution of commercial drug delivery technologies. *Nat Biomed Eng* **5,** 951–967 (2021).

161. Lee, P. I. & Li, J.-X. in *Oral Controlled Release Formulation Design and Drug Delivery* 21–31 (2010).

162. Laffleur, F. & Keckeis, V. Advances in drug delivery systems: Work in progress still needed? *Int J Pharm* **590,** 119912 (2020).

163. Abdelkader, H., Fathalla, Z., Seyfoddin, A., Farahani, M., Thrimawithana, T., Allahham, A., Alani, A. W. G., Al-Kinani, A. A. & Alany, R. G. Polymeric long-acting drug delivery systems (LADDS) for treatment of chronic diseases: Inserts, patches, wafers, and implants. *Adv Drug Deliv Rev* **177,** 113957 (2021)

164. Tiwari, G., Tiwari, R., Bannerjee, S., Bhati, L., Pandey, S., Pandey, P. & Sriwastawa, B. Drug delivery systems: An updated review. *Int J Pharm Investig* **2,** 2-11 (2012).

165. Priyadarshi, R., Roy, S., Purohit, S. D. & Ghosh, T. Biopolymers for Food Packaging and Biomedical Applications: Options or Obligations? *Coatings* **12,** 1261 (2022).

166. Liechty, W. B., Kryscio, D.R., Slaughter, B. V. and Peppas, N. A. Polymers for drug delivery systems. *Annu. Rev. Chem. Biomol. Eng.* **1,** 149–173 (2010).

167. Park, K. Controlled drug delivery systems: Past forward and future back. *Journal of Controlled Release* **190,** 3–8 (2014).

168. Vinarov, Z., *et al*. Impact of gastrointestinal tract variability on oral drug absorption and pharmacokinetics: An UNGAP review. *Eur J Pharma Sci* **162,** 105812 (2021).

169. Prausnitz, M. R. & Langer, R. Transdermal drug delivery. *Nat Biotechnol* **26,** 1261–1268 (2008).

170. Yun, Y. H., Lee, B. K. & Park, K. Controlled Drug Delivery: Historical perspective for the next generation. *J Control Release* **219,** 2–7 (2015).

171. te Kulve, H. Anticipating Market Introduction of Nanotechnology-Enabled Drug Delivery Systems, In Application of Nanotechnology in Drug Delivery*, IntechOpen* (2014).

172. Singh, R. & Lillard, J. W. Nanoparticle-based targeted drug delivery. *Exp Mol Pathol* **86,** 215–223 (2009).

173. Zainal-Abidin, M. H., Hayyan, M., Ngoh, G. C., Wong, W. F. & Looi, C. Y. Emerging frontiers of deep eutectic solvents in drug discovery and drug delivery systems. *J Control Release* **316,** 168–195 (2019).

174. Huang, C., Chen, X., Wei, C., Wang, H. & Gao, H. Deep Eutectic Solvents as Active Pharmaceutical Ingredient Delivery Systems in the Treatment of Metabolic Related Diseases. *Front Pharmacol* **12,** (2021).

175. Wang, J., Li, M., Duan, L., Lin, Y., Cui, X., Yang, Y. & Wang, C. Deep Eutectic Systems as Novel Vehicles for Assisting Drug Transdermal Delivery. *Pharmaceutics* **14,** 2265 (2022).

176. Gad, S. C. Pharmaceutical Manufacturing Handbook: Production and Processes. *John Wiley & Sons, Inc.* 314–316 (2008).

177. Adepu, S. & Ramakrishna, S. Controlled Drug Delivery Systems: Current Status and Future Directions. *Molecules* **26,** 5905 (2021).

178. Patra, J. K., Das, G., Fraceto, L. F., Campos, E. V. R., Rodriguez-Torres, M. del P., Acosta-Torres, L. S., Diaz-Torres, L. A., Grillo, R., Swamy, M. K., Sharma, S., Habtemariam, S. & Shin, H.-S. Nano based drug delivery systems: recent developments and future prospects. *J Nanobiotechnology* **16,** 71 (2018).

179. Hegde, R. R., Verma, A. & Ghosh, A. Microemulsion: New Insights into the Ocular Drug Delivery. *ISRN Pharm* **2013,** 826798 (2013).

180. Colucci, G., Santamaria-Echart, A., Silva, S. C., Fernandes, I. P. M., Sipoli, C. C. & Barreiro, M. F. Development of Water-in-Oil Emulsions as Delivery Vehicles and Testing with a Natural Antimicrobial Extract. *Molecules* **25,** 2105 (2020).

181. Chen, B., Hou, M., Zhang, B., Liu, T., Guo, Y., Dang, L. & Wang, Z. Enhancement of the solubility and antioxidant capacity of α-linolenic acid using an oil in water microemulsion. *Food Funct* **8,** 2792–2802 (2017).

182. Sharma, A. K., Garg, T., Goyal, A. K. & Rath, G. Role of microemuslsions in advanced drug delivery. *Artif Cells Nanomed Biotechnol* **44,** 1–9 (2015).

183. Bjerregaard, S., Pedersen, H., Vedstesen, H., Vermehren, C., Sö Derberg B, I. & Frokjaer, S. Parenteral water/oil emulsions containing hydrophilic compounds with enhanced in vivo retention: formulation, rheological characterisation and study of in vivo fate using whole body gamma-scintigraphy. *Int J Pharm* **215,** 13-27 (2001).

184. Guzmán, E., Fernández-Peña, L., Rossi, L., Bouvier, M., Ortega, F. & Rubio, R. G. Nanoemulsions for the Encapsulation of Hydrophobic Actives. *Cosmetics* **8,** 45 (2021).

185. Mundada, A. S. & Avari, J. G. In Situ Gelling Polymers in Ocular Drug Delivery Systems: A Review. *Crit Rev Ther Drug Carrier Syst* **26,** 85–118 (2009).

186. Dou, Q., Karim, A. A. & Loh, X. J. Modification of thermal and mechanical properties of PEG-PPG-PEG copolymer (F127) with MA-POSS. *Polymers* **8,** 341 (2016).

187. Chowhan, A. & Giri, T. K. Polysaccharide as renewable responsive biopolymer for in situ gel in the delivery of drug through ocular route. *Int J Biol Macromol* **150,** 559–572 (2020).

188. Nazar, M. F., Khan, A. M. & Shah, S. S. Microemulsion System with Improved Loading of Piroxicam: A Study of Microstructure. *AAPS PharmSciTech* **10,** 1286-1294 (2009).

189. Aliberti, A. L. M., de Queiroz, A. C., Praça, F. S. G., Eloy, J. O., Bentley, M. V. L. B. & Medina, W. S. G. Ketoprofen Microemulsion for Improved Skin Delivery and In Vivo Anti-inflammatory Effect. *AAPS PharmSciTech* **18,** 2783–2791 (2017).

190. Hegde, R. R., Bhattacharya, S. S., Verma, A. & Ghosh, A. Physicochemical and pharmacological investigation of water/oil microemulsion of non-selective beta blocker for treatment of glaucoma. *Curr Eye Res* **39,** 155–163 (2014).

191. Almeida, H., Lobão, P., Frigerio, C., Fonseca, J., Silva, R., Manuel, J., Lobo, S., Amaral, M. H., Preparation, characterization and biocompatibility studies of thermoresponsive eyedrops based on the combination of nanostructured lipid carriers (NLC) and the polymer Pluronic F-127 for controlled delivery of ibuprofen Preparation , characterization a. *Pharm Dev Technol* **22,** 336-349 (2015).

192. Souza, J. G., Dias, K., Pereira, T. A., Bernardi, D. S. & Lopez, R. F. v. Topical delivery of ocular therapeutics: carrier systems and physical methods. *J Pharm Pharmacol* **66,** 507–530 (2014).

193. Dhingra, D., Behera, K., Bhawna & Pandey, S. Formation of water-in-oil microemulsions within a hydrophobic deep eutectic solvent. *Phys Chem Chem Phys* **17,** 10629–10635 (2021).

194. Supaweera, N., Chulrik, W., Jansakun, C., Bhoopong, P., Yusakul, G. & Chunglok, W. Therapeutic deep eutectic solvent-based microemulsion enhances anti-inflammatory efficacy of curcuminoids and aromatic-turmerone extracted from Curcuma longa L. *RSC Adv* **12,** 25912–25922 (2022).

195. Almoshari, Y. Novel Hydrogels for Topical Applications: An Updated Comprehensive Review Based on Source. *Gels* **8,** 174 (2022).

196. Aravamudhan, A., Ramos, D. M., Nada, A. A. & Kumbar, S. G. Natural Polymers: Polysaccharides and Their Derivatives for Biomedical Applications, In Natural and Synthetic Biomedical Polymers. *Elsevier*, 67–89 (2014).

197. Lee, H.-R., Jung, S. M., Yoon, S., Yoon, W. H., Park, T. H., Kim, S., Shin, H. W., Hwang, D. S. & Jung, S. Immobilization of planktonic algal spores by inkjet printing. *Sci Rep* **9,** 12357 (2019).

198. Campo, V. L., Kawano, D. F., Silva, D. B. da & Carvalho, I. Carrageenans: Biological properties, chemical modifications and structural analysis – A review. *Carbohydr Polym* **77,** 167–180 (2009).

199. Malafaya, P. B., Silva, G. A. & Reis, R. L. Natural–origin polymers as carriers and scaffolds for biomolecules and cell delivery in tissue engineering applications. *Adv Drug Deliv Rev* **59,** 207–233 (2007).

200. Pal, K., Paulson, A. T. & Rousseau, D. Biopolymers in Controlled-Release Delivery Systems. In Modern Biopolymer Science. *Academic Press*, 519-557 (2009).

201. Abasalizadeh, F., Moghaddam, S. V., Alizadeh, E., akbari, E., Kashani, E., Fazljou, S. M. B., Torbati, M. & Akbarzadeh, A. Alginate-based hydrogels as drug delivery vehicles in cancer treatment and their applications in wound dressing and 3D bioprinting. *J Biol Eng* **14,** 8 (2020).

202. Fonseca, D. F. S., Carvalho, J. P. F., Bastos, V., Oliveira, H., Moreirinha, C., Almeida, A., Silvestre, A. J. D., Vilela, C. & Freire, C. S. R. Antibacterial multi-layered nanocellulose-based patches loaded with dexpanthenol for wound healing applications. *Nanomaterials* **10,** 2469 (2020).

203. Carvalho, T., Guedes, G., Sousa, F. L., Freire, C. S. R. & Santos, H. A. Latest Advances on Bacterial Cellulose-Based Materials for Wound Healing, Delivery Systems, and Tissue Engineering. *Biotechnol J* **14,** 1900059 (2019).

204. Troncoso, O. P. & Torres, F. G. Non-conventional starch nanoparticles for drug delivery applications. *Med Devices Sens* **3,** e10111 (2020).

205. Lauto, A., Mawad, D., Barton, M., Gupta, A., Piller, S. C. & Hook, J. Photochemical tissue bonding with chitosan adhesive films. *Biomed Eng Online* **9**, 47 (2010).

206. Kicková, E., Sadeghi, A., Puranen, J., Tavakoli, S., Sen, M., Ranta, V.-P., Arango-Gonzalez, B., Bolz, S., Ueffing, M., Salmaso, S., Caliceti, P., Toropainen, E., Ruponen, M. & Urtti, A. Pharmacokinetics of Pullulan–Dexamethasone Conjugates in Retinal Drug Delivery. *Pharmaceutics* **14,** 12 (2021).

207. Gopi, S. & Amalraj, A. Effective Drug Delivery System of Biopolymers Based On Nanomaterials and Hydrogels - A Review. *Drug Des* **5,** (2016).

208. Thu, H.-E., Zulfakar, M. H. & Ng, S.-F. Alginate based bilayer hydrocolloid films as potential slow-release modern wound dressing. *Int J Pharm* **434,** 375–383 (2012).

209. Karki, S., Kim, H., Na, S. J., Shin, D., Jo, K. & Lee, J. Thin films as an emerging platform for drug delivery. *Asian J Pharm Sci* **11,** 559–574 (2016)

210. Vuddanda, P. R., Montenegro-Nicolini, M., Morales, J. O. & Velaga, S. Effect of plasticizers on the physico-mechanical properties of pullulan based pharmaceutical oral films. *Eur J Pharma Sci* **96,** 290–298 (2017).

211. Morais, E. S., Silva, N. H. C. S., Sintra, T. E., Santos, S. A. O., Neves, B. M., Almeida, I. F., Costa, P. C., Correia-Sá, I., Ventura, S. P. M., Silvestre, A. J. D., Freire, M. G. & Freire, C. S. R. Anti-inflammatory and antioxidant

nanostructured cellulose membranes loaded with phenolic-based ionic liquids for cutaneous application. *Carbohydr Polym* **206,** 187–197 (2019).

212. Chantereau, G., Sharma, M., Abednejad, A., Vilela, C., Costa, E. M., Veiga, M., Antunes, F., Pintado, M. M., Sèbe, G., Coma, V., Freire, M. G., Freire, C. S. R. & Silvestre, A. J. D. Bacterial nanocellulose membranes loaded with vitamin B-based ionic liquids for dermal care applications. *J Mol Liq* **302,** 112547 (2020).

213. Chandna, S., Paul, S., Kaur, R., Gogde, K. & Bhaumik, J. Photodynamic Lignin Hydrogels: A Versatile Self-Healing Platform for Sustained Release of Photosensitizer Nanoconjugates. *ACS Appl Polym Mater* **4**, 8962-8976 (2022).

214. Xie, Y., Gao, P., He, F. & Zhang, C. Application of Alginate-Based Hydrogels in Hemostasis. *Gels* **8,** 109 (2022)

215. Carvalho, J. P. F., Silva, A. C. Q., Silvestre, A. J. D., Freire, C. S. R. & Vilela, C. Spherical cellulose micro and nanoparticles: A review of recent developments and applications. *Nanomaterials* **11,** 2744 (2021).

216. Silva, N. H. C. S., Vilela, C., Almeida, A., Marrucho, I. M. & Freire, C. S. R. Pullulan-based nanocomposite films for functional food packaging: Exploiting lysozyme nanofibers as antibacterial and antioxidant reinforcing additives. *Food Hydrocoll* **77,** 921–930 (2018).

217. Carvalho, T., Ezazi, N. Z., Correia, A., Vilela, C., Santos, H. A. & Freire, C. S. R. Gelatin-Lysozyme Nanofibrils Electrospun Patches with Improved Mechanical, Antioxidant, and Bioresorbability Properties for Myocardial Regeneration Applications. *Adv Funct Mater* **32,** 2113390 (2022).

218. Pawar, R., Jadhav, W., Bhusare, S., Borade, R., Farber, S., Itzkowitz, D. & Domb, A. Polysaccharides as carriers of bioactive agents for medical applications. *Natural-Based Polymers for Biomedical Applications* 3–53 (2008).

219. Nilsson, A., Wallin, B., Rotstein, A., Care, I. & Control, A. P. The EMLA patch--a new type of local anaesthetic application for dermal analgesia in children. *Anaesthesia* **49**, 70–72 (1994).

220. Scherlund, M., Brodin, A. & Malmsten, M. Nonionic Cellulose Ethers as Potential Drug Delivery Systems for Periodontal Anesthesia. *J Colloid Interface Sci* **229,** 365–374 (2000).

221. Li, Y., Wu, X., Zhu, Q., Chen, Z., Lu, Y., Qi, J. & Wu, W. Improving the hypoglycemic effect of insulin via the nasal administration of deep eutectic solvents. *Int J Pharm* **569,** 118584 (2019).

222. Bianchi, M. B., Zhang, C., Catlin, E., Sandri, G., Calderón, M., Larrañeta, E., Donnelly, R. F., Picchio, M. L. & Paredes, A. J. Bioadhesive eutectogels supporting drug nanocrystals for long-acting delivery to mucosal tissues. *Mater Today Bio* **17,** 100471 (2022).

223. Qu, W., Qader, I. B. & Abbott, A. P. Controlled release of pharmaceutical agents using eutectic modified gelatin. *Drug Deliv Transl Res* **12,** 1187–1194 (2022).

224. Roda, A., Santos, F., Matias, A. A., Paiva, A., Rita, A. & Duarte, C. Design and processing of drug delivery formulations of therapeutic deep eutectic systems for tuberculosis. *J Supercrit Fluids* **161,** 104826 (2020).

225. Almeida, C. M. R., Magalhães, J. M. C. S., Souza, H. K. S. & Gonçalves, M. P. The role of choline chloride-based deep eutectic solvent and curcumin on chitosan films properties. *Food Hydrocoll* **81,** 456–466 (2018).

226. Silva, J. M., Silva, E. & Reis, R. L. Therapeutic deep eutectic solvents assisted the encapsulation of curcumin in alginate-chitosan hydrogel beads. *Sustain Chem Pharm* **24,** 100553 (2021).

227. Bhattarai, N., Ramay, H. R., Chou, S.-H. & Zhang, M. Chitosan and lactic acid-grafted chitosan nanoparticles as carriers for prolonged drug delivery. *Int J Nanomedicine* **1,** 181–187 (2006).

228. Mano, F., Martins, M., Sá-Nogueira, I., Barreiros, S., Borges, J. P., Reis, R. L., Duarte, A. R. C. & Paiva, A. Production of Electrospun Fast-Dissolving Drug Delivery Systems with Therapeutic Eutectic Systems Encapsulated in Gelatin. *AAPS PharmSciTech* **18**, 2579-2585 (2017).

229. Cheng, K.-C., Demirci, A. & Catchmark, J. M. Pullulan: biosynthesis, production, and applications. *Appl Microbiol Biotechnol* **92,** 29–44 (2011).

230. Coltelli, M.-B., Danti, S., de Clerck, K., Lazzeri, A. & Morganti, P. Pullulan for Advanced Sustainable Body- and Skin-Contact Applications. *J Funct Biomater* **11,** 20 (2020).

231. de Arce Velasquez, A., Ferreira, L. M., Stangarlin, M. F. L., da Silva, C. de B., Rolim, C. M. B. & Cruz, L. Novel Pullulan–Eudragit® S100 blend microparticles for oral delivery of risedronate: Formulation, in vitro evaluation and tableting of blend microparticles. *Mater Sci C Mater Biol Appl* **38,** 212–217 (2014).

232. Dionísio, M., Cordeiro, C., Remuñán-López, C., Seijo, B., Rosa da Costa, A. M. & Grenha, A. Pullulan-based nanoparticles as carriers for transmucosal protein delivery. *Eur J Pharma Sci* **50,** 102–113 (2013).

233. Chen, L., Wang, X., Ji, F., Bao, Y., Wang, J., Wang, X., Guo, L. & Li, Y. New bifunctional-pullulan-based micelles with good biocompatibility for efficient co-delivery of cancer-suppressing p53 gene and doxorubicin to cancer cells. *RSC Adv* **5,** 94719–94731 (2015).

234. Bae, B. & Na, K. Self-quenching polysaccharide-based nanogels of pullulan/folate-photosensitizer conjugates for photodynamic therapy. *Biomaterials* **31,** 6325–6335 (2010).

235. Gehrcke, M., Martins, C. C., de Bastos Brum, T., da Rosa, L. S., Luchese, C., Wilhelm, E. A., Soares, F. Z. M. & Cruz, L. Novel Pullulan/Gellan Gum Bilayer Film as a Vehicle for Silibinin-Loaded Nanocapsules in the Topical Treatment of Atopic Dermatitis. *Pharmaceutics* **14,** 2352 (2022).

236. Teramoto, N. & Shibata, M. Synthesis and properties of pullulan acetate. Thermal properties, biodegradability, and a semi-clear gel formation in organic solvents. *Carbohydr Polym* **63,** 476–481 (2006).

237. Singh, R. S., Kaur, N., Sharma, R. & Rana, V. Investigating the potential of carboxymethyl pullulan for protecting the rabbit eye from systematically induced precorneal tear film damage. *Exp Eye Res* **184,** 91–100 (2019).

238. Guo, H., Liu, Y., Wang, Y., Wu, J., Yang, X., Li, R., Wang, Y. & Zhang, N. pH-sensitive pullulan-based nanoparticle carrier for adriamycin to overcome drug-resistance of cancer cells. *Carbohydr Polym* **111,** 908–917 (2014).

239. Singh, R. S., Kaur, N. & Kennedy, J. F. Pullulan and pullulan derivatives as promising biomolecules for drug and gene targeting. *Carbohydr Polym* **123,** 190–207 (2015).

240. Carvalho, L. T., Moraes, R. M., Teixeira, A. J. R. M., Tada, D. B., Alves, G. M., Lacerda, T. M., Santos, J. C., Santos, A. M. & Medeiros, S. F. Development of pullulan-based carriers for controlled release of hydrophobic ingredients. *J Appl Polym Sci* **138,** 51344 (2021).

241. Vora, L. K., Courtenay, A. J., Tekko, I. A., Larrañeta, E. & Donnelly, R. F. Pullulan-based dissolving microneedle arrays for enhanced transdermal delivery of small and large biomolecules. *Int J Biol Macromol* **146,** 290–298 (2020).

242. Fonseca, D. F. S., Costa, P. C., Almeida, I. F., Dias-Pereira, P., Correia-Sá, I., Bastos, V., Oliveira, H., Duarte-Araújo, M., Morato, M., Vilela, C., Silvestre, A. J. D. & Freire, C. S. R. Pullulan microneedle patches for the efficient transdermal administration of insulin envisioning diabetes treatment. *Carbohydr Polym* **241,** 116314 (2020).

243. Priya, V. S., Iyappan, K., Gayahtri, V. S., William, S. & Suguna, L. Influence of pullulan hydrogel on sutureless wound healing in rats. *Wound Med* **14,** 1–5 (2016).

244. Wong, V. W., Rustad, K. C., Glotzbach, J. P., Sorkin, M., Inayathullah, M., Major, M. R., Longaker, M. T., Rajadas, J. & Gurtner, G. C. Pullulan Hydrogels Improve Mesenchymal Stem Cell Delivery into High-Oxidative-Stress Wounds. *Macromol Biosci* **11,** 1458-1466 (2011).

245. Lee, K. Y. & Mooney, D. J. Alginate: Properties and biomedical applications. *Prog Polym Sci* **37,** 106–126 (2012).

246. Helgerud, T., Gserd, O., Fjreide, T., Andersen, P. O. & Larsen, C. K. Alginates, In Food Stabilisers, Thickeners and Gelling Agents. *Wiley-Blackwell*, 50–72 (2010).

247. Wee, S. F & Gombotz, W. R. Protein release from alginate matrices. *Adv Drug Deliv Rev* **31,** 194–205 (1998).

248. Sellimi, S., Younes, I., Ayed, H. ben, Maalej, H., Montero, V., Rinaudo, M., Dahia, M., Mechichi, T., Hajji, M. & Nasri, M. Structural, physicochemical and antioxidant properties of sodium alginate isolated from a Tunisian brown seaweed. *Int J Biol Macromol* **72,** 1358–1367 (2015).

249. Choe, G., Park, J., Park, H. & Lee, J. Hydrogel Biomaterials for Stem Cell Microencapsulation. *Polymers* **10,** 997 (2018).

250. Rosiak, P., Latanska, I., Paul, P., Sujka, W. & Kolesinska, B. Modification of Alginates to Modulate Their Physic-Chemical Properties and Obtain Biomaterials with Different Functional Properties. *Molecules* **26,** 7264 (2021).

251. Elzatahry, A. A., Eldin, M. S. M., Soliman, E. A. & Hassan, E. A. Evaluation of alginate-chitosan bioadhesive beads as a drug delivery system for the controlled release of theophylline. *J Appl Polym Sci* **111,** 2452–2459 (2009).

252. Sookkasem, A., Chatpun, S., Yuenyongsawad, S. & Wiwattanapatapee, R. Alginate beads for colon specific delivery of self-emulsifying curcumin. *J Drug Deliv Sci Technol* **29,** 159–166 (2015).

253. Hu, Y., Hu, S., Zhang, S., Dong, S., Hu, J., Kang, L. & Yang, X. A double-layer hydrogel based on alginate-carboxymethyl cellulose and synthetic polymer as sustained drug delivery system. *Sci Rep* **11,** (2021).

254. Gupta, P., Vermani, K. & Garg, S. Hydrogels: From controlled release to pH-responsive drug delivery. *Drug Discov Today* **7,** 569–579 (2002).

255. Jacob, S., Nair, A. B., Shah, J., Sreeharsha, N., Gupta, S. & Shinu, P. Emerging Role of Hydrogels in Drug Delivery Systems, Tissue Engineering and Wound Management. *Pharmaceutics* **13,** 357 (2021).

256. Almoshari, Y. Novel Hydrogels for Topical Applications: An Updated Comprehensive Review Based on Source. *Gels* **8,** 174 (2022).

257. Zhao, F., Yao, D., Guo, R., Deng, L., Dong, A. & Zhang, J. Composites of Polymer Hydrogels and Nanoparticulate Systems for Biomedical and Pharmaceutical Applications. *Nanomaterials* **5,** 2054–2130 (2015).

258. Coşkun, G., Karaca, E., Ozyurtlu, M., Özbek, S., Yermezler, A. & Çavuşoğlu, I. Histological evaluation of wound healing performance of electrospun

poly(vinyl alcohol)/sodium alginate as wound dressing in vivo. *Biomed Mater Eng* **24,** 1527–1536 (2014).

259. Abebe, M. W., Appiah-Ntiamoah, R. & Kim, H. Gallic acid modified alginate self-adhesive hydrogel for strain responsive transdermal delivery. *Int J Biol Macromol* **163,** 147–155 (2020).

260. Pradeepkumar, P., Rajan, M., Almoallim, H. S. & Alharbi, S. A. Targeted Delivery of Doxorubicin in HeLa Cells Using Self-Assembled Polymeric Nanocarriers Guided by Deep Eutectic Solvents. *ChemistrySelect* **6,** 7232–7241 (2021).

261. Liu, C., Qu, X., Song, L., Shang, R., Wan, X. & Fang, L. Investigation on the effect of deep eutectic formation on drug-polymer miscibility and skin permeability of rotigotine drug-in-adhesive patch. *Int J Pharm* 118852 (2019).

262. Bird, D. & Ravindra, N. M. Transdermal drug delivery and patches—An overview. *Med Devices Sens* **3,** e10069 (2020).

263. Pastore, M. N., Kalia, Y. N., Horstmann, M. & Roberts, M. S. Transdermal patches: history, development and pharmacology. *Br J Pharmacol* **172,** 2179–2209 (2015).

264. Gutschke, E., Bracht, S., Nagel, S. & Weitschies, W. Adhesion testing of transdermal matrix patches with a probe tack test – In vitro and in vivo evaluation. *Eur J Pharma Biopharma* **75,** 399–404 (2010).

265. Banerjee, S., Chattopadhyay, P., Ghosh, A., Datta, P. & Veer, V. Aspect of adhesives in transdermal drug delivery systems. *Int J Adhes Adhes* **50,** 70–84 (2014).

266. Yuk, H., Varela, C. E., Nabzdyk, C. S., Mao, X., Padera, R. F., Roche, E. T. & Zhao, X. Dry double-sided tape for adhesion of wet tissues and devices. *Nature* **575,** 169–174 (2019).

267. Yang, J., Li, Y., Ye, R., Zheng, Y., Li, X., Chen, Y., Xie, X. & Jiang, L. Smartphone-powered iontophoresis-microneedle array patch for controlled transdermal delivery. *Microsyst Nanoeng* **6,** (2020).

268. Rajabi, M., Roxhed, N., Shafagh, R. Z., Haraldson, T., Fischer, A. C., Wijngaart, W. van der, Stemme, G. & Niklaus, F. Flexible and Stretchable Microneedle Patches with Integrated Rigid Stainless Steel Microneedles for Transdermal Biointerfacing. *PLoS One* **11,** e0166330 (2016).

269. Moon, S. S., Richter-Roche, M., Resch, T. K., Wang, Y., Foytich, K. R., Wang, H., Mainou, B. A., Pewin, W., Lee, J., Henry, S., McAllister, D. v. & Jiang, B. Microneedle patch as a new platform to effectively deliver inactivated polio vaccine and inactivated rotavirus vaccine. *NPJ Vaccines* **7,** 26 (2022).

270. Manikkath, J. & Subramony, J. A. Toward closed-loop drug delivery: Integrating wearable technologies with transdermal drug delivery systems. *Adv Drug Deliv Rev* **179,** 113997 (2021).

271. Almeida, C. M. R., Magalhães, J. M. C. S., Souza, H. K. S. & Gonçalves, M. P. The role of choline chloride-based deep eutectic solvent and curcumin on chitosan films properties. *Food Hydrocoll* **81,** 456–466 (2018).

272. Lončarić, M., Jakobek, L. & Molnar, M. Deep Eutectic Solvents in the Production of Biopolymer-Based Materials. *Croatica Chemica Acta* **94,** 75-82 (2021).

273. Sousa, A. M. M., Souza, H. K. S., Latona, N., Liu, C.-K., Gonçalves, M. P. & Liu, L. Choline chloride based ionic liquid analogues as tool for the fabrication of agar films with improved mechanical properties. *Carbohydr Polym* **111,** 206–214 (2014).

274. Wang, S., Peng, X., Zhong, L., Jing, S., Cao, X., Lu, F. & Sun, R. Choline chloride/urea as an effective plasticizer for production of cellulose films. *Carbohydr Polym* **117,** 133–139 (2015).

275. Sokolova, M. P., Smirnov, M. A., Samarov, A. A., Bobrova, N. v., Vorobiov, V. K., Popova, E. N., Filippova, E., Geydt, P., Lahderanta, E. & Toikka, A. M. Plasticizing of chitosan films with deep eutectic mixture of malonic acid and choline chloride. *Carbohydr Polym* **197,** 548–557 (2018).

276. Tillotson, G. S. & Zinner, S. H. Burden of antimicrobial resistance in an era of decreasing susceptibility. *Expert Rev Anti Infect Ther* **15,** 663–676 (2017).

277. Baker, S. J., Payne, D. J., Rappuoli, R. & de Gregorio, E. Technologies to address antimicrobial resistance. *Proc Natl Acad Sci* **115,** 12887–12895 (2018).

278. Årdal, C., Balasegaram, M., Laxminarayan, R., Mcadams, D., Outterson, K., Rex, J. H., Sumpradit, N., Årdal, C. & Mcadams, D. Antibiotic development — economic, regulatory and societal challenges. *Nat Rev Microbiol* **18,** 267-274 (2019).

279. World Health Organisation, WHO Report on Surveillance of Antibiotic Consumption. (2019). Available at: https://www.who.int/publications/i/item/who-report-on-surveillance-ofantibiotic-consumption.

280. Bothwell, L. E., Greene, J. A., Podolsky, S. H. & Jones, D. S. Assessing the Gold Standard — Lessons from the History of RCTs. *NEJM* **374,** 2175–2181 (2016).

281. Gao, P., Nie, X., Zou, M., Shi, Y. & Cheng, G. Recent advances in materials for extended-release antibiotic delivery system. *J Antibiot* **64,** 625–634 (2011).

282. Domalaon, R., Idowu, I., Zhanel, G. G. & Schweizer, F. Antibiotic Hybrids: the Next Generation of Agents and Adjuvants against Gram-Negative Pathogens? *Clin Microbiol Rev* **31,** e00077-17 (2018).

283. Thu D. M. Pham, Z. M. Z. and M. A. T. B. Quinolone antibiotics. *Med. Chem. Commun.* 1719–1739 (2019).

284. Fief, C. A., Hoang, K. G., Phipps, S. D., Wallace, J. L. & Deweese, J. E. Examining the Impact of Antimicrobial Fluoroquinolones on Human. 4049−4055 (2019).

285. Li, B. & Webster, T. J. Bacteria Antibiotic Resistance: New Challenges and Opportunities for Implant-Associated Orthopaedic Infections. *J Orthop Res* **36,** 22–32 (2018).

286. Haslund, J. M., Dinesen, M. R., Brit, A., Nielsen, S., Llor, C. & Bjerrum, L. Different recommendations for empiric first-choice antibiotic treatment of uncomplicated urinary tract infections in Europe. *Scand J Prim Health Care* **31,** 235–240 (2013).

287. Gill, E. E., Franco, O. L., Hancock, R. E. W., Catolica, U., Bosco, D., Biotecnologia, P. & Grande, C. Antibiotic Adjuvants : Diverse Strategies for Controlling Drug-Resistant Pathogens. *Chem Bio Drug Des* **85,** 56–78 (2015).

288. Varanda, F.; Pratas de Melo, M. J.; Caço, A. I.; Dohrn, R.; Makrydaki, F. A.; Voutsas, E.; Tassios, D.; Marrucho, I. M. Solubility of Antibiotics in Different Solvents. 1. Hydrochloride Forms of Tetracycline, Moxifloxacin, and Ciprofloxacin. *Ind Eng Chem Res* **45**, 6368–6374 (2006).

289. Wiegand, I., Hilpert, K. & Hancock, R. E. W. Agar and broth dilution methods to determine the minimal inhibitory concentration (MIC) of antimicrobial substances. *Nat Protoc* **3,** 163–175 (2008).

290. Clinical and Laboratory Standards Institute, Performance standards for antimicrobial susceptibility testing, Document M100:CLSI, 2020.

291. European Committee on Antimicrobial Susceptibility Testing, MIC and zone diameter distributions and ECOFFs. (2020). Available at https://www.eucast.org/mic_distributions_and_ecoffs/.

292. Nagoba, B., Davane, M., Gandhi, R., Wadher, B. & Suryawanshi, N. Treatment of skin and soft tissue infections caused by Pseudomonas aeruginosa — A review of our experiences with citric acid over the past 20 years. *Wound Medicine* **19,** 5–9 (2017).

293. Mäkinen, K. K. The Latest on Sugar Substitutes of the Alditol Type with Special Consideration of Erythritol and Xylitol — Rectifications and Recommendations Journal of Food: Microbiology, Safety & Hygiene. **2,** 1–13 (2017).

294. Percival, S. L., Finnegan, S., Donelli, G., Vuotto, C., Rimmer, S. & Lipsky, B. A. Antiseptics for treating infected wounds: Efficacy on biofilms and effect of pH. *Crit Rev Microbiol* **42,** 293-309 (2014).

295. Delso, I., Lafuente, C., Muñoz-Embid, J. & Artal, M. NMR study of choline chloride-based deep eutectic solvents. *J Mol Liq* **290,** 111236 (2019).

296. Caço, A. I., Varanda, F., de Melo, M. J. P., Dias, A. M. A., Dohrn, R. & Marrucho, I. M. Solubility of antibiotics in different solvents. Part II. non-

hydrochloride forms of tetracycline and ciprofloxacin. *Ind Eng Chem Res* **47,** 8083–8089 (2008).

297. Yu, X., Zipp, G. L. & Ray Davidson III, G. W. *The effect of temperature and pH on the solubility of quinolone compounds. Pharm Res* **11,** 522-527 (1994).

298. U.S. Food and Drug Administration (FDA), Cipro ® iv (ciprofloxacin) For Intravenous Infusion. (2013). Available at https://www.accessdata.fda.gov/drugsatfda_docs/label/2013/019857s062lbl.pdf.

299. Shimizu, S. & Matubayasi, N. The origin of cooperative solubilisation by hydrotropes. *Physical Chemistry Chemical Physics* **18,** 25621–25628 (2016).

300. Millard, J. W., Alvarez-Núñez, F. A. & Yalkowsky, S. H. Solubilization by cosolvents: Establishing useful constants for the log-linear model. *Int J Pharm* **245,** 153–166 (2002).

301. Atilhan, M., Aparicio, S. & Gutie, A. Behavior of Antibiotics in Natural Deep Eutectic Solvents. *J Chem Eng Data* **65,** 4669–4683 (2020).

302. Kussmann, M., Ferth, A., Obermüller, M., Pichl, P., Zeitlinger, M., Wi, M., Burgmann, H., Poeppl, W. & Reznicek, G. Compatibility of ciprofloxacin with commercial peritoneal dialysis solutions. *Sci Rep* **9,** 1–6 (2019).

303. Donnelly, R. F. Stability of Ciprofloxacin in Polyvinylchloride Minibags. *Can J Hosp Pharm* **64,** 252–256 (2011).

304. Youssef, A., Dudhipala, N. & Majumdar, S. Ciprofloxacin Loaded Nanostructured Lipid Carriers Incorporated into In-Situ Gels to Improve Management of Bacterial Endophthalmitis. *Pharmaceutics* **12,** 572 (2020).

305. Youssef, A. A. A., Cai, C., Dudhipala, N. & Majumdar, S. Design of Topical Ocular Ciprofloxacin Nanoemulsion for the Management of Bacterial Keratitis. *Pharmaceuticals* **14,** 210 (2021).

306. Macário, I. P. E., Oliveira, H., Menezes, A. C., Ventura, S. P. M. & Pereira, J. L. Cytotoxicity profiling of deep eutectic solvents to human skin cells. *Sci Rep* **9,** 3932 (2019).

307. Adamus-białek, W., Wawszczak, M., Arabski, M., Gulba, M., Jarych, D. & Parniewski, P. Ciprofloxacin, amoxicilin, and aminoglycosides stimulate genetic and phenotypic changes in uropathogenic Escherichia coli strains. *Virulence* **10,** 260–276 (2019).

308. Machuca, J., Recacha, E., Briales, A., Díaz-de-alba, P. & Austin, R. H. Cellular Response to Ciprofloxacin in Low-Level Quinolone-Resistant Escherichia coli. *Front Microbiol* **8,** 1370 (2017).

309. Burel, C., Kala, A. & Purevdorj-Gage, L. Impact of pH on citric acid antimicrobial activity against Gram-negative bacteria. *Lett Appl Microbiol* **72,** 332–340 (2021).

310. Pankuch, G. A., Lin, G., Seifert, H., Appelbaum, C., Pankuch, G. A., Lin, G., Seifert, H. & Appelbaum, P. C. Activity of Meropenem with and without Ciprofloxacin and Colistin against Pseudomonas aeruginosa and Acinetobacter baumannii Activity of Meropenem with and without Ciprofloxacin and Colistin against Pseudomonas aeruginosa and Acinetobacter baumannii. *Antimicrob Agents Chemother* **52,** 333–336 (2008).

311. Ermertcan, S., HoŞgör, M., Tünger, O. & Cosar. Investigation of Synergism of Meropenem and Ciprooxacin Against Pseudomonas aeruginosa and Acinetobacter Strains Isolated from Intensive Care Unit Infections. *Scand J Infect Dis* **33,** 818–821 (2001).

312. Troughton, J. A., Millar, G., Smyth, E. T. M., Doherty, L. & Mcmullan, R. Ciprofloxacin use and susceptibility of Gram-negative organisms to quinolone and non-quinolone antibiotics. *J Antimicrob Chemother* **66,** 2152–2158 (2011).

313. Breidenstein, E. B. M., Khaira, B. K., Wiegand, I., Overhage, J. & Hancock, R. E. W. Complex Ciprofloxacin Resistome Revealed by Screening a Pseudomonas aeruginosa Mutant Library for Altered Susceptibility □. *Antimicrob Agents Chemother* **52,** 4486–4491 (2008).

314. Kureishi, A., Diver, J. M., Beckthold, B., Schollaardt, T. & Bryan, L. E. Cloning and Nucleotide Sequence of Pseudomonas aeruginosa DNA Gyrase gyrA Gene from Strain PAO1 and Quinolone-Resistant Clinical Isolates. *Antimicrob Agents Chemother* **38,** 1944–1952 (1994).

315. Nakano, M., Deguchi, T., Kawamura, T., Yasuda, M., Kimura, M., Okano, Y. & Kawada, Y. Mutations in the gyrA and parC Genes in Fluoroquinolone-Resistant Clinical Isolates of Pseudomonas aeruginosa. *Antimicrob Agents Chemother* **41,** 2289–2291 (1997).

316. Rehman, A., Patrick, W. M. & Lamont, I. L. Mechanisms of ciprofloxacin resistance in Pseudomonas aeruginosa: new approaches to an old problem. *J Med Microbiol* **68,** 1–10 (2019).

317. Oh, H., Stenhoff, J., Jalal, S. & Wretlind, B. Role of Efflux Pumps and Mutations in Genes for Topoisomerases II and IV in Fluoroquinolone-Resistant. *Microbial Drug Resistance* **9,** 323–328 (2003).

318. Kiser, T. H., Pharm, D., Obritsch, M. D., Pharm, D., Jung, R., Pharm, D., Maclaren, R., Pharm, D., Fish, D. N. & Pharm, D. Efflux Pump Contribution to Multidrug Resistance in Clinical Isolates of Pseudomonas aeruginosa. *Pharmacotherapy* **30,** 632–638 (2010).

319. Tanimoto, K., Tomita, H., Fujimoto, S., Okuzumi, K. & Ike, Y. Fluoroquinolone Enhances the Mutation Frequency for Meropenem-Selected Carbapenem Resistance in Pseudomonas aeruginosa, but Use of the High-Potency Drug Doripenem Inhibits Mutant Formation. *Antimicrob Agents Chemother* **52,** 3795–3800 (2008).

320. Nikaido, H. & Pagès, J.-M. Broad Specificity Efflux pumps and Their Role in Multidrug Resistance of Gram-Negative Bacteria. *FEMS Microbiol Rev* **36,** 340–363 (2013).

321. Westbrock-wadman, S., Sherman, D. R., Hickey, M. J., Coulter, S. N., Zhu, Y. A. Q. I., Warrener, P., Nguyen, L. Y., Shawar, R. M., Folger, K. I. M. R. & Stover, C. K. Characterization of a Pseudomonas aeruginosa Efflux Pump Contributing to Aminoglycoside Impermeability. *Antimicrob Agents Chemother* **43,** 2975–2983 (1999).

322. Zhang, F., Zhu, C., Peng, Q., Wang, F., Sheng, S., Wu, Q. & Wang, J. Enhanced permeability of recombinant E . coli cells with deep eutectic solvent for transformation of rutin. *J. Chem Technol Biotechnol* 384–393 (2020).

323. Pessina, A., Raimondi, A., Piccirillo, M., Neri, M. G., Croera, C. & Foti, P. High sensitivity of human epidermal keratinocytes (HaCaT) to topoisomerase inhibitors. *Cell Prolif* **34**, 243–252 (2001).

324. Steinmetz, J. D., *et al.* Causes of blindness and vision impairment in 2020 and trends over 30 years, and prevalence of avoidable blindness in relation to VISION 2020: the Right to Sight: an analysis for the Global Burden of Disease Study. *Lancet Glob Health* **9,** e144–e160 (2021).

325. Klotz, S. A., Penn, C. C., Negvesky, G. J. & Butrus, S. I. Fungal and Parasitic Infections of the Eye. *Clin Microbiol Rev* **13,** 662–685 (2000).

326. Petrillo, F., Pignataro, D., di Lella, F. M., Reibaldi, M., Fallico, M., Castellino, N., Parisi, G., Trotta, M. C., D'Amico, M., Santella, B., Folliero, V., della Rocca, M. T., Rinaldi, M., Franci, G., Avitabile, T., Galdiero, M. & Boccia, G. Antimicrobial Susceptibility Patterns and Resistance Trends of Staphylococcus aureus and Coagulase-Negative Staphylococci Strains Isolated from Ocular Infections. *Antibiotics* **10,** 527 (2021).

327. León-Buitimea, A., Garza-Cárdenas, C. R., Garza-Cervantes, J. A., Lerma-Escalera, J. A. & Morones-Ramírez, J. R. The Demand for New Antibiotics: Antimicrobial Peptides, Nanoparticles, and Combinatorial Therapies as Future Strategies in Antibacterial Agent Design. *Front Microbiol* **11,** 1–10 (2020).

328. Lee, A. S., de Lencastre, H., Garau, J., Kluytmans, J., Malhotra-Kumar, S., Peschel, A. & Harbarth, S. Methicillin-resistant Staphylococcus aureus. *Nat Rev Dis Primers* **4,** 18033 (2018).

329. Bergen, P. J., Landersdorfer, C. B., Lee, H. J., Li, J. & Nation, R. L. 'Old' antibiotics for emerging multidrug-resistant bacteria. *Curr Opin Infect Dis* **25,** 626–633 (2012).

330. Rahal, J. J. & Simberkoff, M. S. Bactericidal and Bacteriostatic Action of Chloramphenicol Against Meningeal Pathogens. *Antimicrob Agents Chemother* **16,** 13–18 (1979).

331. Lorenzo. Chloramphenicol Resurrected: A Journey from Antibiotic Resistance in Eye Infections to Biofilm and Ocular Microbiota. *Microorganisms* **7,** 278 (2019).

332. Jithan, A., Mohan, Ck. & Vimaladevi, M. Development and evaluation of a chloramphenicol hypertonic ophthalmic solution. *Indian J Pharm Sci* **70,** 66 (2008).

333. Aiassa, V., Zoppi, A., Albesa, I. & Longhi, M. R. Inclusion complexes of chloramphenicol with β-cyclodextrin and aminoacids as a way to increase drug solubility and modulate ROS production. *Carbohydr Polym* **121,** 320–327 (2015).

334. Xu, Y., Zhang, C., Zhu, X., Wang, X., Wang, H., Hu, G., Fu, Q. & He, Z. Chloramphenicol/sulfobutyl ether-β-cyclodextrin complexes in an ophthalmic delivery system: prolonged residence time and enhanced bioavailability in the conjunctival sac. *Expert Opin Drug Deliv* **16,** 657–666 (2019).

335. Mokhtarpour, M., Shekaari, H. & Shayanfar, A. Design and characterization of ascorbic acid based therapeutic deep eutectic solvent as a new ion-gel for delivery of sunitinib malate. *J Drug Deliv Sci Technol* **56,** 101512 (2020).

336. Souza, J. G., Dias, K., Pereira, T. A., Bernardi, D. S. & Lopez, R. F. v. Topical delivery of ocular therapeutics : carrier systems and physical methods. *J Pharm Pharmacol* **66**, 507-530 (2013).

337. Dhingra, D., Behera, K., Bhawna & Pandey, S. Formation of water-in-oil microemulsions within a hydrophobic deep eutectic solvent. *Physical Chemistry Chemical Physics* **23,** 10629–10635 (2021).

338. Sekharan, T. R., Chandira, R. M., Tamilvanan, S., Rajesh, S. C. & Venkateswarlu, B. S. Deep Eutectic Solvents as an Alternate to Other Harmful Solvents. *Biointerface Res Appl Chem* **12,** 847–860 (2021).

339. Mundada, A. S. & Avari, J. G. In Situ Gelling Polymers in Ocular Drug Delivery Systems: A Review. *Crit Rev Ther Drug Carrier Syst* **26,** 85–118 (2009).

340. Dou, Q., Abdul Karim, A. & Loh, X. Modification of Thermal and Mechanical Properties of PEG-PPG-PEG Copolymer (F127) with MA-POSS. *Polymers* **8,** 341 (2016).

341. Garrett, Q., Khandekar, N., Shih, S., Flanagan, J. L., Simmons, P., Vehige, J. & Willcox, M. D. P. Betaine stabilizes cell volume and protects against

apoptosis in human corneal epithelial cells under hyperosmotic stress. *Exp Eye Res* **108,** 33–41 (2013).

342. Szél, E., Danis, J., Sőrés, E., Tóth, D., Korponyai, C., Degovics, D., Prorok, J., Acsai, K., Dikstein, S., Kemény, L. & Erős, G. Protective effects of glycerol and xylitol in keratinocytes exposed to hyperosmotic stress. *Clin Cosmet Investig Dermatol* **12,** 323–331 (2019).

343. Todoran, N., Ciurba, A., Rédai, E., Ion, V., Lazăr, L. & Sipos, E. Limitations when use chloramphenicol-bcyclodextrins complexes in ophtalmic solutions buffered with boric acid/borax system. *Acta Med Marisiensis* **60,** 269–274 (2014).

344. Abelson, M. B., Udell, I. J. & Weston, J. H. Normal Human Tear pH by Direct Measurement. *Archives of Ophthalmology* **99,** 301–301 (1981).

345. Tong, L., Petznick, A., Lee, S. & Tan, J. Choice of Artificial Tear Formulation for Patients With Dry Eye: Where Do We Start? *Cornea* **1**, S32-36 (2012).

346. Talegaonkar, S., Azeem, A., Ahmad, F., Khar, R., Pathan, S. & Khan, Z. Microemulsions: A Novel Approach to Enhanced Drug Delivery. *Recent Pat Drug Deliv Formul* **2,** 238–257 (2008).

347. Prud'homme, R. K., Wu, G. & Schneider, D. K. Structure and Rheology Studies of Poly(oxyethylene-oxypropylene-oxyethylene) Aqueous Solution. *Langmuir* **12**, 4651-4659 (1996).

348. Arshinoff, S. A., Hofmann, I. & Nae, H. Role of rheology in tears and artificial tears. *J Cataract Refract Surg* **47,** 655–661 (2021).

349. Choi, H.-G., Jung, J.-H., Ryu, J.-M., Yoon, S.-J., Oh, Y.-K. & Kim, C.-K. Development of in situ-gelling and mucoadhesive acetaminophen liquid suppository. *Int J Pharm* **165,** 33–44 (1998).

350. Chaibundit, C., Ricardo, N. M. P. S., Ricardo, N. M. P. S., Muryn, C. A., Madec, M.-B., Yeates, S. G. & Booth, C. Effect of ethanol on the gelation of aqueous solutions of Pluronic F127. *J Colloid Interface Sci* **351,** 190–196 (2010).

351. Matthew, J. E., Nazario, Y. L., Roberts, S. C. & Bhatia, S. R. Effect of mammalian cell culture medium on the gelation properties of Pluronic s F127. *Biomaterials* **23,** 4615-4619 (2002).

352. Thapa, R. K., Cazzador, F., Grønlien, K. G. & Tønnesen, H. H. Effect of curcumin and cosolvents on the micellization of Pluronic F127 in aqueous solution. *Colloids Surf B Biointerfaces* **195,** 111250 (2020).

353. Yong, C. S., Suck Choi, J., Quan, Q.-Z., Rhee, J.-D., Kim, C.-K., Lim, S.-J., Kim, K.-M., Oh, P.-S. & Choi, H.-G. Effect of sodium chloride on the gelation temperature, gel strength and bioadhesive force of poloxamer gels containing diclofenac sodium. *Int J Pharm* **226,** 195-205 (2001).

354. Lv, F., Li, N., Zheng, L. & Tung, C. Studies on the stability of the chloramphenicol in the microemulsion free of alcohols. *Eur J Pharm Biopharm* **62,** 288–294 (2006).

355. Glazko, A. J., Dill, W. A. & Rebstock, M. C. Biochemical studies on Chloramphenicol (Chloromycetin). *JBC* **183,** 679–691 (1950).

356. Jünemann, A. G. M., Chorągiewicz, T., Ozimek, M., Grieb, P. & Rejdak, R. Drug bioavailability from topically applied ocular drops. Does drop size matter? *Ophtalmol J* **1,** 29–35 (2016).

357. Anonye, B. O., Nweke, V., Furner-Pardoe, J., Gabrilska, R., Rafiq, A., Ukachukwu, F., Bruce, J., Lee, C., Unnikrishnan, M., Rumbaugh, K. P., Snyder, L. A. S. & Harrison, F. The safety profile of Bald's eyesalve for the treatment of bacterial infections. *Sci Rep* **10,** 17513 (2020).

358. Karava, A., Lazaridou, M., Nanaki, S., Michailidou, G., Christodoulou, E., Kostoglou, M., Iatrou, H. & Bikiaris, D. N. Chitosan Derivatives with Mucoadhesive and Antimicrobial Properties for Simultaneous Nanoencapsulation and Extended Ocular Release Formulations of Dexamethasone and Chloramphenicol Drugs. *Pharmaceutics* **12,** 594 (2020).

359. Boateng, J. S. & Popescu, A. M. Composite bi-layered erodible films for potential ocular drug delivery. *Colloids Surf B Biointerfaces* **145,** 353–361 (2016).

360. Lv, F.-F., Zheng, L.-Q. & Tung, C.-H. Phase behavior of the microemulsions and the stability of the chloramphenicol in the microemulsion-based ocular drug delivery system. *Int J Pharm* **301,** 237–246 (2005).

361. Furuishi, T., Oda, S., Saito, H., Fukami, T., Suzuki, T. & Tomono, K. Effect of Permeation Enhancers on the in Vitro Percutaneous Absorption of Pentazocine1). *Biol Pharm Bull* **30,** 1350–1353 (2007).

362. Benson, H. & Alto, P. Permeability of the Cornea to Topically Applied Drugs. *Arch Dermatol* **91,** 313–327 (1974).

363. Akiyama, H., Oono, T., Huh, W.-K., Yamasaki, O., Ogawa, S., Katsuyama, M., Ichikawa, H. & Iwatsuki, K. Actions of Farnesol and Xylitol against *Staphylococcus aureus*. *Chemotherapy* **48,** 122–128 (2002).

364. Tao, R., Wang, C., Ye, J., Zhou, H. & Chen, H. Polyprenols of Ginkgo biloba Enhance Antibacterial Activity of Five Classes of Antibiotics. *Biomed Res Int* **2016,** 1–8 (2016).

365. Llor, C. & Bjerrum, L. Antimicrobial resistance: risk associated with antibiotic overuse and initiatives to reduce the problem. *Ther Adv Drug Saf* **5,** 229–241 (2014).

366. David, M. Z. & Daum, R. S. Community-Associated Methicillin-Resistant Staphylococcus aureus : Epidemiology and Clinical Consequences of an Emerging Epidemic. *Clin Microbiol Rev* **23,** 616–687 (2010).

367. Cabral, J. & AG, R. Blue Light Disinfection in Hospital Infection Control: Advantages, Drawbacks, and Pitfalls. *Antibiotics* **8,** 58 (2019).

368. Tavares, A., Dias, S. R. S., Carvalho, C. M. B., Faustino, M. A. F., Tomé, J. P. C., Neves, M. G. P. M. S., Tomé, A. C., Cavaleiro, J. A. S., Cunha, Â., Gomes, N. C. M., Alves, E. & Almeida, A. Mechanisms of photodynamic inactivation of a Gram-negative recombinant bioluminescent bacterium by cationic porphyrins. *Photochem Photobiol Sci* **10,** 1659-1669 (2011).

369. Li, X., Lee, S. & Yoon, J. Supramolecular photosensitizers rejuvenate photodynamic therapy. *Chem Soc Rev* **47,** 1174–1188 (2018).

370. Glass, S., Rüdiger, T., Griebel, J., Abel, B. & Schulze, A. Uptake and release of photosensitizers in a hydrogel for applications in photodynamic therapy: the impact of structural parameters on intrapolymer transport dynamics. *RSC Adv* **8,** 41624–41632 (2018).

371. Gnanasekar, S., Kasi, G., He, X., Zhang, K., Xu, L. & Kang, E.-T. Recent advances in engineered polymeric materials for efficient photodynamic inactivation of bacterial pathogens. *Bioact Mater* **21,** 157–174 (2023).

372. Kim, S. K, Kim, J. H., Kim, J. O., Ku, S., Cho, H., Han, D. H. & Huh, P. Fabrication of poly(ethylene oxide) hydrogels for wound dressing application using E-beam. *Macromol Res* **22,** 131–138 (2014).

373. Feng, C.-C., Lu, W.-F., Liu, Y.-C., Liu, T.-H., Chen, Y.-C., Chien, H.-W., Wei, Y., Chang, H.-W. & Yu, J. A hemostatic keratin/alginate hydrogel scaffold with methylene blue mediated antimicrobial photodynamic therapy. *J Mater Chem B* **10,** 4878–4888 (2022).

374. Chen, C.-P., Hsieh, C.-M., Tsai, T., Yang, J.-C. & Chen, C.-T. Optimization and Evaluation of a Chitosan/Hydroxypropyl Methylcellulose Hydrogel Containing Toluidine Blue O for Antimicrobial Photodynamic Inactivation. *Int J Mol Sci* **16,** 20859–20872 (2015).

375. Frade, M., de Annunzio, S., Calixto, G., Victorelli, F., Chorilli, M. & Fontana, C. Assessment of Chitosan-Based Hydrogel and Photodynamic Inactivation against Propionibacterium acnes. *Molecules* **23,** 473 (2018).

376. Hu, S., Pei, X., Duan, L., Zhu, Z., Liu, Y., Chen, J., Chen, T., Ji, P., Wan, Q. & Wang, J. A mussel-inspired film for adhesion to wet buccal tissue and efficient buccal drug delivery. *Nat Commun* **12,** 1689 (2021).

377. Borges, A. F., Silva, C., Coelho, J. F. J. & Simões, S. Oral films: Current status and future perspectives: I-Galenical development and quality attributes. *J Control Release* **206,** 1–19 (2015)

378. Forooshani, P. K. & Lee, B. P. Recent approaches in designing bioadhesive materials inspired by mussel adhesive protein. *J Polym Sci A Polym Chem* **55,** 9–33 (2017).

379. Huang, T., Zhou, Z., Li, Q., Tang, X., Chen, X., Ge, Y. & Ling, J. Light-Triggered Adhesive Silk-Based Film for Effective Photodynamic Antibacterial Therapy and Rapid Hemostasis. *Front Bioeng Biotechnol* **9,** (2022).

380. Mao, C., Xiang, Y., Liu, X., Cui, Z., Yang, X., Li, Z., Zhu, S., Zheng, Y., Yeung, K. W. K. & Wu, S. Repeatable Photodynamic Therapy with Triggered Signaling Pathways of Fibroblast Cell Proliferation and Differentiation To Promote Bacteria-Accompanied Wound Healing. *ACS Nano* **12,** 1747–1759 (2018).

381. Lei, X., Qiu, L., Lan, M., Du, X., Zhou, S., Cui, P., Zheng, R., Jiang, P., Wang, J. & Xia, J. Antibacterial photodynamic peptides for staphylococcal skin infection. *Biomater Sci* **8,** 6695–6702 (2020).

382. Garnica-Palafox, I. M. & Sánchez-Arévalo, F. M. Influence of natural and synthetic crosslinking reagents on the structural and mechanical properties of chitosan-based hybrid hydrogels. *Carbohydr Polym* **151,** 1073–1081 (2016).

383. Chen, X. & Taguchi, T. Enhanced Skin Adhesive Property of Hydrophobically Modified Poly(vinyl alcohol) Films. *ACS Omega* **5,** 1519–1527 (2020).

384. Coltelli, M. B., Danti, S., de Clerk, K., Lazzeri, A. & Morganti, P. Pullulan for advanced sustainable body- And skin-contact applications. *J Funct Biomater* **11,** 20 (2020)

385. Le, N. M. N., Le-Vinh, B., Friedl, J. D., Jalil, A., Kali, G. & Bernkop-Schnürch, A. Polyaminated pullulan, a new biodegradable and cationic pullulan derivative for mucosal drug delivery. *Carbohydr Polym* **282,** 119143 (2022).

386. Kawasaki, R., Ohdake, R., Yamana, K., Eto, T., Sugikawa, K. & Ikeda, A. Photodynamic therapy using self-assembled nanogels comprising chlorin e6-bearing pullulan. *J Mater Chem B* **9,** 6357–6363 (2021).

387. Baptista, I., Queirós, R. P., Cunha, Â., Saraiva, J. A., Rocha, S. M. & Almeida, A. Inactivation of enterotoxic and non-enterotoxic Staphylococcus aureus strains by high pressure treatments and evaluation of its impact on virulence factors. *Food Control* **57,** 252–257 (2015).

388. Papageorgiou, S., Varvaresou, A., Tsirivas, E. & Demetzos, C. New alternatives to cosmetics preservation. *J Cosmet Sci* **61,** 107–123 (2010).

389. Fernandes, S. C. M., Sadocco, P., Causio, J., Silvestre, A. J. D., Mondragon, I. & Freire, C. S. R. Antimicrobial pullulan derivative prepared by grafting with 3-aminopropyltrimethoxysilane: Characterization and ability toformtransparent films. *Food Hydrocoll* **35,** 247–252 (2014).

390. Li, G., Xie, Q., Liu, Q., Liu, J., Wan, C., Liang, D. & Zhang, H. Separation of phenolic compounds from oil mixtures by betaine-based deep eutectic solvents. *Asia-Pac J Chem Eng* **15,** e2515 (2020).

391. Lynam, J. G., Kumar, N. & Wong, M. J. Deep eutectic solvents' ability to solubilize lignin, cellulose, and hemicellulose; thermal stability; and density. *Bioresour Technol* **238,** 684–689 (2017).

392. Rafael, D., Andrade, F., Martinez-Trucharte, F., Basas, J., Seras-Franzoso, J., Palau, M., Gomis, X., Pérez-Burgos, M., Blanco, A., López-Fernández, A., Vélez, R., Abasolo, I., Aguirre, M., Gavaldà, J. & Schwartz, S. Sterilization Procedure for Temperature-Sensitive Hydrogels Loaded with Silver Nanoparticles for Clinical Applications. *Nanomaterials* **9,** 380 (2019).

393. Lima, I. A. de, Pomin, S. P. & Cavalcanti, O. A. Development and characterization of pullulan-polymethacrylate free films as potential material for enteric drug release. *Braz J Pharm Sci* **53,** 1–9 (2017).

394. Wang, F. Wang, R., Pan, Y., Du, M., Zhao, Y. Gelatin / Chitosan Films Incorporated with Curcumin Based on Photodynamic Inactivation Technology for Antibacterial Food Packaging. *Polymers* **14,** 1600 (2022).

395. Roy, S. & Rhim, J. Carboxymethyl cellulose-based antioxidant and antimicrobial active packaging fi lm incorporated with curcumin and zinc oxide. *Int J Biol Macromol* **148,** 666–676 (2020).

396. Gao, C., Pollet, E. & Avérous, L. Properties of glycerol-plasticized alginate films obtained by thermo-mechanical mixing. *Food Hydrocoll* **63,** 414–420 (2017).

397. Sokolova, M. P., Smirnov, M. A., Samarov, A. A., Bobrova, N. v., Vorobiov, V. K., Popova, E. N., Filippova, E., Geydt, P., Lahderanta, E. & Toikka, A. M. Plasticizing of chitosan films with deep eutectic mixture of malonic acid and choline chloride. *Carbohydr Polym* **197,** 548–557 (2018).

398. Arbeiter, D., Reske, T., Teske, M., Bajer, D., Senz, V., Schmitz, K., Grabow, N. & Oschatz, S. Influence of Drug Incorporation on the Physico-Chemical Properties of Poly(l-Lactide) Implant Coating Matrices—A Systematic Study. *Polymers* **13,** 292 (2021).

399. Ki, V. & Rotstein, C. Bacterial skin and soft tissue infections in adults: A review of their epidemiology, pathogenesis , diagnosis , treatment and site of care. *Can J Infect Dis Med Microbiol* **19,** 173–184 (2008).

400. Spagnul, C., Turner, L. C. & Boyle, W. Immobilized Photosensitisers for antimicrobial applications. *J Photochem Photobiol B* **150,** 11–30 (2015).

401. Li, J., Celiz, A. D., Yang, Q., Wamala, I., Whyte, W., Seo, B. R., Vasilyev, N. v, Vlassak, J. J., Suo, Z. & Mooney, D. J. Tough adhesives for diverse wet surfaces. *Science* **357,** 378–381 (2017).

402. Chen, Y., Yu, D., Chen, W., Fu, L. & Mu, T. Water absorption by deep eutectic solvents†. *Phys.Chem.Chem.Phys.* **21,** 2601–2610 (2019).

403. Singla, S., Amarpuri, G., Dhopatkar, N., Blackledge, T. A. & Dhinojwala, A. Hygroscopic compounds in spider aggregate glue remove interfacial water to maintain adhesion in humid conditions. *Nat Commun* **9,** 1890 (2018).

404. Song, W., Ren, Y., Liu, L., Zhao, Y., Li, Q. & Yang, H. Curcumin induced the cell death of immortalized human keratinocytes (HaCaT) through caspaseindependent and caspase-dependent pathways†. *Food Function* **12,** 8669–8680 (2021).

405. Zhao, Y., Sun, J., Dou, W. & Hu, J. Curcumin inhibits proliferation of interleukin-22-treated HaCaT cells. *Int J Clin Exp Med* **8,** 9580–9584 (2015).

406. Tong, S. Y. C., Davis, J. S., Eichenberger, E., Holland, T. L. & Fowler, V. G. Staphylococcus aureus infections: Epidemiology, pathophysiology, clinical manifestations, and management. *Clin Microbiol Rev* **28,** 603–661 (2015).

407. Branco, T. M., Valério, N. C., Jesus, V. I. R., Dias, C. J., Neves, M. G. P. M. S., Faustino, M. A. F. & Almeida, A. Single and combined effects of photodynamic therapy and antibiotics to inactivate Staphylococcus aureus on skin. *Photodiagnosis Photodyn Ther* **21,** 285–293 (2018).

408. Naksuriya, O., van Steenbergen, M. J., Torano, J. S., Okonogi, S. & Hennink, W. E. A Kinetic Degradation Study of Curcumin in Its Free Form and Loaded in Polymeric Micelles. *AAPS J* **18,** 777–787 (2016).

409. Castro, K. A. D. F., Moura, N. M. M., Figueira, F., Ferreira, R. I., Simões, M. M. Q., Cavaleiro, J. A. S., Faustino, M. A. F., Silvestre, A. J. D., Freire, C. S. R., Tomé, J. P. C., Nakagaki, S., Almeida, A. & Neves, M. G. P. M. S. New Materials Based on Cationic Porphyrins Conjugated to Chitosan or Titanium Dioxide: Synthesis, Characterization and Antimicrobial Efficacy. *Int J Mol Sci* **20,** 2522 (2019).

410. Fontana, C. R., Abernethy, A. D., Som, S., Ruggiero, K., Doucette, S., Marcantonio, R. C., Boussios, C. I., Kent, R., Goodson, J. M., Tanner, A. C. R. & Soukos, N. S. The antibacterial effect of photodynamic therapy in dental plaque-derived biofilms. *J Periodontal Res* **44,** 751–759 (2009).

411. Budzyńska, A., Skowron, K., Kaczmarek, A., Wietlicka-Piszcz, M. & Gospodarek-Komkowska, E. Virulence factor genes and antimicrobial susceptibility of Staphylococcus aureus strains isolated from blood and chronic wounds. *Toxins* **13,** 491 (2021).

412. Maisch, T., Bosl, C., Szeimies, R. M., Love, B. & Abels, C. Determination of the antibacterial efficacy of a new porphyrin-based photosensitizer against MRSA ex vivo. *Photochem & Photobiol Sci* **6,** 545–551 (2007).

413. Wongrakpanich, S., Wongrakpanich, A., Melhado, K. & Rangaswami, J. A Comprehensive Review of Non-Steroidal Anti-Inflammatory Drug Use in The Elderly. *Aging Dis* **9,** 143-150 (2018).

414. Ong, C. K. S., Lirk, P., Tan, C. H. & Seymour, R. A. An Evidence-Based Update on Nonsteroidal Anti-Inflammatory Drugs. *Clin Med Res* **5,** 19–34 (2007).

415. Hadgraft, J., Whitefield, M. & Rosher, P. H. Skin Penetration of Topical Formulations of Ibuprofen 5%: An in vitro Comparative Study. *Skin Pharmacol Physiol* **16,** 137–142 (2003).

416. Deng, Y., Yang, F., Zhao, X., Wang, L., Wu, W., Zu, C. & Wu, M. Improving the skin penetration and antifebrile activity of ibuprofen by preparing

nanoparticles using emulsion solvent evaporation method. *Eur J Pharm Sci* **114,** 293–302 (2018).

417. Haroutiunian, S., Drennan, D. A. & Lipman, A. G. Topical NSAID Therapy for Musculoskeletal Pain. *Pain Medicine* **11,** 535–549 (2010).

418. Schmuck, C. & Weber, E. Solubility of Nonsteroidal Anti-inflammatory Drugs (NSAIDs) in Neat Organic Solvents and Organic Solvent Mixtures. *Chem Int* **36,** 6391–6392 (2014).

419. Pushpamalar, J., Meganathan, P., Tan, H. L., Dahlan, N. A., Ooi, L.-T., Neerooa, B. N. H. M., Essa, R. Z., Shameli, K. & Teow, S.-Y. Development of a Polysaccharide-Based Hydrogel Drug Delivery System (DDS): An Update. *Gels* **7,** 153 (2021).

420. Jabeen, S., Maswal, M., Chat, O. A., Rather, G. M. & Dar, A. A. Rheological behavior and ibuprofen delivery applications of pH responsive composite alginate hydrogels. *Colloids Surf B Biointerfaces* **139,** 211–218 (2015).

421. González, N. & Sumano, H. Design of Two Liquid Ibuprofen-Poloxamer-Limonene or Menthol Preparations for Dermal Administration. *Drug Deliv* **14,** 287–293 (2007).

422. Kligman, A. M. & Christophers, E. Preparation of Isolated Sheets of Human Stratum Corneum. *Arch Dermatol* **88,** 702–705 (1963).

423. Watkinson, R. M., Herkenne, C., Guy, R. H., Hadgraft, J., Oliveira, G. & Lane, M. E. Influence of Ethanol on the Solubility, Ionization and Permeation Characteristics of Ibuprofen in Silicone and Human Skin. *Skin Pharmacol Physiol* **22,** 15–21 (2009).

424. Rhee, Y.-S., Chang, S.-Y., Park, C.-W., Chi, S.-C. & Park, E.-S. Optimization of ibuprofen gel formulations using experimental design technique for enhanced transdermal penetration. *Int J Pharm* **364,** 14–20 (2008).

425. Heyneman, C. A., Lawless-Liday, C. & Wall, G. C. Oral versus Topical NSAIDs in Rheumatic Diseases. *Drugs* **60,** 555–574 (2000).

426. Lachenmeier, D. W. Safety evaluation of topical applications of ethanol on the skin and inside the oral cavity. *J Occup Med Toxicol* **3,** 26 (2008).

427. Anderson, P. C. & Dinulos, J. G. Are the new moisturizers more effective? *Curr Opin Pediatr* **21,** 486–490 (2009).

428. Hnia, K., Gayraud, J., Hugon, G., Ramonatxo, M., De La Porte, S., Matecki, S. & Mornet, D. L-Arginine Decreases Inflammation and Modulates the Nuclear Factor-κB/Matrix Metalloproteinase Cascade in Mdx Muscle Fibers. *Am J Pathol* **172,** 1509–1519 (2008).

429. Razali, N. A., Conte, M. & McGregor, J. The role of impurities in the La2O3 catalysed carboxylation of crude glycerol. *Catal Letters* **149,** 1403–1414 (2019).

430. Ebrahiminezhad, A., Ghasemi, Y., Rasoul-Amini, S., Barar, J. & Davaran, S. Impact of Amino-Acid Coating on the Synthesis and Characteristics of Iron-Oxide Nanoparticles (IONs). *Bull Korean Chem Soc* **33,** 3957–3962 (2012).

431. Walker, S. E., Choudhury, J., Law, S. & Iazzetta, J. Stability of Ibuprofen Solutions in Normal Saline or 5 % Dextrose in Water. *Can J Hosp Pharm.* **64,** 354–361 (2011).

432. Paavola, A. & Kilpela, I. Controlled release injectable liposomal gel of ibuprofen for epidural analgesia. *Int J Pharm* **199,** 85–93 (2000).

433. Greene, J. M., Feugang, J. M., Pfeiffer, K. E., Stokes, J. V., Bowers, S. D. & Ryan, P. L. L-arginine enhances cell proliferation and reduces apoptosis in human endometrial RL95-2 cells. *Reprod Biol Endocrinol* **11,** 15 (2013).

434. Chantereau, G., Sharma, M., Abednejad, A., Neves, B. M., Se, G., Freire, M. G., Freire, C. S. R. & Silvestre, A. J. D. Design of Nonsteroidal Anti-Inflammatory Drug-Based Ionic Liquids with Improved Water Solubility and Drug Delivery. *ACS Sustain Chem Eng* **7,** 14126–14134 (2019).

435. Tucureanu, M. M., Rebleanu, D., Constantinescu, C. A., Deleanu, M., Voicu, G., Butoi, E., Calin, M. & Manduteanu, I. Lipopolysaccharide-induced inflammation in monocytes/macrophages is blocked by liposomal delivery of Gi-protein inhibitor. *Int J Nanomedicine* **13,** 63–76 (2017).

436. Basiak, E., Lenart, A. & Debeaufort, F. How Glycerol and Water Contents Affect the Structural and Functional Properties of Starch-Based Edible Films. *Polymers* **10,** 412 (2018).

437. Sirviö, J. A., Visanko, M., Ukkola, J. & Liimatainen, H. Effect of plasticizers on the mechanical and thermomechanical properties of cellulose-based biocomposite films. *Ind Crops Prod* **122,** 513–521 (2018).

438. Skowrońska, D. & Wilpiszewska, K. Deep Eutectic Solvents for Starch Treatment. *Polymers (Basel)* **14,** 220 (2022).

439. Ahn, Y., Kim, H. & Kwak, S.-Y. Self-reinforcement of alginate hydrogel via conformational control. *Eur Polym J* **116,** 480–487 (2019).

440. Jannah, N., Sebri, M., Anuar, K. & Amin, M. Slow Drug Release of Encapsulated Ibuprofen in Cross-linked Hydrogel for Tissue Engineering Application. *Aust J Basic & Appl Sci* **9,** 48–52 (2015).

441. Konstan, M. W., Krenicky, J. E., Finney, M. R., Kirchner, H. L., Hilliard, K. A., Hilliard, J. B., Davis, P. B. & Hoppel, C. L. Effect of Ibuprofen on Neutrophil Migration in Vivo in Cystic Fibrosis and Healthy Subjects. *J Pharmacol Exp Ther* **306,** 1086–1091 (2003).

442. Lima, A. de F., Pegorin, G. S., Miranda, M. C. R., Cachaneski-Lopes, J. P., Silva, W. de M., Borges, F. A., Guerra, N. B., Herculano, R. D. & Batagin-Neto, A. Ibuprofen-loaded biocompatible latex membrane for drug release: Characterization and molecular modeling. *J Appl Biomater Funct Mater* **19,** 228080002110053 (2021).

443. Ossowicz-Rupniewska, P., Rakoczy, R., Nowak, A., Konopacki, M., Klebeko, J., Świątek, E., Janus, E., Duchnik, W., Wenelska, K., Kucharski, Ł. & Klimowicz, A. Transdermal Delivery Systems for Ibuprofen and Ibuprofen Modified with Amino Acids Alkyl Esters Based on Bacterial Cellulose. *Int J Mol Sci* **22,** 6252 (2021).

444. Gaur, P. K., Bajpai, M., Mishra, S. & Verma, A. Development of ibuprofen nanoliposome for transdermal delivery: Physical characterization, in vitro/in vivo studies, and anti-inflammatory activity. *Artif Cells Nanomed Biotechnol* **44,** 370–375 (2016).

445. Luo, L., Patel, A., Sinko, B., Bell, M., Wibawa, J., Hadgraft, J. & Lane, M. E. A comparative study of the in vitro permeation of ibuprofen in mammalian skin, the PAMPA model and silicone membrane. *Int J Pharm* **505,** 14–19 (2016).

446. Trovatti, E., Freire, C. S. R., Pinto, P. C., Almeida, I. F., Costa, P., Silvestre, A. J. D., Neto, C. P. & Rosado, C. Bacterial cellulose membranes applied in topical and transdermal delivery of lidocaine hydrochloride and ibuprofen: In vitro diffusion studies. *Int J Pharm* **435,** 83–87 (2012).

447. Janus, E., Ossowicz, P., Klebeko, J., Nowak, A., Duchnik, W., Kucharski, Ł. & Klimowicz, A. Enhancement of ibuprofen solubility and skin permeation by conjugation with L-valine alkyl esters. *RSC Adv* **10,** 7570–7584 (2020).

448. Duarte, A. R. C., Ferreira, A. S. D., Barreiros, S., Cabrita, E., Reis, R. L. & Paiva, A. A comparison between pure active pharmaceutical ingredients and therapeutic deep eutectic solvents: Solubility and permeability studies. *European Journal of Pharmaceutics and Biopharmaceutics* **114,** 296–304 (2017).